

A STUDY OF NEUROMODULATION USING THE  
ISOLATED LOCUST (SCHISTOCERCA GREGARIA)  
FIRST BASALAR MOTONEURONE AS AN 'IN VITRO'  
MODEL

Larissa S. Prothero

A Thesis Submitted for the Degree of PhD  
at the  
University of St Andrews



1997

Full metadata for this item is available in  
St Andrews Research Repository  
at:

<http://research-repository.st-andrews.ac.uk/>

Please use this identifier to cite or link to this item:

<http://hdl.handle.net/10023/14875>

This item is protected by original copyright

413

A study of neuromodulation using the isolated locust  
(*Schistocerca gregaria*) first basalar flight  
motoneurone as an *in vitro* model

A thesis submitted to the University of St. Andrews for the degree of Doctor of  
Philosophy

by  
Larissa S. Prothero

University of St. Andrews  
School of Biological and Medical Sciences  
December 1996





ProQuest Number: 10167076

All rights reserved

INFORMATION TO ALL USERS

The quality of this reproduction is dependent upon the quality of the copy submitted.

In the unlikely event that the author did not send a complete manuscript and there are missing pages, these will be noted. Also, if material had to be removed, a note will indicate the deletion.



ProQuest 10167076

Published by ProQuest LLC (2017). Copyright of the Dissertation is held by the Author.

All rights reserved.

This work is protected against unauthorized copying under Title 17, United States Code  
Microform Edition © ProQuest LLC.

ProQuest LLC.  
789 East Eisenhower Parkway  
P.O. Box 1346  
Ann Arbor, MI 48106 – 1346

Th  
C246

I, Larissa S. Prothero, hereby certify that this thesis has been written by me, that it is the record of work carried out by me and that it has not been submitted in any previous application for a higher degree.

date 19.12.96..... signature of candidate .

I was admitted as a research student under Ordinance No. 12 in October, 1992 and as a candidate for the degree of Ph.D. in September, 1993; the higher study for which this is a record was carried out in the University of St. Andrews between 1992 and 1996.

date 19.12.96..... signature of candidate ..

I hereby certify that the candidate has fulfilled the conditions of the Resolutions and Regulations for the degree of Ph.D. in the University of St. Andrews and that the candidate is qualified to submit this thesis in application for that degree.

date 19.12.96..... signature of supervisor'.

In submitting this thesis to the University of St. Andrews I understand that I am giving permission for it to be made available for use in accordance with the regulations of the University Library for the time being in force, subject to any copyright vested in the work not being affected thereby. I also understand that the title and abstract will be published, and that a copy of the work may be made and supplied to any *bona fide* library or research worker.

date 19.12.96..... signature of candidate ...

## ABSTRACT

1. A technique has been developed to isolate the first basalar (BA1) motoneurone of the locust (*Schistocerca gregaria*) from its ganglionic environment. The isolated neurone soma remained viable (often for up to 9hrs), enabling its electrophysiological and pharmacological properties to be investigated. The findings of these studies were comparable with those from the BA1 motoneurone *in situ*, and with other insect neurones whether studied *in vitro* or *in situ*.

2. The application of selected agonists to the isolated BA1 motoneurone soma demonstrated the presence of nicotinic and muscarinic acetylcholine receptors, GABA receptors and dopamine (DA) receptors. The membrane depolarization evoked by nicotine was blocked by  $\alpha$ -BTX, while the GABA-induced membrane hyperpolarization response was sensitive to picrotoxin. Muscarinic receptor and DA receptor activation both induced membrane depolarization which was evoked without a detectable change in membrane conductance. The ionic dependency of these agonist-induced responses is discussed.

3. When applied between pressure applications of GABA, DA could induce either membrane depolarization or hyperpolarization, both of which were associated with a increase in membrane conductance. Furthermore, the amplitude and/or duration of the GABA response was potentiated by DA. Possible mechanisms underlying these observations are proposed.

4. Using the  $\text{Ca}^{2+}$ -sensitive fluorescence probe, fluo-3, and confocal laser scanning microscopy, the effects of the muscarinic agonist, McN A-343, and DA on  $[\text{Ca}^{2+}]_i$  in the isolated BA1 motoneurone were examined. McN evoked an increase in  $[\text{Ca}^{2+}]_i$ , whilst DA evoked a decrease in  $[\text{Ca}^{2+}]_i$ . Similar observations were made from isolated cockroach fast coxal depressor ( $\text{D}_f$ ) motoneurones. The cellular events underlying these observations are discussed.

5. A technique was established to maintain dissociated unidentified adult locust neurones in culture for up to two weeks; a similar protocol was used to maintain isolated BA1 motoneurones in culture. Electrophysiological recording techniques demonstrated that the neurones remained viable in culture.

# TABLE OF CONTENTS

	<u>page</u>
Declaration	ii
Abstract	iii
Table of contents	iv
List of figures	ix
List of tables	xii
Acknowledgements	xiii
 <u>Chapter 1. General Introduction</u>	 1
1.1. Neuromodulation	2
1.1.1. Introduction	2
1.1.2. Modulation of cellular function	3
1.1.3. Modulation of ion channel activity	8
1.1.3.1. Introduction	8
1.1.3.2. Modulation by GTP-binding proteins	9
1.1.3.3. Modulation by second messengers and protein kinases	10
1.1.3.3.1. cAMP and cAMP-dependent Protein Kinase (PKA)	10
1.1.3.3.2. cGMP and cGMP-dependent Protein Kinase (PKG)	12
1.1.3.3.3. Ca <sup>2+</sup> /Phospholipid-dependent Protein Kinase (PKC)	13
1.1.3.3.4. Ca <sup>2+</sup> and calmodulin-dependent Protein Kinase (CaMK)	14
1.1.3.3.5. Protein Tyrosine Kinase (PTK)	15
1.1.3.3.6. Calcium	15
1.1.4. Defensive-withdrawal reflexes of <i>Aplysia</i>	18
1.1.4.1 Introduction	18
1.1.4.2. Sensitization	18
1.1.4.2.1. Short-term sensitization	19
1.1.4.2.2. Long-term sensitization	20
1.2. Neurotransmitter Pharmacology	21
1.2.1. Acetylcholine (ACh)	21
1.2.1.1. Introduction	21
1.2.1.2. Vertebrate nicotinic acetylcholine receptor	22
1.2.1.3. Vertebrate muscarinic acetylcholine receptors	24
1.2.1.4. Insect cholinergic receptors	26
1.2.1.5. 'Mixed' cholinergic receptors	30
1.2.2. $\gamma$ -Aminobutyric acid (GABA)	31
1.2.2.1. Introduction	31

1.2.2.2. Vertebrate GABA receptors	31
1.2.2.3. Insect GABA receptors	35
1.2.3. Dopamine (3-hydroxytyramine; DA)	36
1.2.3.1. Introduction	36
1.2.3.2. Vertebrate dopamine receptors	37
1.2.3.3. Dopamine as a neuromodulator	39
1.2.3.4. Insect dopamine receptors	40
1.3. Confocal Laser Scanning Microscopy (CLSM)	41
1.3.1. Introduction	41
1.3.1.2. The principle of CLSM	41
1.4. Neuronal tissue culture	43
1.4.1. Use of neuronal tissue culture	43
1.4.2. Use of invertebrate neural tissue for tissue culture studies	44
1.5. Thesis in context	49
 <u>Chapter 2. A pharmacological profile of the freshly isolated first basalar motoneurone <i>in vitro</i></u>	 53
2.1. Introduction	54
2.2. Materials and methods	58
2.2.1. Animals	58
2.2.2. Neurone identification	58
2.2.2.1. Identification	58
2.2.2.2. Technique for labelling the first basalar motoneurone cell body	59
2.2.3. Electrophysiological study of the first basalar motoneurone	61
2.2.3.1. Dissection	61
2.2.3.2. Illumination	61
2.2.4. Electrophysiological recording techniques	62
2.2.4.1. Experimental chamber	62
2.2.4.2. Isolation of the first basalar motoneurone	62
2.2.4.3. Microelectrodes	63
2.2.4.4. Impalement of the isolated motoneurone	64
2.2.4.5. Input resistance	65
2.2.4.6. Administration of pharmacological agents	66
2.2.5. Voltage-clamp studies	67
2.2.5.1. Preparation	67
2.2.5.2. Illumination	67

2.2.5.3. Isolation of the first basalar motoneurone	68
2.2.5.4. Microelectrodes	68
2.2.5.5. Impalement of the isolated motoneurone	69
2.2.5.6. Reversal potentials	69
2.2.6. Data capture and storage	70
2.3. Results	71
2.3.1. Electrophysiological properties of the isolated BA1 motoneurone	71
2.3.2. The presence of cholinergic receptors on isolated BA1 motoneurones	71
2.3.2.1. The effects of acetylcholine on isolated BA1 motoneurones	72
2.3.2.2. The effects of nicotine on isolated BA1 motoneurones	74
2.3.2.3. The effects of muscarinic agonists on isolated BA1 motoneurones	76
2.3.3. The effects of GABA and muscimol on isolated BA1 motoneurones	81
2.3.4. The effects of dopamine on isolated BA1 motoneurones	84
2.3.5. The effects of dopamine on the GABA response in isolated BA1 motoneurones	87
2.4. Discussion	91
2.4.1. Electrophysiological properties of the isolated BA1 motoneurones	91
2.4.2. A pharmacological profile of the isolated BA1 motoneurones	93
2.4.2.1. The presence of cholinergic receptors on the isolated motoneurone soma	93
2.4.2.2. The presence of GABAergic receptors on the isolated motoneurone soma	103
2.4.2.3. The presence of dopaminergic receptors on the isolated motoneurone soma	106
2.3.2.4. Modulation of the GABA response by dopamine in isolated BA1 motoneurones	110
<u>Chapter 3. Investigation of the effects of McN-A-343 and dopamine on intracellular <math>Ca^{2+}</math> concentration in the first basalar motoneurone using a fluorescence imaging technique</u>	117
3.1. Introduction	118
3.1.1. Introduction	118
3.1.2.1. Calcium-sensitive fluorescent probes	118
3.1.2.2. Methods of application	120
3.1.3. Applications of calcium-sensitive fluorescent indicators	120
3.2. Materials and methods	123

3.2.1. Dissection	123
3.2.2. Protocol for pressure injection of isolated motoneurons with fluo-3	123
3.2.2.1. Microelectrodes	123
3.2.2.2. Microelectrode impalement and pressure-injection of fluo-3	123
3.3. Results	126
3.3.1. Appearance of insect motoneurons pressure-injected with fluo-3	126
3.3.2. The effect of McN-A-343 on intracellular calcium in isolated BA1 motoneurons	127
3.3.3. The effect of McN-A-343 on intracellular calcium in isolated D <sub>r</sub> motoneurons	129
3.3.4. The effect of dopamine on intracellular calcium in isolated BA1 motoneurons	132
3.3.5. The effects of dopamine on intracellular calcium in isolated D <sub>r</sub> motoneurons	135
3.4. Discussion	136
<u>Chapter 4. A study of cultured isolated locust neurones</u>	146
4.1. Introduction	147
4.2. Materials and methods	153
4.2.1. Culturing of unidentified dissociated locust neurones	153
4.2.1.1. Dissection and preparation	153
4.2.1.2. Culture media	155
4.2.1.3. Preparation of culture dishes	156
4.2.2. Culturing isolated first basalar motoneurons	156
4.3. Results	158
4.3.1. Maintenance of isolated unidentified locust neurones in culture	158
4.3.2. Maintenance of first basalar motoneurons in culture	166
4.3.3. Electrophysiological properties of isolated locust neurones	167
4.4. Discussion	171
<u>Chapter 5. General Discussion</u>	182
General Discussion	183
<u>Bibliography</u>	191
References	192



## Appendices

226

Appendix 1. Composition of Toluidine Blue stain and Bodian's fixative

Appendix 2. Composition of locust and cockroach saline

Appendix 3. Diagrammatic representation of two microelectrode current clamp

Appendix 4. Diagrammatic representation of single microelectrode current clamp

Appendix 5. Diagrammatic representation of the pressure application of pharmacological agents

Appendix 6. Diagrammatic representation of two microelectrode voltage clamp

Appendix 7. Composition of the culture media

Appendix 8. Sources of compounds

Appendix 9. List of abbreviations

## LIST OF FIGURES

	<u>follows page</u>
Figure 1.1.1. The five stages of G protein-mediated transmembrane signalling.	9
Figure 1.1.2. How receptor-activated mechanisms acting via the phosphatidyl inositol system modify calcium release from intracellular stores and entry from the extracellular fluid (diagrammatic).	13
Figure 1.2.1. The pentameric structure of the nicotinic cholinergic receptor of <i>Torpedo</i> electroplax tissue.	23
Figure 1.2.2. Proposed transmembrane structure of the myocardial muscarinic receptor.	25
Figure 1.2.3. Model of the GABA <sub>A</sub> receptor-chloride channel protein complex.	31
Figure 1.2.4. Proposed membrane topography of the human D <sub>1</sub> dopamine receptor	37
Figure 1.3.1. The principles of confocal laser scanning microscopy.	41
Figure 2.2.1. Identification of the first basalar motoneurone (BA1) in the locust mesothoracic ganglion.	58
Figure 2.2.2. The Perspex bath used for isolation of the BA1 motoneurone soma.	61
Figure 2.2.3. A schematic diagram illustrating the procedure for cell isolation and the arrangement of the recording chamber for the isolated BA1 motoneurone.	62
Figure 2.2.4. The experimental bath used for voltage- and current-clamp studies.	67
Figure 2.3.1. The typical electrophysiological properties of a freshly isolated BA1 motoneurone soma <i>in vitro</i> .	71
Figure 2.3.2. The effects of excitatory non-specific cholinergic agents upon isolated BA1 motoneurones.	73
Figure 2.3.3. The effects of the nicotinic acetylcholine receptor agonist, nicotine (NIC), on isolated BA1 motoneurones.	74
Figure 2.3.4. The effects of muscarinic receptor agonists on isolated BA1 motoneurones.	76
Figure 2.3.5. The arecoline (ARE) response of isolated BA1 motoneurones consists of a nicotinic and a muscarinic component.	79
Figure 2.3.6. The effects of the inhibitory neurotransmitter, GABA, on isolated BA1 motoneurones.	81
Figure 2.3.7. The effects of the vertebrate GABA <sub>A</sub> agonist, muscimol, on isolated BA1 motoneurones.	82
Figure 2.3.8. The inhibitory neurotransmitter, GABA, evokes a dose-dependent membrane hyperpolarization at resting membrane potential, in isolated BA1 motoneurones.	83
Figure 2.3.9. The effects of the biogenic amine, dopamine, on isolated BA1 motoneurones.	84
Figure 2.3.10. The effects of dopamine on the GABA response of isolated BA1 motoneurones.	88

Figure 3.1.1. The biophysical properties of the $\text{Ca}^{2+}$ -sensitive fluorescent dyes, fura-2 and fluo-3.	119
Figure 3.3.1. The effect of $10^{-4}\text{M}$ McN-A-343 on $[\text{Ca}^{2+}]_i$ of isolated BA1 motoneurons.	127
Figure 3.3.2. The effect of $10^{-3}\text{M}$ McN-A-343 on $[\text{Ca}^{2+}]_i$ of isolated BA1 motoneurons.	128
Figure 3.3.3. The effect of $10^{-2}\text{M}$ McN-A-343 on $[\text{Ca}^{2+}]_i$ of isolated BA1 motoneurons.	129
Figure 3.3.4. The effect of $10^{-4}\text{M}$ McN-A-343 on $[\text{Ca}^{2+}]_i$ of isolated BA1 motoneurons is blocked by the cholinergic antagonist, atropine ( $10^{-4}\text{M}$ ).	129
Figure 3.3.5. The effect of $10^{-3}\text{M}$ McN-A-343 on $[\text{Ca}^{2+}]_i$ of isolated $\text{D}_f$ motoneurons.	130
Figure 3.3.6. The effect of $10^{-2}\text{M}$ McN-A-343 on $[\text{Ca}^{2+}]_i$ of an isolated $\text{D}_f$ motoneuron.	131
Figure 3.3.7. The dose-dependent effect of dopamine ( $10^{-4}\text{M}$ and $10^{-3}\text{M}$ ) on $[\text{Ca}^{2+}]_i$ of isolated BA1 motoneurons.	132
Figure 3.3.8. The dose-dependent effect of dopamine ( $10^{-3}\text{M}$ and $10^{-2}\text{M}$ ) on $[\text{Ca}^{2+}]_i$ of isolated BA1 motoneurons.	133
Figure 3.3.9. The effect of $10^{-4}\text{M}$ dopamine on $[\text{Ca}^{2+}]_i$ of isolated BA1 motoneurons is blocked by the $\text{D}_1/\text{D}_2$ dopaminergic antagonist, fluphenazine ( $10^{-4}\text{M}$ ).	134
Figure 3.3.10. The effect of dopamine ( $10^{-3}\text{M}$ ) on $[\text{Ca}^{2+}]_i$ of isolated $\text{D}_f$ motoneurons.	135
Figure 3.4.1. Schematic diagram summarizing a hypothesis of the cellular events of DA regulation of $[\text{Ca}^{2+}]_i$ in isolated BA1 motoneurons and $\text{D}_f$ motoneurons.	143
Figure 4. 2. 1. Schematic diagram of the preparation of isolated locust thoracic neurone cultures.	154
Figure 4.3.1. Neuritic outgrowth from a dissociated unidentified adult thoracic locust neurone cultured in Chen and Montalcini's '5 + 4' growth medium.	158
Figure 4.3.2. Varied forms of neuritic outgrowth were observed from dissociated thoracic locust neurones, when cultured in Hayashi and Hildebrand's chemically undefined growth medium (in the absence of fetal calf serum).	161
Figure 4.3.3. Directed neuritic outgrowth from dissociated locust thoracic neurones.	161
Figure 4.3.4. Neurones without prominent axonal stumps, plated in close proximity to one another, were seen to extend neuritic processes which appeared to contact one another.	162
Figure 4.3.5. Neurones with prominent axonal stumps, plated in close proximity to one another, were seen to extend neuritic processes which appeared to contact one another.	162

Figure 4.3.6. The adapted version of the 'hanging column' technique described by Beadle and Hicks (1985) was successful for culturing dissociated adult locust neurones when using Hayashi and Hildebrand's growth medium (in the absence of fetal calf serum).	164
Figure 4.3.7. The isolated adult locust first basalar motoneurone maintained in culture.	166
Figure 4.3.8. Both freshly isolated and dissociated adult locust neurones in culture elicit spontaneous membrane activity.	168
Figure 4.3.9. Locust neurones <i>in vitro</i> could produce membrane oscillations upon membrane depolarization which were not associated with the production of spontaneous 'spiking' activity.	169
Figure 4.3.10. Locust neurones <i>in vitro</i> could fail to show spontaneous 'spiking' activity or multiple membrane oscillations in response to depolarizing current injection.	170

## LIST OF TABLES

Table 1.2.1. The pharmacological profiles of vertebrate and insect ionotropic GABA receptors.	<u>follows page</u> 36
Table 1.2.2. The pharmacological profile of the dopamine receptor present on an identified insect motoneurone	40
Table 4.3.1. Comparison of the resting membrane potential of freshly isolated and cultured locust neurones.	167

## ACKNOWLEDGEMENTS

I wish to express my gratitude to my supervisor, Dr Bob Pitman, for his guidance and support throughout my PhD. I would also like to say a big 'Thank you' to Dr Janette Mills and Dr Jon David for their encouragement, answering my questions and proof-reading the early drafts of this thesis. I am especially grateful to Dr Jon David for introducing me to calcium imaging and making the confocal microscopy experiments of this study possible.

I am indebted to all my friends in and outside of St. Andrews. There are too many of you to mention you all, however, you all made sure I got to the end... I couldn't have done it without you!!

I would like to thank everybody else who has given me advice and support, particularly Dr Isabel Bermudez of Oxford Brookes University for her advice regarding techniques of dissociated insect neuronal cultures, Miss Jane McLelland for her work in the investigation of the effects of dopamine on locust neurones, Mr John Mackie for his technical support with the confocal microscope, and Mr David Ogden for keeping me supplied with locusts. I would also like to acknowledge the Company of Biologists for their financial support, enabling me to attend the 1995 Society for Neuroscience Conference (San Diego). The work presented here was funded by the BBSRC.

I dedicate this thesis to my family. Without their continual support and words of encouragement, this would not have been possible.

## **Chapter 1**

### **General Introduction**

# GENERAL INTRODUCTION

## 1.1. Neuromodulation

### 1.1.1. Introduction

A neuronal circuit has been defined as a limited ensemble of interconnected neurones whose combined activity subserves a particular function or set of functions (from Katz and Frost, 1996). For example, the generation of timing cues for repetitive movements of specific muscles, such as required for wing motion during locust flight, are generated by central pattern generators (CPGs). These are neural circuits, which, in the absence of descending and sensory input, produce a rhythmic motor pattern.

Existing within distinct functional circuits, neurones are subject to modulation. Neuromodulation is the ability of neurones to alter their properties in response to intracellular biochemical changes resulting from synaptic or hormonal stimulation (see Kaczmarek & Levitan, 1987). There are two forms of neuromodulation which can change the activity of neuronal circuits by altering neuronal membrane excitability and/or synaptic efficacy; these are *extrinsic* and *intrinsic* modulation (for recent detailed review see Katz and Frost, 1996). *Extrinsic* neuromodulation of a circuit is caused by neurotransmitters and neurohormones released from sites anatomically and functionally separate from the circuit. Consequently, this type of modulation tends to have a widespread effect on the nervous system of an organism. A well illustrated example of this is the modulation of the crustacean stomatogastric CPGs that control the movements of the foregut. *Intrinsic* neuromodulation, on the other hand, arises from substances released by neurones of a circuit that then affect neurones and synapses within that circuit. Unlike extrinsic modulation which is optional, intrinsic modulation is present when the circuit is active, is dependent on the level of



activity within the circuit itself and can act as a self-regulatory mechanism. An example of intrinsic modulation is the escape-swim CPG of the mollusc *Tritonia*. It is believed that activity of a specific serotonergic dorsal swim interneurone, found within the escape-swim CPG circuit, enables this neuronal circuit to function as a rhythmic-pattern generator for swimming (cited by Katz and Frost, 1996). Thus, neuromodulation is an important phenomenon that allows the nervous system of an animal to adapt to a continually changing environment, and furthermore, is the basis for some of the long term changes seen in animal behaviour.

#### 1.1.2. Modulation of cellular function

Cellular function is maintained by a number of ionic currents, and it is the modification of neuronal ion channel function which regulates neuronal membrane excitability, which is fundamental to neuromodulation. Four basic changes in the electrical properties of neurones are seen as a result of the modulation of channel function are:

1. An alteration in the shape of action potentials
2. A change in frequency and pattern of firing
3. The inhibition and onset of bursting
4. A change in cellular response to stimulation.

A brief description of the ion currents involved in the maintenance of neuronal excitability and function is given below (see Levitan and Kaczmarek, 1987).

#### Sodium current ( $I_{Na}$ )

This is an inward sodium ( $Na^+$ ) current whose activation (channel opening) and inactivation (channel closure) are strongly voltage-dependent.

Activation occurs at positive to  $-40\text{mV}$ ; inactivation is almost complete at the peak of an action potential. Generally, the  $\text{Na}^+$  current is blocked by treatment with tetrodotoxin (TTX).

### Calcium current ( $I_{\text{Ca}}$ )

The voltage-dependent calcium ( $\text{Ca}^{2+}$ ) current is the other major inward current elicited by membrane depolarization.  $\text{Ca}^{2+}$  channels are activated at potentials positive to  $-20\text{mV}$ , and display slower inactivation kinetics than those of  $\text{Na}^+$  channels. Inactivation can be both voltage- and  $\text{Ca}^{2+}$ -dependent; in the case of the latter, the  $\text{Ca}^{2+}$  that enters the cell during depolarization feeds back and inhibits the voltage-dependent  $\text{Ca}^{2+}$  channels. The  $\text{Ca}^{2+}$  channels are blocked by  $\text{Cd}^{2+}$ ,  $\text{Co}^{2+}$  and  $\text{Ni}^{2+}$ , however,  $\text{Ba}^{2+}$  is often used in electrophysiological studies to replace  $\text{Ca}^{2+}$  ions. Although it does not cause  $\text{Ca}^{2+}$  channel inactivation,  $\text{Ba}^{2+}$  carries current through the  $\text{Ca}^{2+}$  channels and blocks  $\text{K}^+$  channels and thus, enables a clearer examination of  $\text{Ca}^{2+}$  channel characteristics. There are four main different types of  $I_{\text{Ca}}$ , which can be separated into two classes, depending on their respective activation thresholds. The properties of these  $I_{\text{Ca}}$  channels are outlined below (for further details see Keibabian and Neumeyer, 1994; Tsien *et al*, 1988):

#### *High voltage activated (HVA)*

L-type: The slow inactivating L-type (large, long-lasting) channels are activated at potentials positive to  $-10\text{mV}$  and are more permeable to  $\text{Ba}^{2+}$  than to  $\text{Ca}^{2+}$ . Their inactivation is dependent on both voltage and  $\text{Ca}^{2+}$ . L-type channel blockers include the groups of compounds known as dihydropyridines (DHPs) and phenylalkylamines (for example, verapamil). These channels are usually associated with muscle contraction.

N-type: These  $\text{Ca}^{2+}$  channels are associated with neural tissue (neuronal) and are activated at potentials more positive than -20mV; they are inactivated at potentials more negative than -80mV. N-type channels are more permeable to  $\text{Ba}^{2+}$  than  $\text{Ca}^{2+}$ , and are blocked by  $\omega$ -conotoxin GVIA (CTX) of the marine snail *Conus geographus*. Populations of N-type channels appear only to be associated with neurones and are linked with neurotransmitter release.

P-type: Like the N-type channels, these P- type channels (*Purkinje neurone*) are only associated with neuronal tissue and neurotransmitter release. They are activated at potentials positive to -15mV, and selectively blocked by funnel web spider (*Agelenopsis aperta*) toxin (FTX). Like the other HVA channels, the P-type channel is more permeable to  $\text{Ba}^{2+}$  than to  $\text{Ca}^{2+}$  ions.

#### *Low voltage activated (LVA)*

T-type: T-type (transient, tiny conductance) channels open transiently upon depolarization from holding potentials more negative than -100mV to command potentials to -50mV; they are inactivated at potentials more positive than -80mV. The permeability of the channels to  $\text{Ca}^{2+}$  and  $\text{Ba}^{2+}$  is very similar. There are no highly selective blockers of these channels and these channels are associated with the heart and neuronal membrane bursting activity.

#### Calcium-dependent Cation channel ( $I_{\text{cation/Ca}}$ )

This inward current carries both  $\text{Na}^{+}$  and potassium ( $\text{K}^{+}$ ) ions, consequently, the reversal potential is between -10 and -20mV. Activation of these channels is dependent on  $\text{Ca}^{2+}$ , and is only weakly dependent on voltage.

### Potassium current ( $I_K$ )

There are at least six voltage-dependent outward  $K^+$  currents present in most neurones (as described below). They are distinguished by their voltage-dependencies, activation and inactivation kinetics, and their respective sensitivities to various pharmacological agents.

### Delayed Rectifying Potassium current ( $I_{K(V)}$ )

The voltage-dependent  $K^+$  current activates rapidly during prolonged depolarizations - activation occurs at potentials positive to  $-70\text{mV}$  which is followed by a relatively long inactivation period (full recovery can take up to a minute). This current is the major outward current responsible for the repolarizing phase of an action potential. Tetraethylammonium (TEA) ions are routinely used to block  $I_{K(V)}$ .

### Calcium-dependent Potassium current ( $I_{K(Ca)}$ )

This outward  $K^+$  current contributes to membrane repolarization and afterhyperpolarization of an action potential and thus, is involved in determining interspike intervals. Channel activation is dependent on  $\text{Ca}^{2+}$  ions; binding of  $\text{Ca}^{2+}$  causes a conformational change in the channel protein, to result in channel opening. Consequently, there is a large increase in  $I_{K(Ca)}$  associated with membrane depolarization. Blockers of  $I_{Ca}$  also block  $I_{K(Ca)}$ , however, following  $I_{Ca}$  block, injection of  $\text{Ca}^{2+}$  ions into the cell activates this current.

### Transient Potassium current ( $I_{K(A)}$ )

The A current ( $I_{K(A)}$ ) is a rapidly activating and inactivating  $K^+$  current - although dependent on cell type, activation and inactivation of the current occur at approximately  $-60\text{mV}$  and approximately  $-40\text{mV}$ , respectively. Since activation and inactivation can occur at subthreshold potentials for action potential generation,  $I_{K(A)}$  is involved in determining interspike intervals.

### Inward Rectifying Potassium current ( $I_{K(r)}$ )

This  $K^+$  current obtains its name from the decrease in the slope of the I/V relationship with depolarization. This current is active at hyperpolarized membrane potentials and begins to inactivate at the potassium equilibrium potential ( $E_K$ ).  $I_{K(r)}$  is not a perfect rectifier, that is, some outward current flows at membrane potentials in the range of +30mV of  $E_K$ . Since few other ion currents are active at hyperpolarized potentials,  $I_{K(r)}$  contributes significantly to the resting membrane potential.

### M current ( $I_{K(M)}$ )

The M current, so named because of its sensitivity to muscarine (Brown and Adams, 1980), is another  $K^+$  current active in the hyperpolarized range of the membrane potential. It is activated at -50mV and does not inactivate. This relatively small current influences the activity of a cell at the resting membrane potential.

### S current ( $I_{K(S)}$ )

The S current is found in sensory neurones of *Aplysia* and shows only some voltage dependency. Like the M current, it is activated at approximately -50mV, and exhibits no significant inactivation or dependency on intracellular  $Ca^{2+}$ . It is so named because of its sensitivity to serotonin (Klein *et al*, 1982).  $I_{K(S)}$  remains active during an action potential and contributes to spike repolarization.

There is also an additional ionic current, known as the leak current. However, it is simply the underlying, voltage-independent, passive movement of  $K^+$  and  $Cl^-$  across the neuronal plasma membrane.

### 1.1.3. Modulation of ion channel activity

#### 1.1.3.1. Introduction

Ion channel proteins and neurotransmitter receptors are amongst a number of proteins found in the nervous system, which can be phosphorylated by protein kinases. This phosphorylation is believed to have a critical role in at least some forms of synaptic plasticity. Other proteins which also undergo phosphorylation include enzymes involved in neurotransmitter biosynthesis, synaptic vesicle-associated proteins and cytoskeletal proteins (see Huganir, 1987). The protein kinases catalyze the transferral of a phosphoryl group from adenosine triphosphate (ATP) to an amino acid residue of the substrate protein, and this results in an alteration of the functional properties of the protein. The identity of the amino acid phosphorylated depends on the specific kinase catalyzing the reaction, however, it is usually either serine, threonine or tyrosine (see Stryer, 1988). Possible effects of phosphorylation of the amino acids resulting in modulation of the ion channel function are (see Siegelbaum and Tsien, 1983):

- (a) alteration of the open channel flux (that is, the movement of ions through the channel)
- (b) alteration of the probability of channel opening
- (c) alteration of the availability of functional channels
- (d) alteration of the total number of channels.

Many neurotransmitters and hormones modulate ion channel function either directly, via guanyl-nucleotide-binding proteins (GTP-binding proteins/G-proteins), or indirectly, by altering the levels of intracellular second messenger molecules (themselves mediated by G-proteins) as components of cascade pathways (for review see Swope *et al*, 1992). The involvement of G-proteins,

second messengers and protein kinases that are activated by second messenger molecules in the modulation of neuronal activity is described below.

#### 1.1.3.2. Modulation by GTP-binding proteins

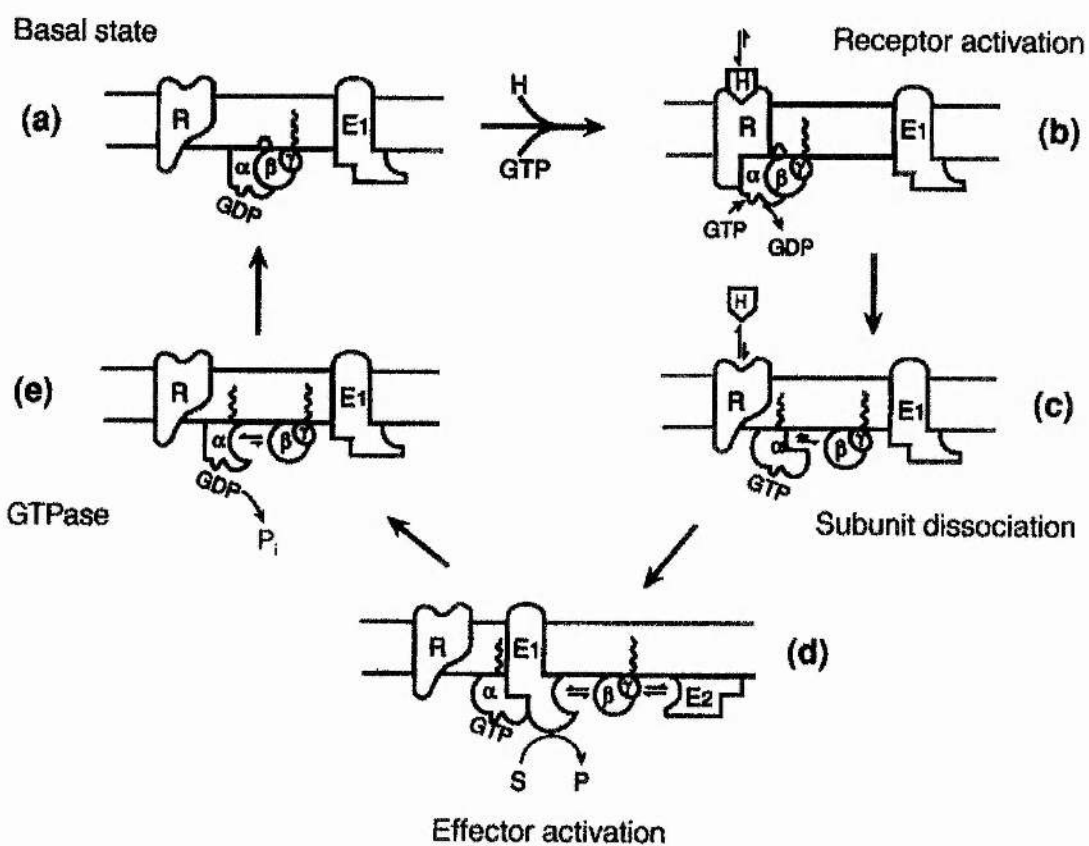
GTP-binding proteins (G-proteins) are membrane-bound heterotrimeric protein complexes, which act as signal transducers. Various neurotransmitters bind to G-protein-coupled receptors to mediate their effects on intracellular processes; the neurotransmitter receptors include the muscarinic acetylcholine receptor, the GABA<sub>B</sub> receptor, the dopamine receptor subtypes, neuropeptidergic, all but one of the serotonergic and glutamatergic receptors (see Hulme *et al.*, 1990). The G-protein macromolecule is composed of  $\alpha$  (40K),  $\beta$  (35K) and  $\gamma$  (10K) subunits which are present in equal stoichiometry (see Figure 1.1.1). Whilst there are over 20 different G-proteins, it is the  $\alpha$  subunit (of which there are several subtypes) that determines the function and specificity of the protein (see Majewski and Barrington, 1995).

The involvement of G-proteins in signal transduction following agonist-receptor binding are shown in Figure 1.1.1. In the resting state, guanosine diphosphate (GDP) is bound to the G $_{\alpha}$  subunit. However, binding of the agonist to its receptor results in a conformational change in the guanyl nucleotide binding site on this subunit, and GDP is replaced with GTP (guanosine triphosphate). This is followed by the activation of the G-protein and the subsequent dissociation of the G $_{\alpha}$  subunit (with the GTP molecule) from the  $\beta\gamma$  complex. The G $_{\alpha}$  subunit then binds to and modifies the activity of its target protein (for example, an ion channel protein, such as the N-type Ca<sup>2+</sup> channels following the activation of a variety of receptors (see Hille, 1994) or a catalytic enzyme involved in second messenger cascades (see below). G $_{\alpha}$  is active as long as GTP is bound to it; the subunit has intrinsic GTPase activity which results in GTP hydrolysis to GDP.

Figure 1.1.1. The five stages of G protein-mediated transmembrane signalling. In the inactivated state (a), G proteins exist as heterotrimers, with GDP bound to the G protein. Upon agonist binding and receptor activation, the receptor-agonist complex binds to the  $\alpha$  subunit, altering the guanyl nucleotide binding site on  $G_\alpha$ : the GDP molecule dissociates and GTP binds to  $G_\alpha$  (b). The binding of GTP activates the G protein and allows  $G_\alpha$ -GTP to dissociate from  $G_{\beta\gamma}$  and the receptor-agonist complex (c). The free  $G_\alpha$  subunit can now bind to and modify the activity of an effector molecule (d). In some cases,  $G_{\beta\gamma}$  interacts with a second effector,  $E_2$ .  $G_\alpha$  possesses an intrinsic GTPase activity and will slowly hydrolyze the GTP molecule to GDP. When this occurs, the G protein is inactivated and dissociates from the enzyme (e) and returns to the basal state (a).

(adapted from Hepler and Gilman, 1992).





Consequently, the  $\alpha$  subunit is able to reassociate with the receptor- $\beta\gamma$  complex to terminate its activity.

#### 1.1.3.3. Modulation by second messengers and protein kinases

The involvement of second messengers in metabolism was first demonstrated in the 1950s; an increase in the synthesis of cyclic adenosine monophosphate (cAMP) was shown to mediate the stimulation of glycogenolysis by adrenaline in the liver (Sutherland and Rall, 1958). It was somewhat later that it was reported that cAMP activated a protein kinase in skeletal muscle and that the stimulation of glycogenolysis by adrenaline was mediated by cAMP-dependent protein kinase (Krebs and Beavo, 1979). Since this time, a number of protein kinases dependent on cAMP, cyclic guanosine monophosphate (cGMP), diacylglycerol and  $\text{Ca}^{2+}$  for their activation, have been associated with the modulation of ion channel and receptor protein function (see below).

##### 1.1.3.3.1. cAMP and cAMP-dependent Protein Kinase (PKA)

The synthesis of cAMP from ATP is catalysed by adenylate cyclase, a plasma membrane-associated enzyme. The activation of adenylate cyclase by the binding of neurotransmitters and hormones to their specific receptors is mediated by G-proteins (see above). The actions of the G-proteins on adenylate cyclase can be stimulatory (in the case of  $G_s$ ) or inhibitory (in the case of  $G_i$ ) and, therefore, the level of intracellular cAMP is regulated. Phosphodiesterases also participate in the regulation of intracellular cAMP; these enzymes hydrolyze cAMP to AMP to terminate its activity. cAMP-dependent protein kinase (PKA) is a major intracellular receptor for cAMP. It is widely distributed within cells, being found both within membrane and cytosolic compartments, and the action of cAMP

within a cell is mediated almost entirely by this kinase (see Majewski and Barrington, 1995).

PKA is a tetrameric protein complex of regulatory and catalytic subunits, which on binding with cAMP, results in its dissociation. The free catalytic subunits are then active to phosphorylate their substrate proteins. The catalytic subunits can autophosphorylate one of the regulatory subunits, thus causing a decrease in the rate of reassociation and enhancing the response to cAMP. As with all the protein kinases, substrate specificity is primarily determined by the primary structure of the substrate protein, although the secondary and tertiary structures do play a role. PKA, like cGMP-dependent,  $\text{Ca}^{2+}$ /calmodulin-dependent, and  $\text{Ca}^{2+}$ /phospholipid-dependent protein kinases, phosphorylates serine and threonine residues which are preceded by 2 to 3 basic amino acids, usually arginine and lysine (see Huganir, 1987).

From the vast array of literature published it is seen that most of the voltage-dependent ion channels described previously can be modulated by PKA (see Levitan, 1988). The result of PKA-dependent phosphorylation is the enhancement or depression of ion flux through the ion channel. In addition to these voltage-dependent ion channels, the receptor proteins for the neurotransmitters comprising the ligand-gated ion channel superfamily also act as substrates for this kinase, to be modulated by phosphorylation (see Swope *et al.*, 1992). Phosphorylation of the neuronal nicotinic acetylcholine receptor results in an increase peak ionic current, which appears to be the result of an increase in the number of functional receptors (Margiotta *et al.*, 1987; Vijayaraghavan *et al.*, 1990). The effects of PKA phosphorylation of the GABA<sub>A</sub> receptor are complex; it can cause depression or potentiation of the response to GABA; whether depression or potentiation occurs, appears to be dependent on the identity of the cell type being used in the investigation. For example, using cultured embryonic

rat neurones, PKA evokes a decrease in peak GABA-current amplitude by increasing the fast component of desensitization (Moss *et al*, 1992). However, using rat pyramidal neurones, it has been suggested that cAMP-dependent mechanisms are responsible for the noradrenaline-induced potentiation of the GABA response (Sessler *et al*, 1995). Glutamate receptors offer another example of PKA-induced potentiation of channel function. A study using rat hippocampal neurones has shown that PKA increases the frequency and duration of kainate-gated channel opening. This suggests, by phosphorylating kainate receptor proteins, PKA has an important direct role in long-term potentiation (Greengard *et al*, 1991).

#### 1.1.3.3.2. cGMP and cGMP-dependent Protein Kinase (PKG)

cGMP is produced in a similar manner to cAMP, in that it is synthesized from a nucleotide (guanosine) triphosphate (GTP) in a reaction catalysed by guanylate cyclase, which is also a G-protein coupled event. cGMP-dependent protein kinase (PKG) is dependent on cGMP for its activation, in a manner similar to the dependence of PKA on cAMP. It is one of several types of intracellular binding protein for cGMP (others include ion channel proteins and phosphodiesterases; for detailed review see Lincoln and Cornwell, 1993). PKG is a dimeric protein which, when it binds to cGMP, undergoes a conformational change resulting in its activation. Like PKA, it too is affected by autophosphorylation - in its case, it results in an increase in its maximal velocity ( $V_{max}$ ; de Jonge and Rosen, 1977). This means that the concentration of substrate (cGMP) required for enzyme (PKG) saturation is increased, and subsequently, enzyme turnover is increased (see Stryer, 1988).

Whilst the roles of cAMP and PKA in neuromodulation are well understood, those of cGMP and PKG in neuronal functioning are not clear. It has

been suggested that PKG may regulate catecholamine neurotransmitter synthesis, by altering the phosphorylation state of transcription factors (which regulate gene expression) and/or tyrosine hydroxylase (Roskoski *et al*, 1987). More recently, PKG has been shown to phosphorylate the  $\beta$  subunit of the GABA<sub>A</sub> receptor (McDonald and Moss, 1994). Thus it may have a role in the modulation of GABA<sub>A</sub> receptor function *in vivo*.

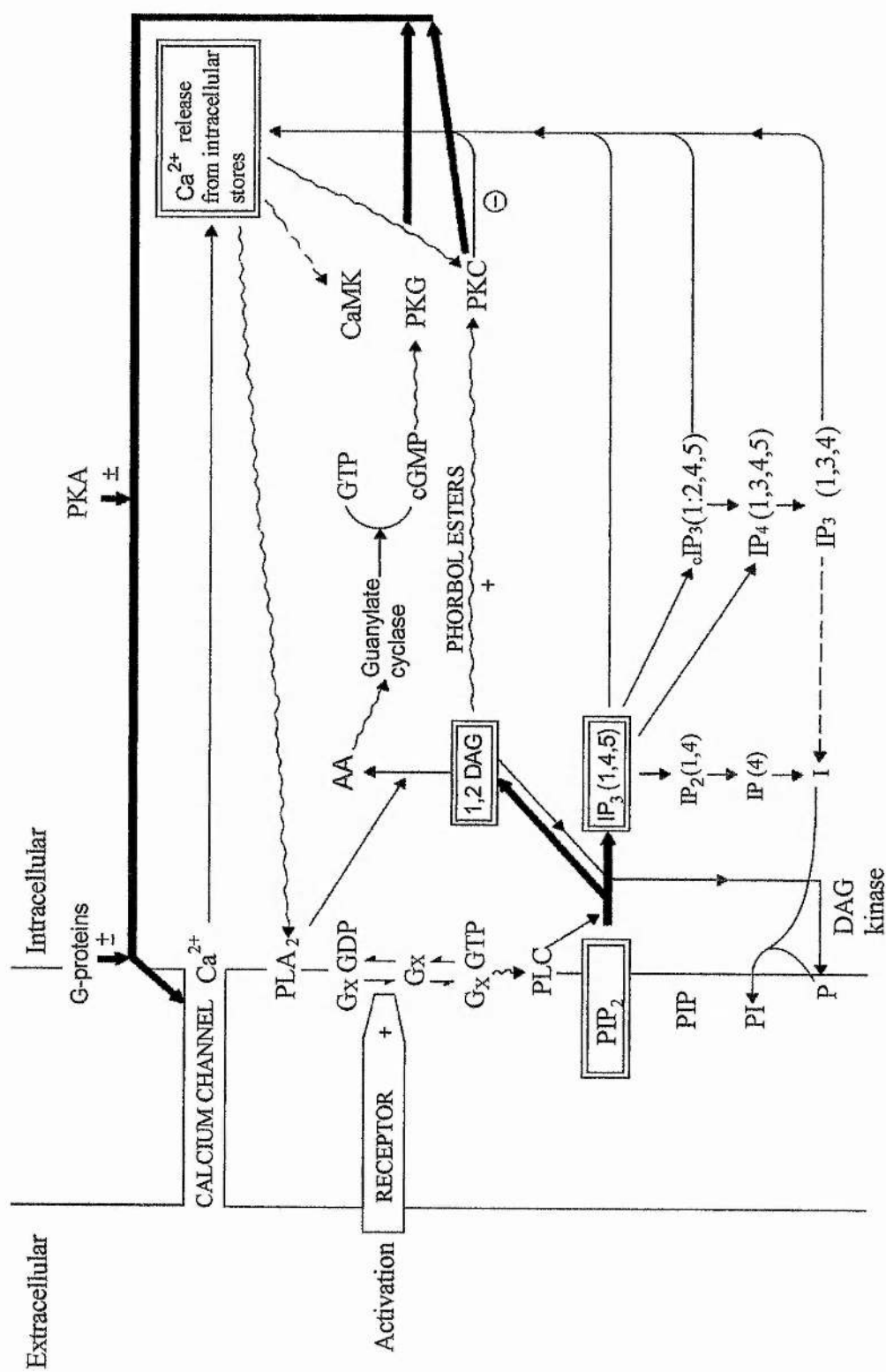
#### 1.1.3.3.3. $\text{Ca}^{2+}$ /Phospholipid-dependent Protein Kinase (PKC)

Another second messenger-dependent protein kinase known to have key roles in neuromodulation, is  $\text{Ca}^{2+}$ /phospholipid-dependent protein kinase (PKC). This phosphorylatory enzyme is activated on binding to  $\text{Ca}^{2+}$  or to diacylglycerol, which is a product of phosphatidylinositol (PI) hydrolysis (see Figure 1.1.2).

PI hydrolysis is catalysed by the membrane-associated enzyme, phospholipase C (PLC) following its G-protein-dependent activation. PLC hydrolyzes the membrane-associated lipid phosphatidylinositol 4, 5-bisphosphate ( $\text{PIP}_2$ ) to form diacylglycerol (DAG) and inositol 1, 4, 5-triphosphate ( $\text{IP}_3$ ). Both DAG, which is associated with the plasma membrane, and  $\text{IP}_3$ , which is located in the cytosol, are important in the regulation of neuronal function. DAG is the second messenger responsible for the activation of PKC in the presence of normal intracellular  $\text{Ca}^{2+}$  concentrations (Nishizuka, 1984), whilst  $\text{IP}_3$  causes the release of  $\text{Ca}^{2+}$  from intracellular stores, such as the endoplasmic reticulum (Streb *et al*, 1983). For an overview of  $\text{Ca}^{2+}$  in neuronal function, see Section 1.1.3.3.6.

The actions of PKC upon voltage-dependent ion channels do not appear to be as universal as those of PKA. That is, most reports are of  $I_{\text{Na}}$  and  $I_{\text{Ca}}$  channel modulation by this protein kinase, for example, Sigel and Baur (1988). However, ligand-gated receptor proteins are modulated by PKC to a similar extent as those by PKA. PKC-induced phosphorylation inhibits both neuromuscular and neuronal

Figure 1.1.2. How receptor-activated mechanisms acting via the phosphatidyl inositol system modify calcium release from intracellular stores and entry from the extracellular fluid (diagramatic representation). Receptor stimulation, via a guanosine-nucleotide regulatory protein ( $G_x$ ), activates a phospholipase C (PLC) - specifically phosphatidylinositolase C - to hydrolyze phosphatidylinositol diphosphate ( $PIP_2$ ) with the formation of inositol trisphosphate ( $IP_3$ ) and 1,2 diacylglycerol (DAG). These two intermediate messengers then affect release of calcium from intracellular stores (-, inhibition) and the resultant formation of three phosphokinases (PKs) namely  $Ca^{2+}$ -calmodulin (CaMK), cyclic GMP-dependent (PKG) and protein kinase C (PKC). Thick lines indicate receptor-operated factors affecting calcium channels (+/-, opening and closing depending upon the tissue involved). Wavy lines indicate activation of enzymes; interrupted lines indicates multi-stage process (adapted from Grundy, 1990).



nicotinic acetylcholine receptor function. Following treatment with phorbol esters, which are activators of PKC, the receptors exhibit an increased rate of desensitization (Downing and Role, 1987; Ross *et al*, 1988). PKC phosphorylation also inhibits GABA<sub>A</sub> receptor function. Using *Xenopus* oocytes expressing GABA channels from rat brain RNA, it has been shown that PKC acts to modulate the function of this ligand-gated ion channel by reducing the amplitude of the receptor current (Moran and Dascal, 1989). Similar findings have been reported for the PKC phosphorylation of GABA<sub>C</sub> receptors, and it has been suggested that PKC-induced phosphorylation is involved in ionotropic GABA receptor run-down (Feigenspan and Bormann, 1994). Glutamate receptors are also substrates for PKC; phosphorylation of AMPA receptors of Purkinje neurones by PKC appears to result in receptor desensitization (Crepel and Krupa, 1988). It has been suggested that it is by this mechanism that PKC has a key role in long-term depression, as seen in the cerebellum.

#### 1.1.3.3.4. Ca<sup>2+</sup> and calmodulin-dependent Protein Kinase (CaMK)

The Ca<sup>2+</sup>/calmodulin-dependent protein kinase (CaMK) is dependent on the binding of Ca<sup>2+</sup> to the cytosolic protein calmodulin for its activation. When calmodulin binds to Ca<sup>2+</sup>, it undergoes a large conformational change to expose a hydrophobic domain. This region interacts with a variety of kinases for their activation.

A number of neuronal Ca<sup>2+</sup>/calmodulin-dependent protein kinases exist (Nairn *et al*, 1985). However, of these, one in particular is seen to have modulatory effects on ligand-gated ion channels. Ca<sup>2+</sup>/calmodulin-dependent protein kinase II (CaMKII) has been shown to phosphorylate a purified GABA<sub>A</sub> receptor subunit (McDonald and Moss, 1994). Furthermore, the  $\alpha$ -subunit of CaMKII has recently been reported to potentiate GABA-induced currents using



the whole-cell patch-clamp technique on isolated rat neurones. The action of the kinase was associated with reduced desensitization of the GABA responses (Wang *et al*, 1995). Evidence is accumulating for a central role for this kinase in long-term depression in the hippocampus because of its involvement in the regulation of AMPA receptor phosphorylation (see Schulman, 1995; Larkman and Jack, 1995).

#### 1.1.3.3.5. Protein Tyrosine Kinase (PTK)

In addition to the protein kinases described above, there is a second messenger-independent protein kinase, the protein tyrosine kinase (PTK), which appears to be involved in ion channel modulation. PTK only phosphorylates tyrosine residues that are preceded by the acidic amino acids glutamic acid and aspartic acid. Although the extracellular signals that trigger the kinase have not been established for neurones, it regulates the function of the GABA<sub>A</sub> receptor by phosphorylation (Moss *et al*, 1995; Valenzuela *et al*, 1995).

#### 1.1.3.3.6. Calcium

It is now well established that calcium ( $\text{Ca}^{2+}$ ) has a pivotal role in neuronal cell function and the contraction of muscle; cytosolic  $\text{Ca}^{2+}$  concentration is critical in neurotransmitter release, neuronal excitability and its modulation, the regulation of protein synthesis and gene expression, neuronal growth and cytotoxicity (see Tsien *et al*, 1988; Choi, 1988). In a neurone at rest,  $\text{Ca}^{2+}$  is found at relatively low concentrations within the cytoplasm (approximately  $10^{-7}\text{M}$ ). However, this level does increase several-fold (see Miller, 1988). Increases in intracellular  $\text{Ca}^{2+}$  can occur either as a result of the opening of voltage-dependent  $\text{Ca}^{2+}$  channels with membrane depolarization, or the release of  $\text{Ca}^{2+}$  from intracellular stores (primarily the endoplasmic reticulum), mediated by the

activation of two distinct intracellular receptor proteins (for detailed review see Simpson *et al*, 1995).

The first type of receptor, the ryanodine (RyR) receptor, is so named from its sensitivity to the plant alkaloid, ryanodine. There are apparently three RyR subtypes. The subtype associated with neural tissue, RyR III, appears to be activated by local accumulations of  $\text{Ca}^{2+}$ . Thus,  $\text{Ca}^{2+}$  release via the activation of these receptors is known as CICR -  $\text{Ca}^{2+}$ -induced  $\text{Ca}^{2+}$  release. RyRs are subject to a range of endogenous modulators, which include the protein kinases. The second type of receptor by which  $\text{Ca}^{2+}$  can be released from intracellular stores, is the inositol triphosphate receptor ( $\text{IP}_3\text{R}$ ) which is activated by the second messenger molecule,  $\text{IP}_3$  (for detailed review see Pozzan *et al*, 1994). The production of  $\text{IP}_3$  is induced by the activation of extracellular neurotransmitter receptors coupled to G-proteins linked to the activation of PLC. Since the activity of the  $\text{IP}_3\text{R}$ -channels is highly sensitive to cytoplasmic concentrations of  $\text{Ca}^{2+}$  in a 'bell shaped' manner (Bezprozvanny *et al*, 1991), it has been suggested that the activation of  $\text{IP}_3\text{Rs}$  at low  $\text{Ca}^{2+}$  concentrations and the inactivation of  $\text{IP}_3\text{Rs}$  at high  $\text{Ca}^{2+}$  concentrations may play important roles in regenerative intracellular signals, such as  $\text{Ca}^{2+}$  waves and oscillations (Berridge, 1993; see Pozzan *et al*, 1994). Like the RyRs, the activity of  $\text{IP}_3$ -sensitive  $\text{Ca}^{2+}$ -release channels are modulated by a range of endogenous factors, including protein kinases (see Pozzan *et al*, 1994).

Of equal importance to cell function and the maintenance of cell viability are the mechanisms by which elevated cytoplasmic  $[\text{Ca}^{2+}]$  is regulated. There are three main cellular mechanisms by which cytoplasmic  $\text{Ca}^{2+}$  can be lowered. First, by the active transport (involving the hydrolysis of ATP) of  $\text{Ca}^{2+}$  across plasma membranes by membrane-bound  $\text{Ca}^{2+}\text{ATPases}$ . When this occurs across the plasma membrane,  $\text{Ca}^{2+}$  is expelled from the cytosol of the neurone, into the

extracellular space. Since  $\text{Ca}^{2+}$ ATPases are also present on cytoplasmic organelles, such as the endoplasmic reticulum and mitochondria, their activation provides a mechanism for simultaneously lowering cytosolic  $\text{Ca}^{2+}$  concentrations and refilling the neuronal  $\text{Ca}^{2+}$  stores. Second,  $\text{Ca}^{2+}$  can also leave the cytosolic environment of a neurone by an exchange mechanism present on the plasma membrane, known as the  $\text{Na}^{+}$ - $\text{Ca}^{2+}$  exchange. The exchange mechanism is driven by the  $\text{Na}^{+}$  electrochemical gradient across the plasma membrane, rather than ATP hydrolysis, and results in one  $\text{Ca}^{2+}$  ion being exchanged for three  $\text{Na}^{+}$  ions and the generation of an inward current (for further details see Lederer *et al*, 1990). Third, there are a number of  $\text{Ca}^{2+}$  binding molecules (aside from the  $\text{Ca}^{2+}$ -dependent kinases) present within the cytoplasm, such as parvalbumin and vitamin D-dependent  $\text{Ca}^{2+}$  binding protein, which act as  $\text{Ca}^{2+}$  buffers. As a result of binding to these molecules,  $\text{Ca}^{2+}$  is effectively rendered inactive (see Blaustein, 1988; Alberts *et al*, 1983).

The mechanisms by which  $\text{Ca}^{2+}$  plays a crucial role in regulating cellular function have already been discussed in the preceding sections. Briefly, cytosolic  $\text{Ca}^{2+}$  is seen to act both directly and indirectly to participate in neuronal modulation. By definition, it directly regulates ion flux through  $I_{K(\text{Ca})}$  and  $I_{\text{cation}(\text{Ca})}$  channels, as changes in intracellular  $\text{Ca}^{2+}$  concentrations ( $[\text{Ca}^{2+}]_i$ ) will result changes in the activation/inactivation status of these ion channels. Since,  $\text{Ca}^{2+}$  channels themselves are affected by  $[\text{Ca}^{2+}]_i$  ( $I_{\text{Ca}}$  channels show  $\text{Ca}^{2+}$ -dependent inactivation; see Section 1.1.2), in effect,  $\text{Ca}^{2+}$  influx is self-regulated, and this can contribute to some of the membrane activity patterns observed in neurones. Indirect pathways by which  $\text{Ca}^{2+}$  affects neuronal function, include the activation of protein kinases, such as PKC and CaMK (see Section 1.1.3.3). By inducing the phosphorylation of specific proteins, both short- and

long-term changes in cell metabolism can be induced; these include changes in neuronal excitability and neuronal growth (see below).

#### 1.1.4. Defensive-withdrawal reflexes of *Aplysia*

##### 1.1.4.1 Introduction

It is understood that by modifying the levels of G-proteins and second messenger molecules, it is possible to induce changes in neurone functioning, and potentially the behavioural patterns of an organism. Well studied examples of this are the neuronal circuits within the abdominal and pleural ganglia of the marine mollusc (sea hare) *Aplysia*, which control the gill-siphon- and tail-withdrawal reflexes, respectively. In these examples, serotonin and cAMP are believed to play central roles in the modulation of a form of simple behaviour.

Both withdrawal reflexes of the *Aplysia* are examples of a non-associative form of learning, that is, they are induced by a single type of stimulus and need not to be associated with other stimuli seen with associative learning. As a result of the gill (or siphon) or tail of the animal being touched, action potentials are generated in sensory neurones which make monosynaptic connections with motoneurones controlling gill or tail withdrawal. If the fast EPSPs that are generated in the motoneurones reach threshold for action potential generation, the result will be withdrawal. It is likely that the neurotransmitter responsible for this fast response is glutamate (Dale and Kandel, 1993). These simple reflex arcs are modulated by interneurones (Xu *et al*, 1994). Repeated stimulation of the sensory neurones results in habituation, that is, the extent of withdrawal decreases. However, sensitization (enhanced withdrawal) occurs when a noxious stimulus is applied to the animal's head or tail (Carew *et al*, 1981). This form of behaviour is discussed below; it is associated with the generation of slow EPSPs, a decrease in

membrane conductance and an increase in action potential duration (Klein and Kandel, 1980; Klein *et al*, 1980).

#### 1.1.4.2. Sensitization

Sensitization is a change in synaptic efficacy at the sensorimotor synapse, occurring as a consequence of heterosynaptic facilitation upon the sensory neurones which enhances neurotransmitter release (Castellucci and Kandel, 1976; Dale *et al*, 1988). Sensitization can manifest itself in two forms: short- and long-term sensitization. Short-term sensitization is understood to occur immediately and locally following the brief exposure to serotonin (5-HT; for example 5 minutes). Long-term facilitation, on the other hand, develops approximately 24 hours after 5HT application, is usually associated with longer exposure times to 5HT (for example 1½ hours) and occurs at sites all over the cell, including those remote to the site of 5HT exposure (for detailed review see Byrne and Kandel, 1996). Whilst the identity of the modulatory neurotransmitter has yet to be verified, there is sufficient evidence to indicate that it is 5-HT. This is based on the ability of 5-HT to mimic the events associated with presynaptic facilitation; that is, (i) the generation of slow EPSPs, (ii) a presynaptic increase in cytosolic cAMP, accompanied by an increase in  $\text{Ca}^{2+}$  influx, occurring as a consequence of a decrease in the  $\text{K}^{+}$  current (Klein and Kandel, 1980).

##### 1.1.4.2.1. Short-term sensitization

The increase in the excitability of the sensory neurones during short-term sensitization arises from a decrease in the specific 5HT-sensitive outward  $\text{K}^{+}$  current ( $I_{\text{K(S)}}$ ; the S current) and the early component of the outward  $I_{\text{K(V)}}$  (Klein *et al*, 1982; Goldsmith and Abrams, 1992) and an increase in  $\text{Ca}^{2+}$  conductance (Boyle *et al*, 1984). Together these alterations prolong action potential duration

and decrease the firing rate during prolonged depolarizations (also known as accommodation; for example see Goldsmith and Abrams, 1992). Consequently, there is an increase in transmitter released from the sensory neurone which increases the level of excitation of the follower neurones and a more intense reflex withdrawal.

It is understood that 5HT acts on the  $K^+$  channels predominantly via cAMP and PKA to phosphorylate the ion channels (Baxter and Byrne, 1989, Hochner and Kandel, 1992). However, the sensitivity of these currents to modulation varies substantially. The reduction in accommodation by 5HT is linked to the 'steady state'  $I_{K(S)}$  and relatively modest activation of PKA, whilst the increase in spike duration is mediated by  $I_{K(V,early)}$  and requires more powerful activation of PKA (Goldsmith and Abrams, 1992). In experiments carried out to block spike broadening using Walsh PKI, a PKA blocker, it was discovered that most of the prolongation was mediated by PKA, however, as it did not accompany the same degree of blocking seen of the increased excitability it has been suggested that a proportion of spike broadening is PKC mediated (Goldsmith and Abrams, 1992).

#### 1.1.4.2.2. Long-term sensitization

As in short-term sensitization, long-term sensitization is associated with a decrease in the outward current. However, it appears that it is only attributed to a decrease in  $I_{K(S)}$  (Scholz and Byrne, 1987). Furthermore, rather than the second messenger, cAMP, contributing to spike broadening, in this instance, evidence suggests that PKC is involved in long-term spike broadening (Sugita *et al.*, 1992). Aside from the time-dependent nature of the two forms of sensitization, the major difference between short-term and long-term facilitation is that the latter requires

an alteration in neuronal gene expression and protein synthesis and thus, can result in changes of neuronal structure (Montarolo *et al*, 1986; Glanzman *et al*, 1990).

In summary; sensitization associated with the withdrawal reflexes in *Aplysia* is a form of neuromodulation, which can result in both short- and long-term increases in synaptic efficacy. In the case of long-term sensitization, it is also associated with structural changes in neuronal morphology. These factors are understood to be critical in the development of memory.

## 1.2. Neurotransmitter Pharmacology

### 1.2.1. Acetylcholine (ACh)

#### 1.2.1.1. Introduction

Acetylcholine (ACh) is a major excitatory neurotransmitter in both vertebrate (Krnjevic, 1974) and invertebrate (Gerschenfeld, 1973) central and peripheral nervous systems. It is synthesized from choline, which is actively transported, via a sodium-dependent transport mechanism, from the cytoplasmic cleft into nerve terminals, where it is a product of ACh hydrolysis by cholinesterase. In the nerve terminal choline is acetylated by choline acetyltransferase, the source of the acetyl groups being acetyl-CoA. Cholinesterase is present in the terminal and ACh is continually being hydrolysed and resynthesized.

The effects of ACh are mediated by its binding to two distinct integral membrane proteins, the nicotinic and muscarinic acetylcholine receptors. The receptor protein structures and cellular events following ACh binding to these receptors are distinctly different (see below).



#### 1.2.1.2. Vertebrate nicotinic acetylcholine receptor

The nicotinic acetylcholine receptor is a member of the superfamily of ligand-gated ion channels, like the GABA<sub>A</sub> and GABA<sub>C</sub>, glycinergic and some of the glutamatergic and serotonergic receptors. This cholinergic receptor exists as two subtypes which can be distinguished by their location; one is located at neuromuscular junctions, whilst the other is located on neuronal membranes. Nicotinic agonists show little selectivity between neuromuscular and neuronal nicotinic receptors. However, nicotinic antagonists do show more specificity. d-Tubocurarine and decamethonium antagonize neuromuscular nicotinic receptors, whilst neurones of the autonomic ganglia are sensitive to hexamethonium and pentamethonium (see Bowman and Rand, 1980). The toxin  $\alpha$ -bungarotoxin ( $\alpha$ -BTX) from the snake *Bungarus multicinctus* has been used as a specific irreversible blocker of neuromuscular nicotinic receptors (for example, Barnard *et al*, 1971; Raferty *et al*, 1973). However, it is now known that it also blocks some neuronal nicotinic receptors (Fumagalli *et al*, 1976; Brown and Fumagalli, 1977); given the differential sensitivity of neuronal nicotinic receptors to  $\alpha$ -BTX it may suggest that the receptors exist as a heterogeneous population.

The high density of nicotinic receptors in both the electroplax of the electric fish of the genus *Torpedo* and in mammalian skeletal muscle, has enabled the purification (Olsen *et al*, 1972, Schmidt and Raferty, 1972; Brockes and Hall, 1975; Dolly and Barnard, 1975), cloning and structural analysis and physiological properties of the neuromuscular nicotinic acetylcholine receptor. The receptor is a heteropentameric glycoprotein comprising of 4 different ( $\alpha$ ,  $\beta$ ,  $\delta$  and  $\gamma$ ) polypeptide subunits (Weill *et al*, 1974; Raferty *et al*, 1975). As seen in other ligand-gated ion channels (for example, the GABA<sub>A</sub> receptor), the secondary structure of the receptor subunits consists of an extracellular amino (N) terminus, 4 membrane spanning hydrophobic domains (M1 - M4) with alternating

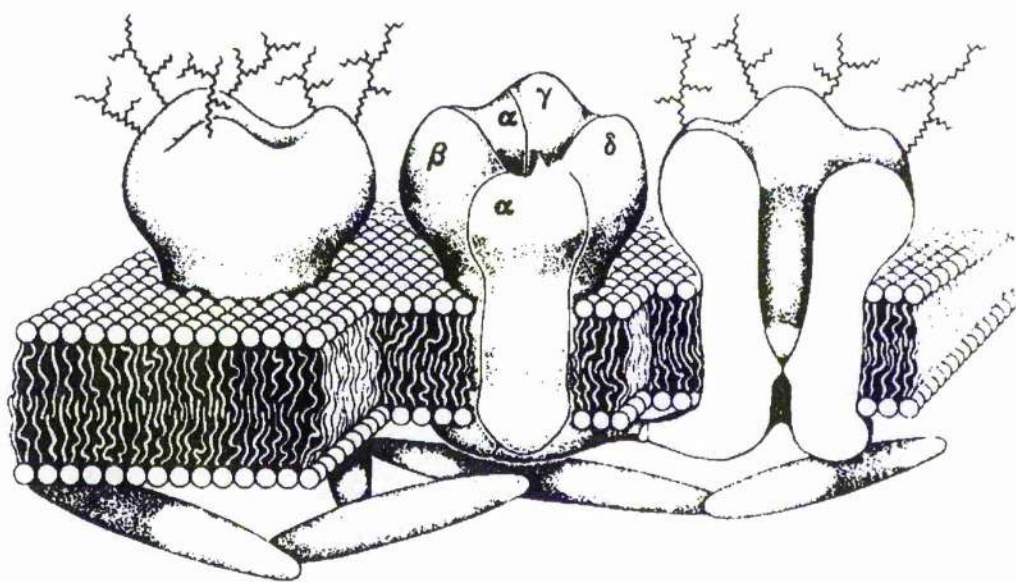


cytoplasmic and extracellular loops and a carboxy (C) terminus, which in the nicotinic receptor is believed to be extracellular (Karlin, 1993). The receptor has a stoichiometry of  $\alpha_2, \beta, \delta, \gamma$  (Reynolds and Karlin, 1978; Lindstrom *et al.*, 1979), and the subunits are arranged regularly around a central axis to form a cation-permeable pore (approximately 290kD) showing a high degree of pentagonal symmetry (see Figure 1.2.1; Brisson and Unwin, 1985). A fifth subunit,  $\epsilon$ , has been discovered from mature calf muscle (but not that of fetal or newborn muscle) and resembles the calf  $\gamma$  subunit (Takai *et al.*, 1985). Its function is not clear, however, it is thought to be involved in developmental changes in receptor kinetics. The channel formed by the arrangement of polypeptide subunits is predominantly permeable to  $\text{Na}^+$  ions, however, it is also permeable to  $\text{K}^+$  and  $\text{Ca}^{2+}$  ions. It has been shown using affinity labelling techniques that the ACh binding site is located on the  $\alpha$  subunit (Reiter *et al.*, 1972; Karlin and Cowburn, 1973; Weill *et al.*, 1974). Consequently, it is understood that there are two ACh binding sites per molecule. More recently, the primary structure of the receptor  $\alpha$ -subunit of *Torpedo californica* has been deduced from DNA sequencing (Noda *et al.*, 1982), and the residues thought to be involved in ACh binding and signal transduction have been located (Mishina *et al.*, 1985).

Neuronal nicotinic receptors are similar in their structural and functional properties to those located at neuromuscular junctions, although, the stoichiometry of the subunits does differ. Whilst it is believed that they are heteropentameric macromolecules, they are composed of five subunits of the  $\alpha$  and  $\beta$  subtype, most likely with a  $\alpha_2\beta_3$  stoichiometric configuration (see Huganir and Greengard, 1990; Conti-Tronconi *et al.*, 1994). As there are currently 7  $\alpha$  ( $\alpha 2$  -  $\alpha 8$ ) subunits and 4  $\beta$  ( $\beta 2$  -  $\beta 5$ ) subunits that have been sequenced from vertebrate neural tissue, the structure of the receptor protein is complicated. However, sensitivity to  $\alpha$ -BTX appears to be designated to the  $\alpha 7$  and  $\alpha 8$  subunits. Subunits resembling  $\delta$ ,  $\gamma$  or  $\epsilon$ ,

Figure 1.2.1. The pentameric structure of the nicotinic cholinergic receptor of *Torpedo* electroplax tissue. The receptor is a macromolecule comprising an integral receptor and non-specific cation channel, and is made up of five polypeptide chains arranged around the pore. The agonist-binding sites are located on the  $\alpha$  subunits (but see Karlin, 1993), implying that two molecules of ACh must bind to the receptor in order for the channel to open. Conserved tyramine, tryptophan and cysteine residues located at the agonist-binding sites are thought to be involved in ligand binding (Karlin, 1993).

(Figure adapted from Rang and Dale, 1987).



as found in neuromuscular nicotinic receptors, have not yet been identified with this receptor subtype.

Regarding the modulation of nicotinic acetylcholine-gated ion channel function by protein kinase-regulated phosphorylation, the neuromuscular nicotinic receptor has been shown to be phosphorylated by PKA (upon the  $\delta$  and  $\gamma$  subunits), PKC (upon the  $\delta$  subunit) and a protein tyrosine kinase (upon the  $\beta$ ,  $\delta$  and  $\gamma$  subunits). Each of the protein kinases phosphorylates a single site on the relevant subunit(s), and the location of these sites have either been proposed (Huganir *et al*, 1984) or determined to be located (Yee and Huganir, 1987; Safran *et al*, 1987) on the major intracellular loop (between M3 and M4) of each subunit (see Huganir and Greengard, 1990). The physiological roles of nicotinic receptor phosphorylation include modulation of receptor desensitization (Hoffmann *et al*, 1994) and assembly (Green *et al*, 1991a, b; Ross *et al*, 1991). Structural details concerning the phosphorylation of neuronal nicotinic receptors is limited. PKA has been shown to phosphorylate  $\alpha 4$  subunits of nicotinic receptors in rat brain neurones *in vitro* (Nakayama *et al*, 1993), and there is evidence to support PKA-mediated phosphorylation of the  $\alpha 3$  subunit of nicotinic receptors of chick ciliary ganglion neurones (Vijayaraghavan *et al*, 1990).

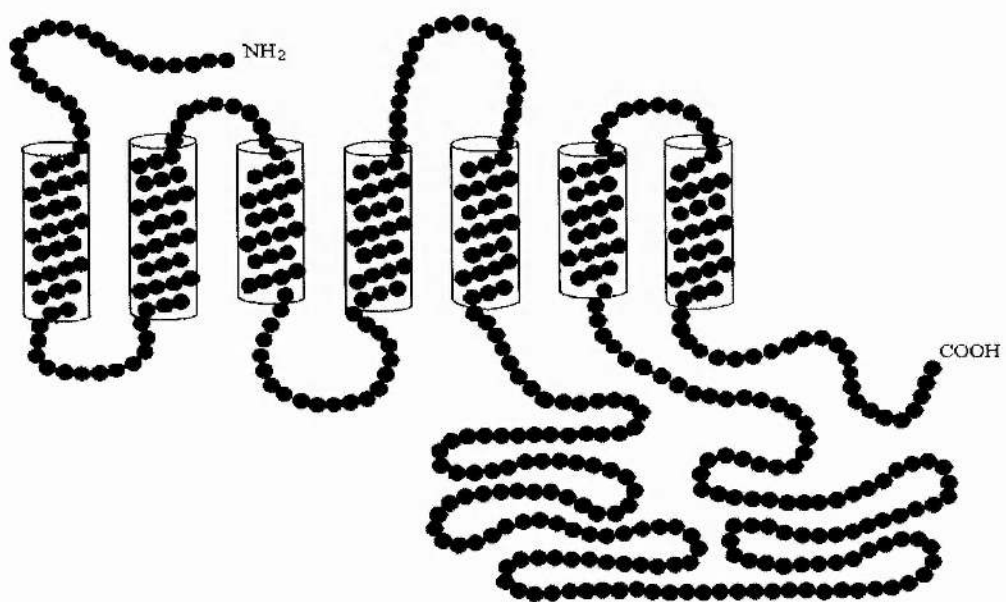
#### 1.2.1.3. Vertebrate muscarinic acetylcholine receptors

In the vertebrate central nervous system the majority of cholinergic receptors are of the muscarinic receptor subtype (Ben-Barak and Dudai, 1979). In contrast to the ligand-gated nicotinic receptors, the muscarinic receptors are members of the superfamily of integral membrane proteins that constitute the G-protein-coupled (also termed metabotropic) receptors to mediate signal transduction (see Nathanson, 1987). Other members of this group include the GABA<sub>B</sub> (see Section 1.2.2.2), dopamine (see Section 1.2.3.2), serotonin,

metabotropic glutamate receptors and most neuropeptide receptors. Figure 1.2.2 shows the proposed topology of the muscarinic receptor. The receptor consists of a long polypeptide chain (approximately 500 amino acids), whose basic topology is an extracellular N terminus region, 7 transmembrane hydrophobic spanning regions (M1 - M7) with alternating cytoplasmic and extracellular loops and a cytoplasmic C terminus region. Furthermore, a region has been identified on the cytoplasmic loop between M5 and M6 which is involved in selective G-protein coupling as part of the transduction pathway that follows receptor activation (Kubo *et al*, 1988).

Pharmacological experiments have distinguished three distinct vertebrate muscarinic receptor subtypes, termed M<sub>1</sub> (neuronal), M<sub>2</sub> (cardiac) and M<sub>3</sub> (glandular) (see below; see Hulme *et al*, 1990). The pharmacological profiles of vertebrate muscarinic receptors differ dramatically from those of the vertebrate nicotinic receptors. There are number of non-selective muscarinic agonists and antagonists routinely used in pharmacological investigations (see Keabian and Neumeyer, 1994). Muscarine, oxotremorine and pilocarpine are used as muscarinic agonists, whilst quinuclidinyl benzilate (QNB), atropine and scopolamine are used as antagonists. Owing to the potent nature of QNB, tritiated QNB is routinely used in radioligand binding studies to identify muscarinic receptors (for example, Waelbroeck *et al*, 1991). In contrast to the number of subtype-selective antagonists that are available, McN-A-343 is the only selective receptor subtype (M<sub>1</sub>) agonist routinely used. Regarding selective muscarinic antagonists, M<sub>1</sub> muscarinic receptors are distinguished by their sensitivity to pirenzepine; the antagonist is ineffective at the M<sub>2</sub> receptor subtype. AF-DX 116 and methoctramine are characteristic M<sub>2</sub> receptor selective antagonists, whilst, hexahydro-sila-difenidol (HHSiD) selectively antagonizes the M<sub>3</sub> receptor. One distinct feature of the muscarinic receptors is their insensitivity to  $\alpha$ -BTX.

Figure 1.2.2. Proposed transmembrane structure of the myocardial muscarinic receptor (adapted from Peralta *et al.*, 1987).



Molecular cloning studies, on the other hand, have revealed the existence of five molecularly distinct mammalian muscarinic receptor proteins (termed m1 - m5). However, these proteins do share a high degree of sequence homology in the membrane spanning regions (Peralta *et al*, 1987; Liao *et al*, 1989). When some of the cloned muscarinic receptors have been expressed in non-native cell types, pharmacological analysis has confirmed their identity. That is, when expressed in *Xenopus* oocytes, cloned porcine brain muscarinic receptors have been reported to resemble M<sub>1</sub> receptors (Kubo *et al*, 1986a); similarly, when expressed in Chinese hamster ovary cells, cloned porcine heart muscarinic receptors resemble M<sub>2</sub> receptors (Kubo *et al*, 1986b). Cloned muscarinic receptors have also enabled the investigation of the cellular events following receptor activation, to indicate distinct muscarinic receptor subtypes. It has been demonstrated that the m1, m3, and m5 receptors generally couple to G proteins that stimulate PI hydrolysis (and consequently increase [Ca<sup>2+</sup>]<sub>i</sub>), whilst, m2 and m4 couple to G proteins that inhibit adenylate cyclase to decrease levels of cytosolic cAMP (Fukuda *et al*, 1988; Peralta *et al*, 1988; Pinkas-Kramarski *et al*, 1988; Liao *et al*, 1989).

#### 1.2.1.4. Insect cholinergic receptors

There is substantial evidence to demonstrate that ACh is an important excitatory neurotransmitter at insect central synapses (Pitman and Kérkut, 1970; for reviews see Pitman, 1971, 1985; Benson, 1993). Furthermore, the effects of this neurotransmitter are known to be mediated by both nicotinic and muscarinic acetylcholine receptors; evidence supporting this has been provided by ligand binding and pharmacological studies (see below).

The antagonists,  $\alpha$ -BTX and QNB, have been used in binding studies to show that nicotinic and muscarinic acetylcholine receptors are present in the central nervous system of various insect species. These include the fruit fly,



*Drosophila* (Dudai, 1977; Dudai and Ben-Barak, 1977; Dudai and Amsterdam, 1977), the locusts *Locusta* and *Schistocerca* (Breer, 1981; Aguilar and Lunt, 1984), the honey bee, *Apis* (Abdallah *et al*, 1991; Huang and Knowles, 1990), and the cockroach *Periplaneta* (Lummis and Sattelle, 1985; Abdallah *et al*, 1991). From these studies it is shown that the number of nicotinic receptors found is approximately an order of magnitude greater than that determined for muscarinic receptors (Breer, 1981; Lummis and Sattelle, 1985). This finding is in contrast to that observed from vertebrate neuronal preparations, where the muscarinic receptor dominates the cholinergic receptor population (Ben-Barak and Dudai, 1979).

Electrophysiological and pharmacological techniques verified the presence of such functional cholinergic receptors on identified insect neurones *in situ*. Both nicotinic and muscarinic receptors are present on the cockroach giant interneurone (Sattelle *et al*, 1983; Le Corrionc *et al*, 1991), the cockroach fast coxal depressor motoneurone ( $D_f$ ) (Sattelle *et al*, 1980; David and Sattelle, 1984, David and Pitman, 1990, 1993a), the principal planta retractor (PPR) motoneurons of *Manduca sexta* (Trimmer, 1992; Trimmer and Weeks, 1989, 1993) and the first basalar motoneurone of the locust (Leitch *et al*, 1993; Anderson, 1995). Furthermore, a recent extensive study has investigated the cholinergic pharmacological profile of unidentified dissociated locust neurones; both the nicotinic and muscarinic responses of these neurones is described in detail (Benson, 1992).

The majority of insect nicotinic receptors are thought to resemble the vertebrate neuromuscular nicotinic receptor because the membrane response mediated by the receptor is blocked by  $\alpha$ -BTX (Sattelle *et al*, 1980). However, whether they exist as a homogeneous population of receptor proteins is not clear at present. It has been suggested that they may exist as a heterogeneous population

(see Gundelfinger, 1992), since dorsal unpaired midline (DUM) neurones of the cockroach (Sattelle *et al*, 1980; Lapied and Hue, 1991) and the locust (Goodman and Spitzer, 1980) exhibit a lower sensitivity to  $\alpha$ -BTX. Further studies are required to clarify this. Native insect nicotinic receptors gate non-specific cation channels (David and Sattelle, 1990), and are assumed to have a pentameric structure similar to the vertebrate nicotinic receptor. However, whether the receptor exists as a homo-oligomer or a hetero-oligomer has yet to be established. Receptor subunits which resemble the vertebrate neuronal  $\alpha$  subunits have been cloned from *Drosophila* (Bossy *et al*, 1988; Jonas *et al*, 1990) and *Schistocerca* (Marshall *et al*, 1990), in addition to a non- $\alpha$  subunit from *Drosophila* (Hermans-Borgmeyer *et al*, 1986; Sawruk *et al*, 1990). There is evidence for the existence of both functional homo-oligomeric receptors (Breer *et al*, 1985; Hanke and Breer, 1986, Amar *et al*, 1995) and hetero-oligomeric receptors (Hermans-Borgmeyer *et al*, 1986; Schloss *et al*, 1991). Few pharmacological studies using reconstituted nicotinic receptors have been reported. However, it has been found that  $\alpha$ -BTX binds to the cloned *Schistocerca*  $\alpha$  subunit (Marshall *et al*, 1990) and one of the  $\alpha$  subunits cloned from *Drosophila* (Bertrand *et al*, 1994).

A *Drosophila* muscarinic receptor is the only invertebrate muscarinic receptor protein to have been cloned (Onai *et al*, 1989; Shapiro *et al*, 1989). This receptor showed approximately 60 - 70% homology with the 5 mammalian cloned muscarinic receptors and contained the conserved sequences common to G-protein coupled receptors. Furthermore, the receptor most resembled the m1 muscarinic receptor subtype (69% homology: Onai *et al*, 1989). One major difference between this receptor and the mammalian muscarinic receptor subtypes was observed. The *Drosophila* receptor protein was found to be considerably longer than its mammalian counterparts (Shapiro *et al*, 1989). However, combining expression and pharmacological studies it has been shown that the cloned

*Drosophila* muscarinic receptor stimulates phosphatidylinositol metabolism, and its pharmacology broadly resembles that of the vertebrate M<sub>1</sub>, M<sub>3</sub> and M<sub>5</sub> receptor subtypes (Shapiro *et al*, 1989; Blake *et al*, 1993).

Whereas the nicotinic receptor tends to be located on postsynaptic neuronal membranes (however, see Wonnacott, 1997) to mediate fast synaptic transmission, muscarinic receptors are found both pre- and postsynaptically, and have been found to have contrasting effects on neuronal function (for detailed review see Trimmer, 1995). Presynaptic muscarinic receptors on sensory neurones act as autoreceptors to inhibit neurotransmitter release, thereby reducing the effectiveness of the afferent input upon a postsynaptic neurone (for example, Leitch and Pitman, 1995). Activation of muscarinic receptors on the postsynaptic membrane, on the other hand, results in membrane depolarization and a decrease in the spike threshold of the cell to increase membrane excitability (Le Corrionc *et al*, 1991; Trimmer, 1994; Trimmer and Weeks, 1993). Consequently, this facilitates synaptic transmission and increases the probability of receptor-mediated depolarization (such as that evoked by the activation of the nicotinic receptor) evoking action potentials. Postsynaptic muscarinic receptors have been associated with the generation of rhythmic motor activity; muscarinic agonists have been shown to drive bursts of activity in the pharyngeal muscles of *Drosophila* (Gorczyca *et al*, 1991) and rhythmic depolarizations in neurones of *Manduca sexta* (Trimmer and Weeks, 1989) and locust (Ryckebusch and Laurent, 1993).

The pharmacological profiles of insect muscarinic receptors depend upon whether they are found on the pre- or postsynaptic neuronal membranes. Muscarinic receptors of synaptosome preparations or those on presynaptic membranes most closely resemble the vertebrate M<sub>2</sub> receptor subtype. These receptors are sensitive to the vertebrate M<sub>2</sub> receptor antagonist, methoctramine and generally are insensitive to the M<sub>1</sub> receptor antagonist, pirenzepine. Such

receptors have been identified on locust synaptosomes (Breer and Knipper, 1984; Knipper and Breer, 1989), and at the cercal nerve - giant interneurone synapse of the cockroach (Hue *et al*, 1989; Le Corrionc *et al*, 1991), the forewing hinge stretch receptor - first basalar (BA1) motoneurone of the locust (Leitch *et al*, 1993; Leitch and Pitman, 1995). In contrast, muscarinic receptors of postsynaptic neuronal membranes do not conform to the vertebrate classification system, that is, although they show pirenzepine sensitivity, they tend to have a broad pharmacological profile. For example, the BA1 motoneurone of the locust (Anderson, 1995), and the giant interneurone (Le Corrionc and Hue, 1993) and the D<sub>f</sub> motoneurone of the cockroach (David and Pitman, 1993a).

#### 1.2.1.5. 'Mixed' cholinergic receptors

In addition to the nicotinic and muscarinic acetylcholine receptors described above, there is evidence for a third acetylcholine receptor subtype, that is, the 'mixed', nicotinic-muscarinic acetylcholine receptor. Biochemical studies have exposed a cholinergic receptor that binds both nicotinic and muscarinic ligands in tissue of various animal species, including insects, namely, the electroplax of *Electrophorus* (Eldefrawi *et al*, 1971), bovine chromaffin cells (Shirvan *et al*, 1991), housefly (*Musca*) neurones (Aziz and Eldefrawi, 1973; Harris *et al*, 1981) and cultured cockroach (*Periplaneta*) neurones (Lees *et al*, 1983). Furthermore, pharmacological studies have shown the existence of such functional nicotinic-muscarinic receptors in dissociated locust neurones (Benson and Neumann, 1987; Benson, 1992), and the skin of *Rana catesbiana* (Cox, 1993). However, until the molecular biology of this proposed cholinergic receptor is examined, it could be suggested that the receptor actually corresponds to a muscarinic receptor which lacks a high degree of specificity in its ligand binding.

## 1.2.2. $\gamma$ -Aminobutyric acid (GABA)

### 1.2.2.1. Introduction

$\gamma$ -Aminobutyric acid (GABA) is the major inhibitory neurotransmitter in vertebrates (Mody *et al*, 1994) and invertebrates (Pitman, 1971). This neutral amino acid is formed from the decarboxylation of glutamic acid by glutamate decarboxylase and when released from GABAergic neurones it mediates its effects by binding to specific integral membrane proteins which constitute the GABA receptor family.

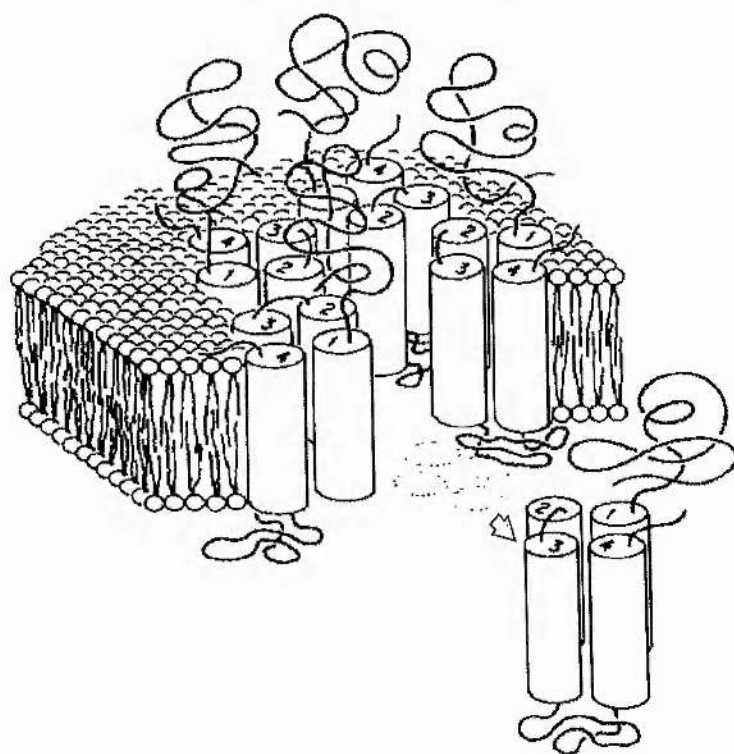
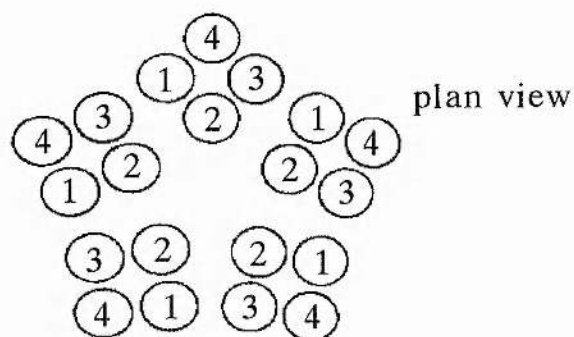
### 1.2.2.2. Vertebrate GABA receptors

In vertebrates, GABA has been found to act at at least three pharmacologically and structurally distinct subclasses of receptor, these being the GABA<sub>A</sub>, GABA<sub>B</sub> and GABA<sub>C</sub> receptor subtypes. Detailed reviews of these GABA receptors have recently been published; GABA<sub>A</sub>: MacDonald and Olsen (1994) and Stephenson (1995); GABA<sub>B</sub>: Bowery (1993) and GABA<sub>C</sub>: Bormann and Feigenspan (1995) and Djamgoz, (1995).

#### *GABA<sub>A</sub> receptors*

The abundant nature of GABA<sub>A</sub> receptors in the mammalian nervous system, particularly the brain (see McKernan and Whiting, 1996), has resulted in the elucidation of many of the biochemical properties of this GABA receptor subtype. As a member of the superfamily of ligand-gated ion channels, the GABA<sub>A</sub> receptor complex is a pentameric structure consisting of five polypeptide subunits ( $\alpha_{1-6}$ ,  $\beta_{1-4}$ ,  $\gamma_{1-3}$ ,  $\delta$ ) which are believed to form a hetero-oligomeric (approximately 275kDa) glycoprotein chloride channel (see Figure 1.2.3). It is understood that these subunits have putative N-glycosylation sites, four  $\alpha$ -helical hydrophobic membrane-spanning regions, and a cytoplasmic region of highly

Figure 1.2.3. Model of the GABA<sub>A</sub> receptor-chloride channel protein complex. The ligand-gated ion channel is proposed to be a hetero-oligomer composed of five subunits. Each subunit has four membrane-spanning domains (cylinder numbered 1-4), one or more of which contribute to the wall of the ion channel. The structure is patterned after the well-characterized nicotinic acetylcholine receptor, another member of the same gene superfamily. The naturally occurring oligomers are composed of some of the  $\alpha$ ,  $\beta$ ,  $\gamma$  and  $\delta$  polypeptides, but the exact subunit composition, stoichiometry and number of subunits are not known at this time (adapted from Olsen and Tobin, 1990).



variable sequence between the third and fourth membrane-spanning regions. It is this cytoplasmic loop that is involved in regulatory mechanisms such as phosphorylation (Bormann *et al*, 1987; Schofield *et al*, 1987). A number of different GABA<sub>A</sub> receptor isoforms exist, owing to the different combinations available of the polypeptide subunits; for example, in the rat brain 12 different subtypes have been identified using techniques such as *in situ* hybridization, radioligand binding and immunoprecipitation (see McKernan and Whiting, 1996).

In addition to the activation of the GABA<sub>A</sub> receptor by GABA, it is activated by the agonists muscimol (from the hallucinogenic mushroom *Amanita muscaria*), isoguvacine, and 3-aminopropyl sulphonic acid (3-APS), and THIP (4,5,6,7-tetrahydroisoxazolo[5,4-c]pyridin-3-ol) (see Rauh *et al*, 1990; Barker and Mathers, 1981). This receptor has a number of binding sites on its structure for compounds some of which are of great therapeutic importance, such as bicuculline, benzodiazepines, barbiturates and neurosteroids. These agents act to modify the agonist-evoked chloride current, the main (95%) conductance being of 27-30 pS (MacDonald *et al*, 1989a).

Bicuculline, a plant-derived convulsant, is used as a GABA<sub>A</sub> antagonist in pharmacological studies. It blocks GABA<sub>A</sub> responses by decreasing channel open frequency and mean open duration (MacDonald *et al*, 1989a). Picrotoxin is another plant-derived convulsant used as a GABA<sub>A</sub> antagonist. The active component, picrotoxinin, acts to reduce average channel open duration and burst duration (Twyman *et al*, 1989). On the other hand, barbiturates (which include those with sedative-hypnotic, anaesthetic and anticonvulsant properties) enhance the GABA response by mimicking GABA and increasing the receptor affinity for GABA. Findings suggest that the evoked current is increased because these compounds act on GABA<sub>A</sub> channels to favour the opening of long-lasting open states (MacDonald *et al*, 1989b). Neurosteroids also enhance the GABA response



by increasing the channel open and burst durations. However, it is thought that they act by increasing channel opening frequency and increase the probability of longer channel opening (Twyman and MacDonald, 1992). Benzodiazepines (used for antianxiety, muscle relaxation and hypnotic activity) enhance GABA<sub>A</sub> currents by increasing channel opening frequency (Study and Barker, 1981). How this is achieved is not clear at present.

### *GABA<sub>B</sub> receptors*

The concept of a second GABA receptor subtype arose from work of Bowery and his co-workers. They proposed to designate the classical GABA binding site as the GABA<sub>A</sub> receptor, whilst a novel GABA binding site, which was baclofen-sensitive and bicuculline-insensitive, was the GABA<sub>B</sub> receptor (Hill and Bowery, 1981).

The GABA<sub>B</sub> receptor, like the muscarinic acetylcholine receptor and the dopamine receptor, is a metabotropic receptor. Whereas there is information about the structure of the muscarinic receptor (for review see Wess, 1993) and dopamine receptor (for review see Sibley and Monsma, 1992), such literature is not available for the GABA<sub>B</sub> receptor. However, it would not be unreasonable to assume that the sequence of the GABA<sub>B</sub> receptor will have greater homology with these G-protein linked receptors than with the pentameric structure of the GABA<sub>A</sub> receptor.

Activation of GABA<sub>B</sub> receptors results in a decrease in voltage-dependent Ca<sup>2+</sup> conductance and/or an increase in K<sup>+</sup> conductance. The consequences of this modulation upon a neurone depend on whether the receptors are located pre- or postsynaptically. At presynaptic sites GABA<sub>B</sub> receptors act directly on ion channels and neurotransmitter secretory machinery (Wall and Dale, 1993) to decrease neurotransmitter release. However, at postsynaptic sites they appear to

enhance the GABA response, via phospholipase A<sub>2</sub> and arachidonic acid. As the cellular effects of these receptors also appear to differ between different neuronal cell types, it has been difficult to fully elucidate the mechanisms of action of GABA at the GABA<sub>B</sub> receptor (for review see Gage, 1992).

The GABA<sub>B</sub> receptor is clearly distinguishable from the GABA<sub>A</sub> receptor subtype on the basis of its pharmacological profile. Whilst GABA also activates this receptor, the GABA<sub>A</sub> agonists (such as muscimol and isoguvacine), antagonists (bicuculline and picrotoxin) and GABA<sub>A</sub> modulatory substances are not active at the GABA<sub>B</sub> site. Instead, (-)baclofen ( $\beta$ -p-chlorophenyl-GABA), which is used as a major treatment for spasticity, and its phosphonic analogues, 3-APA (3-aminopropylphosphonic acid) and 3-APPA (3-aminopropylphosphonous acid) are used as GABA<sub>B</sub> agonists. Antagonists used to block the vertebrate GABA<sub>B</sub> response include phaclofen, saclofen and CGP35348 ([p-(3-aminopropyl)-P-diethoxymethylphosphonic acid]).

#### *GABA<sub>C</sub> receptors*

Relatively recently a third subtype of GABA receptor, the GABA<sub>C</sub> receptor, was proposed based on its electrophysiological and pharmacological properties (Drew *et al*, 1984). Such receptors have only recently been localized *in situ* to subpopulations of rat and fish retinal neurones (Feigenspan *et al*, 1993; Qian and Dowling, 1993; Djamgoz, 1995).

The GABA<sub>C</sub> receptor structure resembles that of the GABA<sub>A</sub> receptor subtype, although it is thought to be composed only of the newly discovered polypeptide  $\rho$  subunits, which are not associated with the GABA<sub>A</sub> receptor subtype (Enz *et al*, 1995; Shimada *et al*, 1992). This receptor subtype is a homopentameric ionotropic complex that also gates a chloride channel. As observed with the GABA<sub>A</sub> receptor, there is a cytoplasmic loop between the third

and fourth intramembrane subunits, which has consensus sequences for protein kinase C. Consequently, the receptor function is open to modulation by phosphorylation (Cutting *et al*, 1991; Feigenspan and Bormann, 1994). From single-channel recordings, a conductance value of 7pS has been determined for this receptor subtype, which is approximately 4 times smaller than that of the GABA<sub>A</sub> receptor. In addition, the mean channel open time (150ms) is approximately five times longer than that of the GABA<sub>A</sub> receptor (Feigenspan *et al*, 1993).

Since these GABA receptors are primarily identified on the basis of their pharmacological profile, as expected this differs markedly from GABA<sub>A</sub> and GABA<sub>B</sub> receptor subtypes. GABA<sub>C</sub> receptors are insensitive to bicuculline, baclofen, benzodiazepines, barbiturates and neurosteroids. Like GABA<sub>A</sub> receptors they are activated by GABA and muscimol, but they are preferentially activated by CACA (*cis*-4-aminocrotonic acid), and the *cis*- and *trans*- enantiomers of 2-aminomethyl-cyclopropane carboxylic acid (CAMP and TAMP) which are without effect at the GABA<sub>A</sub> receptor. GABA<sub>C</sub> receptors are antagonized by picrotoxin and picrotoxinin, the active component of picrotoxin (Feigenspan *et al*, 1993, Kusama *et al*, 1993; Qian and Dowling, 1994).

#### 1.2.2.3. Insect GABA receptors

Using electrophysiological recording techniques it has been demonstrated that insect neurones are sensitive to the application of GABA, and the response is mediated by a chloride current (Kerkut *et al*, 1969a, b; Pitman and Kerkut, 1970; Usherwood *et al*, 1980). It is known that the pharmacological profile of these GABA receptors notably differs from any single class of vertebrate GABA receptor. The receptors share many of the properties of the vertebrate GABA<sub>A</sub>

receptor subtype. However, like the vertebrate GABA<sub>C</sub> receptors, the majority of them appear to be bicuculline-insensitive (Lees *et al*, 1987; Lummis *et al*, 1987).

One feature insect GABA receptors have in common with both these vertebrate GABA receptor subtypes is their insensitivity to baclofen, the vertebrate GABA<sub>B</sub> receptor agonist. Closer examination of the pharmacological profile of the insect receptors shows that the insect GABA receptor has properties similar to both the vertebrate GABA<sub>A</sub> and GABA<sub>C</sub> receptor subtypes (Aydar *et al*. 1995; see Table 1.2.1). However, using a cloned homo-oligomeric *Drosophila* GABA receptor, it has been recently been shown that the amino acid sequence of this receptor demonstrates a higher overall sequence similarity to the vertebrate glycine receptor subunits (31-32% amino acid identity) than to the GABA<sub>A</sub> and GABA<sub>C</sub> subunits (27-29%) (ffrench-Constant and Rocheleau, 1992).

An exception to these chloride-gated insect GABA receptors has recently been described by Bai and Sattelle (1995). They reported the presence of a GABA<sub>B</sub>-like receptor on an identified (D<sub>1</sub>) cockroach motoneurone. Whilst the neurone responded to the vertebrate GABA<sub>B</sub> receptor agonists 3-APA and 3-APPA and was insensitive to picrotoxin, it did not respond to baclofen. In addition, the vertebrate GABA<sub>B</sub> receptor antagonists saclofen and CGP35348 had no effect. Further work is necessary to clarify the presence of this GABA receptor subtype on insect neurones.

### 1.2.3. Dopamine (3-hydroxytyramine; DA)

#### 1.2.3.1. Introduction

Dopamine is a member of the class of catecholamine neurotransmitters, which also includes adrenaline and noradrenaline. It is formed from the hydroxylation and decarboxylation of the aromatic amino acid tyrosine, as part of the metabolic pathway for the synthesis of noradrenaline and adrenaline. The

Table 1.2.1. The pharmacological profiles of vertebrate and insect ionotropic GABA receptors (adapted from Rauh *et al*, 1990).

<sup>1</sup>: Millar *et al*, 1995.

<sup>2</sup>: Rauh *et al*, 1990.

<sup>3</sup>: (CACA) Aydar *et al*, 1995.

\*: Cloned receptor (Rdl) used in this study is resistant to the cyclodiene, dieldrin.

+/- indicates the degree of activity; +++: high, ++: moderate, +, weak, --- inactive

(blank, not tested)

GABA:  $\gamma$ -aminobutyric acid; CACA: *cis*-4-aminocrotonic acid; TACA: *trans*-4-aminocrotonic acid; TBPS: *t*-butylbicyclophosphorothionate.

Ligand	Vertebrate (GABA <sub>A</sub> )	Vertebrate (GABA <sub>C</sub> )	Insect <sup>2</sup>	Cloned <i>Drosophila</i> mutant <i>Rdl</i> receptor <sup>1</sup>
<b>Agonists</b>				
GABA	+++	+++	+++	+++
muscimol	+++	++	+++	+++
3-APS	+++	---	+	
TACA/CACA	++/+	++/++++	+++ <sup>3</sup>	+++/++
baclofen	---	---	---	---
<b>Antagonists</b>				
bicuculline	+++	---	---	---
<b>Benzodiazepines</b>				
Ro5-4864	---	---	+++	---
clonazepam	+++	---	+	
<b>Steroids</b>				
pregnane steroids	+++	---	+	+++
RU5135	+++	---	+	
<b>Barbiturates</b>				
pentobarbital	+++	---	++	+/-
<b>Convulsants</b>				
TBPS	+++	+++	+	+
			+++ <sup>3</sup>	
cyclodienes	+++		++	*
picrotoxin(in)	+++	+++	+++ <sup>3</sup>	+++

effects of dopamine are mediated by its binding to specific GTP-protein coupled integral membrane proteins, that make up the dopamine receptor family.

#### 1.2.3.2. Vertebrate dopamine receptors

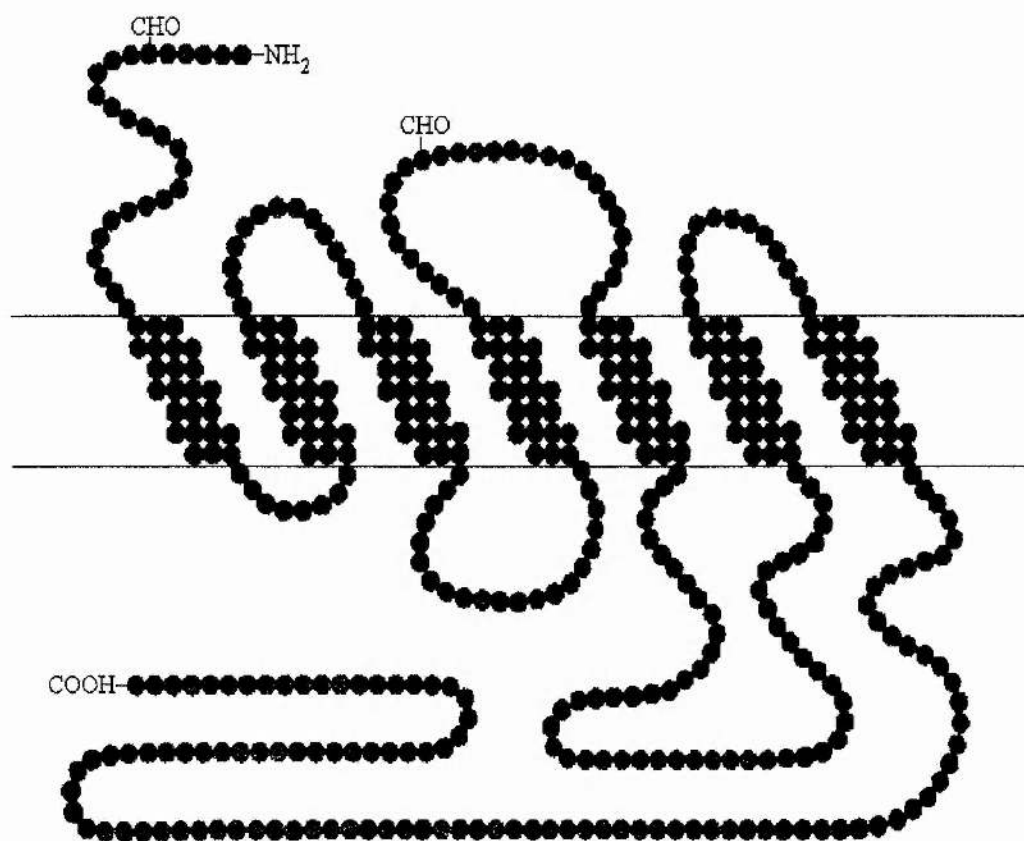
Until recently, dopamine receptors were classified into two distinct groups. The criteria used to distinguish between the two subtypes was based on whether they activate adenylyl cyclase and increase intracellular levels of cAMP ( $D_1$ ) or exert an inhibitory influence on this enzyme ( $D_2$ ) (for review see Keabadian and Calne, 1979). With the development of molecular biological methods, in particular recombinant DNA techniques, five different pharmacologically distinct vertebrate dopamine receptors have now been cloned and identified. The  $D_1$ -like receptors now include the  $D_1$  and  $D_5$  receptors, whilst the  $D_2$ -like receptors include the  $D_2$ ,  $D_3$  and  $D_4$  subtypes (for reviews see Sibley and Monsma, 1992; Seeman and Van Tol, 1994). The main feature of these receptor proteins that distinguishes them from the ligand-gated ion channels is that they consist solely of seven transmembrane domains with an extracellular amino (N) terminus and an intracellular carboxy (C) terminus.

#### $D_1$ receptor subfamily

The proposed membrane topography of the human  $D_1/D_5$  dopamine receptor is shown in Figure 1.2.4. The  $D_1$ -like receptor is believed to have a smaller 3rd cytoplasmic loop and a longer C-terminus than the  $D_2$ -like receptor. The latter feature is apparently a characteristic of receptors that are coupled to  $G_s$  and activate adenylyl cyclase. There are two extracellular consensus glycosylation sites, one consensus site for cAMP-dependent phosphorylation in the third cytoplasmic loop and a number of potential phosphorylation sites in the C-terminus associated with this protein. Aside from changes in the primary structure

Figure 1.2.4. Proposed membrane topography of the human D<sub>1</sub> dopamine receptor. CHO, potential N-linked glycosylation sites (adapted from Sibley and Monsma, 1992).





of the receptor protein, the main difference between D<sub>1</sub> and D<sub>5</sub> receptor subtypes is that dopamine is approximately 10 times more potent at D<sub>5</sub> than at D<sub>1</sub>. An outline of the pharmacological profile of the D<sub>1</sub>-like and D<sub>2</sub>-like receptor subtypes is shown in Table 1.2.2.

### D<sub>2</sub> receptor subfamily

#### *D<sub>2</sub> receptor*

Noted features of the D<sub>2</sub> receptor protein that differ from the D<sub>1</sub>-like subtype include (1) the existence of three consensus sequences for potential glycosylation sites on the N-terminus, (2) the relatively small C-terminus and (3) the large cytoplasmic loop between the membrane-spanning regions 5 and 6 which contains a potential site for phosphorylation by PKA. The latter two features are characteristic of most receptors whose activation inhibits adenylyl cyclase activity (see Dohlman *et al*, 1991). The use of cloned D<sub>2</sub> receptors in mammalian cell lines has demonstrated that the activation of this dopamine receptor subtype can also evoke changes in a number of different intracellular messenger systems. These include the stimulation of PI hydrolysis and Ca<sup>2+</sup> mobilization (Vallar *et al*, 1990), the reduction of intracellular Ca<sup>2+</sup> and membrane hyperpolarization (Albert *et al*, 1990) and potentiation of cAMP-independent ATP-mediated arachidonic acid release (Felder *et al*, 1991).

#### *D<sub>3</sub> receptors*

Whilst the D<sub>3</sub> receptor subtype closely resembles the D<sub>2</sub> receptor, its topology does differ slightly - one of the glycosylation sites is on the first extracellular loop rather than on the N-terminus. The pharmacological profile of a cloned D<sub>3</sub> receptor revealed that dopamine was about 20 times more selective for D<sub>3</sub> receptors than for D<sub>2</sub> receptors (see Sibley and Monsma, 1992).

### *D<sub>4</sub> receptors*

The D<sub>4</sub> receptor is the most recent dopamine receptor subtype to be identified and cloned (Van Tol *et al.*, 1991). There are two main differences between the D<sub>4</sub> receptor and the other two D<sub>2</sub>-like receptor subtypes. First, there is only one glycosylation site on the N-terminus and second, whilst it displays similar pharmacological properties to the D<sub>2</sub> and D<sub>3</sub> receptors, the antagonist clozapine (an antipsychotic) exhibits a 10-fold higher affinity for the D<sub>4</sub> receptor subtype.

### 1.2.3.3. Dopamine as a neuromodulator

As a modulator of ion channel activity, dopamine is of great importance in vertebrate nervous system functioning. This is illustrated using the following examples. (1) Dopamine modulates Ca<sup>2+</sup> conductance of voltage-dependent Ca<sup>2+</sup> channels in turtle retinal ganglion cells via a D<sub>1</sub> dopamine receptor cAMP-PKA pathway. This results in alterations in the signalling properties of these neurones (Liu and Lasater, 1994). (2) Dopamine, whilst not having a direct effect on Ca<sup>2+</sup> entry, via a cAMP-dependent mechanism, down-modulates GABA<sub>C</sub> receptor sensitivity of bipolar cells. Consequently, there is an increase in neurotransmitter release from these neurones and an enhancement of postsynaptic activity in amacrine and ganglion cells (Wellis and Werblin, 1995). (3) D<sub>1</sub> stimulation in rat prefrontal cortex neurones results in the enhancement of Na<sup>+</sup> current duration and the attenuation of a K<sup>+</sup> and a Ca<sup>2+</sup> current, which results in a decrease in first spike latency and a reduction in spike threshold in these neurones. Therefore, dopamine is seen to have an important role in signal processing (Yang and Seamans, 1996).

#### 1.2.3.4. Insect dopamine receptors

As seen other invertebrate species (*Lymnaea* respiratory CPG: Barnes *et al*, 1994; lobster stomatogastric ganglion pyloric CPG: Harris-Warrick *et al*, 1995a, b), dopamine appears to play a primarily neuromodulatory role in insects. This biogenic amine, along with serotonin and octopamine which are also biogenic amines, has been shown to modify central (Claassen and Kammer, 1986; Goldstein and Camhi, 1991) and peripheral neural activity (for review see Evans, 1980).

Biochemical and histochemical studies have revealed dopamine is widespread in the insect central nervous system (see Pitman, 1985). In comparison to the extensive literature on dopamine receptors in the vertebrate central nervous system, relatively little is known about such receptors that mediate the effects of dopamine in the insect nervous system. Pharmacological studies have demonstrated that dopamine can have excitatory and inhibitory actions on insect neurones *in situ* (Kerkut *et al*, 1969a, Steiner and Pieri, 1969; Pitman and Davis, 1988; J. C. McLelland unpublished observations), however, the ionic basis of the observed responses to dopamine is not clear (Pitman and Davis, 1988). Experimental data suggests that the pharmacological profile of the insect dopamine receptor(s) differs from the vertebrate D<sub>1</sub> and D<sub>2</sub> receptor subtypes (see Table 1.2.2: Davis and Pitman, 1991; Kokay and Mercer, 1996). Reports of cAMP involvement in the actions of insect dopamine receptors varies (Uzzan and Dudai, 1982; Pitman and Baker, 1989) and details of the identity of the dopamine receptor(s) are limited. A receptor with significant functional homology to the human D<sub>1</sub>/D<sub>5</sub> receptor but with a genomic organization resembling the D<sub>2</sub> receptor gene, has recently been identified in *Drosophila* (Gotzes *et al*, 1994).

Table 1.2.2. The pharmacological profile of the dopamine receptor present on an identified insect motoneurone (adapted from Davis and Pitman, 1991).

<sup>1</sup>: Data from Davis and Pitman, 1991.

<sup>2</sup>: ADTN: hydrobromide[(±)-2-amino-6,7-dihydroxy-1,2,3,4-tetrahydronaphthalene hydrobromide

	Vertebrate target	Insect motoneurone <sup>1</sup> (D <sub>3</sub> : <i>Periplaneta americana</i> )
<b>Agonists</b>		
dopamine	D <sub>1</sub> /D <sub>2</sub>	potent
SK&F 82526	D <sub>1</sub>	inactive
ergometrine	D <sub>2</sub>	potent
apomorphine	D <sub>2</sub>	potent
bromocryptine	D <sub>2</sub>	potent
ADTN <sup>2</sup>	D <sub>2</sub>	potent
LY 171555	D <sub>2</sub>	inactive
<b>Antagonists</b>		
(+)-butaclamol	D <sub>1</sub> /D <sub>2</sub>	potent
fluphenazine	D <sub>1</sub> /D <sub>2</sub>	potent
flupenthixol	D <sub>1</sub> /D <sub>2</sub>	potent
SCH 23390	D <sub>1</sub>	potent
haloperidol	D <sub>2</sub>	potent
spiroperidol	D <sub>2</sub>	potent
YM 09151-2	D <sub>2</sub>	potent
metoclopramide	D <sub>2</sub>	inactive

### 1.3. Confocal Laser Scanning Microscopy (CLSM)

#### 1.3.1. Introduction

In the current study confocal laser scanning microscopy (CLSM) was used to visualize agonist-evoked changes in intracellular calcium ( $\text{Ca}^{2+}$ ) concentrations in isolated living neurone somata. With this type of microscopy a laser is used (in this case an argon/krypton laser) as a high intensity illumination source which enables the use of fluorescent probes (fluorochromes) as tools for highly sensitive and selective examination of components of cell structure and metabolism. The laser is used to excite an appropriate fluorescent probe (that is, the excitation and emission maxima of the probe complement the laser output), so that, on binding to its substrate molecule(s), it produces a fluorescence emission (see Section 3.1.2.). There are many fluorescent probes available for the study of a diverse range of physiological and other cellular features, ranging from the dynamic properties of cells, such as cytosolic ion concentrations and membrane potentials (such probes are based on specific chelators), to relatively static components such as specific membrane or cytosolic proteins and lipids (for this the fluorescent markers are conjugated specific antibody probes).

#### 1.3.1.2. The principle of CLSM

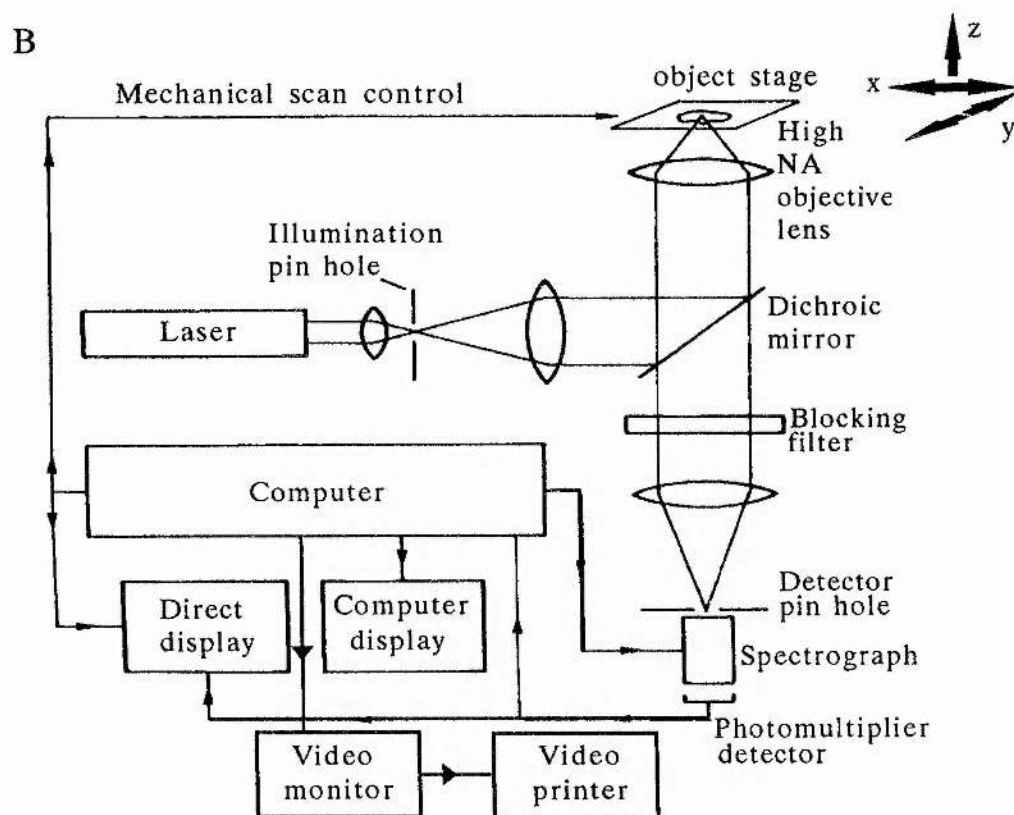
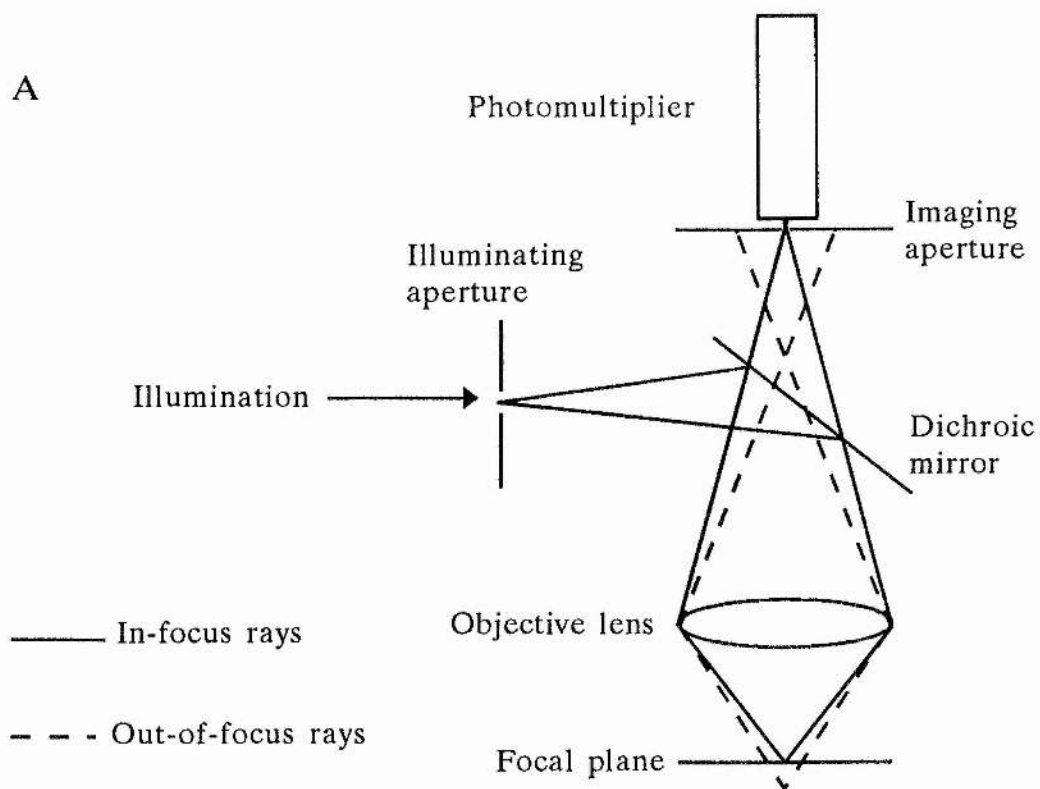
The basic principle of confocal microscopy is that one point in the object is optimally illuminated by a point light source as well as imaged on a point detector (photomultiplier). Owing to the high intensity of laser light sources generally used with CLSM, the illumination pinhole can be made sufficiently small that, in fact, it functions as a point light source (see Figure 1.3.1A; see Brakenhoff *et al*, 1989). The combined effect of the point source illumination and the effect of the detection pinhole is that only the in-focus fluorescence emissions generated in the specimen layer being imaged will reach the photomultiplier; the

Figure 1.3.1. The principles of confocal laser scanning microscopy.

A. The confocal principle in fluorescence scanning microscopy. Laser light required for the excitation of the fluorescent probe passes from the illuminating aperture through an excitation filter (not shown), to be reflected by the dichroic mirror and focussed by the microscope objective to a diffraction limited spot at the focal plane within the specimen. Fluorescence emissions, excited both within the illuminated in-focus planes and within the illuminated cones above and below it, are collected by the objective lens to pass through the dichroic mirror and the emission filter (not shown). Only the emissions from the in-focus plane pass unimpeded through the imaging aperture to be detected by the photomultiplier. The emissions from above and below the in-focus plane are attenuated by the imaging aperture, and thus, effectively do not contribute to the final confocal image.

B. Schematic diagram of the confocal scanning fluorescence microscope. Light originating from the laser-illuminated pinhole is focussed on a certain point in the object (NA refers to the numerical aperture of the lens). The same point is subsequently imaged on the detector pinhole. The term 'confocal' relates to the fact that the image of the illumination pinhole and the back-projection of the detection pinhole have a common focus in the object. The specimen is scanned mechanically (in the x, y, and z planes) through this confocal point. A direct image is displayed on a cathode-ray tube, and at the same time, the image data are digitized and stored in the computer system. The spectrograph enables one to select a certain band from the fluorescence radiation for image formation. The bandwidth as well as the wavelength selection of the spectrograph can be set by the computer (adapted from Brakenhoff *et al*, 1989).





out-of-focus areas are eliminated. Each image obtained using CLSM is a representation of the points of in-focus emissions detected by the photomultiplier. These are easily stored in a digitized form, making subsequent computerized image processing possible (see Figure 1.3.1B).

Since (i) out-of-focus fluorescence emissions are eliminated in the construction of images and (ii) lasers are used as high intensity illumination sources in CLSM, the resolution obtained, whilst not as great as gained using electron microscopy (EM), is greater than that of conventional epifluorescence microscopy. With conventional microscopy all the fluorescence radiation generated over the depth of the specimen reaches the image plane. The in-focus layer is imaged sharply, whilst the out-of-focus layers introduce blurring, and thus, a reduction in image resolution. Other advantages of CLSM are that (i), unlike electron microscopy, live tissue can be visualized without fixation, dehydration and embedding processes, (ii) the temporal and spatial development of living tissue can be rapidly and accurately observed by utilizing the on-line 'time-series' and 'z-series' (serial, spatial sectioning) applications. In addition, there are stereoscopic imaging and dual-channel imaging facilities; the latter allows substances labelled with fluorochromes having different excitation maxima to be simultaneously visualized (see Section 3.2.2.). (iii) images are acquired much more quickly with CLSM compared to EM, and can be rapidly processed using off-line processing software packages. In the current study, images were constructed by moving the confocal spot with respect to the specimen. Images were then stored onto optical disc as graded tones of white and black pixels. The software package CoMOS was used for data processing; facilities used included magnification of defined areas, local contrast manipulation and visualization in pseudocolour.

#### 1.4. Neuronal tissue culture

##### 1.4.1. Use of neuronal tissue culture

The advancement of neural tissue culture studies has enabled the study of elements of neurotransmission and neuronal growth and plasticity from isolated neurone preparations. Dissociated neurones can be maintained in both short-term (i.e. up to three weeks) and long-term (i.e. three to six months) culture. As a result, many neurophysiological and pharmacological problems are being understood. The advantages and disadvantages of using dissociated neurones are:

##### *Advantages*

1. These *in vitro* preparations allow the maximum visualization of the cellular morphology of the neurones.

2. They permit direct access to the neurones, their processes and their synaptic connections so that experiments can be performed on them whilst they are under continual observation. Conventional single and two microelectrode electrophysiological techniques are used in addition to the various patch-clamping configurations.

3. Experiments can be carried out on cultured neurones in the absence of other neurones and other cell types, such as glial cells, which can affect experimental analysis and interpretation of results. The possibility of heterosynaptic modulation of synaptic connections can be eliminated using dissociated neuronal cultures. Isolated glial cells do not tend to survive the process of trituration - they are usually destroyed, owing to their flat, irregular morphology (Hicks and Beadle, 1980).

4. The population density of cultured neurones can be controlled by altering the neuronal tissue mass : volume of culture medium used, since, the density of the neurones is seen to influence the degree of neurite outgrowth.

5. Dissociated neurone cultures offer improved access for pharmacological agents. In the absence of connective tissue and glial cells around neurones, neuronal membrane accessibility is improved. Consequently, drug-receptor binding is aided, to reflect the true receptor sensitivities *in vivo*.

6. Such cultures offer the best opportunity for genetic manipulation, the use of 'knockout' strains and genetic analysis of neurobiological events.

### *Disadvantages*

1. It may be expected that the dramatic process of dissociation itself would have an effect on the neurones which may affect subsequent development and the pharmacological profiles. Therefore, the degree to which neurones *in vitro* and those *in vivo* can be related should be considered.

2. Comparing studies using whole ganglia/tissue explants and dissociated neurones, it is harder to relate back the behaviour of dissociated cultured neurones to that of neurones *in vivo*. This is because the environment of dissociated cultured neurones is so different from that of explant material and the intact animal. The extent to which the isolated neurones resemble those *in situ* and *in vivo* must be taken into account when analyzing experimental data.

### 1.4.2. Use of invertebrate neural tissue for tissue culture studies

A number of researchers have developed techniques for culturing neurones from undifferentiated embryonic neural tissue and fully differentiated adult nervous systems of invertebrates, and tissue from these animal species offer a number of advantages for electrophysiologists. Firstly, invertebrates have an accessible central nervous system in both the adult and embryonic stages of development. Secondly, compared with vertebrate systems, the invertebrate nervous system is relatively simple in its anatomical organization. In addition, the

cell body diameter of invertebrate neurones tends to be larger than that of vertebrates which improves the ease of microelectrode penetration and maintenance of stable electrophysiological recordings along with easier recognition of identified neurones. Thirdly, the neurones appear to have the ability to survive experimental procedures well. It has been found that experimental data obtained from insect neurones *in vitro* is qualitatively similar to that obtained from neurones *in situ* and *in vivo*, and the neurones demonstrate plasticity in their regeneration.

Neuronal tissue from species of the phyla Mollusca and Annelida (notably the sea hare *Aplysia*, the snail *Helisoma*, and the medicinal leech, *Hirudo*) have been extensively studied using *in vitro* techniques to investigate synaptogenesis and neurotransmission in the period following cell contact (see below). In comparison, the success of studies of insect neurones in culture has trailed behind that of molluscs and annelids. Evidence supporting the formation of neurone-neurone synaptic connections between insect neurones *in vitro* is lacking. Consequently, the progress of studies regarding the growth and development of isolated insect neurones *in vitro* has been limited.

### *Aplysia*

Studies using isolated *Aplysia* neurones have demonstrated that these cells extend neuritic outgrowth, exhibit synaptic and action potentials, are sensitive to neurotransmitters (Strumwasser *et al*, 1978) and form specific and novel electrical and chemical connections *in vitro* (Kaczmarek *et al*, 1979; Bodmer *et al*, 1984; Schacher *et al*, 1985). Consequently, isolated *Aplysia* neurones *in vitro* have been used to examine a number of phenomena, including the factors controlling neurite extension and synaptogenesis, and the mechanisms involved in synaptic plasticity (for review see Schacher, 1988)

It is well understood that choice of growth medium is critical for the growth and development of neurones in culture, and it has been shown that use of growth medium supplemented with *Aplysia* haemolymph influences the nature and morphology of neuritic outgrowth from *Aplysia* neurones (Schacher and Proshansky, 1983). Another parameter known to be of great importance is the choice of substrate material for neurite growth. In addition to modifying the patterns of neuronal outgrowth, some are known to alter the synaptic specificity of neurones, for example concanavalin A (Lin and Levitan, 1987). The morphology of the freshly isolated neurone also influences neuritic outgrowth; in the presence of an initial axonal stump, the time for the initiation of neuritic outgrowth of a neurone is reduced and the pattern of extension is restricted to monopolar processes, rather than multipolar processes (Schacher and Proshansky, 1983; see Section 4.3.).

Regarding the mechanisms of synaptic plasticity, since isolated sensory and motoneurones are readily maintained and form chemical connections in culture, they have been used as *in vitro* models to study the cellular mechanisms of short- and long-term facilitation associated with the defensive-withdrawal mechanisms in *Aplysia*. For example, (i) the contributions of PKA and PKC to the actions of 5-HT on a  $\text{Ca}^{2+}$  current of sensory neurones have been examined (Braham *et al*, 1993) and (ii) the 5-HT induction of long-term facilitation was shown to be dependent on protein or RNA synthesis using sensorimotor connections in culture (Montarolo *et al*, 1986).

### *Helisoma*

The initial studies using isolated *Helisoma* neurones were dominated by Kater and his co-workers; they established a technique for the culturing of isolated *Helisoma* neurones (Wong *et al*, 1981). In determining that brain-derived

conditioning factors were a major requirement for neuritic growth of *Helisoma* neurones, their protocol allowed the mechanisms underlying neuronal growth and the formation of synaptic connections to be studied. The formation of both specific and novel electrical (Hadley *et al*, 1983, 1985) and chemical (Haydon, 1988; Haydon and Kater, 1988) connections between these isolated molluscan neurones in culture have been reported. Mutual neurite extension by neurones has been shown to be a prerequisite for the formation of electrical synapses (Hadley *et al*, 1983, 1985), but not for chemical synapses (Haydon, 1988). In addition, it has been noted that one can observe conjoint (i.e. both electrical and chemical) connections between neurones, however, the formation of chemical synapses does not depend on the previous formation of electrical connections (Haydon and Kater, 1988).

Using cultured *Helisoma* neurones, two main lines regarding the growth and development of these molluscan neurones have been investigated. First, the mechanisms by which various factors (in particular  $[Ca^{2+}]_i$ ) influence neurite growth and growth cone properties which potentially are involved in synaptogenesis, and second, the factors controlling the formation of specific neuronal connections have been studied. High  $[Ca^{2+}]_i$  inhibits neurite elongation and growth cone motility, and low  $[Ca^{2+}]_i$  results in the cessation of elongation and growth cone motility (Mattson and Kater, 1987). Factors that regulate the growth and development of neurites and growth cones include (i) neurotransmitters and (ii) electrical activity (Cohan and Kater, 1986). The neurotransmitters known to affect neurones in this way include serotonin (Haydon *et al*, 1984), dopamine (McCobb *et al*, 1985), glutamate (Bulloch and Hauser, 1990) and acetylcholine (McCobb and Kater 1986).

Most of this work has been performed on the B19-SLT (supralateral radular tensor) muscle fiber cholinergic synapse, which is the appropriate



postsynaptic target of B19 *in vivo*. Connectivity has been shown to be initially dependent on the contact of the growth cone with the target cell. Upon contact, further development is dependent on a yet-unidentified retrograde signal from the postsynaptic to the presynaptic neurone. This enhances presynaptic  $\text{Ca}^{2+}$  influx via the activation of cAMP-dependent protein kinase and enhances the responsiveness of the secretory machinery to internal  $\text{Ca}^{2+}$  levels, thereby imparting the presynaptic cell with the ability to couple action potentials with neurotransmitter release (Zoran *et al*, 1990, 1991; Funte and Haydon 1993; see Haydon and Drapeau, 1995).

### Annelids

Ready and Nicholls (1979) first described the growth and formation of selective electrical and chemical synaptic connections of dissociated identified leech neurones *in vitro*. Since then, cultured leech neurones have provided excellent *in vitro* models for the study of factors affecting neuronal growth patterns and signals underlying synapse formation and function (see Fernández-de-Miguel and Drapeau, 1995).

Of particular interest have been the various electrical connections made by the serotonergic Retzius neurone, and the chemical synapse made by the Retzius cell and the pressure sensitive (P cell) neurone (Fuchs *et al*, 1982; Henderson *et al*, 1983; Arechiga *et al*, 1986; Nicholls *et al*, 1990). Using the Retzius and P neurones as experimental models, it is now believed, at least for these cells, that cell surface contact mediates neuronal outgrowth, cellular ion channel populations (Masuda-Nakagawa and Nicholls, 1991) and cell recognition and synapse formation (Merz and Drapeau, 1994). In addition, it has been demonstrated that tyrosine phosphorylation is a signal for synapse formation (Catarsi and Drapeau, 1993; Catarsi *et al*, 1995).



### 1.5. Thesis in context

The main focus of the present study has been the examination of the pharmacological profile of the isolated first basalar motoneurone (BA1) soma, in order to gain an insight into the mechanisms by which the membrane activity of this neurone may be regulated. To place this work in context; the BA1 motoneurone is an integral component of the neuronal circuitry that controls the rhythmic motor output generated by a number of interneurons for locust flight. By innervating one of the principal wing depressor muscles, which controls the downstroke of the wingbeat, the BA1 motoneurone has a central role in the production of the wingbeat cycle. A brief description of the physiological basis for locust flight and its modulation is given below.

The locust has two pairs of wings; (i) the forewings, which are attached to the mesothoracic segment and (ii) the hindwings, which are attached to the metathoracic segment. Each wing has its own stretch receptor, located just inside the thorax, at the base of the wing (Gettrup, 1962). Whilst neuronal activity from the stretch receptors is not necessary for generating the basic flight motor pattern (Wilson, 1961), when stimulated by wing elevation, the stretch receptors are able to entrain and reset flight rhythm, co-ordinate the activities of both pairs of wings and modulate wing-beat frequency (Pearson *et al.*, 1983; Pearson and Ramirez, 1990). The stretch receptor neurones are able to do this as both pairs of forewing and hindwing stretch receptors branch extensively throughout the thoracic ganglia (Altman and Tyrer, 1977; Burrows, 1975), forming synapses with interneurons and motoneurons (Reye and Pearson, 1987; Burrows, 1975). Following stretch receptor stimulation, EPSPs are generated in the depressor motoneurons (including the BA1 motoneurone), and IPSPs in elevator motoneurons, which results in the switching of wing upstroke to wing downstroke (Burrows, 1975).

Since the activity of the stretch receptor is also known to be under octopaminergic modulation (Ramirez and Orchard, 1990), it is seen that sensory input from the stretch receptors is an important form of extrinsic modulation for the generation of the flight motor pattern.

The stretch receptor-BA1 synapse is known to be monosynaptic (Burrows, 1975) and cholinergic in nature (Leitch *et al*, 1993; Leitch and Pitman, 1995). Recent pharmacological studies by Pitman and his co-workers have examined the pharmacological profile of these synaptic cholinergic receptors *in situ*. It was revealed that both nicotinic and muscarinic acetylcholine receptors are present on the postsynaptic membrane (Leitch *et al*, 1993; Anderson, 1995), whilst only muscarinic receptors with a pharmacological profile broadly similar to that of the M<sub>2</sub>-subclass of vertebrate muscarinic receptors, are present on the presynaptic membrane (Leitch *et al*, 1993; Leitch and Pitman, 1995). It is believed that activation of nicotinic receptors is responsible for EPSP generation in the BA1 motoneurone, whilst the post-synaptic muscarinic receptors modulate synaptic transmission by decreasing spike threshold at the postsynaptic membrane (Anderson, 1995). Recent evidence has shown that the presynaptic muscarinic receptors act as autoreceptors to modulate ACh release from the nerve terminals of the stretch receptor neurone (Leitch *et al*, 1993; Leitch and Pitman, 1995), consequently the stretch receptor neurone may also act as an important intrinsic modulator of flight motor pattern.

In summary, the stretch receptor-BA1 sensorimotor synapse provides us with a model to study synaptic transmission and the mechanisms of its modulation. It may be anticipated that the findings of such a study can be directly related to the control of the flight cycle pattern, which is solely an adult form of behaviour in the locust.

Until recently, it was believed that insect motoneurons did not exhibit active electrical properties; that is, patterned motor output underlying rhythmic activity such as flight, resulted entirely from the synaptic connectivity of neural networks, and that intrinsic inherent membrane properties of individual neurons played little or no part in this process. It has been shown, however, that insect neurons can produce such activity under the influence of certain neuromodulatory agents such as octopamine (Rameriz and Pearson; 1991a, b) and muscarinic agonists (Trimmer and Weeks, 1989; Ryckebusch and Laurent, 1993; J. D. Mills, personal communication). Furthermore, it is thought that this modulation could have a significant role in shaping the motor output patterns which generate insect locomotion (for review see Pitman *et al*, 1993).

#### The aims of this study

1. To establish a pharmacological profile of the neurotransmitter receptors present on the isolated BA1 motoneurone soma, using conventional microelectrode recording techniques. Included in these studies will be an investigation of possible neurotransmitter interactions with GABA receptors on this motoneurone because these could alter the effectiveness of GABAergic synaptic inputs under different physiological conditions.
2. Examine the cellular mechanisms by which dopamine and the muscarinic M<sub>1</sub>-subtype agonist, McN-A-343, acting at somal receptors, could influence the membrane activity of BA1 motoneurons, using Ca<sup>2+</sup> fluorescence imaging techniques.

3. To establish a technique for the maintenance of isolated adult locust neurones, including the BA1 motoneurone, in culture. In addition to allowing the electrophysiological and pharmacological properties of the isolated neurones to be studied, it is intended that the protocol will allow BA1 motoneurones to be co-cultured with the presynaptic neurone, the forewing hinge stretch receptor, with which it may form synaptic connections. Consequently, it will be possible to study synaptic transmission and its modulation between these two identified neurones, in the absence of heterosynaptic input, and relate the findings to the flight pattern cycle of the intact animal. Of particular interest will be the mechanisms of muscarinic receptor-mediated acetylcholine release and their modulation.

## **Chapter 2**

### **A pharmacological profile of the freshly isolated first basalar motoneurone *in vitro***

## INTRODUCTION

It would appear, from the substantial amount of evidence obtained from pharmacological and ligand binding studies, that insect central neurones possess an array of neurotransmitter receptors on the somal membrane and on neuritic arborizations (for detailed review see Benson, 1993). The technique established by Usherwood and his co-workers which involved the mechanical dissociation of neural tissue, whilst maintaining the viability of the isolated neurones, has greatly facilitated pharmacological studies of insect somata *in vitro* (Usherwood *et al*, 1980). In particular, a pharmacological profile of isolated locust neurones has been established. Electrophysiological and pharmacological investigations are routinely performed from neurones isolated by this method, whether they are freshly isolated neurones or are being maintained *in vitro* using tissue culture protocols (see Chapter 4.1.). Electrophysiological techniques employed for these investigations include intracellular microelectrode recordings (both current- or voltage-clamp protocols), and the various configurations of the patch-clamping technique.

In the initial studies by Usherwood and his co-workers, it was demonstrated, using a single microelectrode recording technique, that isolated somata from the locust, *Schistocerca gregaria*, responded to the pressure-application of a number of neurotransmitters and putative neurotransmitters, including acetylcholine, GABA, serotonin, octopamine, glycine, taurine and cysteine. Furthermore, the response to acetylcholine was blocked by the cholinergic agonists atropine and d-tubocurarine (Usherwood *et al*, 1980; Suter and Usherwood, 1985; Suter, 1986). Subsequent studies, using modifications of the original isolation protocol described by Usherwood *et al* (1980), has enabled the detailed examination of the voltage and underlying ionic

basis of the responses to the various neurotransmitters and their analogues in detail, in particular, the excitatory neurotransmitter acetylcholine, the inhibitory neurotransmitter, GABA and proposed neuromodulator, serotonin of the locust (*Locusta migratoria*) (Benson and Neumann, 1987; Benson, 1992; Lees *et al*, 1983, 1987; Bermudez *et al*, 1992).

The findings of an extensive investigation have demonstrated that the acetylcholine response of these neurones consists of a fast nicotinic component (ACh1) which dominates the action of acetylcholine, and a slow muscarinic (ACh2) component. These responses are activated by different receptors and are mediated by different membrane currents (Benson and Neumann, 1987; Benson, 1992). The nicotinic response of the neurones is blocked by the potent snake venom toxin,  $\alpha$ -bungarotoxin, which has also been shown in comparative studies using the cockroach D<sub>f</sub> motoneurone and the locust BA1 motoneurone *in situ* (David and Sattelle, 1984; Anderson, 1995). Block of the muscarinic response recorded from locust neurones *in vitro* and *in situ*, and the D<sub>f</sub> motoneurone *in situ*, can be produced by the broad spectrum antagonists scopolamine and atropine (Benson, 1992; David and Sattelle, 1984; Anderson, 1995). Attempts to identify the nature of the muscarinic response of the dissociated locust neurones, the locust BA1 motoneurone *in situ* and the cockroach D<sub>f</sub> motoneurone *in situ* using vertebrate receptor (M<sub>1</sub>, M<sub>2</sub> and M<sub>3</sub>) subtype-selective muscarinic antagonists, have demonstrated that the pharmacology of the receptor does not fit the vertebrate classification system (Benson, 1992; Anderson, 1995; David and Pitman, 1993a). The pharmacological profile of the muscarinic response of these insect neurones indicates that the receptor mediating the response resembles both the M<sub>1</sub> and M<sub>3</sub> vertebrate receptor subtypes.

From investigations examining the pharmacological profile of the GABA response of dissociated insect neurones, the receptor has been said to most closely

resemble that of the vertebrate GABA<sub>A</sub> receptor subtype. That is, the GABA response is dependent on extracellular Cl<sup>-</sup> ions, mimicked by the GABA<sub>A</sub> agonist, muscimol, and antagonized by the GABA<sub>A</sub> antagonist, picrotoxin (Usherwood *et al*, 1980; Lees *et al*, 1987; Neumann *et al*, 1987). Similar findings are reported from insect neurones *in situ* (Kerkut *et al*, 1969a; Pitman and Kerkut, 1970; Lummis *et al*, 1987; Pinnock *et al* 1988). However, since the insect receptor shares some properties with the vertebrate GABA<sub>C</sub> receptor, such as bicuculline-insensitivity, there may be some correlation between this receptor and the insect GABA receptor (see Section 1.2.2.3).

To date, no evidence has been reported, demonstrating the effects of the biogenic amine, dopamine, on isolated insect neurones. Dopamine has been shown to have an excitatory effect upon identified cockroach motoneurones *in situ* (Pitman and Baker, 1989; Pitman and Davis, 1988) and an inhibitory effect on ant neurones (Steiner and Pieri, 1969). Using vertebrate D<sub>1</sub>- and D<sub>2</sub>- subtype-selective agonists and antagonists, it has been shown that the receptor mediating the response in the cockroach common inhibitory motoneurone (D<sub>3</sub>) resembles neither vertebrate subtype closely (Davis and Pitman, 1991).

### Aims

The aims of experiments presented here were fourfold: (i) to establish a protocol in order to isolate the first basalar (BA1) motoneurone from the mesothoracic ganglion and maintain it in a viable state *in vitro* for a number of hours, to enable an electrophysiological and pharmacological profile to be made of this neurone, using current- and voltage-clamp recording techniques; (ii) to examine the nicotinic and muscarinic acetylcholine responses of the neurone, and compare the findings with the those from this neurone *in situ* (Anderson, 1995); (iii) to examine the GABA response of the isolated BA1 motoneurone and



compare it to that observed from other insect neurones; and (iv) to investigate the response of the BA1 motoneurone to dopamine, and investigate any modulatory effect the amine has on the GABA response of this neurone.

## MATERIALS AND METHODS

### 2.2.1. Animals

Adult locusts (*Schistocerca gregaria*) of both sexes were obtained from a colony maintained at the laboratory; their diet consisted of fresh barley shoots and bran. If the colony became depleted additional animals were obtained from Blades Biological (Kent).

### 2.2.2. Neurone identification

#### 2.2.2.1. Identification

The soma of the first basalar motoneurone (BA1) is located in the mesothoracic ganglion; it is a paired (that is, it has a contralateral homologue), relatively large cell (approximately 80µm in diameter) and situated near the midline of the ventral surface of the ganglion (Burrows, 1975; Anderson, 1995; Leitch and Pitman, 1995). The motoneurone extends an axon through the neuropile which leaves the ganglion through ipsilateral Nerve 3. A branch of Nerve 3, N3A<sub>2</sub> (nomenclature after Campbell, 1961), carries the axon to the first basalar muscle. Figure 2.2.1. shows the motoneurone soma after N3A<sub>2</sub> was backfilled with the fluorescent dye Lucifer Yellow and the ganglion counterstained with Toluidine Blue according to the technique described below. The large unstained area of the ganglion is the neuropile which contains nerve tracts and dendrites, but no neuronal somata. As N3A<sub>2</sub> contains axons from other neurones within the mesothoracic ganglion the first basalar motoneurone soma is not the only cell to be labelled using this technique.

The cell bodies of the ventral surface of the mesothoracic ganglion are arranged in three groups: there are two bilaterally symmetrical clusters at the rostral end of the ganglion (top of the photograph) and one cluster that extends distally from the caudal region of the midline. The first basalar motoneurone cell

Figure 2.2.1. Identification of the first basalar motoneurone (BA1) in the locust mesothoracic ganglion.

The BA1 motoneurone soma is readily identified by its characteristic size (approximately 80µm) and position in the mesothoracic ganglion. In this photomicrograph the soma (arrowed, left-hand side of the ganglion) and a number of other motoneurones have been stained by backfilling Nerve 3 with Lucifer Yellow. BA1 is found on the ventral surface of the ganglion, close to the midline on the caudal margin of the rostral group of somata. The ganglion has been counter-stained with Toluidine Blue to reveal its position relative to its neighbours.

Scale bar = 200µm.



bodies are found on the caudal margin of the rostral groups of cells, however, only one has been labelled as only the right-hand side N3A<sub>2</sub> trunk was backfilled.

#### 2.2.2.2. Technique for labelling the first basalar motoneurone cell body

The locusts were decapitated and, once their legs and wings and abdominal cavity had been removed, were pinned dorsal surface uppermost on a Sylgard-filled Petri dish. The thoracic cavity was opened along the mid-dorsal line and the gut removed to expose the dorsal surface of the thoracic ganglia. Using the anatomical study of the *Locusta* mesothoracic nervous system (Campbell, 1961) as a reference, fat and trachea were carefully dissected from the thoracic cavity and blocks of muscle were carefully pinned aside, using fine dissecting pins, to expose N3A<sub>2</sub>. Care was taken to prevent touching of the nerve trunk with dissecting implements and the preparation was kept moist with locust saline. N3A<sub>2</sub> was then cut close to its point of insertion into the first basalar muscle and together with the thoracic ganglia was isolated from the thoracic cavity and placed into locust saline.

The protocol employed to backfill the BA1 soma with Lucifer Yellow was based on that of Pitman, Tweedle and Cohen (1972) for labelling neurones with cobalt chloride. The conditions used for dehydrating and counterstaining this preparation, resulting in maximal visualization of the BA1 motoneurone, were established by Anderson (1995). A small Vaseline bridge (approximately 15mm long, 1mm high) was made in a Petri dish and locust saline was placed on one side of the bridge. The thoracic ganglia were placed in the saline and the N3A<sub>2</sub> branch of the mesothoracic ganglion was very carefully drawn over the bridge. More Vaseline was placed over the bridge and gently sealed using a laboratory-made wax melter so that the nerve was sealed; this prevented bulk movement of liquid between compartments. Lucifer Yellow (2.5% in 1.5M LiAc) was then placed on

the other side of the bridge to immerse the nerve trunk. Extreme care was taken to prevent the tissue from drying and a successful Vaseline seal was indicated by no mixing of the orange-coloured Lucifer Yellow with the saline. Dampened tissue paper was then placed in the Petri dish and the lid replaced. The preparation was then left for 24 to 36 hours at 4 to 5°C. After the incubation period with Lucifer Yellow, the ganglia were removed from the saline, and briefly rinsed in locust saline.

Preparations were then transferred to 5% formalin for 15 minutes to prevent leaching of the Lucifer Yellow from the cells. They were then dehydrated through an ascending alcohol series (70, 90, 96, 100 and 100% ethanol again; 10 minutes each) and cleared in methyl salicylate. Preparations were then checked by temporarily mounting in methyl salicylate on a cavity slide and viewed using a fluorescence microscope (Zeiss) using a 495nm filter.

Before counterstaining the ganglion with Toluidine Blue, it was rehydrated by transferring it through an descending alcohol series (100, 100, 96, 90, and 70% ethanol; 10 minutes each); from the 70% ethanol solution the preparation was transferred to the Toluidine Blue stain (composition given in Appendix 1) for 15 minutes. Bodian's fixative (composition given in Appendix 1) was then used to differentiate staining of the ganglion (which removed excess stain and enhanced the contrast between the stained cells and non-stained tissue). This usually took 10 to 15 minutes depending on the age of the stain. The preparation was then dehydrated as previously described and cleared in methyl benzoate. To photograph the labelled cells the ganglion was temporarily mounted in methyl benzoate on a cavity slide. The preparation was then viewed using the fluorescence microscope as described above and photographs were taken using Fujichrome DX 400 slide film and an Olympus OM-2 camera back; the film was developed commercially.

### 2.2.3. Electrophysiological study of the first basalar motoneurone

#### 2.2.3.1. Dissection

The locusts were decapitated, their legs removed then pinned ventral surface uppermost on a Sylgard-filled Petri dish (Sylgard; Dow Corning). The cuticle of the thorax was removed to expose the pro-, meso- and metathoracic ganglia. The three ganglia were dissected out of the thoracic cavity and placed in locust saline (composition given in Appendix 2). Once the tracheal tissue and fat were removed from the surface of the mesothoracic ganglion, the thoracic cord was placed on a Perspex slide and secured using two rubber bands (insert, Figure 2.2.2). Locust saline was used to keep the preparation moist whilst the mesothoracic ganglion was desheathed. The preparation was then placed in a chamber for soma isolation (Figure 2.2.2; dimensions 81mm long, 25 width and 36mm depth), where it was perfused with oxygenated locust saline (oxygen; BOC) - the rising oxygen bubbles generated a continuous movement of oxygenated saline over the ganglion.

#### 2.2.3.2. Illumination

The preparation was illuminated using a lamp (6V, 48W; Prior, U.K.) positioned such that the light was reflected off a mirror and then focused down onto the mesothoracic ganglion using a converging lens. This extended pathway of light allowed the light to be focused to a small spot on the ganglion and virtually eliminated any heating of the preparation. Using a Nikon zoom (x16 to x80) dissecting microscope the preparation was viewed horizontally through the glass front of the chamber. The soma of first basalar motoneurone (BA1) was reliably located on the surface of the mesothoracic ganglion by its characteristic relatively large diameter and location (Figure 2.2.1).

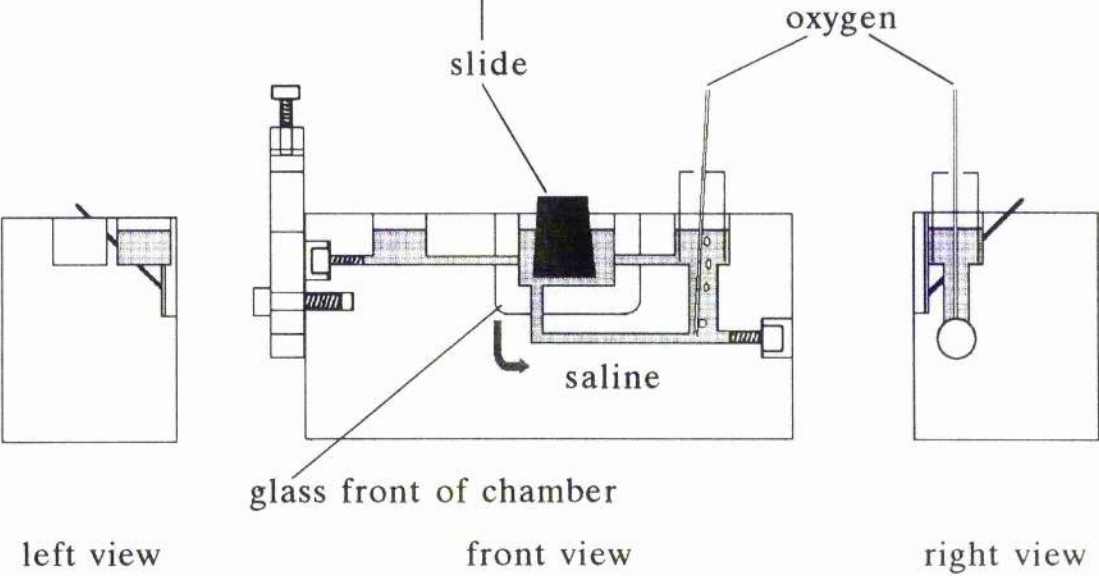
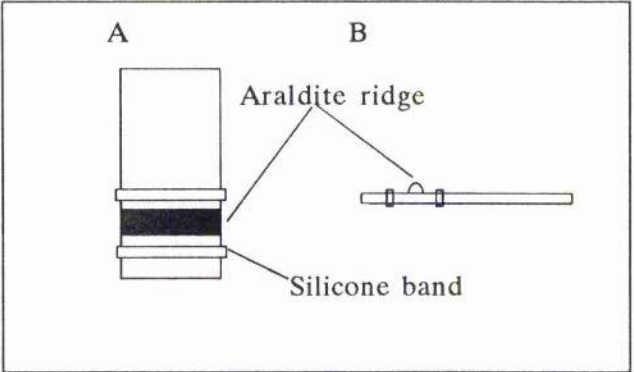
Figure 2.2.2. The Perspex bath used for isolation of the BA1 motoneurone soma.

The areas containing locust saline are indicated by 'stippling'. Saline entered the bath via the right-hand compartment and was circulated throughout the chambers by means of bubbling oxygen into the right-hand compartment. The direction of saline flow is shown by the arrow. Shortly before isolation of the neurone was due to commence, the oxygen supply was turned off, preventing the isolated soma from being carried away with the saline around the bath. The dimensions of the bath were 81mm x 25mm x 36mm, to give a bath volume of 2ml.

The insert shows the Perspex preparation slide, both front (A) and profile (B) views. The nerve cord was arranged on the slide so that the mesothoracic ganglion lay on the Araldite ridge. Silicone elastic bands were used to secure the nerve cord in position. The dimensions of the slide were 10mm x 19mm x 1.5mm.

(Figure adapted from Anderson, 1995).





#### 2.2.4. Electrophysiological recording techniques

##### 2.2.4.1. Experimental Chamber

The recording chamber consisted of a Petri dish (50mm diameter, 9mm depth; Falcon 1006) and a clear Perspex slide (dimensions: 23mm long, 20mm width and 3mm depth) which had three interlinking wells milled out of it (Figure 2.2.3B). This slide was secured to the Petri dish using silicone grease (Radio Spares). A pump-driven circulation system was attached to the recording bath which allowed drugs to be perfused over the preparation. In addition there was a perfusion system consisting of a saline inflow (oxygenated locust saline) and an outflow. This enabled the preparation to be washed whenever necessary. The bath volume (500 $\mu$ l) was kept constant by continuous surface suction (Figure 2.2.3C). The apparatus was carefully earthed to a baseplate and housed in a Faraday cage. The saline was held at earth potential using an electrode (the 'bath electrode') consisting of a silver wire the tip of which had been electrolytically chlorided using a 9V battery and 1M potassium chloride solution. The electrode was connected to the input of a virtual earth current monitor (for experimental set-up see Appendix 3).

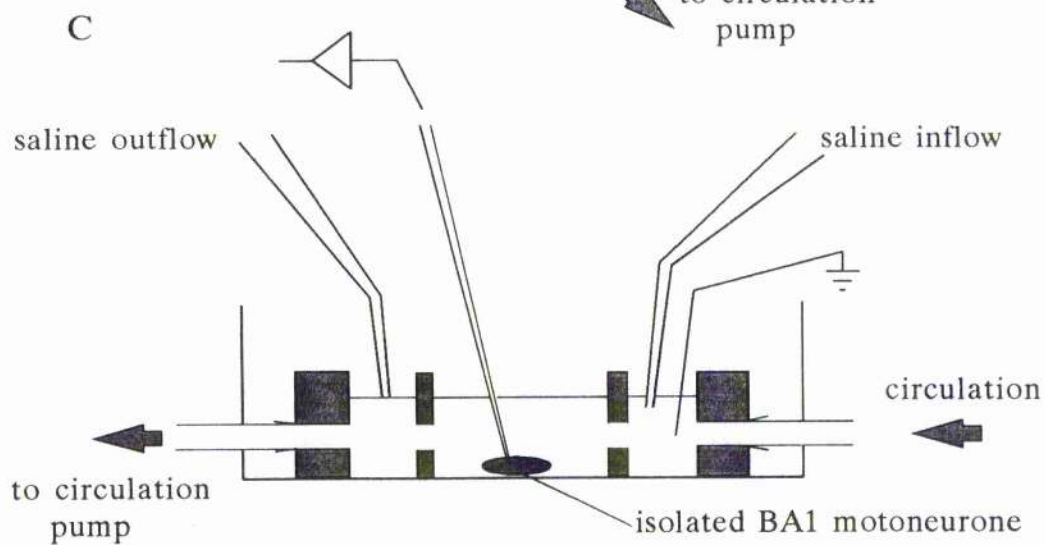
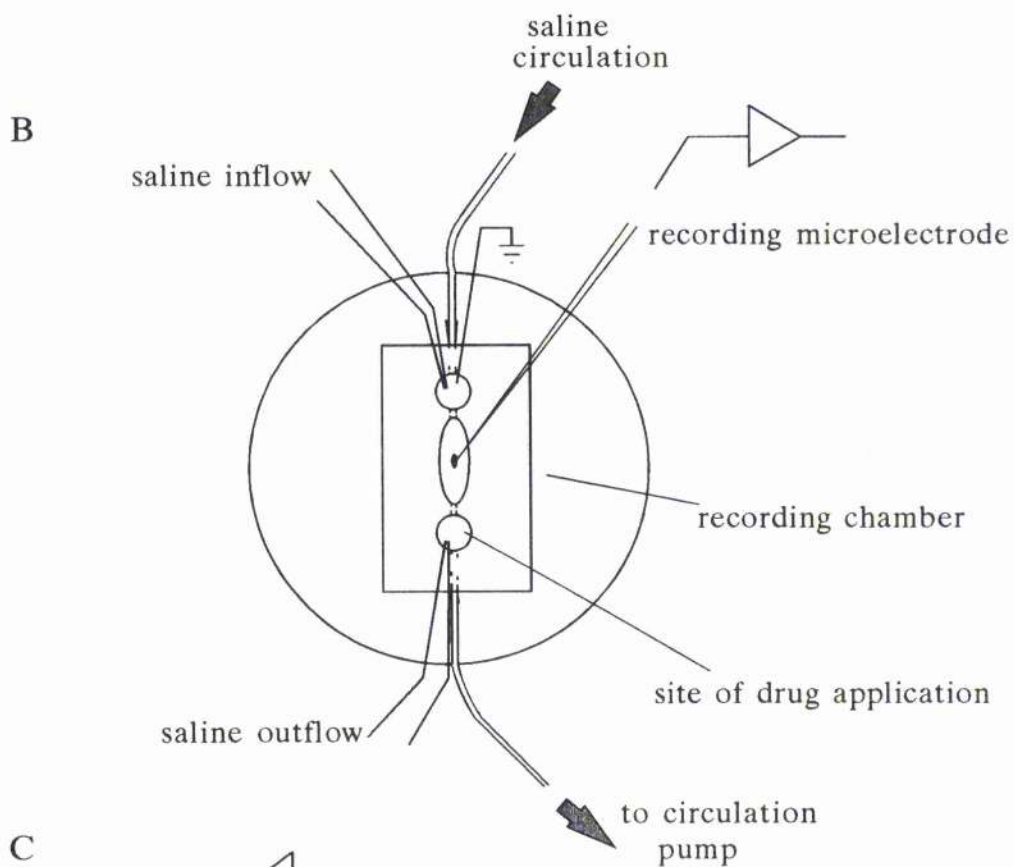
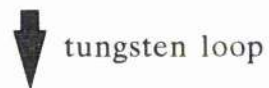
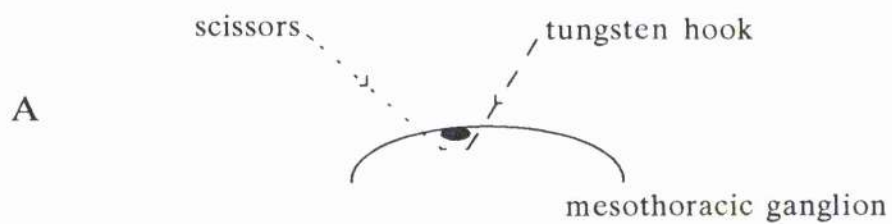
##### 2.2.4.2. Isolation of the first basalar motoneurone

Once identified, the soma of BA1 was removed, together with surrounding tissue (approximately 0.5mm diameter and 0.2mm depth) from the ganglion using a pair of fine scissors (Fine Science Tools: U.K. agents Interfocus Ltd., Withersfield, Suffolk) and an etched tungsten hook (tungsten; Clark Electromedical Instruments; TW8-3). A small etched tungsten loop was used to transfer the identified isolated neurone from the isolation bath to the recording chamber (Figure 2.2.3). This loop prevented the small cluster of neurones, which included the BA1 cell body, from dissociating as the tissue was passed up through

Figure 2.2.3. A schematic diagram illustrating the procedure for cell isolation and the arrangement of the recording chamber for the isolated BA1 motoneurone.

A. shows how the BA1 motoneurone soma was isolated from its ganglionic environment. Using fine scissors the soma was cut free from surrounding tissue, any remaining points of attachment being broken using a fine etched tungsten hook. The neurone was isolated as a small cluster of cells (up to 7 somata) - the somata around the BA1 motoneurone were damaged (using the tungsten hook or loop) during isolation, to prevent any possibility of synaptic connections forming. Once isolated, the small cluster of cells was transferred from the isolation bath to the recording chamber, using a small tungsten loop.

B and C. A diagrammatic representation of the apparatus used for electrophysiological experiments, as observed from above (B) and in profile (C). The recording chamber, a Perspex slide (23mm long x 20mm width x 3mm depth) with three interlinking wells, milled as shown, was placed into a Petri dish (Falcon 1006; diameter 50mm) and secured to the surface of the dish with silicone grease. The three wells were filled with locust saline and once isolated, the BA1 motoneurone was placed into the middle well. A circulation system (comprising of a length of silicone rubber tubing and an electric pump) joined the two end wells, allowing continued exposure of the BA1 motoneurone to agonists and antagonists. For washing of the preparation gravity-fed oxygenated saline entered the bath via the top well (see B), which also housed the bath electrode. The level of saline within the three chambers was maintained by a suction line which drew off excess saline from the lower well.



the meniscus of the saline. The neurones were then pushed onto the surface of the Petri dish with a dissecting pin (the ventral surface of the cluster being uppermost) and the position of BA1 with respect to the other cells was noted. Great care was taken during the whole isolation process not to touch the BA1 motoneurone with any of the implements or allow the ventral surface of the cluster to come into contact with the Petri dish. If either of these events occurred the preparation was abandoned, since it could not be guaranteed that the viability of the neurone had not been impaired prior to impalement. The recording chamber was then secured onto the stage of an inverted phase contrast microscope (Olympus, CK-2) which enabled visualization of the preparation prior to, and during, impalement with microelectrodes and throughout the course of each experiment.

#### 2.2.4.3. Microelectrodes

Microelectrodes were drawn from thin-walled filamented capillary glass (Clark Electromedical Instruments; external diameter, 1.5mm, internal diameter, 1.17mm) using a Narishige PE-2 vertical puller inclined at 45°; they were filled with 1M potassium acetate (KAc) and had electrical resistances of 10 to 20M $\Omega$ . Each microelectrode was held in a Perspex holder containing 1M KAc in which was placed a chlorided silver wire (see above) connected to the input of a high impedance amplifier/bridge via pre-amplifiers (all laboratory-made). The microelectrodes were then positioned in the bath using Prior micromanipulators; these were fitted with reduction drives which allowed for finely controlled movement of the microelectrodes.

During an experiment, changes in membrane potential and neuronal input resistance were monitored using either a single microelectrode or two microelectrode recording technique (for experimental setup see Appendices 3 and 4). Using the single microelectrode recording technique, current was injected into

the neurone whilst changes in membrane potential were monitored simultaneously. Following bridge-balancing, this technique enabled changes in membrane conductance to be approximated. To determine changes in membrane conductance more accurately, the two microelectrode recording technique was employed - one microelectrode (the 'voltage' microelectrode; resistance approximately  $18\text{M}\Omega$ ) was used to monitor membrane potential, whilst a second microelectrode (the 'current' microelectrode; resistance approximately  $12\text{M}\Omega$ ) was used to inject current into the cell in order to monitor changes in cell input resistance (see below).

#### 2.2.4.4. Impalement of the isolated motoneurone

Whilst visualizing the BA1 soma under relatively low powers of magnification (x40 or x100) the two microelectrodes were positioned close to the neurone. Also at this time, 0mV was set on the oscilloscope (Tektronix single beam storage) by adjusting the amplified voltage deflection. Its position was equivalent to that of the beam when the oscilloscope input was set to the level predetermined by the experimenter as being 'ground'. In a similar fashion, 0mV was set on a second oscilloscope/thermal array plotter (Gould, 'Windograf') that displayed both voltage and current signals from the Tektronix oscilloscope. As the 'Windograf' had a printer facility incorporated into it, hard copies of experimental data were produced during the course of an experiment.

Under higher magnification (x200), the recording microelectrode was lowered onto the surface of the soma until a very slight movement of the cell membrane was observed - this moment was also signified by a small deflection in the oscilloscope trace. In order to facilitate penetration of the cell membrane, a series of brief hyperpolarizing current pulses (approximately 30ms, 100nA) were applied through the electrode using a battery powered stimulus isolator (Digitimer

Model DS2); a successful stable impalement was indicated by a sudden and maintained negative shift in potential to between -45 and -55mV; very little variation in membrane potential indicated a stable penetration. This procedure was repeated for the 'current' microelectrode, with the exception that the hyperpolarizing current pulses used were approximately 10ms in duration and 150nA in amplitude. As the current microelectrode was advanced towards the cell the membrane potential was monitored using the recording electrode; penetration was marked by large hyperpolarizing responses corresponding to the pulses applied through the 'current' electrode.

#### 2.2.4.5. Input resistance

Input resistance ( $R_i$ ) was determined by injecting hyperpolarizing current pulses into the cell through the 'current' electrode so that the amplitude of deflection was 10mV (200ms pulses; 0.4 - 0.5Hz). Current pulses were applied using a Grass SD9 stimulator which was connected to a laboratory-made stimulus attenuating device and a laboratory-made amplifier/bridge. The attenuating device was used to make fine adjustments to the stimulus amplitude. The amplitude of the injected current was measured using a current monitor (laboratory-made) the input of which was connected to the 'bath' electrode whilst the output fed into the second channel of the oscilloscope.

Input resistance is calculated from Ohm's Law:

$$\text{input resistance } (\Omega) = \frac{\text{voltage deflection (V)}}{\text{applied current (A)}}$$

Input resistance ( $R_i$ ) measurements provided an indication of the viability of a neurone in addition to drug-induced membrane conductance changes, since, conductance is the reciprocal of resistance.



#### 2.2.4.6. Administration of pharmacological agents

The pharmacological agents used were dissolved in locust saline and the pH of solutions was checked before use (desired pH ~ 7.4). Two methods were adopted to apply agents to the isolated neurone; (i), via the front well of the recording chamber (concentrations referred to in the text are final bath concentrations) and (ii) by local pressure-application of the drug through a microelectrode close to the isolated neurone soma (for further details, see below).

#### *Pressure application of agonists*

Thin-walled filamented capillary glass (external diameter, 1.5mm; internal diameter, 1.17mm) was used to make microelectrodes in the same manner as described above for intracellular microelectrodes; these were then filled with  $10^{-4}\text{M}$  to  $10^{-2}\text{M}$   $\gamma$ -aminobutyric acid (GABA) or the vertebrate GABA<sub>A</sub> receptor agonist, muscimol. The filled microelectrode, once placed in its holder, was connected to a Picospritzer II (General Valve Corporation) triggered by a Grass S44 stimulator through a laboratory-made relay switch (see Appendix 4). The microelectrode was positioned in the bath close to the neurone using a Prior micromanipulator. To ease the expulsion of the agonist, the tip of the microelectrode was broken off by carefully touching the surface of the Petri dish. A 'puff' of agonist, between 10ms and 1s in duration was applied approximately every 100s at 10psi, generated using a garden spray unit (Killaspray Courier 8). When the effect of dopamine (DA) on the GABA response was examined, DA was applied after three consecutive GABA responses were of similar amplitude and duration.



#### 2.2.5. Voltage-clamp studies

In addition to studying the effects of pharmacological agents on the isolated BA1 soma using the two microelectrode current-clamp technique described above, the response to GABA and muscimol was examined under two microelectrode voltage-clamp. To do this, a different arrangement of apparatus was used from that described above. This apparatus also allowed the agonist-induced responses to be examined under current-clamp.

##### 2.2.5.1. Preparation

After the ganglia were dissected from the locust and secured onto the Perspex slide, the preparation was placed into the experimental chamber. This resembled the chamber used to isolate BA1 somata, which has been previously described. However, as shown in Figure 2.2.4, there were a number of additions to the chamber that enabled electrophysiological recordings to be made. A virtual earth electrode consisting of a chlorided silver wire placed in an agar-filled 200 $\mu$ l plastic pipette tip was placed in the rear left-hand chamber. This electrode was connected to the main chamber via an agar bridge. This effectively isolated it from any ionic changes happening in the main chamber.

Pharmacological agents and saline for washing were applied to the right-hand compartment of the experimental chamber, whilst the bath volume was kept constant by a continuous surface suction from the front left-hand compartment of the bath.

##### 2.2.5.2. Illumination

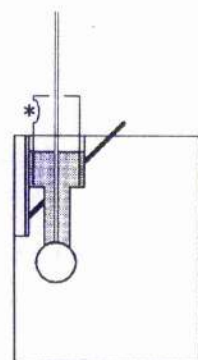
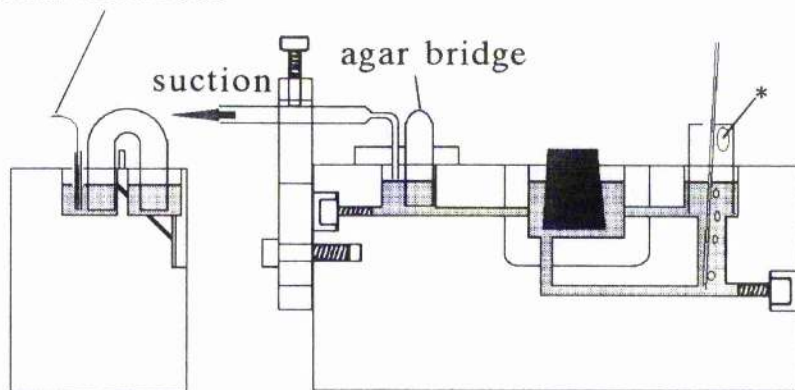
The preparation was illuminated using a lamp located outside the Faraday cage and the light beam was reflected off a mirror inside the cage and focused down onto the cell body by a converging lens. Using an Olympus zoom binocular

Figure 2.2.4. The experimental bath used for voltage- and current-clamp studies.

This bath closely resembled the bath used for the isolation of the BA1 motoneurone from the mesothoracic ganglion (see Figure 2.2.2). That is, oxygen was bubbled into the right-hand compartment of the bath, to generate an anticlockwise movement of saline over the isolated BA1 motoneurone. The neurone, once isolated was held in position on the top of the mesothoracic ganglion (secured on the Perspex slide), using a flame polished microelectrode.

However, to enable voltage- and current-clamp studies to be made from the isolated BA1 motoneurone, there were several additions to the bath. A 'bath electrode' was placed in the rear left compartment to provide a virtual ground for electrophysiological experiments. It was connected to the main chamber by an agar bridge was placed between the front and rear left compartments. The point of addition (right-hand compartment) of saline and pharmacological agents to the circulating saline of the bath, which allowed for thorough mixing of both, is shown by the asterisks. The volume of saline in the bath was maintained by a suction line (left-hand compartment).

bath electrode



dissecting microscope (magnifications of x16 to x80), the preparation was viewed horizontally through the glass front of the chamber.

#### 2.2.5.3. Isolation of the first basalar motoneurone

The BA1 cell body was isolated from the mesothoracic ganglion as previously described, however, it was not removed from the experimental chamber. Instead, the small cluster of cells was placed on top of the ganglion and held in position by a flame-polished microelectrode which prevented movement of the neurone generated by the circulating saline.

#### 2.2.5.4. Microelectrodes

Microelectrodes were made as previously described (see Section 2.2.4.3.), however, the 'voltage' microelectrode, which monitored changes in membrane potential was connected to the 'voltage' amplifier/bridge (Dagan 8800 Total Clamp) via a Dagan pre-amplifier 8870 and a x10 amplifier (for experimental setup see Appendix 6). The 'current' microelectrode was connected to the second amplifier/bridge (laboratory-made) via a current(I)/voltage(V)-clamp switch, and a pre-amplifier (both laboratory-made). The output from the voltage amplifier was fed directly to the voltage-clamp amplifier (laboratory-made), and the output from the latter was fed to the current microelectrode via a switch that allowed rapid and smooth switching of the current-clamp circuit to the voltage-clamp circuit. The output signals from both amplifiers were connected to an oscilloscope (Tektronix Dual Beam Storage Oscilloscope) via an analogue-digital converter (Medical Systems Corporation; MSC PCM-4/8 CO) and video cassette recorder (Mitsubishi VHS HQ; HS-B21).

The current pulses used to aid microelectrode penetration or monitor membrane input resistance were applied using a Grass S88 stimulator via a

stimulation isolation unit (Grass SIU5). The stimulator (Grass S88) was also used to drive the Picospritzer II (General Valve Corporation) which was used for pressure-application of the agonists as previously described.

#### 2.2.5.5. Impalement of the isolated motoneurone

Once the 'current', 'voltage' and the pressure-application microelectrodes were secured in their respective holders, they were lowered into the experimental bath towards the isolated BA1 soma. To prevent capacitative coupling between the 'current' and 'voltage' microelectrodes an earthed brass shield, supported by a small retort stand, was placed between the two microelectrodes. The technique of penetrating the neurone was very similar to that described for impaling it when it was placed in the recording chamber (see Section 2.2.4.4). One exception, however, was that one knew when the microelectrodes were just on the cell surface as a slight depression in the membrane was observed. Also, rather than breaking the tip of the pressure-application microelectrode on part of the experimental chamber in order to facilitate the expulsion of the agonists, the tip was damaged by carefully touching the Perspex specimen slide.

#### 2.2.5.6. Reversal potentials

In order to determine the membrane potentials at which the GABA- and muscimol-evoked responses reversed, the membrane potential of the isolated neurone was progressively hyperpolarized in 5 or 10mV increments from the resting membrane potential (usually between -40mV and -50mV) to -100mV. Under voltage-clamp the amplitudes of the induced currents associated with the agonist applications at different holding potentials were measured, in order to demonstrate the current(I)/voltage(V) relationships of the responses. To hyperpolarize the cell body under current-clamp, hyperpolarizing current was

injected from the current amplifier/bridge under manual control. Once in voltage-clamp, i.e. the current-clamp/voltage-clamp switch had been changed from current to voltage mode, the holding potential was also under manual control.

#### 2.2.6. Data capture and storage

Copies of experimental data were recorded onto videotape. Selected data were then played-back and displayed using a Gould DSO 1604 Storage Oscilloscope; using this oscilloscope the peak currents of the GABA- and muscimol-evoked responses were measured.

## RESULTS

### 2.3.1. Electrophysiological properties of the isolated BA1 motoneurone

Examination of the electrophysiological properties of the mechanically isolated BA1 motoneurone soma indicated that this preparation was viable and closely resembled the BA1 motoneurone *in situ*. Furthermore, subsequent pharmacological experiments demonstrated that the isolated motoneurone, generally, responded to various pharmacological agents in a similar manner to that observed from the motoneurone in its ganglionic environment.

When penetrated with a single microelectrode, the resting membrane potential of isolated BA1 motoneurons was  $-51.8 \pm 0.8\text{mV}$  (mean  $\pm$  S.E.M.;  $n = 44$ ), whilst two electrode recordings gave a value of  $-45.2 \pm 0.4\text{mV}$  (mean  $\pm$  S.E.M.;  $n = 105$ ). The mean input resistance of the neurone, determined using the two microelectrode current clamp technique was  $7.1 \pm 0.4\text{M}\Omega$  (mean  $\pm$  S.E.M.;  $n = 61$ ). Following injection of small hyperpolarizing current pulses into the BA1 motoneurone at the resting membrane potential a 'rebound' in the membrane potential was seen. Figure 2.3.1A shows an isolated BA1 motoneurone with a resting membrane potential of  $-43\text{mV}$ , injected with  $1\text{nA}$ ,  $200\text{ms}$  duration hyperpolarizing current pulses at  $24\text{s}$  intervals. These evoked approximately  $7\text{mV}$  membrane hyperpolarizations (therefore, from Ohm's Law, the input resistance of this neurone was  $7\text{M}\Omega$ ) which were associated with distinct membrane 'rebounds'. The importance of membrane 'rebounds' is they give an indication of membrane excitability because they reflect the balance of inward and outward currents across the neuronal membrane. An increase in membrane 'rebound' amplitude represents an increase in the net inward current of the neurone and, therefore, an increase in membrane excitability.

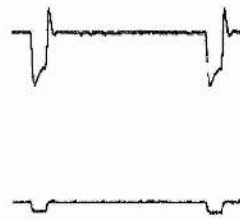
Figure 2.3.1. The typical electrophysiological properties of a freshly isolated BA1 motoneurone soma *in vitro*.

A. The injection of small hyperpolarizing current pulses into the neurone at resting membrane potential evoked a corresponding membrane hyperpolarization; upon termination of the current pulse, a small membrane depolarization, termed a membrane 'rebound', was observed. In the example given, the resting membrane potential of the isolated BA1 motoneurone was  $-43\text{mV}$ . The injection of hyperpolarizing current (bottom trace:  $1\text{nA}$ ,  $200\text{ms}$ , approximately  $0.04\text{Hz}$ ) evoked approximately  $7\text{mV}$  membrane hyperpolarizations which were associated with  $3\text{mV}$  membrane 'rebounds' (top trace). Using Ohm's Law (see Section 2.2.4.5), the membrane input resistance of this neurone was estimated to be  $7\text{M}\Omega$ .

B. Injection of depolarizing current into the isolated BA1 motoneurone soma at resting membrane potential evoked membrane oscillations; upon termination of the current pulses, distinct membrane afterhyperpolarizations were seen. In the example shown the resting membrane potential of the neurone was  $-59\text{mV}$ . The top trace shows that the amplitude of the evoked membrane oscillations and the amplitude of membrane afterhyperpolarization increased, as the amplitude of the injected current was increased (bottom trace). As a single electrode recording technique was used and microelectrode resistance was not continuously monitored, the amplitude of the injected current could not be accurately determined.

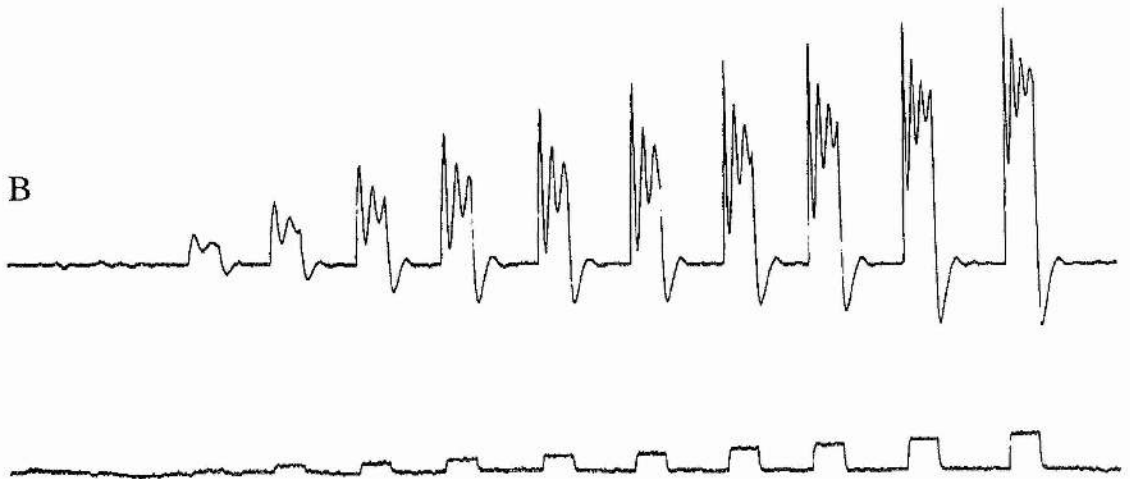


A



10mV  
5nA  
400ms

B



10mV  
10nA  
400ms

Figure 2.3.1B shows the responses of a different isolated BA1 motoneurone preparation (resting membrane potential  $-59\text{mV}$ ) to small depolarizing current pulses (400ms) of increasing amplitude, measured using the single microelectrode recording technique. As shown, a viable isolated BA1 motoneurone typically elicited membrane oscillations on injection of depolarizing current pulses and on the termination of each pulse, prominent transient membrane afterhyperpolarizations were observed ( $n = 30$ ). The amplitude of the membrane oscillations and afterhyperpolarizations increased as the amplitude of the injected current increased (up to approximately  $5.5\text{nA}$ ; see Figure 2.3.1B).

### 2.3.2. The presence of cholinergic receptors on isolated BA1 motoneurons

It has previously been shown that cholinergic receptors are present on BA1 motoneurons *in situ* (Anderson, 1995). This population of receptors include receptors with a distinct nicotinic pharmacology (i.e. are sensitive to  $\alpha$ -bungarotoxin; see below) and those with a broadly muscarinic pharmacology. However, the data of this study indicated that the latter type of receptor had a 'mixed' (nicotinic/muscarinic) pharmacology. One of the aims of the current study was to investigate the pharmacological profile of cholinergic receptors upon the soma membrane of the BA1 motoneurone. The series of experiments described below demonstrate that functional cholinergic receptors are present on the soma membrane. Furthermore, these receptors consist of two populations of acetylcholine receptor subtypes: nicotinic and  $\alpha$ -bungarotoxin-resistant (termed 'muscarinic') acetylcholine receptors.

#### 2.3.2.1. The effects of acetylcholine on isolated BA1 motoneurons

The initial evidence for the presence of acetylcholine (ACh) receptors on the isolated BA1 motoneurone soma was obtained from experiments in which

ACh ( $10^{-5}\text{M}$  to  $10^{-2}\text{M}$ ) was bath-applied to the isolated neurones. The bath-application of this neurotransmitter evoked membrane depolarization and an increase in membrane conductance in a dose-dependent manner ( $n = 29$ ). The threshold for ACh to evoke a change in membrane potential was between  $10^{-5}\text{M}$  and  $10^{-4}\text{M}$  in isolated BA1 motoneurones.

Figure 2.3.2A shows the dose-dependent nature of the ACh-induced response on an isolated BA1 motoneurone (single microelectrode recording, continuously perfused with locust saline). In this preparation the bath-application of  $10^{-5}\text{M}$  ACh did not appear to evoke any response (Figure 2.3.2Ai), however,  $10^{-4}\text{M}$  ACh evoked a 1mV membrane depolarization which was not associated with any apparent change in membrane input resistance (Figure 2.3.2Aii). Following the bath-application of  $10^{-3}\text{M}$  ACh, the membrane potential was depolarized by 4.5mV which was associated with a 15% increase in membrane conductance (Figure 2.3.2Aiii). Figure 2.3.2Aiv shows the effect of the bath-application of  $10^{-2}\text{M}$  ACh to this preparation. In this instance, ACh evoked a 13mV membrane depolarization with a 127% increase in membrane conductance.

The presence of acetylcholine receptors on the BA1 motoneurone soma was further suggested using the non-selective cholinergic agonist, carbachol (carbamylcholine chloride; CCh). Since it is a non-hydrolyzable analogue of ACh, and, therefore, it is not affected by cholinesterase, it is a more potent cholinergic agonist than ACh on preparations which possess cholinesterase activity. This was demonstrated using isolated BA1 motoneurone preparations. The bath-application of CCh evoked a more pronounced membrane depolarization, which was associated with a greater increase in membrane conductance than that observed when the same concentration of ACh was bath-applied to the neurone ( $n = 5$ ). Using a different preparation to that used in Figure 2.3.2A (single microelectrode recording, not continuously perfused with locust saline), the responses of the

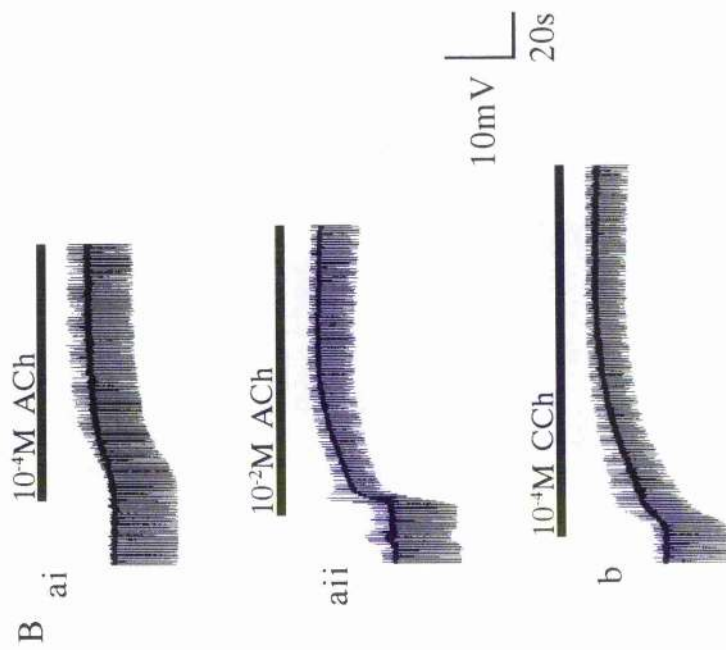
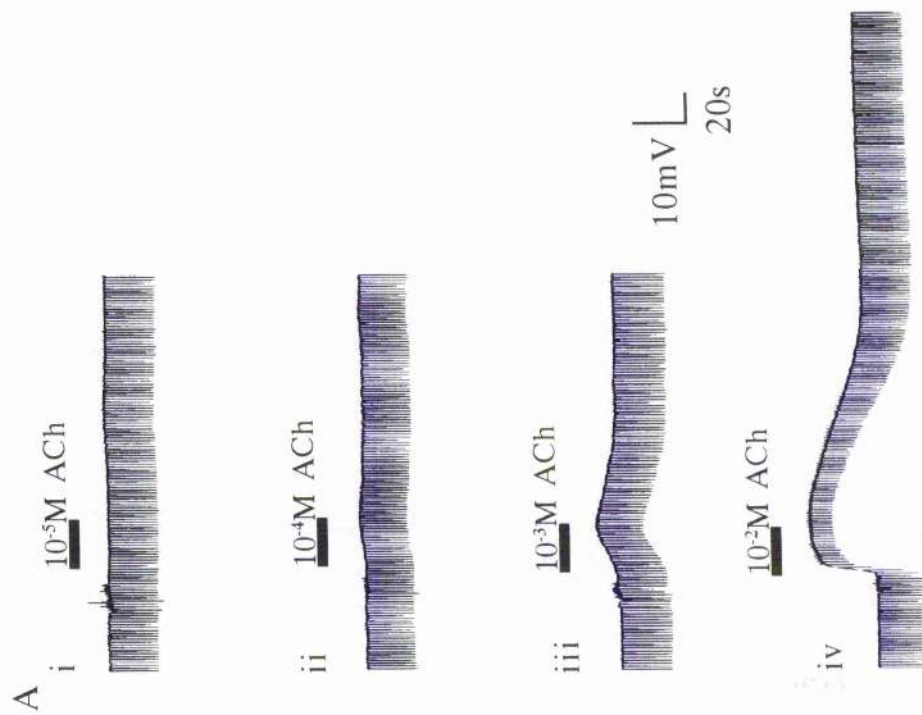
Figure 2.3.2. The effects of excitatory non-specific cholinergic agents upon isolated BA1 motoneurons.

A. Acetylcholine (ACh) evokes a dose-dependent change in membrane potential, which at higher concentrations is associated with a detectable increase in membrane conductance ( $10^{-5}\text{M}$  to  $10^{-2}\text{M}$ ;  $n = 29$ ). From Ohm's Law, an increase in membrane conductance was seen as a decrease in membrane input resistance, which was monitored by the amplitude of the voltage deflections evoked by small hyperpolarizing current pulses injected into the neurone (approximately 0.5Hz). The solid bars above each trace (and in subsequent figures) represents the duration of drug application. The right-hand side end of each bar signifies when washing commenced.

In this preparation (resting membrane potential was  $-56\text{mV}$ ; preparation continuously perfused with locust saline), the threshold for ACh to induce membrane depolarization was between  $10^{-5}\text{M}$  and  $10^{-4}\text{M}$ ; the bath-application of  $10^{-5}\text{M}$  ACh (i) did not appear to evoke a detectable change in membrane potential or membrane input resistance. However,  $10^{-4}\text{M}$  ACh evoked a  $1\text{mV}$  membrane depolarization (no detectable change in membrane input resistance was observed). Increasing the concentration of ACh ( $10^{-3}\text{M}$ : (iii) and  $10^{-2}\text{M}$ : (iv)) applied to the motoneurone resulted in greater membrane depolarization which was associated with a dose-dependent decrease in input resistance. The effects of ACh upon the BA1 motoneurone were seen to reverse with washing.

B. Carbachol (carbamylcholine chloride; CCh), a non-selective, non-hydrolyzable cholinergic agonist, evoked membrane depolarization which was associated with an increase in membrane conductance; this response was dose-dependent (not shown). The effects of this agonist were more pronounced than those observed using the same concentration of ACh ( $n = 5$ ).

Using a different preparation to that used in Figure 2.3.2A (resting membrane potential was  $-59\text{mV}$ ; preparation not continuously perfused with locust saline), the effects of bath-applied  $10^{-4}\text{M}$  and  $10^{-2}\text{M}$  ACh are shown (Bai and Baii, respectively). ACh evoked membrane depolarization associated with an increase in membrane conductance in both experiments. The bath-application of CCh ( $10^{-4}\text{M}$ ; Bb) evoked membrane depolarization and an increase in membrane conductance of similar magnitude to that evoked by  $10^{-2}\text{M}$  ACh. Furthermore, in each experiment there was a prominent increase in the amplitude of after-hyperpolarization membrane 'rebounds', demonstrating the agonist-induced increase in membrane excitability.



isolated neurone to the bath-application of  $10^{-4}\text{M}$  and  $10^{-2}\text{M}$  ACh are shown in Figures 2.3.2Bai and 2.3.2Baii, respectively.  $10^{-4}\text{M}$  ACh evoked a 4mV membrane depolarization which was associated with a 46% increase in membrane conductance, whilst  $10^{-2}\text{M}$  ACh evoked an 11mV membrane depolarization with a 100% increase in membrane conductance. However, the bath-application of  $10^{-4}\text{M}$  CCh to this preparation evoked a membrane depolarization of 10mV, which was associated with a 125% increase in membrane conductance (Figure 2.3.2Bb). In each of these examples and Figure 2.3.2Aiv, it was noted that the responses evoked by the cholinergic agonists were accompanied with an increase in neuronal excitability. This was shown by the increase in amplitude of the membrane 'rebound's that occurred on the termination of the hyperpolarizing current pulses, used to monitor membrane input resistance.

#### 2.3.2.2. The effects of nicotine on isolated BA1 motoneurones

After it had been established that cholinergic receptors were present on the BA1 motoneurone soma, the nature of these receptors was investigated. The bath-application of the nicotinic acetylcholine receptor agonist, nicotine (NIC), confirmed the presence of such receptors on the BA1 soma membrane. That is, following its application to isolated BA1 motoneurones, NIC ( $10^{-9}\text{M}$  to  $5 \times 10^{-3}\text{M}$ ;  $n = 43$ ) evoked a dose-dependent membrane depolarization and an increase in membrane conductance. This agent was found to be the most potent cholinergic agonist tested on the BA1 motoneurone soma.

An example of the dose-dependent responses evoked by NIC on an isolated BA1 motoneurone (resting membrane potential -48mV; not continuously perfused with locust saline) are shown in Figure 2.3.3A. Whilst no response was apparent following the bath-application of  $10^{-7}\text{M}$  NIC (Figure 2.3.3Ai),  $10^{-6}\text{M}$  NIC evoked a 2mV membrane depolarization with a 18% increase in membrane

Figure 2.3.3. The effects of the nicotinic acetylcholine receptor agonist, nicotine (NIC), on isolated BA1 motoneurons.

A. The bath-application of NIC evoked a dose-dependent membrane depolarization in isolated BA1 motoneurons which was associated with an increase in membrane conductance ( $10^{-9}\text{M}$  to  $5 \times 10^{-3}\text{M}$ ,  $n = 43$ ). In this preparation (resting membrane potential  $-48\text{mV}$ ; not continuously perfused with locust saline) no response was apparent following the bath-application of  $10^{-7}\text{M}$  NIC (Ai), however, as the concentration of NIC was increased ( $10^{-6}\text{M}$ : Aii,  $10^{-5}\text{M}$ : Aiii and  $10^{-4}\text{M}$ : Aiv), the agonist induced membrane depolarization associated with an increase in membrane conductance, the magnitude of which increased as the concentration of bath-applied NIC increased.

The ability of nicotinic receptors to desensitize is illustrated in the above traces (Aii to Aiv). That is, in the absence of washing (i.e. in the continued presence of NIC), the NIC-induced effects appear to reverse with time (for further details regarding receptor desensitization see Discussion).

B. The nicotinic response of the isolated BA1 motoneurone is irreversibly blocked by the irreversible vertebrate nicotinic antagonist,  $\alpha$ -bungarotoxin ( $\alpha$ -BTX). Using a different preparation to that used in Figure 2.3.3A (resting membrane potential  $-45\text{mV}$ ; continuously perfused with locust saline), the bath-application of NIC ( $10^{-3}\text{M}$ ) alone evoked membrane depolarization which was associated with an increase in membrane conductance, and the effects of nicotine were shown to be reversible with washing (Bi). Following incubation with  $\alpha$ -BTX (BTX:  $10^{-5}\text{M}$ ; 50 minutes), NIC ( $10^{-3}\text{M}$ ) did not evoke a change in membrane potential or input resistance (Bii). Furthermore, no response was observed when the concentration of NIC was increased to  $10^{-1}\text{M}$  (Biii), indicating the receptors mediating the response were completely blocked by the toxin.



A

i

$10^{-7}$ M NIC



10mV

ii

$10^{-6}$ M NIC

20s



iii

$10^{-5}$ M NIC



iv

$10^{-4}$ M NIC



B

i

$10^{-3}$ M NIC



ii

( $10^{-5}$ M BTX)

$10^{-3}$ M NIC



iii

( $10^{-5}$ M BTX)

$10^{-1}$ M NIC



10mV

40s



conductance (Figure 2.3.3Aii). Increasing the concentration of NIC to  $10^{-5}\text{M}$  and then to  $10^{-4}\text{M}$  increased the size of response evoked, as shown in Figures 2.3.3Aiii and 2.3.3Aiv, respectively. The bath-application of  $10^{-5}\text{M}$  NIC induced a 4mV membrane depolarization with a 43% increase in membrane conductance, whilst  $10^{-4}\text{M}$  NIC induced a 7mV membrane depolarization which was associated with a 117% increase in membrane conductance. These examples show how the NIC receptors desensitize with time in the continued presence of the agonist. That is, without washing the preparation, the membrane potential and membrane conductance return to that seen pre-NIC application.

$\alpha$ -bungarotoxin ( $\alpha$ -BTX) is known to be highly potent in its ability to block the ACh response of insect neurones (David and Sattelle, 1984; Benson, 1992). At  $10^{-6}\text{M}$ , it is routinely used as an antagonist of nicotinic responses in insect neurones (for examples, see David and Pitman, 1993a; Anderson, 1995). When the ability of  $10^{-6}\text{M}$   $\alpha$ -BTX to antagonize the nicotinic response was tested in this preparation (incubation period 50 minutes), it could not fully block the response evoked by the bath-application of NIC at concentrations equal or greater than that of itself ( $n = 4$ ). However, it was found that when  $10^{-5}\text{M}$   $\alpha$ -BTX (50 minutes incubation) was used, it fully blocked the response evoked by the bath-application of NIC (up to  $10^{-1}\text{M}$ ; see Figure 2.3.3B). When  $10^{-3}\text{M}$  NIC alone was bath-applied to this preparation (resting membrane potential -45mV; continuously perfused with locust saline), the membrane potential was depolarized by 3mV, and this associated with a 117% increase in membrane conductance. These effects reversed on washing (Figure 2.3.3Bi). However, when the neurone was tested with the same dose of NIC again in the presence of  $10^{-5}\text{M}$   $\alpha$ -BTX (50 minutes incubation), no change in membrane potential or input resistance was observed (Figure 2.3.3Bii). Figure 2.3.3Biii shows that when the concentration of

NIC was increased to  $10^{-1}$  M, still no response was observed, indicating that the population of NIC receptors was fully blocked.

#### 2.3.2.3. The effects of muscarinic agonists on isolated BA1 motoneurons

To investigate the presence of muscarinic acetylcholine receptors on the BA1 motoneurone soma, responses of known muscarinic agonists, arecoline (ARE), pilocarpine (PILO), oxotremorine (OXO) and McN-A-343 (McN) were tested under current-clamp, for their effects on the resting membrane potential and input resistance of isolated BA1 motoneurons. ARE is established as a preferential muscarinic agonist in vertebrate preparations, however, when applied to insect neurones it can evoke both muscarinic and nicotinic effects (Benson, 1992; Tribut *et al*, 1994). This observation appears to be dependent upon in the dose of agonist applied (Tribut *et al*, 1994). Consequently, the effects of ARE were examined in the absence and presence of  $\alpha$ -BTX ( $10^{-5}$ M; 50mins). PILO and OXO are both non-selective vertebrate muscarinic receptor agonists, whilst McN is a selective vertebrate  $M_1$  subtype agonist; all have been shown to have an effect on insect neurones (Benson, 1992; David and Pitman, 1993a; Anderson, 1995).

The bath-application of muscarinic agonists to isolated BA1 motoneurons usually evoked membrane depolarization which was dose-dependent and reversed on washing. Whether a change in membrane conductance was associated with the change in membrane potential was dependent on the agonist concentration and on individual preparations. The order of potency of these agonists evoking membrane depolarization in isolated BA1 motoneurons was ARE > PILO > OXO > McN.

Figures 2.3.4Aa and 2.3.4Ab show the dose-dependent membrane depolarization evoked by the bath-application of ARE to isolated BA1 motoneurons ( $10^{-4}$ M to  $10^{-2}$ M;  $n = 40$ ). ARE normally induced a monophasic membrane depolarization ( $n = 24$  out of 27 preparations; Figures 2.3.4Aai and

Figure 2.3.4. The effects of muscarinic receptor agonists on isolated BA1 motoneurons.

A. When tested on isolated BA1 motoneurons, the vertebrate muscarinic agonist, arecoline (ARE;  $10^{-4}\text{M}$  to  $10^{-2}\text{M}$ ;  $n = 40$ ), induced a dose-dependent membrane depolarization which could be either monophasic (a) or biphasic (b); whether a change in input resistance (i.e. membrane conductance) was associated with the membrane depolarization, was dependent upon the individual preparation.

Aa shows the monophasic membrane depolarization induced by the bath-application of  $10^{-4}\text{M}$  (Aai) and  $10^{-3}\text{M}$  (Aaia) ARE in an isolated BA1 motoneurone (resting membrane potential  $-59\text{mV}$ ; not continually perfused with locust saline). A prominent increase (122%) in membrane conductance was associated with the ARE-induced membrane depolarization (Aaia) in this preparation, and these changes in membrane potential and membrane conductance were seen to reverse on washing (Aaiib; seen after 13 minutes).

Ab shows the biphasic membrane depolarization induced by the bath-application of ARE in an isolated BA1 motoneurone (resting membrane potential  $-43\text{mV}$ ; not continually perfused with locust saline). The bath-application of  $10^{-3}\text{M}$  induced a small ( $0.5\text{mV}$ ) membrane depolarization and a 4% increase in membrane conductance (Abi). When the concentration of ARE was increased to  $5 \times 10^{-3}\text{M}$  (Abii) and  $7.5 \times 10^{-3}\text{M}$  (Abiii), the amplitude of the induced membrane depolarization increased, and was seen to be biphasic in nature. No change in input resistance was associated with these latter responses. The agonist-induced effects reversed on washing (not shown).

Aa

i

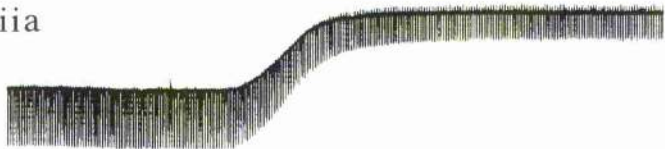
$10^{-4}$ M ARE



10mV   
20s

$10^{-3}$ M ARE

ii a



ii b

WASH



Ab

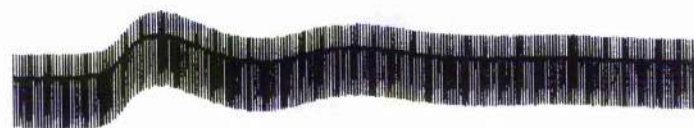
i

$10^{-3}$ M ARE



ii

$5 \times 10^{-3}$ M ARE



iii

$7.5 \times 10^{-3}$ M ARE


10mV   
40s



Figure 2.3.4. (continued) The effects of muscarinic receptor agonists on isolated BA1 motoneurons.

B. When tested on isolated BA1 motoneurons, the muscarinic agonist, pilocarpine (PILO), induced membrane depolarization in most preparations ( $n = 3$  out of 4).

In this preparation (resting membrane potential  $-47\text{mV}$ )  $10^{-4}\text{M}$  PILO induced gradual membrane depolarization which was not associated with a detectable change in input resistance; the change in membrane potential was seen to reverse on washing the preparation with locust saline (Ba). The dose-dependent nature of this agonist-induced response was observed using this preparation:  $10^{-3}\text{M}$  PILO induced a more rapid depolarization which was associated with a 18% increase in membrane conductance; these agonist induced effects reversed on washing.

Using a different preparation to that used in Figure 2.3.4Ba (resting membrane potential  $-40\text{mV}$ ), the excitatory effects of PILO ( $10^{-4}\text{M}$ ) were seen as an increase membrane excitability, shown by an increase in amplitude of the post-hyperpolarization membrane 'rebounds'. PILO had only a small effect ( $1\text{mV}$  depolarization) on the membrane potential.

C. The effects of the muscarinic agonist oxotremorine (OXO;  $10^{-4}\text{M}$ ) on isolated BA1 motoneurons were investigated. Membrane depolarization was evoked in 1 preparation out of 4 (shown here). In this preparation (resting membrane potential  $-47\text{mV}$ ) membrane depolarization was evoked without a detectable change in membrane input resistance, which reversed on washing.

D. When the vertebrate  $M_1$  receptor-specific agonist, McN-A-343 (McN), was tested on isolated BA1 motoneurons at  $10^{-4}\text{M}$  (Di), it did not induce a change in membrane potential or a detectable change in membrane input resistance ( $n = 3$ ). In this preparation (resting membrane potential  $-50\text{mV}$ ), McN ( $10^{-3}\text{M}$ ) also appeared not to affect the neurone (Dii).

Bai

10<sup>-4</sup>M PILO



Baii

10<sup>-3</sup>M PILO



10mV  
└  
40s

Bb

10<sup>-4</sup>M PILO



10mV  
└  
40s

C

10<sup>-4</sup>M OXO



10mV  
└  
40s

Di

10<sup>-4</sup>M McN



Dii

10<sup>-4</sup>M McN



10mV  
└  
40s



2.3.4Aaiia), but in a few preparations gave biphasic membrane depolarization ( $n = 3$  out of 27 preparations; Figure 2.3.4Abii and 2.3.4Abiii). Figure 2.3.4Aai shows a 2mV membrane depolarization evoked by  $10^{-4}$ M ARE on isolated BA1 motoneurone, resting membrane potential -59mV (using the single microelectrode recording technique). When  $10^{-3}$ M ARE was bath-applied to the same neurone, the membrane potential was depolarized by 15mV and this was associated with a 122% increase in membrane conductance (Figure 2.3.4.Aaia). This effect was reversed on washing - after 13 minutes the membrane potential and input resistance had returned to that seen before the application of ARE (Figure 2.3.4Aaiib). Figure 2.3.4Ab shows the dose-dependent biphasic response evoked by ARE on an isolated BA1 motoneurone (two microelectrode recording; resting membrane potential -43mV). It was observed that this preparation exhibited a prominent membrane 'rebound' following the termination of each hyperpolarizing current pulse used to monitor changes in membrane input resistance. The bath-application of  $10^{-3}$ M ARE evoked approximately 0.5mV membrane depolarization and a 4% increase in membrane conductance (Figure 2.3.4Abi). When the concentration of ARE was increased to  $5 \times 10^{-3}$ M, a biphasic membrane depolarization with no apparent change in membrane conductance was evoked by the agonist in this preparation (Figure 2.3.4Abii). The first 'wave' of depolarization was 8mV in amplitude, whilst the second was 5mV. Figure 2.3.4Abiii shows that the bath-application of  $7.5 \times 10^{-3}$ M ARE evoked a biphasic membrane depolarization of greater magnitude than that observed following the application of  $5 \times 10^{-3}$ M ARE. In this case, the first 'wave' of depolarization was 12.5mV in amplitude, whilst the second was 8.5mV in amplitude. Again, no change in input resistance was observed. Possible explanations for this phenomenon are discussed in the Discussion.

When the selective muscarinic agonists PILO, OXO and McN ( $10^{-4}\text{M}$ ) were tested on isolated BA1 motoneurons at the resting membrane potential, PILO was the most effective in inducing a change in membrane potential ( $n = 3$  out of 4; Figure 2.3.4B). Figure 2.3.4Bai shows the bath-application of  $10^{-4}\text{M}$  PILO to an isolated BA1 motoneurone, resting membrane potential  $-47\text{mV}$ , to induce a gradual membrane depolarization. At approximately 4.75 minutes post-PILO application the membrane potential had depolarized by  $3\text{mV}$  - there was no change in membrane input resistance. In this preparation it was possible to demonstrate the dose-dependent nature of the response. Following the bath-application of  $10^{-3}\text{M}$  PILO, a more rapid membrane depolarization was evoked ( $3\text{mV}$  after approximately 2.75 minutes), and this was associated with a 18% increase in membrane conductance (Figure 2.3.4Baii). In both instances the PILO-induced effects were shown to reverse on washing. Using a different isolated BA1 motoneurone preparation (resting membrane potential  $-40\text{mV}$ ), the bath-application of  $10^{-4}\text{M}$  PILO induced a gradual small membrane depolarization ( $1\text{mV}$ ), and as indicated by the increase in amplitude of the post-hyperpolarization membrane 'rebound's, an increase in membrane excitability (Figure 2.3.4Bb).

Bath-application of OXO ( $10^{-4}\text{M}$ ) to isolated BA1 motoneurons at resting membrane potential, was not as effective in inducing a change in membrane potential as PILO. In only one preparation out of four was a membrane depolarization induced. Figure 2.3.4C shows the effect of the bath-application of  $10^{-4}\text{M}$  OXO on this preparation (resting membrane potential  $-47\text{mV}$ ). After approximately 2.5 minutes in the presence of OXO, the membrane potential had depolarized by  $1\text{mV}$ ; this change in membrane depolarization reversed on washing.

The  $M_1$  receptor-specific agonist McN ( $10^{-4}\text{M}$ ) did not appear to affect isolated BA1 motoneurons at resting membrane potential ( $n = 3$ ). Figure 2.3.4Di



shows the effect of the bath-application of  $10^{-4}\text{M}$  McN on an isolated BA1 motoneurone, at resting membrane potential  $-50\text{mV}$ . McN appeared to have no effect on membrane potential or membrane input resistance. When the concentration of McN was increased to  $10^{-3}\text{M}$ , similar observations were recorded (Figure 2.3.4Dii). These findings may suggest that (i) the muscarinic response is voltage-dependent and at resting membrane potential, McN-induced effects have little influence on the membrane potential (see Discussion) or (ii) the muscarinic receptors present on the BA1 motoneurone soma do not resemble the vertebrate  $M_1$  receptor subtype. However, using the  $\text{Ca}^{2+}$ -sensitive fluorescence dye, fluo-3 and confocal microscopy techniques, this was found not to be the case, see Section 3.3.2.

Whilst it was demonstrated that isolated BA1 motoneurons are sensitive to ARE, the separate muscarinic and nicotinic components of the response were not easily distinguishable. Consequently,  $\alpha$ -BTX was used to block the nicotinic component of the ARE response, and the subsequent response evoked by the bath-application of ARE was examined.

It was seen that after blocking nicotinic receptors with  $\alpha$ -BTX ( $10^{-5}\text{M}$ ; 50 to 60 minutes incubation), the bath-application of ARE still evoked membrane depolarization ( $2 \times 10^{-4}\text{M}$  to  $10^{-2}\text{M}$ ;  $n = 5$ ). In this preparation prior to  $\alpha$ -BTX application (resting membrane potential  $-55\text{mV}$ ),  $10^{-3}\text{M}$  ARE evoked  $1.5\text{mV}$  depolarization which was associated with a 29% increase in membrane conductance (Figure 2.3.5.i). Following 50 minutes incubation with  $10^{-5}\text{M}$   $\alpha$ -BTX, the bath-application of  $10^{-3}\text{M}$  ARE evoked  $0.5\text{mV}$  membrane depolarization (Figure 2.3.5ii). No change in input resistance was observed, which may suggest that the  $\alpha$ -BTX-sensitive component (the nicotinic response) is associated with the change in membrane conductance. Figure 2.3.5iii shows that when the concentration of ARE was increased to  $10^{-2}\text{M}$ , the membrane potential

Figure 2.3.5. The arecoline (ARE) response of isolated BA1 motoneurons consists of a nicotinic and a muscarinic component.

When ARE ( $2 \times 10^{-4}\text{M}$  to  $10^{-2}\text{M}$ ;  $n = 5$ ) is applied to isolated BA1 motoneurons in the presence of the nicotinic receptor antagonist,  $\alpha$ -BTX (BTX:  $10^{-5}\text{M}$ ; 50 minutes incubation), the agonist still induces membrane depolarization.

In this preparation (resting membrane potential  $-55\text{mV}$ ), ARE ( $10^{-3}\text{M}$ ) alone induced membrane depolarization which was associated with an increase in membrane conductance. In the presence of  $\alpha$ -BTX (BTX:  $10^{-5}\text{M}$ ; 50 minutes incubation)  $10^{-3}\text{M}$  ARE evoked a small ( $0.5\text{mV}$ ) membrane depolarization with no detectable change in input resistance (ii). Increasing the concentration of ARE to  $10^{-2}\text{M}$  increased the magnitude of depolarization (no detectable change in input resistance was observed), and this reversed on washing (iii).

Attempts to antagonize this ARE-evoked ( $10^{-3}\text{M}$  to  $10^{-2}\text{M}$ ;  $n = 2$ )  $\alpha$ -BTX-resistant response with scopolamine (SCOP) and atropine (ATR) ( $10^{-4}\text{M}$  and  $10^{-3}\text{M}$ ) were unsuccessful. Using the same preparation as before, in the presence of  $\alpha$ -BTX ( $10^{-5}\text{M}$ ; 50 minutes incubation) and SCOP ( $10^{-4}\text{M}$ ; 50 minutes incubation), ARE ( $10^{-2}\text{M}$ ) induced membrane depolarization without a detectable change in input resistance (iv). Similar responses were obtained when SCOP was replaced by  $10^{-4}\text{M}$  ATR (8 minutes incubation; see v) and  $10^{-3}\text{M}$  ATR (20 minutes incubation; see vi).

i

10<sup>-3</sup>M ARE



ii

(10<sup>-5</sup>M BTX)

10<sup>-3</sup>M ARE



iii

(10<sup>-5</sup>M BTX)

10<sup>-2</sup>M ARE



Also in the presence of 10<sup>-5</sup>M BTX

iv

(10<sup>-4</sup>M  
SCOP)

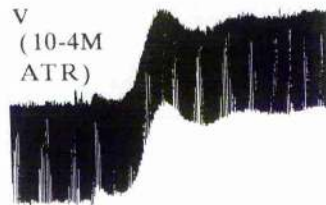
10<sup>-2</sup>M ARE



v

(10<sup>-4</sup>M  
ATR)

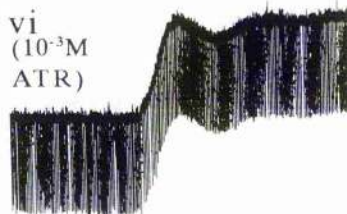
10<sup>-2</sup>M ARE



vi

(10<sup>-3</sup>M  
ATR)

10<sup>-2</sup>M ARE



10mV  
40s

was depolarized by 6mV and no change in input resistance was observed. With washing the ARE-evoked response reversed; at 25 minutes after washing commenced, the membrane potential returned to that pre-ARE application (not shown).

Attempts to antagonize the  $\alpha$ -BTX-resistant (muscarinic) component of the ARE response, using known antagonists of the muscarinic response in insect neurones (Benson, 1992; David and Pitman, 1993a; Anderson, 1995), were unsuccessful. At concentrations of  $10^{-4}$ M to  $10^{-3}$ M, the specific muscarinic antagonist scopolamine (SCOP) and the cholinergic antagonist atropine (ATR) were ineffective as antagonists of the muscarinic response evoked by ARE ( $10^{-3}$ M to  $10^{-2}$ M), in the presence of  $10^{-5}$ M  $\alpha$ -BTX ( $n = 2$ ; see Figure 2.3.5.). Figure 2.3.5.iv shows the response to ARE ( $10^{-2}$ M) in the presence of  $\alpha$ -BTX and after 50 minutes incubation with SCOP  $10^{-4}$ M (same preparation as before). The bath-application of ARE evoked an 8mV membrane depolarization which did not appear to be associated with a change in membrane conductance. Similar responses were observed in the presence of ATR. After 8 minutes incubation in  $10^{-4}$ M ATR, the bath-application of  $10^{-2}$ M ARE the membrane potential was depolarized by 10mV (Figure 2.3.5v). Similarly, after 20 minutes incubation in  $10^{-3}$ M ATR, the bath-application of  $10^{-2}$ M ARE evoked a membrane depolarization of 11mV (Figure 2.3.5vi). One possible explanation for the inability to block the response is agonist saturation of these cholinergic receptor sites. In the presence of relatively high concentrations of ARE (as used here to evoke a change in membrane potential), the agonist may displace the antagonist at the binding sites of the receptors, thus, the antagonist is rendered ineffective. There was concern that at these high concentrations ATR was acting as an agonist of the muscarinic component of the response. However, using the fluorescent dye, fluo-3, it was indicated that this was not likely to be the case (see Discussion 3.4).

### 2.3.3. The effects of GABA and muscimol on isolated BA1 motoneurons

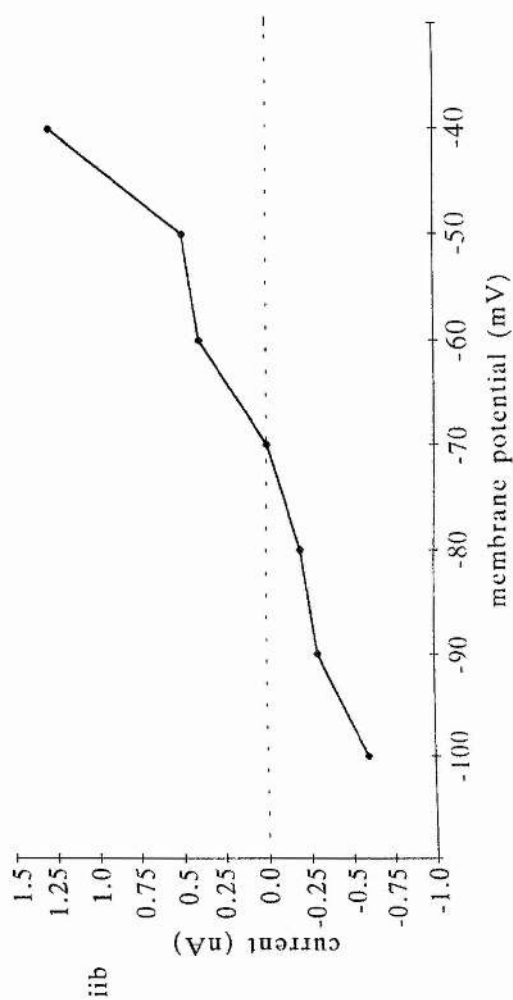
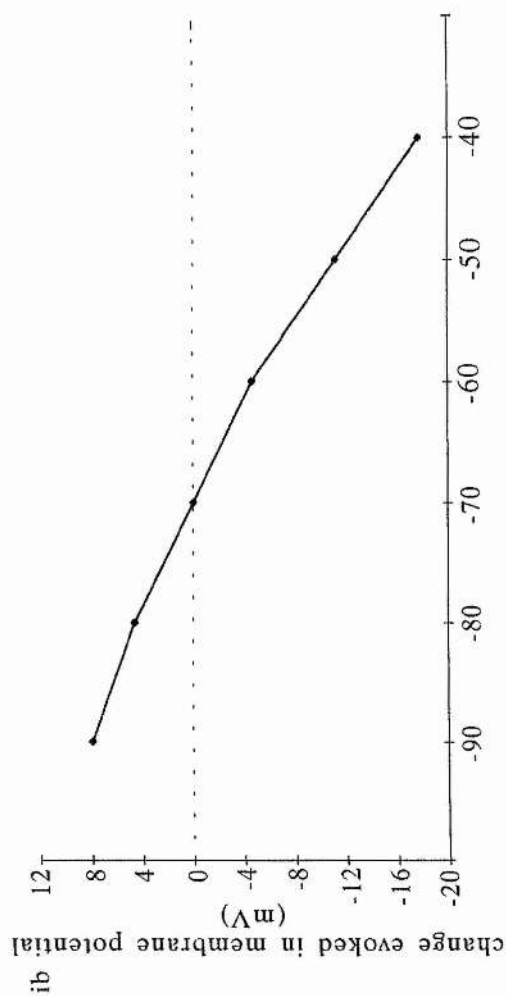
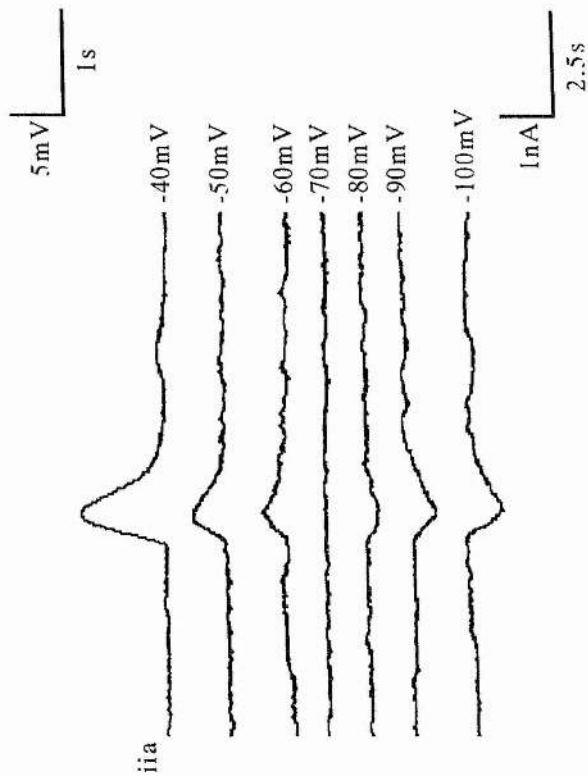
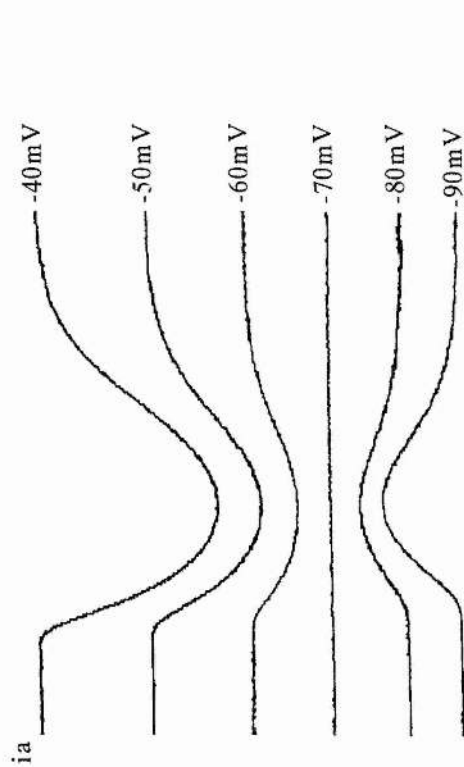
Since GABA is known to be a major inhibitory neurotransmitter in insects (see Pitman, 1985), the possibility that GABA receptors are present on the BA1 motoneurone soma was investigated. The results presented here demonstrate the presence of such receptors on this neurone. Local pressure-application of GABA onto BA1 motoneurons at the resting membrane potential, evoked a brief dose-dependent membrane hyperpolarization ( $n = 52$  of  $53$ ) which under voltage-clamp appeared as an outward current ( $n = 7$ ). Figure 2.3.6ia shows the responses of an isolated BA1 motoneurone to the pressure-application of  $10^{-4}\text{M}$  GABA (10ms; 10psi). The resting membrane potential of this cell was  $-40\text{mV}$ . At this potential GABA evoked a membrane hyperpolarization with a peak amplitude of  $17.5\text{mV}$ . As the membrane potential was made progressively more negative (by the injection of constant negative current), the GABA-evoked membrane hyperpolarization decreased in amplitude and, negative to  $-70\text{mV}$ , changed sign and became a membrane depolarization ( $8\text{mV}$  at  $-90\text{mV}$ ). The estimated reversal potential of the GABA response in isolated BA1 motoneurons was  $-69.8 \pm 2.1\text{mV}$  (mean  $\pm$  S.E.M.;  $n = 11$ ). Figure 2.3.6ib shows the linear relationship between the holding membrane potential and the GABA-evoked change in membrane potential.

Using the same preparation, Figure 2.3.6iia shows the response of the neurone to GABA under voltage-clamp. At  $-40\text{mV}$  the pressure application of GABA induced an outward current ( $1.3\text{nA}$ ), and, as the holding potential was made progressively more negative, the induced current decreased in amplitude and became an inward current at potentials negative to  $-70\text{mV}$  ( $0.6\text{nA}$  at  $100\text{mV}$ ; note the different time scale between Figure 2.3.6ia and Figure 2.3.6iia). Figure 2.3.6iib shows the voltage-dependence of the GABA-induced current in this

Figure 2.3.6. The effects of the inhibitory neurotransmitter, GABA, on isolated BA1 motoneurones.

When GABA ( $10^{-4}\text{M}$ ) was pressure-applied to an isolated BA1 soma through a microelectrode (10ms, 10psi) at its resting membrane potential (-40mV) it evoked membrane hyperpolarization (ia and ib) and an outward current (iia and iib). The reversal potential of this response under current-clamp (ia and ib) was  $-69.8 \pm 2.1\text{mV}$ ; mean  $\pm$  S.E.M.;  $n = 11$ , whilst under voltage-clamp (iia and iib) it was  $-68.9 \pm 2.8\text{mV}$ ; mean  $\pm$  S.E.M.;  $n = 5$ . iia and iib show the current/voltage relationships for the responses seen in ia and ib (note the different time courses between ia and iia).

It appeared that the duration of the agonist-evoked response was unaffected by changes in membrane potential.





isolated neurone; like the GABA-evoked response under current-clamp, the estimated reversal potential under voltage-clamp was close to  $-70\text{mV}$ ; the estimated reversal potential of the GABA-evoked response in BA1 motoneurons under voltage-clamp was  $-68.9 \pm 2.8\text{mV}$  (mean  $\pm$  S.E.M.;  $n = 5$ ). When the mean reversal potential values for the GABA response under current- and voltage-clamp were analyzed using the two-tailed unpaired t-test, their differences were not statistically significant ( $P > 0.05$ ). Furthermore, since the GABA-induced current showed a linear voltage-dependence, it implied that the GABA-activated channels did not show significant voltage-dependence. This was supported by the observation that under current- and voltage-clamp, the duration of the GABA response did not appear to be affected by changes in membrane potential.

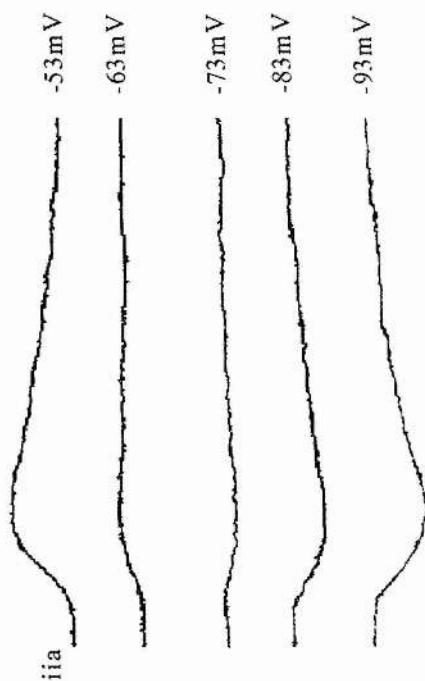
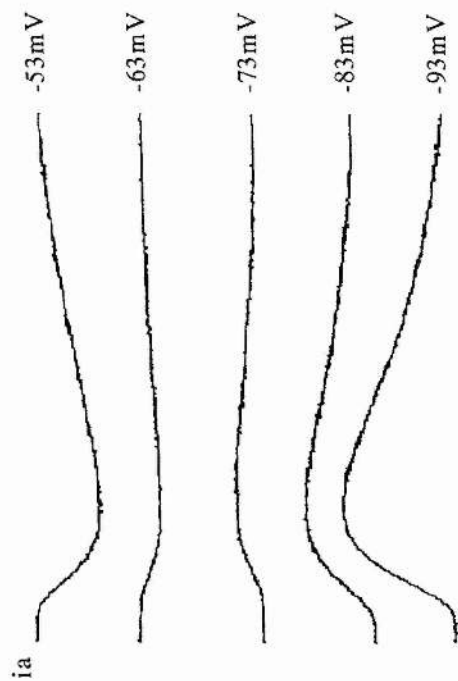
When the vertebrate GABA<sub>A</sub> receptor agonist muscimol ( $10^{-3}\text{M}$ ) was pressure-applied to isolated BA1 motoneurons under current-clamp or voltage-clamp responses were observed which were similar to those evoked by GABA. Figure 2.3.7ia shows the membrane response evoked by  $10^{-3}\text{M}$  muscimol (1s; 10psi). Under current clamp, at the resting membrane potential, an application of muscimol evoked membrane hyperpolarization (in this preparation a  $6\text{mV}$  hyperpolarization); when examined under voltage-clamp this was associated with an outward (for this preparation  $0.8\text{nA}$ ) current (Figure 2.3.7iia). On membrane hyperpolarization, this response reduced in amplitude and, at membrane potentials negative to  $-68\text{mV}$ , muscimol evoked membrane depolarization (Figure 2.3.7ia). The muscimol-evoked response showed a similar linear relationship with the holding membrane potential under current-clamp to that for GABA (compare Figure 2.3.6ib with 2.3.7ib). The estimated reversal potential of the muscimol-evoked response in isolated BA1 motoneurons under current-clamp was  $-67.3 \pm 1.5\text{mV}$  (mean  $\pm$  S.E.M.;  $n = 7$ ). The response evoked by muscimol under voltage-clamp and its relationship with the holding membrane potential, in this



Figure 2.3.7. The effects of the vertebrate GABA<sub>A</sub> agonist, muscimol, on isolated BA1 motoneurones.

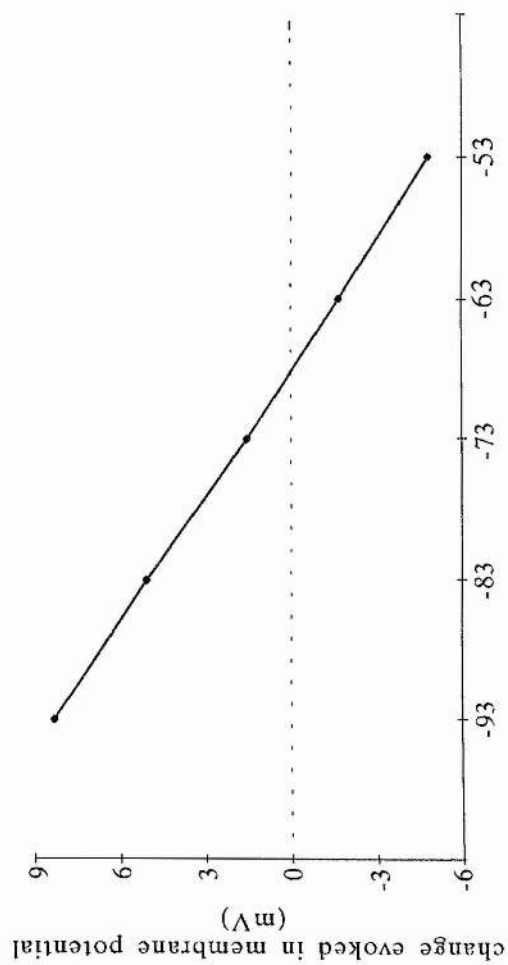
When muscimol ( $10^{-3}\text{M}$ ) was pressure-applied to an isolated BA1 soma through a microelectrode (1s, 10psi) at its resting membrane potential ( $-53\text{mV}$ ) it evoked membrane hyperpolarization (ia and ib) and an outward current (iia and iib). The reversal potential of this response under current-clamp (ia and ib) was  $-67.3 \pm 1.4\text{mV}$ ; mean  $\pm$  S.E.M.;  $n = 7$ , whilst under voltage-clamp (iia and iib) it was  $-66.0 \pm 2.8\text{mV}$ ; mean  $\pm$  S.E.M.;  $n = 7$ . iia and iib show the current/voltage relationship for the responses seen in ia and ib.

It appeared that the duration of the agonist-evoked response was unaffected by changes in membrane potential.

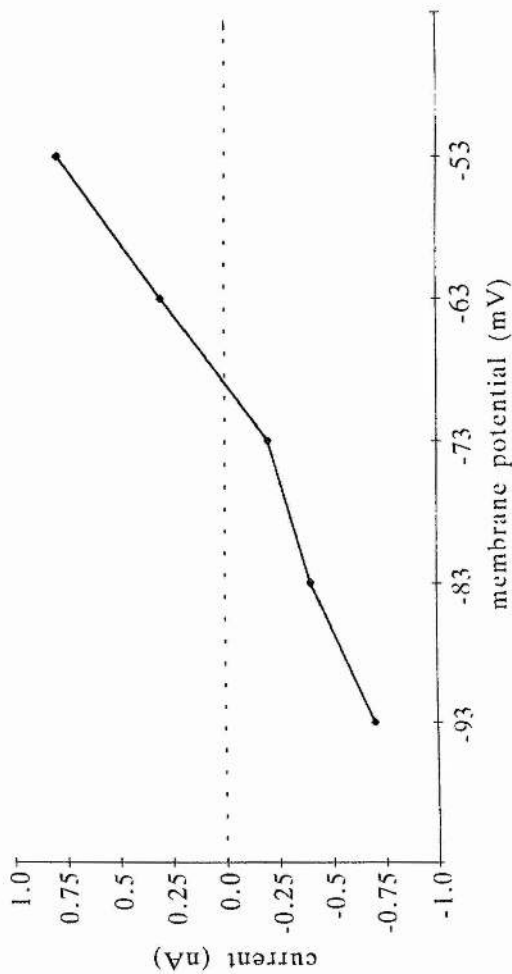


5mV  
1nA  
2.5s

ib



iiib



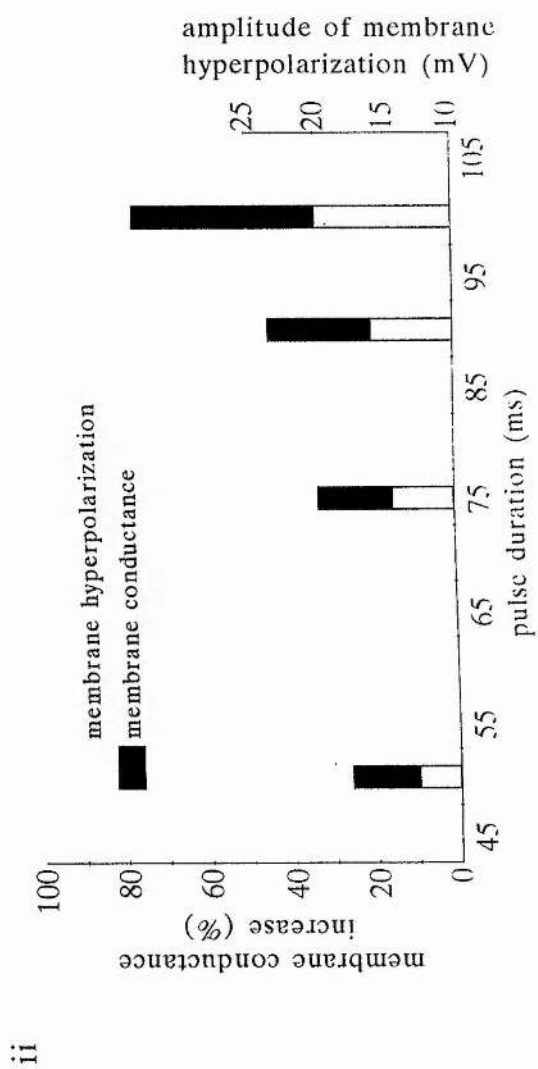
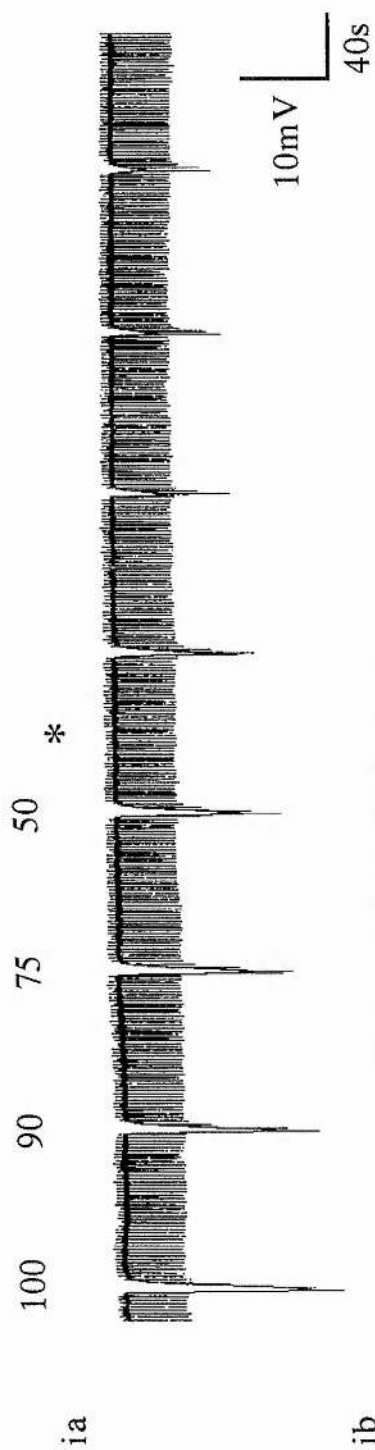
neurone, is shown in Figures 2.3.7iia and 2.3.7iib. The estimated reversal potential was  $-69\text{mV}$  in this preparation (mean reversal potential was  $-66 \pm 3.2\text{mV}$ ;  $n = 7$ ) and, as was observed with the GABA-evoked response, at membrane potentials more negative than the reversal potential, the muscimol evoked membrane depolarization and the associated currents became inward - at  $-93\text{mV}$  the evoked current was  $0.7\text{nA}$  at peak amplitude. When the mean reversal potential values for muscimol (under current- and voltage-clamp) were analyzed using the two-tailed unpaired t-test, their differences were not statistically significant ( $P > 0.05$ ).

Comparison of the mean reversal potential values for GABA and muscimol obtained under both current- and voltage-clamp, made using the two-tailed unpaired t-test, showed the differences were not statistically significant ( $P > 0.05$ ). Thus, the responses evoked by GABA and the GABA<sub>A</sub> receptor agonist, muscimol, were very similar in isolated BA1 motoneurons (Figures 2.3.6 and 2.3.7).

The dose-dependent nature of the GABA response of an isolated BA1 motoneurone is shown in Figure 2.3.8. Whilst using the two microelectrode recording technique to monitor the agonist-evoked changes in membrane conductance ( $1\text{nA}$  hyperpolarizing current pulses were injected into the neurone at  $0.5\text{Hz}$ ), GABA ( $10^{-2}\text{M}$ ;  $10\text{psi}$ ;  $0.01\text{Hz}$ ) was pressure-applied on to the neurone (resting membrane potential  $-45\text{mV}$ ). As the duration of the GABA pulse decreased, so did the amplitude of the membrane hyperpolarization and the magnitude of increase in membrane conductance evoked by the agonist. In this isolated neurone, a  $100\text{ms}$  pulse of GABA evoked a  $20\text{mV}$  membrane hyperpolarization which was associated with an approximately  $77\%$  increase in membrane conductance (Figure 2.3.8ia); a  $90\text{ms}$  pulse of GABA evoked a  $16\text{mV}$  hyperpolarization with approximately a  $45\%$  increase in membrane conductance; a  $75\text{ms}$  pulse of GABA evoked a  $14.5\text{mV}$  membrane hyperpolarization with an

Figure 2.3.8. The inhibitory neurotransmitter, GABA, evokes a dose-dependent membrane hyperpolarization at resting membrane potential, in isolated BA1 motoneurons.

GABA ( $10^{-2}\text{M}$ ; 10psi; 0.01Hz) was pressure-applied onto an isolated BA1 motoneurone (resting membrane potential  $-45\text{mV}$ ), continuously injected with small hyperpolarizing current pulses (1nA; 0.5Hz) to monitor changes in input resistance (and therefore, changes in membrane conductance). The agonist induced membrane hyperpolarization which was associated with an increase in membrane conductance, and as the duration of the GABA pulse was decreased from 100ms to 50ms (as indicated by the numbers above trace ia), the magnitude of the GABA-induced effects decreased. Figure 2.3.8ii shows a graphical representation of this. In order to obtain consistent and small (approximately  $2.5\text{mV}$ ) GABA-induced membrane hyperpolarizations using a pulse duration of 50ms, the GABA pressure-application microelectrode was gradually moved away from the neurone (after \*) until such responses were obtained (ib). ib is a continuation of the trace shown in ia; GABA responses of similar amplitude and duration are produced by the motoneurone.



approximately 33% increase in membrane conductance and 50ms pulse of GABA evoked a 13mV membrane hyperpolarization which was associated with an approximately 26% increase in membrane conductance (see Figure 2.3.8ii). The subsequent responses to GABA shown in Figure 2.3.8ia (after \*) were obtained using a pulse duration of 50ms, however, the amount of agonist reaching the neurone for each test was reduced by moving the microelectrode away from the cell, so that GABA evoked membrane hyperpolarizations of approximately 2.5mV. Figure 2.3.8ib shows the continuation of the trace shown in Figure 2.3.8ia. Pressure-application of GABA under the set conditions consistently evoked membrane hyperpolarization of approximately 2.5mV (Figure 2.3.8ib). Consequently, this would indicate that the reduction in amplitude of the GABA response shown in Figure 2.3.8ia was predominantly a dose-dependent effect rather than the result of receptor desensitization. Had it been the latter, one would have expected to see an enhancement of the GABA response on receptor recovery from the desensitized state. This was not observed using the described experimental protocol.

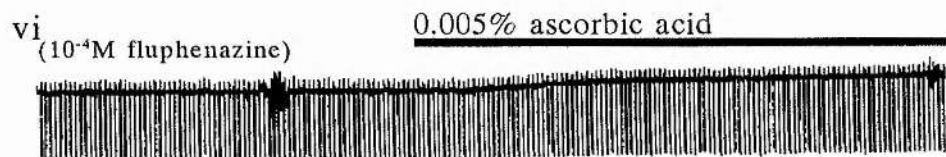
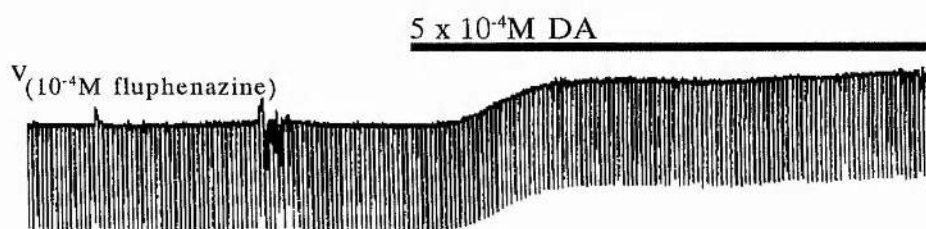
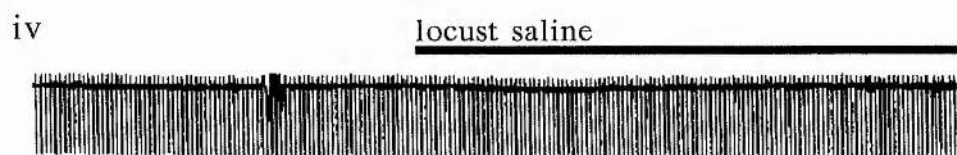
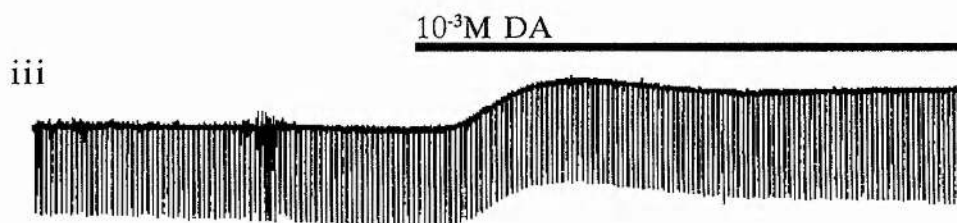
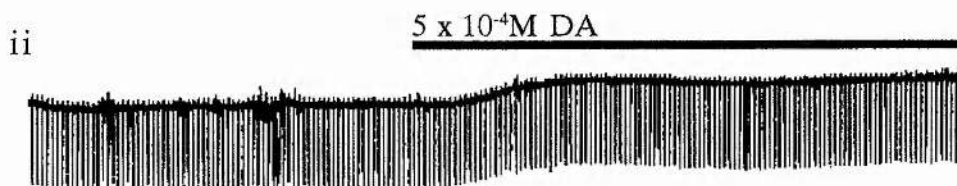
#### 2.3.4. The effects of dopamine on isolated BA1 motoneurones

Since it had been shown that insect motoneurones could respond to the application of the biogenic amine, dopamine (DA; Pitman and Davis, 1988; Pitman and Baker, 1989; J. C. McLelland, personal communication), the effects of this agonist upon the isolated BA1 motoneurone soma were investigated. The effect of bath-applying DA ( $10^{-4}\text{M}$  to  $10^{-2}\text{M}$ ) to isolated BA1 motoneurones was to evoke a membrane depolarization ( $n = 11$  out of 12), which was not usually associated with a detectable change in membrane conductance ( $n = 10$  out of 11). This response was dose-dependent ( $n = 6$ ; for example, see Figure 2.3.9) and reversible on washing. Figure 2.3.9i shows the effect of the bath-application of

Figure 2.3.9. The effects of the biogenic amine, dopamine, on isolated BA1 motoneurons.

When dopamine (DA;  $10^{-4}\text{M}$  to  $10^{-2}\text{M}$ ) was bath-applied to isolated BA1 motoneurons, it induced membrane depolarization ( $n = 11$  out of 12) which was not usually associated with a detectable change in membrane conductance ( $n = 10$  out of 11). The DA-induced change in membrane potential was seen to be a dose-dependent effect ( $n = 6$ ), which reversed on washing (not shown).

The effect of  $1.8 \times 10^{-4}\text{M}$ ,  $5 \times 10^{-4}\text{M}$  and  $10^{-3}\text{M}$  DA upon an isolated BA1 motoneurone (resting membrane potential  $-45\text{mV}$ ) is shown in i, ii and iii respectively. To show that the membrane depolarization was not an experimental artefact, locust saline was bath-applied to the neurone (iv). Attempts to antagonize the DA-induced membrane depolarization with established DA antagonists were unsuccessful ( $n = 3$ ; see v); it is shown using the same preparation, that the  $D_1/D_2$  receptor subtype antagonist, fluphenazine ( $10^{-4}\text{M}$ ; 41 minutes incubation) fails to prevent membrane depolarization following the bath-application of  $5 \times 10^{-4}\text{M}$  DA; a similar response was observed following 60 minutes incubation in  $10^{-3}\text{M}$  fluphenazine (not shown). A additional control experiment (vi) was performed using ascorbic acid (0.005%), in the presence of fluphenazine ( $10^{-4}\text{M}$ ), to confirm the membrane depolarization following the bath-application of DA was not caused by the presence of this anti-oxidant.



10mV

40s



$1.8 \times 10^{-4}\text{M}$  DA on an isolated BA1 motoneurone - following bath-application a membrane depolarization of approximately 1mV in amplitude was evoked. No change in membrane conductance was observed. Upon bath-application of  $5 \times 10^{-4}\text{M}$  DA the membrane potential was depolarized by approximately 2.5mV. Again no detectable change in membrane conductance was observed (Figure 2.3.9ii). The effect of bath-application of  $10^{-3}\text{M}$  DA onto this neurone is shown in Figure 2.3.9iii. In this instance DA evoked approximately 5.5mV membrane depolarization. The small increase in input resistance observed may have been a result of slight blocking of the 'voltage' microelectrode, rather than a drug-induced response. The blocking of the microelectrode results in increased microelectrode resistance, and consequently (from Ohm's Law), larger voltage deflections are associated with the hyperpolarizing current pulses of constant amplitude. As a control for these DA-induced effects, a test application of locust saline was added to the experimental bath. No significant changes in membrane potential or input resistance were seen following administration (Figure 2.3.9iv).

Attempts to antagonize the DA-induced effects when DA was bath-applied to the isolated motoneurone preparation were unsuccessful under these experimental conditions. The vertebrate  $D_1/D_2$  receptor subtype antagonists flupenthixol and fluphenazine had previously been described as antagonists of pressure-applied DA responses in the prothoracic inhibitory neurone of the cockroach (*Periplaneta americana*) (Davis and Pitman, 1991); using a voltage-clamp protocol, they were reported to block DA responses at concentrations of  $10^{-9}\text{M}$  and  $10^{-6}\text{M}$ , respectively. However, in this preparation, when changes in neuronal excitability were studied under current-clamp, they were found to be ineffective antagonists; that is, bath-application of DA evoked membrane depolarization after 45 to 60 minutes incubation of the isolated neurone with the antagonist (fluphenazine:  $10^{-4}\text{M}$  to  $10^{-3}\text{M}$ ,  $n=2$ ; flupenthixol:  $10^{-4}\text{M}$ ,  $n=1$ ).

These findings should be compared with results in Chapter 3; data presented in this section showed that fluphenazine blocked the DA-induced response in isolated BA1 motoneurons. Figure 2.3.9v shows the response of an isolated BA1 neurone to  $5 \times 10^{-4}\text{M}$  DA after the preparation had been left in the presence of  $10^{-4}\text{M}$  fluphenazine for 41 minutes. DA evoked a membrane depolarization of approximately 5mV with no apparent change in membrane conductance, in the presence of fluphenazine. A similar response was observed following 60 minutes incubation in  $10^{-3}\text{M}$  fluphenazine (not shown). One possible explanation for the inability to block the DA response was agonist saturation of the DA receptor sites. In the presence of the relatively high concentrations of DA (as used here to evoke a change in membrane potential) fluphenazine may have been displaced from the binding sites, thus, rendering it ineffective as an antagonist of the DA-induced response. Preliminary attempts were made to antagonize membrane depolarizations evoked by the pressure-application of DA ( $10^{-1}\text{M}$ ; 10psi; up to 1s) onto isolated BA1 motoneurons. DA applied in this way to the BA1 isolated cell body (protocol similar to Pitman and Davis, 1988) evoked 2 to 3mV membrane depolarizations. These small responses to DA were not affected by the bath-application of  $10^{-4}\text{M}$  fluphenazine ( $n = 2$ ).

Another control experiment was performed to demonstrate that the observations were the result of the bath-application of DA (Figure 2.3.9vi). Since the stock solution of DA ( $10^{-1}\text{M}$ ) was dissolved in 1% ascorbic acid solution to prevent oxidation (which rapidly occurs to DA when it is normally placed in solution), the appropriate concentration of diluted ascorbic acid (in locust saline) was also used as a control. In some preparations ascorbic acid had no apparent effect on the membrane potential ( $n = 2$  out of 4), whilst in others it induced small (1mV) membrane depolarization ( $n = 2$  out of 4). Figure 2.3.9vi shows the bath-application of 0.005% ascorbic acid, in the presence of  $10^{-4}\text{M}$  fluphenazine.

This concentration of ascorbic acid was present with the application of  $5 \times 10^{-4}\text{M}$  DA. Ascorbic acid alone induced an approximate 1mV membrane depolarization, which was less than that evoked by  $5 \times 10^{-4}\text{M}$  DA (approximately 2.5mV, see Figure 2.3.9ii); 0.004% ascorbic acid had a similar effect on the membrane potential in the absence of fluphenazine in this preparation (not shown). These results infer that the depolarization observed following the application of DA was a DA-induced response and not the result of an experimental artefact, associated with the addition of ascorbic acid.

#### 2.3.5. The effects of dopamine on the GABA response in isolated BA1 motoneurones

The effects of DA on the response of isolated BA1 motoneurones to the pressure-application of GABA were investigated. Pressure-application of GABA onto isolated BA1 motoneurones consistently evoked membrane hyperpolarization ( $n = 52$  out of 53; see Section 2.3.3). When DA ( $10^{-4}\text{M}$  to  $10^{-2}\text{M}$ ) alone was bath-applied to isolated BA1 motoneurones, it evoked membrane depolarization in 92% of the preparations ( $n = 11$  out of 12; see Section 2.3.4); DA alone was never seen to evoke membrane hyperpolarization. However, if DA was applied to the preparation in between the GABA responses, in some neurones it evoked membrane hyperpolarization ( $n = 5$ ;  $2 \times 10^{-5}\text{M}$  -  $10^{-3}\text{M}$  DA), whilst in others it caused membrane depolarization ( $n = 6$ ;  $10^{-5}\text{M}$  -  $10^{-3}\text{M}$  DA). In one preparation no change in membrane potential was evident. Furthermore, the bath-application of DA potentiated the amplitude and/or duration of the response to GABA in 11 out of 12 preparations tested.

It was established that the changes in membrane potential and the GABA response observed following DA application had been induced by DA, and not by a time-dependent change in the GABA response or a decrease in neuronal

viability. In control experiments in which GABA was pressure-applied to isolated BA1 motoneurons for time periods up to 2 hours, the peak amplitude of the GABA responses was not potentiated ( $n = 6$  out of 7). In fact, with time, the responses gradually diminished in amplitude, as the input resistance of the neurone decreased. When the membrane input resistance fell to approximately  $1\text{ M}\Omega$  (indicating notable cell deterioration), no response to GABA was observed ( $n = 6$ ). Therefore, in isolated BA1 motoneurons, the potentiation of GABA responses following the bath-application of DA was a drug-induced effect.

Figures 2.3.10Ai and 2.3.10Aii show the enhancement of GABA responses in an isolated BA1 motoneurone following the application of  $7.5 \times 10^{-5}\text{M}$  DA (resting membrane potential  $-50\text{mV}$ ; continuously perfused with locust saline). Initially, when GABA was pressure-applied to the neurone ( $10^{-2}\text{M}$ ; 25s, 10psi) it evoked  $4\text{mV}$  membrane hyperpolarizations. Bath-application of DA ( $7.5 \times 10^{-5}\text{M}$ ) caused a  $10\text{mV}$  membrane hyperpolarization which was associated with a 60% increase in membrane conductance ( $*_1$ ). Following these changes, the GABA response was potentiated and the DA-induced enhancement in membrane conductance of the neurone gradually returned to that seen before the DA application. The DA-induced potentiation of GABA response was long-lasting; that is, the effect did not reverse following washing with locust saline. Figure 2.3.10Aii shows that approximately 75 minutes after washing off DA, the peak amplitude and duration of response had increased further. As long as GABA was pressure-applied to the neurone, the membrane potential remained hyperpolarized by approximately  $5.5\text{mV}$ . However, when GABA was no longer applied the membrane potential returned to  $-51\text{mV}$  ( $*_2$ ). It should be noted that the pressure used to apply GABA in Figure 2.3.10Aii had been reduced from 10psi to 5psi; although the pressure was normally kept constant throughout experiments, it was lowered to (and remained at) 5psi because the GABA-induced response was near

Figure 2.3.10. The effects of dopamine on the GABA response of isolated BA1 motoneurons.

When DA ( $10^{-5}\text{M}$  to  $10^{-3}\text{M}$ ) is bath-applied to isolated BA1 motoneurons in between repeated pressure-applications of GABA, membrane hyperpolarization ( $n = 5$  out of 12) or depolarization ( $n = 6$  out of 12) was evoked. Furthermore, DA potentiated the response evoked by GABA, that is following the bath-application of DA, the amplitude and/or duration of the GABA response was increased (see Figures 2.3.10A and 2.3.10B). These effects did not reverse on washing.

Ai. In this preparation (resting membrane potential  $-50\text{mV}$ ; continuously perfused with locust saline), initially the pressure-application of GABA ( $10^{-2}\text{M}$ ; 25ms, 10psi) was seen to evoke approximately 4mV membrane hyperpolarizations. The bath-application of DA ( $7.5 \times 10^{-5}\text{M}$ ) induced a 10mV membrane hyperpolarization ( $\ast_1$ ) which was associated with an increase in membrane conductance. Following this, the GABA response was potentiated and the change in membrane conductance returned to the control value. The potentiation was seen to be long-lasting, that is, it did not reverse on washing; 75 minutes after washing off DA further enhancement of the GABA response was observed (Aii). The repeated pressure-application of GABA appeared to have an effect on the membrane potential during the potentiation of the GABA-induced membrane hyperpolarization. As long as GABA was applied to the neurone, the membrane potential remained hyperpolarized; on stopping the pressure-application of GABA, the membrane potential returned to  $-51\text{mV}$  ( $\ast_2$  and as indicated by the horizontal dotted line).

B. Using a different preparation (resting membrane potential  $-45\text{mV}$ ; continuously perfused with locust saline), initially the pressure-application of GABA ( $10^{-2}\text{M}$ ; 10psi) was seen to evoke approximately 5mV membrane hyperpolarizations. The bath-application of DA ( $10^{-3}\text{M}$ ) induced a 14mV membrane depolarization which was associated with an increase in membrane conductance. Following this, the GABA response was potentiated and the change in membrane conductance returned to the control value ( $\star$ ). The potentiation of the GABA response persisted following washing.

Ai

7.5 x 10<sup>-5</sup> M DA



Ai cont.

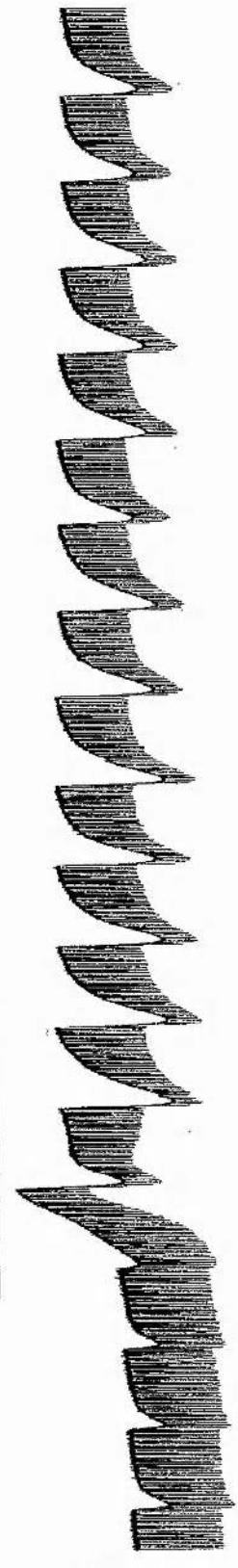
\*<sub>2</sub>      Aii



10mV  
40s

B

10<sup>-3</sup> M DA



10mV  
40s



maximal. It was believed that keeping the pressure at 10psi may have resulted in receptor desensitization, which could have impinged on the DA-induced potentiation of the GABA response. Under the conditions used, DA had increased the mean peak amplitude and the mean duration (measured at 1/2 peak amplitude) of the GABA response by 344% and 547%, respectively (values obtained by comparing the responses prior to DA application and those shown in Figure 2.3.10Aii).

Whilst DA could induce membrane hyperpolarization and potentiation of the GABA response in some isolated BA1 motoneurones ( $n = 5$ ), in others it induced membrane depolarization which was also associated with the potentiation of GABA responses ( $n = 6$ ). This indicated that potentiation of the GABA response was not merely a result of change in membrane potential. Figure 2.3.10B shows DA-induced membrane depolarization and potentiation of the GABA response following bath-application of  $10^{-3}\text{M}$  DA on an isolated BA1 motoneurone (resting membrane potential  $-45\text{mV}$ ; continuously perfused with locust saline). Prior to DA application the pressure-application of GABA evoked  $5\text{mV}$  membrane hyperpolarizations of approximately 11s duration at 1/2 peak amplitude which were associated with a 34% increase in membrane conductance. The bath-application of  $10^{-3}\text{M}$  DA to this isolated motoneurone evoked a  $14\text{mV}$  membrane depolarization with a 20% increase in membrane conductance. The membrane potential was prevented from depolarizing further by the subsequent applications of GABA, and these responses to GABA were markedly potentiated, both in the presence of DA and after washing. The DA-induced change in membrane conductance was transient, since the value of membrane conductance had returned to normal 5.5 minutes after DA application (indicated by ★). Comparing the four GABA responses obtained following membrane depolarization with those obtained before the bath-application of DA ('control'

responses), it was estimated that the parameters of the GABA response had increased as follows: amplitude by 205%, duration at 1/2 peak amplitude by 125% and membrane conductance at peak amplitude by 100%. Despite the slow and gradual decline in neuronal input resistance that developed during this experiment, the GABA response remained potentiated. As a consequence of the continued reduction in input resistance of this preparation, the long-term effects of DA application (as shown in Figure 2.3.10A) could not be studied.



## DISCUSSION

In the current study a technique has been established for the isolation of the first basalar motoneurone from its ganglionic environment, to enable the electrophysiological and pharmacological properties of this isolated soma to be compared with those observed *in situ*. The results presented in Section 2.3.1. illustrated that this isolated neurone preparation was suitable for such studies. That is, BA1 motoneurones were routinely isolated, maintained in a viable state supported by locust saline, and electrophysiological recordings were made from the neurones for time periods often up to 9 hours. It was observed that the electrophysiological properties of the isolated somata were similar to those of the neurone *in situ*. By bath-applying various cholinergic agents to the preparation, the cholinergic profile of the isolated BA1 motoneurone was found to be similar to that of the neurone in its ganglionic environment (Anderson, 1995). It was also shown that the isolated BA1 motoneurone soma responded to the application of the inhibitory neurotransmitter, GABA, and the neuromodulator, dopamine (DA). Furthermore, it was of great interest to discover that DA potentiated the GABA-induced response of this neurone *in vitro*.

### 2.4.1. Electrophysiological properties of the isolated BA1 motoneurones

The resting membrane potential of the isolated BA1 motoneurone was found to be  $-51.8 \pm 0.8\text{mV}$  when determined using the single microelectrode recording technique, and  $-45.2 \pm 0.4\text{mV}$  when estimated using the two microelectrode recording technique. These values were not dissimilar from the resting membrane potential of  $-54.0 \pm 0.9\text{mV}$  obtained from the neurone *in situ* (Anderson, 1995); the slightly more positive resting membrane potential values obtained from the isolated neurones may be attributed to subtle changes in the composition of the cytoplasm, resulting from the severing of the axon process

(Usherwood *et al.*, 1980). It is most likely that the difference seen in the resting membrane potential values obtained from the isolated BA1 motoneurone, using either a single or paired microelectrodes, was the result of damage to the plasma membrane from the impalement of the second microelectrode. The mean membrane input resistance value determined for the isolated BA1 motoneurone was approximately  $7\text{M}\Omega$ . This value was slightly higher than that obtained *in situ* ( $4.3\text{M}\Omega$ ; Anderson, 1995). This was understood to be the consequence of the loss of the axonal and dendritic processes following isolation, since, membrane input resistance is inversely proportional to membrane surface area (Aidley, 1991).

The injection of current pulses, whether hyperpolarizing or depolarizing, evoked characteristic changes in membrane potential. Along with the resting membrane potential and neuronal input resistance values, the membrane responses to current injection were used as determinants of neuronal viability. Viable isolated BA1 motoneurons elicited a membrane hyperpolarization and a prominent membrane 'rebound' on the injection of hyperpolarizing current. Owing to the relatively positive resting membrane potential of these cells and the presence of a voltage-dependent calcium ( $I_{\text{Ca}}$ ) current in the BA1 motoneurone (Anderson, 1995), it is likely that the membrane 'rebound' observed on current pulse termination is the result of  $I_{\text{Ca}}$  activation. It was shown that depolarizing current pulses evoke membrane oscillations in isolated BA1 motoneurons.

Whilst the amplitude of the oscillations could vary between preparations, 'overshooting' action potentials were never evoked, even when relatively large depolarizing currents were injected into the soma. Such observations have been reported from isolated cockroach  $\text{D}_1$  motoneurons (Pitman, 1988). Furthermore, identified insect motoneurons *in situ* have been shown not to generate 'overshooting' action potentials upon depolarization (Pitman, 1975; Goodman and Heitler, 1979; L. J. Anderson, personal communication). It would suggest that

such membrane activity is due to a prevalence of outward membrane currents counteracting inward membrane currents to a degree that action potentials cannot be generated in many insect motoneurons under 'normal' conditions. Action potentials have been reported to develop, however, during long-term recordings from the cockroach  $D_f$  motoneurone, in the absence of pharmacological treatment. Whilst the mechanisms for their development remains to be determined, they are  $Ca^{2+}$ -dependent and evoked on membrane depolarization (Hancox and Pitman, 1992).

#### 2.4.2. A pharmacological profile of the isolated BA1 motoneurons

##### 2.4.2.1. The presence of cholinergic receptors on the isolated motoneurone soma

In the series of pharmacological experiments presented here, it has been shown that a population of functional nicotinic ( $\alpha$ -BTX-sensitive) and muscarinic ( $\alpha$ -BTX-insensitive) cholinergic receptors exist on the somal membrane of the BA1 motoneurone. These findings are in agreement with a recent study which reported the presence of such cholinergic receptors, on the BA1 motoneurone *in situ* (Anderson, 1995).

The presence of cholinergic receptors on the isolated BA1 motoneurone preparation was demonstrated by the bath-application of ACh and the non-selective cholinergic agonist, carbachol, to the neurone. Both agonists induced a dose-dependent membrane depolarization with an increase in membrane conductance. The threshold for induction of membrane depolarization was usually between  $10^{-5}M$  and  $10^{-4}M$  ACh. When the effects of carbachol were tested on isolated BA1 motoneurons, it was seen to evoke a more potent response than ACh on the neurone. That is, when the same concentration of agonist was bath-applied to isolated BA1 motoneurons, the degree of change in membrane depolarization and membrane input resistance was greater with carbachol. This is

because carbachol is a non-hydrolyzable analogue of ACh, i.e. it is unaffected by the hydrolytic enzyme acetylcholinesterase - an enzyme known to be widely distributed in the insect CNS (see Pitman, 1985). Since, the agonist cannot be degraded, it is a more persistent agonist than ACh.

*The presence of a nicotinic ( $\alpha$ -BTX-sensitive) acetylcholine receptor population*

Although the presence of acetylcholine receptors on freshly isolated unidentified adult locust thoracic neurones has previously been demonstrated (Usherwood *et al.*, 1980; Suter and Usherwood, 1985), more recently the pharmacological profiles of both nicotinic and muscarinic acetylcholine receptors of isolated locust neurones have been thoroughly examined (Benson, 1992). The nicotinic response has been described as the fast component of the cholinergic response (ACh1), whilst the muscarinic response is the slow component (ACh2) (Benson and Neumann, 1987; Benson, 1992). The coexistence of these receptor subtypes on other insect neurones has been shown using electrophysiological techniques on the cockroach D<sub>f</sub> motoneurone (David and Pitman, 1990), cockroach dorsal unpaired median (DUM) neurones and giant interneurones (Lapied and Hue, 1991; Le Corrionc and Hue, 1993) and the principal planta retractor (PPR) motoneurone of *Manduca sexta* (Trimmer and Weeks, 1989).

The bath-application of nicotine evoked a dose-dependent membrane depolarization which was accompanied by an increase in membrane conductance; it was found to be the most potent agonist tested on the isolated BA1 motoneurone, inducing a response at bath concentrations of  $\geq 10^{-9}$ M. It is believed that the high sensitivity of the isolated neurone to the agonist is a closer reflection of the sensitivity of the receptor *in vivo*, which has been exposed by the increased accessibility of the plasma membrane, as a result of cell isolation (Usherwood *et al.*, 1980). The sensitivity of the BA1 motoneurone may indicate the high

physiological importance of nicotinic receptor activation in fast synaptic transmission at the stretch receptor neurone - BA1 motoneurone synapse modulating wingbeat frequency in the intact animal.

The nicotine-induced membrane depolarization and increase in membrane conductance observed in the isolated BA1 motoneurone, could be the result of activation of a predominantly  $\text{Na}^+$ -mediated current (nicotinic acetylcholine receptor channels are also permeable to  $\text{K}^+$  and possibly  $\text{Ca}^{2+}$ : David and Sattelle, 1990). This is because studies using insect neurone preparations have demonstrated the nicotinic response has a dependence on external  $\text{Na}^+$  concentration (Kerkut *et al*, 1969a), and analysis of the reversal potential of the response is consistent with this (values between -40 and +20mV have been reported: Pitman and Kerkut, 1970; David and Sattelle, 1990; Benson, 1992). The ability of the nicotinic acetylcholine receptor ion channel on the BA1 motoneurone to desensitize was demonstrated in this study. Ligand-gated ion channels, such as the nicotinic acetylcholine receptor and the  $\text{GABA}_A$  receptor, open following agonist binding to receptor binding sites, and can then close for long periods with the agonist still bound. This is termed desensitization. Desensitization can be an important mechanism for the shaping of synaptic potentials, however, this is not thought likely for nicotinic acetylcholine receptor-gated channels due to their desensitization kinetics (see Jones and Westbrook, 1996). These channels show slow desensitization and fast recovery kinetics, as opposed to  $\text{GABA}_A$ -gated channels, which spend a relatively large fraction of their time in a desensitized state following activation (Jones and Westbrook, 1996). Desensitization was seen in the current study as the gradual return to the normal resting membrane potential and membrane input resistance in the presence of nicotine, following the induction of membrane depolarization and conductance increase.

Neuronal nicotinic acetylcholine receptors in other insect preparations resemble the vertebrate neuromuscular junction cholinergic receptors in their high sensitivity to the potent snake (*Bungarus multicinctus*) toxin,  $\alpha$ -bungarotoxin, (David and Sattelle, 1990; Benson, 1992) which is routinely used as a tool to verify the presence of nicotinic acetylcholine receptors, and to unmask the muscarinic ( $\alpha$ -BTX-insensitive) component of the acetylcholine response.  $\alpha$ -BTX is an irreversible antagonist of the acetylcholine response in insect neurones, being an effective antagonist at nanomolar concentrations (Sattelle *et al*, 1980). The nicotinic nature of the response evoked by the bath-application of nicotine to the isolated BA1 motoneurone was verified using  $\alpha$ -BTX. However, full antagonism of the nicotine-induced response did require  $10^{-5}$ M (50 minutes)  $\alpha$ -BTX, which is greater than that usually used (Anderson, 1995; J. A. David, personal communication). This is a reflection of the potent nature of nicotine as an agonist, since acetylcholine and carbachol are less potent in this preparation.

*The presence of a muscarinic ( $\alpha$ -BTX-insensitive) acetylcholine receptor population*

Having established the presence of nicotinic acetylcholine receptors on the somal membrane of the BA1 motoneurone, to confirm the observations of Anderson (1995), the presence of a muscarinic cholinergic receptor was investigated. Previous preliminary voltage-clamp experiments have indicated that muscarinic receptors, with a 'mixed' nicotinic/muscarinic receptor pharmacology are present on the isolated neurone (Anderson 1995). These cholinergic receptors are sensitive to both nicotinic and muscarinic cholinergic ligands. The existence of insect cholinergic receptors with muscarinic or 'mixed' nicotinic/muscarinic properties has been reported on various insect neurone preparations, including isolated locust thoracic neurones (Benson and Neumann, 1987; Benson, 1989,



1992, for review see Benson, 1993), locust synaptosomes (Knipper and Breer, 1988), the cockroach D<sub>f</sub> motoneurone *in situ* (David and Pitman, 1990, 1992, 1993a), cockroach DUM neurones (Lapied *et al*, 1990, 1992; Tribut *et al*, 1994) and the PPR motoneurone of *Manduca sexta* (Trimmer and Weeks, 1989). In the present study, the effects of muscarinic receptor activation by several known vertebrate muscarinic agonists were examined using the intracellular current-clamp recording technique.

The vertebrate muscarinic agonist, arecoline (ARE), induced a dose-dependent membrane depolarization (threshold  $10^{-5}\text{M}$  to  $10^{-4}\text{M}$ ) in isolated BA1 motoneurones which was associated with an increase in membrane conductance in some preparations. Whether an increase in membrane conductance was evoked by the agonist, did not appear to be dependent on the resting membrane potential of the isolated neurone. In fact, the conductance increase appeared to be associated with a nicotinic component of the ARE response in this neurone. In the presence of  $\alpha$ -BTX, bath-application of ARE (even at relatively high concentrations, for example,  $10^{-2}\text{M}$ ) evoked membrane depolarization with no detectable change in membrane conductance, when it had done so before incubation in  $\alpha$ -BTX. A non-specific cholinergic action of ARE on the BA1 motoneurone has also been reported using isolated locust neurones (Benson, 1992) and cockroach DUM neurones *in situ* (Tribut *et al*, 1994).

When the effects of the non-specific vertebrate muscarinic receptor agonists pilocarpine (PILO) and oxotremorine (OXO) and the specific M<sub>1</sub> receptor agonist McN-A-343 (McN) on the neurone were compared with those of ARE, they were found to be less potent in their ability to induce membrane depolarization. The order of potency for these muscarinic agonists to induce a response in the isolated BA1 motoneurone was found to be ARE > PILO > OXO > McN, in descending order.

It was of interest to note that PILO (in the absence of  $\alpha$ -BTX) induced membrane depolarization with a decrease in membrane input resistance, which reversed on washing, in one isolated BA1 motoneurone preparation. Since, the muscarinic response of the isolated BA1 motoneurone did not appear to be associated with an increase in membrane conductance, it was thought that PILO could be acting as a non-specific cholinergic agonist like ARE. This muscarinic agonist has been reported to desensitize the nicotinic response of isolated locust neurones (Benson, 1992), suggesting the response observed in this study could have a nicotinic component.

Unfortunately, there is insufficient evidence to determine the muscarinic receptor subtype mediating the responses observed in the isolated BA1 motoneurone, from the experiments discussed above. However, because the bath-application of McN to isolated BA1 motoneurons increased  $[Ca^{2+}]_i$  (see Section 3.3.2.), it would appear that the receptor at least resembles the vertebrate  $M_1$  muscarinic receptor subtype.

Whether this receptor is a classical muscarinic receptor with a distinct pharmacological profile that resembles the  $M_1$  vertebrate receptor has yet to be established. This scenario, however, is thought unlikely. A muscarinic receptor with a 'mixed' cholinergic pharmacology has already been identified on the BA1 motoneurone *in situ* (Anderson, 1995). Furthermore, using selective cholinergic agonists and antagonists in the presence of  $\alpha$ -BTX, the muscarinic component of this receptor-mediated response could not be classified by the established vertebrate classification system i.e. an  $M_1$ ,  $M_2$  or  $M_3$  muscarinic receptor subtype (Anderson, 1995). Other insect preparations have also been reported to possess muscarinic receptors that are sensitive to more than one subtype-selective agonist and antagonist. The muscarinic response of freshly dissociated locust neurones is reported to be preferentially sensitive to  $M_1$  and  $M_3$  muscarinic antagonists



(Benson 1992), whilst the cockroach  $D_f$  motoneurone is sensitive to  $M_1$  and  $M_2$  agonists and antagonists (David and Pitman, 1993a). In addition, muscarinic receptors located on insect presynaptic neuronal membranes, acting as autoreceptors to inhibit synaptic transmission, have been found to have a pharmacological profile resembling the  $M_2$  muscarinic receptor subtype; for example, the muscarinic receptors of the locust winghinge stretch receptor (Leitch and Pitman, 1995) and the cockroach cercal afferent terminals (Le Corrionc *et al*, 1991). The characteristics and functions of insect muscarinic receptors have recently been reviewed by Trimmer (1995). Future studies examining the cholinergic receptors of the BA1 motoneurone should include voltage-clamp experiments to clarify the nature of the muscarinic receptor and the ionic dependency of the agonist-induced response.

It is proposed that the muscarinic agonist-induced responses obtained in the isolated BA1 motoneurone, occur as a result of muscarinic receptor-mediated decrease in  $K^+$  conductance. There are two lines of evidence to support this proposal. Firstly, the effects of McN ( $10^{-4}M$ ) have been studied extensively in the cockroach  $D_f$  motoneurone - a neurone known to have similar pharmacological properties to the locust BA1 motoneurone. Under voltage-clamp, McN induces an inward current, known to be the consequence of a decrease in  $I_{K(Ca)}$  caused by an McN-induced increase in  $[Ca^{2+}]_i$ . It has been established that the increase in  $[Ca^{2+}]_i$  results from the McN-induced  $IP_3$ -mediated release of  $Ca^{2+}$  from intracellular stores (see Sections 3.3.3. and 3.4.; David and Pitman, 1996b), and causes  $Ca^{2+}$ -dependent inactivation of the  $I_{Ca}$  current, which in turn decreases  $I_{K(Ca)}$ . Secondly, when the McN-induced response of the BA1 motoneurone *in situ* was examined under voltage-clamp, McN ( $10^{-4}M$ ) also induced an inward current (Anderson, 1995). This current comprised of two voltage-dependent  $K^+$  currents, one of which was shown to be dependent on intracellular  $Ca^{2+}$  (Anderson, 1995).

However, as it appears that  $I_{K(Ca)}$  is small, and McN does not affect  $I_{Ca}$  in this neurone (Anderson, 1995), it is thought unlikely that the agonist-induced inward current of the BA1 motoneurone is the result of a reduction in  $I_{K(Ca)}$  by  $Ca^{2+}$ -dependent inactivation of the  $I_{Ca}$  (as seen in the  $D_f$  motoneurone). McN is known, however, to increase  $[Ca^{2+}]_i$  in the isolated BA1 motoneurone (see Section 3.3.2.), so it is proposed that the McN-induced rise in  $[Ca^{2+}]_i$  is involved in the reduction of a  $K^+$  conductance of the BA1 motoneurone. Supporting this proposal is the report of an apamin-sensitive  $Ca^{2+}$ -activated  $K^+$  channel, the function of which is modulated  $[Ca^{2+}]_i$  in cultured rat-muscle cells (Blatz and Magleby, 1986), and a  $Ca^{2+}$ -activated  $K^+$  conductance in hippocampal neurones, that is activated by  $Ca^{2+}$ -calmodulin kinase II (Müller *et al*, 1992).

In the current series of experiments, ARE, in the presence of  $\alpha$ -BTX, could induce relatively large membrane depolarizations without a detectable change in membrane conductance. A similar membrane response has been induced by muscarine and oxotremorine in larval *Manduca sexta* PPR motoneurones *in situ* (Trimmer and Weeks, 1989, 1993). It is proposed that the absence of a detectable change could occur under the following conditions. Firstly, the resting membrane potential of the neurone is close to the  $K^+$  equilibrium potential ( $E_K$ ), which is likely because  $K^+$  is the major contributory ion to the resting membrane potential (Hodgkin and Keynes, 1955). Secondly, the equilibrium potentials of both  $Na^+$  ( $E_{Na}$ ) and  $Ca^{2+}$  ( $E_{Ca}$ ) are sufficiently positive to the membrane potential to create large driving forces on both ions. Thirdly, the isolated neurone has a relatively high input resistance; values up to  $12M\Omega$  (mean  $7M\Omega$ ) were obtained from the isolated BA1 motoneurone, as opposed to  $4.3M\Omega$  from this neurone *in situ* (Anderson, 1995). Membrane depolarization occurs as a secondary effect of muscarinic receptor-mediated events. The agonist-induced reduction in the  $K^+$  current occurs, but could go undetected under current-clamp,

because  $E_K$  is close to the resting potential and the small change in membrane conductance would have little effect on the input resistance of the neurone. The relatively large membrane depolarization induced by ARE could occur if the membrane depolarization was sufficient to induce activation of  $I_{Ca}$  and  $I_{Na}$ . Furthermore, this could occur without a detectable change in input resistance given large driving forces on these cations to enter the neurone.

The lack of an observable membrane depolarization following the bath-application of the other muscarinic agonists tested (PILO, OXO, and McN), may also be explained using this hypothesis. If these agonists are less potent in their ability to evoke a decrease in  $K^+$  conductance, the activation of  $I_{Ca}$  and  $I_{Na}$  will not occur, and consequently, membrane depolarization is not observed.

Attempts were made using the non-specific cholinergic antagonist, atropine (ATR), and the muscarinic antagonist scopolamine (SCOP) to verify the ARE-induced membrane depolarization, in the presence of  $\alpha$ -BTX, was the result of muscarinic receptor activation. Both of these compounds are routinely used as antagonists of the muscarinic response of insect neurones (for example, Anderson, 1995; Benson, 1992 and David and Pitman, 1993a). However, in the current study they were found to be ineffective as antagonists of the ARE-induced membrane depolarization (in the presence of  $\alpha$ -BTX). Given the relatively high muscarinic agonist concentrations required to evoke membrane depolarization at resting membrane potential, it is proposed that they were unable to antagonize the response due to agonist saturation and/or greater agonist binding affinity of the muscarinic receptor binding sites. That is, the concentration of agonist (which was normally greater than the antagonist concentration used), was sufficient to displace the bound antagonist from the receptor protein, thus, rendering it ineffective. Similar observations were obtained when attempting to antagonize the DA-induced depolarization recorded from the BA1 motoneurone (see below).

However, using the  $\text{Ca}^{2+}$ -sensitive fluorescent dye, fluo-3, to examine DA-induced changes in  $[\text{Ca}^{2+}]_i$  (DA lowers  $[\text{Ca}^{2+}]_i$ ), when the DA-antagonist, fluphenazine, was used at the same concentration as DA, the DA-induced response was blocked (see Section 3.3.3). Therefore, given both these DA-induced effects are mediated by the activation of DA receptors, it would seem the DA-induced membrane depolarization is not a direct result of a decrease in  $[\text{Ca}^{2+}]_i$ .

In addition to the induction of membrane depolarization, the excitatory nature of the cholinergic response on the isolated BA1 motoneurone soma, was evident from an increase in amplitude of the membrane 'rebounds' that followed each membrane hyperpolarization used to monitor membrane input resistance. The bath-application of acetylcholine, carbachol, nicotine, arecoline and pilocarpine could all be associated with an increase in membrane 'rebound' amplitude, which reversed on washing of the preparation. The appearance of 'rebounds' or an increase in their amplitude from that observed pre-agonist application did not have to be accompanied by a prominent agonist-induced membrane depolarization, as was illustrated following the bath-application of  $10^{-4}\text{M}$  PILO to one isolated BA1 motoneurone. This increase in membrane excitability is understood to be the result of an agonist-induced transient inward current (a steady inward current would cause depolarization). Voltage-clamp studies would determine the nature of this current, however, it is suggested that if they accompany membrane depolarization induced by nicotinic receptor activation, it is likely the membrane 'rebounds' are generated by an  $I_{\text{Na}}$  and/or  $I_{\text{Ca}}$  inward current. However, if they are associated with muscarinic receptor activation, it is likely they would result from a decrease in  $\text{K}^+$  conductance.

Another example of increased membrane excitability is the decrease in spike threshold of a neurone. Although not examined in the current study, preliminary experiments on the BA1 motoneurone *in situ* have demonstrated that

muscarinic receptor activation decreases the spike threshold of this motoneurone (Anderson, 1995). Similar observations have been reported from other insect postsynaptic neurones, such as locust VPLI interneurones (Baines and Bacon, 1994), the cockroach  $D_f$  motoneurone *in situ* (J. D. Mills, personal communication) and giant interneurones (Le Corrionc and Hue, 1993) and *Manduca sexta* PPR motoneurones (Trimmer and Weeks, 1989, 1993). Consequently, the activation of muscarinic receptors on postsynaptic membranes has been implicated in the modulation of membrane excitability and synaptic transmission (for recent review see Trimmer, 1995).

In addition to the ARE-induced responses described above, membrane oscillations were seen to accompany the agonist-induced membrane depolarization in some preparations, both in the presence and absence of  $\alpha$ -BTX. The physiological basis of this observation is not currently known, however, I propose that  $[Ca^{2+}]_i$  oscillations could underlie the ARE-induced changes in membrane potential. Future experiments should examine the effects of ARE on  $[Ca^{2+}]_i$  using  $Ca^{2+}$ -sensitive fluorescent dyes and confocal imaging techniques as described in Chapter 3. These experimental tools can allow the nature of changes in  $[Ca^{2+}]_i$  to be studied; for further details see Section 3.4.

#### 2.4.2.2. The presence of GABAergic receptors on the isolated motoneurone soma

The sensitivity of the isolated BA1 motoneurone soma to the inhibitory neurotransmitter, GABA, and the vertebrate GABA<sub>A</sub> receptor agonist, muscimol, was demonstrated by the local pressure application of each agonist onto the cell membrane. This method of application allowed brief and regular agonist-induced responses to be evoked by the neurone, which did not show evidence of GABA receptor desensitization. Consequently, agonist-induced responses of similar amplitude and duration were consistently evoked, and this facilitated experiments

which examined the nature of the GABAergic response of isolated BA1 motoneurons.

Under current-clamp, both agonists evoked a voltage-dependent change in the membrane potential. At potentials positive to the reversal potential membrane hyperpolarizations were elicited, whilst at more negative potentials, membrane depolarizations were observed. The estimated reversal potential of the GABA and muscimol response under current-clamp in the isolated neurons was  $-69.8 \pm 2.1\text{mV}$  and  $-67.3 \pm 1.5\text{mV}$ , respectively. When tested, these values were not found to be significantly different (ie  $P > 0.05$ ), suggesting that the GABA receptor present on the isolated neurone membrane could resemble either the vertebrate GABA<sub>A</sub> or GABA<sub>C</sub> receptor subtype. Like receptors for other classes of neurotransmitter in invertebrate species, it is expected that it will not fall into the distinct vertebrate neurotransmitter receptor classification system (Millar *et al*, 1994; for reviews see Rauh *et al*, 1990 and Anthony *et al*, 1993). When the agonist-induced responses were examined under voltage-clamp, it was seen that both agonists induced an inward membrane current at holding potentials positive to the reversal potential, and an outward current at potentials negative to this potential. The estimated reversal potential for GABA and muscimol was  $-68.9 \pm 2.8\text{mV}$  and  $-66.0 \pm 3.2\text{mV}$ , respectively. Like the values obtained under current-clamp, they were found to be not statistically different ( $P > 0.05$ ), thus, suggesting that the agonists acted at a similar type of receptor. When the agonist-induced current of both GABA and muscimol responses were examined under voltage-clamp, they displayed a linear voltage-dependent relationship. This implied that they activated non-rectifying voltage-dependent ion channels; together with the reversal potentials values obtained for the agonist-induced responses, it would not be unreasonable to suggest that the GABA receptors gated chloride ion channels (Pitman and Kerkut, 1970; Pinnock *et al*, 1988). Although



such observations indicate that the GABA receptors present on the BA1 motoneurone soma could resemble the GABA<sub>A</sub> or GABA<sub>C</sub> vertebrate receptor subtype, further analysis of the GABA response using selective receptor subtype pharmacological agents is required to establish whether this insect GABA receptor can be classified according to this scheme. It is possible that some GABA<sub>B</sub> receptors are present on the BA1 motoneurone, where they represent only a small proportion of the GABA receptor population, since the Cl<sup>-</sup> channel blocker picrotoxin can abolish the GABA response in this neurone (unpublished observations).

Comparing the peak amplitude of the membrane currents evoked by GABA in insect neurones *in situ*, and those evoked in the isolated BA1 motoneurone, overall, those of the isolated neurone were smaller (<2nA, as opposed to up to 20nA: Sattelle *et al*, 1988). It is known that the amplitude of the GABA response is dose- and voltage-dependent response (Sattelle *et al*, 1988). However, it is believed that there were several contributing factors to the small amplitude of the GABA and muscimol responses of the isolated BA1 motoneurone. Firstly, agonist pulses were deliberately adjusted so that they evoked only small membrane hyperpolarizations (5 - 6mV) at the resting membrane potential (which was found to be approximately 25mV positive to the GABA reversal potential). Secondly, the absence of GABA receptors, usually present on the axonal and dendritic processes could contribute to smaller membrane currents being observed, and thirdly, a relatively low density of somal GABA receptors could result in relatively small responses being recorded. Similar small GABA-evoked membrane currents have been reported in freshly isolated thoracic locust neurones and cultured isolated embryonic cockroach brain neurones (Lees *et al*, 1987; Neumann *et al*, 1987).

It was observed that the isolated neurone preparations were more sensitive to the pressure-application of GABA than other insect neurones *in situ*. That is, the concentration of agonist in the pressure-application microelectrode required to evoke 5 - 10mV membrane hyperpolarizations is greater for neurones within their ganglionic environment, for example  $10^{-1}\text{M}$  to  $1\text{M}$  (R. M. Pitman, personal communication) as opposed to  $10^{-4}\text{M}$  to  $10^{-2}\text{M}$  used in the present study. The use of lower agonist concentrations when examining the pharmacological properties of isolated neurones has previously been noted (see above), and is a reflection of the true sensitivity of a neurone to an agonist.

#### 2.4.2.3. The presence of dopaminergic receptors on the isolated motoneurone soma

The bath-application of DA to isolated BA1 motoneurones consistently induced a dose-dependent membrane depolarization which was not usually associated with a detectable change in membrane conductance; the range of DA concentrations tested was  $10^{-4}\text{M}$  to  $10^{-2}\text{M}$ . Attempts to antagonize this response with known antagonists of the DA response observed in an identified cockroach motoneurone (Davis and Pitman, 1991), were unsuccessful.

Control experiments eliminated the possibility that the membrane depolarization observed following the bath-application of DA was an experimental artefact evoked by saline and/or ascorbic acid (which was used to prevent oxidation of DA). Given the data presented here, it could be suggested that DA acts non-specifically at other neurotransmitter or neuromodulator receptors (for example, octopamine and/or serotonin) present on the BA1 motoneurone. However, this is thought unlikely, since, using fluorescence imaging techniques (see Section 3.3.4) it has been shown in the current study that DA induces dose-dependent decreases in intracellular calcium ( $[\text{Ca}^{2+}]_i$ ) in isolated BA1 motoneurones. The DA-induced lowering of  $[\text{Ca}^{2+}]_i$  was blocked by the



antagonist fluphenazine ( $10^{-4}\text{M}$ ), and such changes in  $[\text{Ca}^{2+}]_i$  were not observed following the addition of ascorbic acid or saline.

Why it was not possible to antagonize the DA-induced changes observed in isolated BA1 motoneurons was not fully established. The same antagonists used at lower concentrations (flupenthixol,  $10^{-9}\text{M}$ ; fluphenazine  $10^{-6}\text{M}$ ) and after shorter incubation times (up to 25 minutes) were reported to antagonize the response evoked by the local pressure application in the cockroach common inhibitory motoneurone ( $\text{D}_3$ ) under voltage-clamp (Pitman and Davis, 1988; Davis and Pitman, 1991). One likely reason for antagonism of these responses was due to the use of short applications of DA ( $10^{-1}\text{M}$ ; 1s) to elicit a response; such a method of administration would enable antagonism of the induced response as DA would be less likely to displace the antagonist from the receptor binding sites. It was noted that responses of this cockroach motoneurone to DA differed slightly from those recorded from the isolated BA1 motoneurone. When pressure-applied to the  $\text{D}_3$  motoneurone under current-clamp, DA evoked membrane depolarization, which was associated with a change in membrane conductance (Pitman and Davis, 1988; Pitman and Baker, 1989). The observed change in conductance is believed to be associated with the application of a high concentration of DA to the neurone ( $10^{-1}\text{M}$ ), because only a slight (10%) increase in membrane conductance was observed in one isolated BA1 motoneurone preparation following the bath-application of  $10^{-2}\text{M}$  DA (not shown).

Since it was not possible to block the DA-induced response using non-specific DA receptor antagonists, in isolated BA1 motoneurons using the experimental techniques as described, the use of specific  $\text{D}_1$ - and  $\text{D}_2$ -type DA receptor agonists and antagonists was not attempted. Consequently, it was not possible to characterize the receptors mediating the actions of DA on this neurone. It is thought that such a task would be facilitated by studying the DA response of

this neurone using a voltage-clamp protocol as employed by Pitman and Davis (1988). Under such experimental conditions one is examining the underlying ionic dependency of the response (the problem of any voltage-dependency in the nature of the response is alleviated), rather than the secondary effects of the changes on the neuronal membrane properties. Consequently, it is anticipated that agonist concentrations required to elicit a response would be lower, making it possible to antagonize the agonist-induced response. It has been shown in this study that this isolated neurone preparation is suitable for voltage-clamp experiments.

#### *Transduction mechanisms of the BA1 motoneurone DA receptor*

Although it has been known for a number of years that as one of the catecholamines, DA is present in the insect nervous system (for review see Evans, 1980; Fleming and Pitman, 1983), little has been established regarding the pharmacological properties of the DA receptor(s) of this group. It would appear that a DA receptor resembles the vertebrate  $D_1$  receptor subtype more than the  $D_2$  subtype (Gotzes *et al*, 1994; Kokay and Mercer, 1996), although  $D_2$  receptor subtype antagonists have been reported to antagonize DA-induced currents in the cockroach  $D_3$  motoneurone (Davis and Pitman, 1991). It may therefore be anticipated that the events following DA binding to its receptor by which it exerts its effects are less clearly defined than those established for the vertebrate DA receptors.

The DA receptors of the cockroach salivary gland acinar cell have been the most extensively studied insect DA receptors. They have been shown to have a  $D_1$ -like pharmacology and appear to be coupled to at least two second messengers (Evans and Green, 1990). Their activation evokes membrane hyperpolarization and fluid secretion (House, 1973; Smith and House, 1977). An increase in  $I_{K(Ca)}$  conductance underlies the change in membrane potential (Ginsborg *et al*, 1980)

and it has been suggested that this is the result of the activation of PLC (A. M. Evans, unpublished observations). On the other hand, increased fluid secretion has been associated with an increase in intracellular cAMP (Grewé and Kebabian, 1982; Gray *et al*, 1984).

Since, the identity of the BA1 motoneurone DA receptor and its mechanisms of action have yet to be established, one can only hypothesize how DA is acting on this neurone. It has been shown in this study that DA induces the lowering of  $[Ca^{2+}]_i$  (see Section 3.3.4) and the possible mechanisms by which DA acts to lower  $[Ca^{2+}]_i$  could involve both cAMP and the stimulation of PLC (see Discussion, Section 3.4.). Although it is not currently known whether the decrease in  $[Ca^{2+}]_i$  or the subsequent rise in  $[Ca^{2+}]_i$  acts to trigger membrane depolarization in the BA1 motoneurone soma or subsequent events in which DA acts as a neuromodulator (see below), it is likely that changes in  $[Ca^{2+}]_i$  have a central role in DA-induced responses. Pitman and Davis (1988) reported that when examined under voltage-clamp, DA induced a membrane current with a complex voltage-dependence in the cockroach  $D_3$  motoneurone. This current did not show a particular dependence on  $Na^+$ ,  $K^+$  or  $Cl^-$ . However, preventing  $Ca^{2+}$  influx via  $I_{Ca}$  by the application of  $Cd^{2+}$ , verapamil or the use of low  $Ca^{2+}$ -saline, abolished the DA-evoked currents. Further clarification of the ionic basis of this DA response has not been reported. Given the observed responses of the isolated BA1 motoneurone to the bath-application of DA using electrophysiological recording techniques and fluo-3 with fluorescence imaging techniques (see Section 3.3.4), the mechanism by which DA is most likely to induce membrane depolarization, without inducing a detectable change in membrane input resistance is that the reversal potential for the ions involved in the DA response could be sufficiently positive that an extremely small, and undetectable change in membrane conductance would be sufficient to cause membrane depolarization. This proposal,

however, is hard to test directly, since the DA response has an unusual voltage-dependence (Pitman and Davis, 1988).

#### 2.3.2.4. Modulation of the GABA response by dopamine in isolated BA1 motoneurons

The modulation of ligand-gated ion channel function has become the focus of a great deal of interest for the understanding of the molecular basis of synaptic plasticity (for reviews see Huganir and Greengard, 1990; Swope *et al*, 1992; Raymond *et al*, 1993). Insect muscarinic receptors have recently been shown to participate in such modulation of neuronal activity (see Trimmer, 1995; David and Pitman, 1996a). However, little is known about the neuromodulatory effects of biogenic amines in insects. A major focal point of these pharmacological studies was to investigate the potential modulatory actions of DA on the GABA response.

It has been shown, irrespective of its effects on the membrane potential, that DA potentiated the GABA-induced membrane hyperpolarization observed in isolated BA1 motoneurons. The enhancement of the GABA response outlasted the period of DA application and washing, even when the membrane potential and input resistance had returned to their respective levels, seen before DA application.

The DA-induced enhancement of the amplitude and/or duration of the GABA response could not be explained by long-term changes in membrane conductance; early changes in input resistance associated with the bath-application of DA recovered to the level seen before DA application, and the GABA responses continued to be potentiated. Neither could they be associated with a change in membrane potential. This is because (i) when the GABA response was examined under current- and voltage-clamp, the duration of the response appeared unaffected by the holding membrane potential (see Section 2.3.3), (ii) when the

membrane potential was allowed to return to that observed before DA application (by temporarily stopping the application of GABA), the subsequent GABA responses remained greater in amplitude and duration than seen before DA application, and (iii) it could be anticipated that with membrane hyperpolarization, the amplitude of the GABA response would decrease as the membrane potential approached the reversal potential of the GABA response, since, the current/voltage relationship of the GABA response in this isolated neurone was shown to have a linear, non-rectifying relationship (see Section 2.3.3). However, it did not, that is the amplitude of the GABA response was seen to increase. Although not directly shown in the current study, the GABA reversal potential could be assumed to be the  $\text{Cl}^-$  equilibrium potential ( $E_{\text{Cl}}$ ), given the reversal potential value of the GABA-induced response and its current/voltage relationship. These features are typical of GABA-gated chloride channels found in insect neurones (Pitman and Kerkut, 1970; Sattelle *et al*, 1988).

One possible explanation for the enhancement of the GABA response is phosphorylation of the GABA receptor protein by protein kinases, since it is understood this GABA receptor may resemble the vertebrate  $\text{GABA}_A$  and/or  $\text{GABA}_C$  receptors in its profile (see above), and the channel function of both subtypes has been shown to be modulated by PKA and PKC (see Swope *et al*, 1992; Feigenspan and Bormann, 1994). Furthermore, although it has not yet been established, it is thought feasible that the transduction mechanisms of the DA receptor of this neurone could involve the activation of PKA and PKC. This is because there is evidence that the DA receptor of the cockroach salivary gland is coupled to cAMP and PLC (A. M. Evans, unpublished observations). In order to evoke potentiation of a ligand-gated ion channel response, phosphorylation must result in one or more of the following: (i) decrease in rate of receptor desensitization so that, following GABA binding to the receptor, the channel

spends proportionally more time in a functionally open state, (2) an increase in the mean open duration time of the channel and (3) an increase the number of functional channel proteins (see Swope *et al*, 1992). To establish which of these mechanisms are involved in the modulation of GABA-gated channel function, in this neurone, further voltage- and patch-clamp studies are necessary. However, in the current study, although premature, it is tempting to speculate that the rate of GABA receptor desensitization is altered by DA. This is because the potentiated responses evoked by GABA were considered to be near maximal in the example in Figure 2.3.10, yet a degree of receptor desensitization was not evident (as indicated by a decrease in response amplitude). Furthermore, receptor desensitization had been observed in other experiments, in the absence of DA, where the response amplitude was less than shown in Figure 2.3.10.

In addition to the DA-mediated modulation of the GABA responses, another interesting phenomenon was the alteration in the DA response during repetitive GABA application. Although DA never produced membrane hyperpolarization and seldom caused a detectable change in membrane conductance when it was applied in the absence of GABA, it could cause an increase in membrane conductance associated with either membrane hyperpolarization or depolarization, when applied between successive pressure pulses of GABA. This was not deemed a concentration dependent effect, since, both could be induced over a similar concentration range of DA.

There were no indications to suggest that membrane depolarization was induced by a mechanism other than those previously proposed. However, to evoke membrane hyperpolarization, either an outward  $K^+$  current or an inward  $Cl^-$  current must be induced. A relatively simple explanation for the activation of a  $K^+$  current, would be the activation of  $I_{K(Ca)}$ , triggered by the rise in  $[Ca^{2+}]_i$  following the DA-induced lowering of  $[Ca^{2+}]_i$  (as observed using fluo-3 and fluorescence



imaging techniques, see Section 3.3.4). This reason seems feasible, however, these channels are apparently saturated by  $\text{Ca}^{2+}$  ions at relatively low  $\text{Ca}^{2+}$  concentrations (Thomas, 1984; J. D. Mills; personal communication), so whether a prominent hyperpolarization, such as seen in Figure 2.3.10, could be induced by this manner, is not known. On the other hand, it may be suggested that either an increase in ionic conductance is the result of phosphorylation of the ion channels mediated by DA-induced increases in the second messenger molecules necessary for protein kinase activation. The  $\text{Cl}^-$  and  $\text{K}^+$  ion channels have been shown to be regulated by PKA and PKC (for example, Hwang *et al*, 1992; Collier and Hume, 1995; Ivanina *et al*, 1994). Therefore, it may be considered that a DA-induced elevation in either kinase may be responsible for the membrane hyperpolarization and increase in membrane conductance. The reason why the events leading to membrane hyperpolarization should occur, apparently only in the presence of GABA and not when DA is applied alone to the neurone, is not known. One possibility is that repeated applications of GABA induce subtle changes in ion concentrations in the cytoplasm close to the intracellular surface of the plasma membrane. This small change in the ionic composition of the cytoplasm maybe sufficient to alter the nature of the DA-induced response.

Since the enhancement of the GABA response outlasts the changes in membrane potential and membrane conductance, it could be suggested that these two observations are regulated by different second messenger transduction mechanisms. It could be speculated that this is a similar scenario to that observed during the sensitisation and long-term facilitation of the withdrawal reflexes in *Aplysia* (see Section 1.1.4). Since it is a possibility that insect DA receptors are linked to the activation of PKA and PKC, the suggestion may not seem as far-fetched as it first appears. If this is so, intracellular protein kinase activities may have a critical role in the DA-induced modulation of ion channel function in BA1

motoneurones. The involvement of protein kinases in insect ion channel function has recently been suggested by David and Pitman (1996a). They have recently shown that the activation of muscarinic receptors mediates an increase in  $[Ca^{2+}]_i$ , which in turn, modulates nicotinic acetylcholine- and GABA-gated ion channels of the  $D_f$  motoneurone in the cockroach. Since, these modulatory effects outlasted the rise in  $[Ca^{2+}]_i$  evoked by muscarinic receptor activation or photolytic  $Ca^{2+}$  release, which mimicked the effect of muscarinic receptor activation, it was suggested that protein kinases play a part in this form of neuromodulation (David and Pitman, 1996a).

Whilst this is a relatively new area of research, it is felt that the modulation of ligand-gated ion channels by G-protein-coupled neurotransmitters in insect neurones, particularly in light of the results presented, is worthy of extensive examination. Questions that must be addressed regarding the DA-induced membrane depolarization and DA-potentiation of the GABA response in the isolated BA1 motoneurone include (i) what is the identity of the DA receptor and the GABA receptor on the somal membrane of this neurone? (ii) what are the effects of DA on the membrane ionic currents of the neurone, what is their ionic dependence and how do these features compare with those of the cockroach  $D_3$  motoneurone? (iii) what happens to the membrane potential, input resistance and GABA-induced response if the effects of DA on intracellular  $Ca^{2+}$  are mimicked by the injection of  $Ca^{2+}$  chelators such as EGTA or BAPTA, or  $[Ca^{2+}]_i$  is increased using caged  $Ca^{2+}$  compounds, such as nitr-5 (see David and Pitman, 1996a)? (iv) the effects of intracellular injection of the active catalytic units of protein kinases and their analogues should be examined on the ligand-gated ion channel function (nicotinic acetylcholine responses, in addition the GABA response). The modulatory effects of other G-protein coupled neurotransmitters on ligand-gated ion channel responses should also be examined, and a comparative



study should be performed using the isolated cockroach D<sub>f</sub> motoneurone as the experimental model.

To summarize:

A technique has been established for the isolation of the first basalar (BA1) motoneurone of the locust (*Schistocerca gregaria*) from its ganglionic environment. This neurone was routinely isolated, maintained in a viable state supported by locust saline, and electrophysiological recordings were made from the neurones for time periods often up to 9 hours. It was observed that the electrophysiological properties of the isolated somata were similar to those of the neurone *in situ*. By bath-applying various cholinergic agents to the preparation, the cholinergic profile of the isolated BA1 motoneurone was found to be similar to that of the neurone in its ganglionic environment (Anderson, 1995). Both nicotinic and muscarinic receptors were present on the somal membrane of this neurone, and the ionic events underlying the muscarinic agonist-induced response in this neurone have been discussed.

It was shown that the isolated BA1 motoneurone soma responded to the pressure-application of the inhibitory neurotransmitter, GABA, and the vertebrate GABA<sub>A</sub> and GABA<sub>C</sub> receptor agonist, muscimol. When these responses were examined under current- and voltage-clamp, the reversal potential and the current/voltage relationship of each response suggested that GABA receptors of this isolated neurone gate Cl<sup>-</sup> channels. Furthermore, the GABA response of this neurone was blocked by the Cl<sup>-</sup> channel blocker, picrotoxin. Therefore, it is proposed that the GABA receptor present on the BA1 motoneurone resembles either the vertebrate GABA<sub>A</sub> and GABA<sub>C</sub> receptor subtype.

The BA1 motoneurone was also shown to be sensitive to the biogenic amine, dopamine. The bath-application of DA evoked a dose-dependent membrane depolarization which was not associated with a detectable change in membrane input resistance. Ionic mechanisms underlying this response were proposed. Although attempts made to block this response with established dopaminergic antagonists were unsuccessful, evidence from this study, suggest that this was due to DA saturation of DA receptor.

It was of great interest to discover that DA potentiated the GABA-induced response of this neurone *in vitro*. When DA was bath-applied to isolated BA1 motoneurons in between repeated pressure-applications of GABA, membrane hyperpolarization or depolarization was evoked. Furthermore, DA potentiated the response evoked by GABA, that is following the bath-application of DA, the amplitude and/or duration of the GABA response was increased. The cellular events underlying this modulatory response have been discussed. It has been suggested that protein kinases may play an important role in the modulatory effects of DA.

## **Chapter 3**

### **Investigation of the effects of McN-A-343 and dopamine on intracellular $\text{Ca}^{2+}$ concentration in the first basalar motoneurone using a fluorescence imaging technique**

## INTRODUCTION

### 3.1.1. Introduction

Since neuronal cell function is dependent on the maintenance of ionic gradients across cellular membranes, particularly those of  $\text{Na}^+$ ,  $\text{K}^+$ ,  $\text{H}^+$ ,  $\text{Ca}^{2+}$  and  $\text{Cl}^-$ , the development of fluorescent indicators for *in situ* ion measurements has been of great importance for neurobiologists (see Tsien, 1989; see Haugland, 1992). It is now understood that calcium ions play a pivotal role in many aspects of neurone function (see Miller, 1988, see Simpson *et al*, 1995). Therefore, the evolution of fluorescent calcium indicators, led by Tsien and his colleagues, along with improved fluorescence microscopy techniques has been extremely important (Tsien, 1989). A range of these fluorescent probes are commercially available for various purposes, including the investigation of mechanisms of cytosolic calcium regulation and calcium-associated second messenger activity, for instance, voltage-gated calcium channels, G-protein coupled receptors, phorbol esters and calmodulin-associated reagents (see Haugland, 1992).

Fluorescent probes have become popular experimental tools because they (i) are non-cytotoxic, (ii) have a rapid temporal resolution (in the millisecond range), (iii) ion activities and free concentrations can be measured and (iv) isolated cells or tissue fragments can be used with the resolution being in the micrometer range.

### 3.1.2.1. Calcium-sensitive fluorescent probes

There is a range of fluorescent indicators used to measure cytosolic free  $[\text{Ca}^{2+}]$  in individual cells; two often used by neurobiologists are fura-2 and fluo-3; others include calcium green (which has similar properties, both spectrally and structurally, to fluo-3), and aequorin (a natural bioluminescent compound from

the marine jellyfish *Aequorea victoria*) (see Haugland, 1992). The structures of fura-2 and fluo-3 are based on the non-fluorescent  $\text{Ca}^{2+}$  chelator ethylene glycol-bis-( $\beta$ -aminoethyl)-N,N,N',N'-tetraacetic acid (EGTA) (see Figure 3.1.1.). The steric arrangement of four carboxylate groups, two amino and two ether ligand groups in the binding site of this molecule gives approximately  $10^5:1$   $\text{Ca}^{2+}$  binding selectivity over that for magnesium ions. Calcium binding diverts the lone pair of electrons on the left-hand amino nitrogen away from the rest of the conjugated system of the probe, causing large spectral changes that mimic disconnection of the nitrogen substituents (Tsien, 1980).

#### *Fura-2*

Fura-2 is the most common probe used to quantify intracellular  $[\text{Ca}^{2+}]$ . It is excited near UV wavelengths (300-400nm) and has an emission maximum of approximately 510nm. On binding to  $\text{Ca}^{2+}$ , the excitation spectrum shifts approximately 30nm to shorter wavelengths and this phenomenon forms the basis of the ratiometric technique of  $[\text{Ca}^{2+}]$  quantification with fura-2 (see Figure 3.1.1.). Following calibration, the ratio of fluorescence intensities obtained from 340/380nm or 350/385nm excitation pairs can be used to obtain an absolute measure of  $[\text{Ca}^{2+}]$ .

#### *Fluo-3*

Fluo-3 is one of a new family of fluorescent  $\text{Ca}^{2+}$  indicators excitable at visible wavelengths rather than near-UV (Minta *et al*, 1989). It has a number of advantages over its predecessors. Firstly, its excitation wavelength is 488nm, which is close to the output of argon lasers and its emission maximum is approximately 520nm (see Figure 3.1.1.). This means that there is no interference between the actinic (that is, the wavelength of light necessary for the reaction to

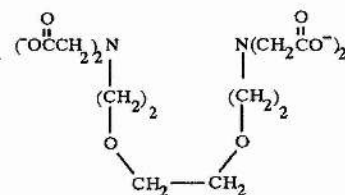
Figure 3.1.1. The biophysical properties of fura-2 and fluo-3.

A. The molecular structure of the  $\text{Ca}^{2+}$  chelator EGTA (ethylene glycol-*bis*-( $\beta$ -aminoethyl)-N, N, N', N'-tetraacetic acid).

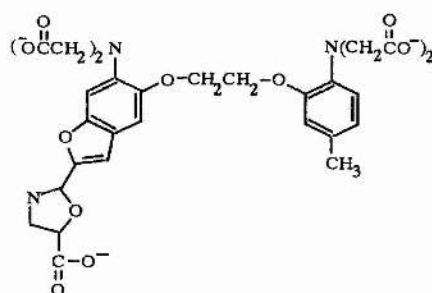
B. The molecular structures of the  $\text{Ca}^{2+}$ -sensitive fluorescent dyes fura-2 (Figure 3.1.1Bi) and fluo-3 (Figure 3.1.1Bii).

C. The excitation and emission spectra of fura-2 (Figure 3.1.1Cia and Figure 3.1.1Ciia, respectively) and fluo-3 (Figure 3.1.1Cib and Figure 3.1.1Ciib, respectively). Conditions with saturating  $\text{Ca}^{2+}$  (Sat.) were obtained with 1mM excess  $\text{CaCl}_2$ . (adapted from Thomas and Delaville, 1991).

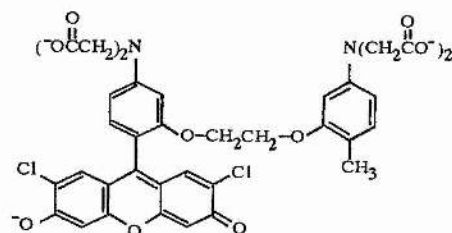
A



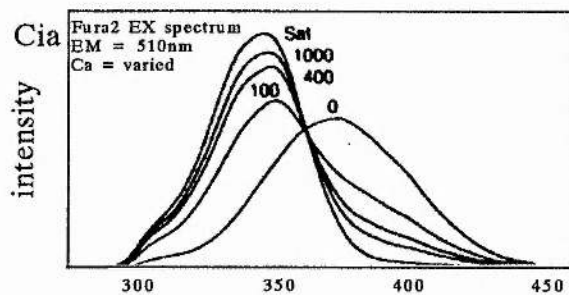
Bi



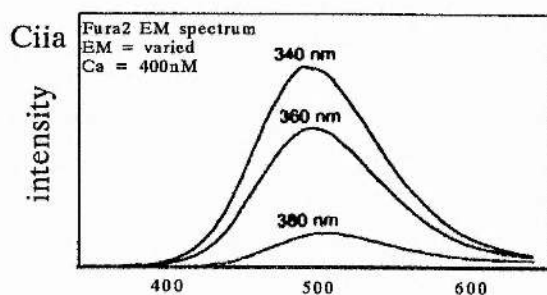
Bii



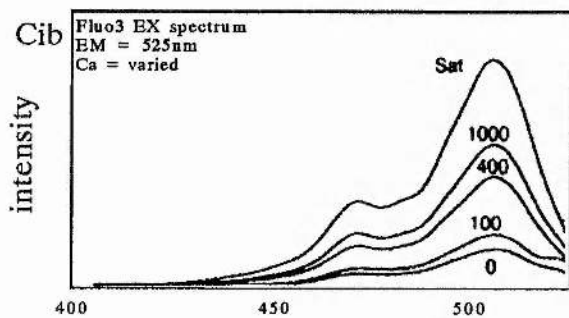
Cia



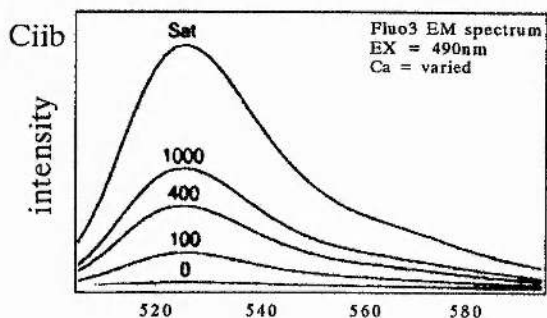
Ciia



Cib



Ciib



wavelength (nm)

occur) and monitoring wavelengths. Furthermore, fluo-3 can be used simultaneously with caged compounds which are sensitive to UV photolysis (Kao *et al*, 1989). Secondly, on binding to  $\text{Ca}^{2+}$ , fluo-3 gives a greater enhancement in fluorescence intensity than other  $\text{Ca}^{2+}$  indicators - it gives a 40 fold enhancement on  $\text{Ca}^{2+}$  binding. Thirdly, fluo-3 has a weaker affinity for  $\text{Ca}^{2+}$  which permits measurements at lower concentrations (5 - 10 $\mu\text{M}$ ). The main drawback of this indicator is that, because it does not undergo a spectral shift (either in excitation or emission) on binding to  $\text{Ca}^{2+}$ , it is not usually used in quantitative studies.

#### 3.1.2.2. Methods of application

There are two basic techniques by which calcium indicators are introduced into cells. One involves direct pressure injection of the free acid form of the probe or its ammonium or potassium salt from an intracellular microelectrode, whilst, with the other method, intact cells are incubated with the acetoxymethyl ester (AM) form of the dye. This esterified form of the indicator readily crosses the cell membrane, to be hydrolyzed to its free form by endogenous esterases; the free acid cannot permeate the cell membrane, and thus, remains in the cytosol where it can monitor the intracellular calcium concentration.

#### 3.1.3. Applications of calcium-sensitive fluorescent indicators

Calcium-sensitive probes have been used to investigate a number of different roles of calcium in cell function. For example, (i) the contributions of calcium influx through voltage-dependent calcium channels and calcium-activated calcium release on cytosolic calcium concentration (Kuba *et al*, 1992), (ii) the roles of calcium in regulating neuritic outgrowth (for example, Dyer *et al*, 1992), (iii) the role of mitochondria in the dynamics of  $\text{IP}_3$ -mediated intracellular



calcium signalling (Jouaville *et al*, 1995), and (iv) the modulation of calcium waves in myocytes (López *et al*, 1996).

Regarding the use of these indicators with neural insect preparations, Howes *et al* (1991), using fura-2, observed changes in intracellular calcium levels in growing isolated adult cockroach neurones in response to  $K^+$  depolarization. Their results indicated the presence of voltage-dependent  $Ca^{2+}$  channels on the neuronal processes of these cells in culture. The same indicator was used to monitor changes in calcium concentration associated with visual motion stimulation in the dendrites of fly visual interneurons *in situ* (Borst and Egelhaaf, 1992). Recently, Sattelle and his co-workers also used fura-2, to demonstrate muscarinic-agonist induced changes in  $[Ca^{2+}]_i$  with a cloned *Drosophila* muscarinic acetylcholine receptor in a stable *Drosophila* cell line (Millar *et al*, 1995), and nicotine-induced increases in  $[Ca^{2+}]_i$  in isolated adult cockroach neurosecretory cells (Grolleau *et al*, 1996).

In the current study, pressure-injection of the potassium salt of fluo-3 was chosen as the preferred dye and method of application for monitoring agonist-evoked changes in  $[Ca^{2+}]_i$  in identified insect neurones. This was because (i) microelectrode pressure-injection techniques had already been established in the laboratory and, therefore, injection of the dye into single identified neurones would be a routine procedure, (ii) the excitation and emission spectra of fluo-3 complemented that of the CLSM system to be used - an argon-krypton laser was installed as the source of illumination for the microscope, (iii)  $Ca^{2+}$  changes in a single neurone could be monitored without any risk of interference from neighbouring cells and (iv) the potassium salt form of fluo-3 was favoured because the potassium ions would have a negligible effect on cell function. It was

not known what, if any, detrimental effects on cell viability would be caused by the injection of ammonium ions into the cytosol.

The aim of this investigation was to examine the effects of dopamine and McN-A-343 on isolated BA1 motoneurones, and perform a comparative study of the effects of these agonists on the fast coxal depressor neurone ( $D_f$ ) of the cockroach (*Periplaneta americana*).

## MATERIALS AND METHODS

### 3.2.1. Dissection

Locusts were dissected as previously described (Section 2.2.3.1.) and the thoracic ganglia, once free from the thoracic cavity and cleared of fat and trachea, were secured onto a Perspex slide. The mesothoracic ganglion was then desheathed and the preparation was transferred to an experimental chamber where it was perfused with oxygenated locust saline; this chamber was similar to that described in Section 2.2.5.1.

### 3.2.2. Protocol for pressure injection of isolated motoneurons with fluo-3

#### 3.2.2.1. Microelectrodes

Microelectrodes were drawn from thick-walled filamented capillary glass (Clark Electromedical Instruments; external diameter, 1.5mm, internal diameter 0.86mm) using a Vertical Pipette Puller (David Kopf Instruments; model 720). Microelectrodes had resistances of 12 to 25M $\Omega$  when filled with 2M KAc. The cell body was penetrated by one of these electrodes for recording membrane potential (the 'voltage' microelectrode). A similar microelectrode was used for injecting the calcium-sensitive fluorescent dye, fluo-3 (Molecular Probes; pentapotassium salt, cell impermeant); the tips of these microelectrodes were filled with 10mM fluo-3.

#### 3.2.2.2. Microelectrode impalement and pressure-injection of fluo-3.

The technique of microelectrode penetration was similar to that described in Section 2.2.5.5.; penetration of the 'voltage' microelectrode was facilitated by briefly adjusting the capacitive compensation facility of the amplifier/bridge and the dye-filled microelectrode was penetrated by injecting a hyperpolarizing

current (50 to 150nA). Following impalement of the BA1 soma with both microelectrodes, fluo-3 was pressure-injected into the neurone. The pressure pulses (10 to 20ms, approximately 2Hz, at 10psi) were generated using a Picospritzer II (General Valve Corporation) which was driven by a Grass S44 stimulator via a stimulus isolation unit (Grass SIU5). Filling times of the BA1 motoneurone varied from 40s to greater than 4 mins depending on microelectrode tip diameter and degree of microelectrode blocking. It was judged that sufficient dye had been injected into a neurone, when the colouration of the neurone contents resembled that of the orange-coloured fluo-3 solution in the pressure-injection microelectrode.

Once filled with fluo-3, the BA1 cell body was isolated from the mesothoracic ganglion and placed in the recording chamber as described in Section 2.2.4.1. However, in this case the Petri dish was finely coated with Sylgard to improve adhesion of the neurone to the surface of the dish. The Sylgard coating was cleaned with 70% ethanol immediately before use and then rinsed with locust saline. To prevent movement of the isolated cell, the edge of the cluster of neurones was carefully surrounded by silicon grease (Radio Spares). The preparation was then viewed (excitation wavelength of fluo-3 is 488nm) using a confocal argon/krypton laser scanning microscope (BioRad Microscience Ltd; MRC-600, Nikon Diaphot 2 inverted microscope) in order to observe the effects of specific receptor agonists (dopamine and McN) on the level of fluo-3 fluorescence (emission wavelength is 510nm). Using this technique the degree of fluorescence gave an indication of agonist-induced changes in intracellular levels of calcium. The computer software package CoMOS was used for calcium imaging and image processing. Data were stored onto rewritable 5¼" optical disks (Phillips) and copies of the data were downloaded using a colour video printer (Sony VP5000) onto colour printer paper.

Agonists were applied in 20 $\mu$ l aliquots directly to the middle well of the recording chamber and the preparation washed by adding locust saline (total volume, 0.6 to 1.0ml) to one of the end wells whilst drawing it off manually from the other using a Gilson pipette. When antagonists were used, they were applied to the experimental bath before the BA1 motoneurone was isolated. The preparation was then incubated with the antagonist for at least 1 hour prior to the isolation of the neurone. The neurone was isolated as previously described and placed into the recording chamber which also contained the appropriate concentration of antagonist.

## RESULTS

### 3.3.1. Appearance of insect motoneurons pressure-injected with fluo-3

Prior to the examination of agonist-induced changes in intracellular calcium levels  $[Ca^{2+}]_i$  using confocal microscopy, the position of the isolated neurones was confirmed using a conventional dissecting microscope (magnification x16 to x80). The filled somata of the neurones were easily identified by the orange colouration of fluo-3; occasionally, filled axons were seen, indicating how readily the dye could diffuse through the cytoplasm to fill the neuronal processes. When preparations were viewed under the confocal microscope, these finer structures became visible (for examples see Figures 3.3.6 and 3.3.7i). It should be noted that prior to isolation, the resting membrane potential of the fluo-3-filled BA1 motoneurone was  $-52.3 \pm 1.2\text{mV}$  (mean  $\pm$  S.E.M.;  $n = 20$ ) which is similar to that obtained in the absence of the dye (Anderson, 1995).

On initial viewing of the filled neurones using the confocal microscope, the desired visual image (optical section) of a neurone was chosen by manually altering the focus of the microscope. Once the image plane was chosen, the level of fluorescence of the neurone was usually modified (increased or decreased) by altering the brightness and contrast scan controls accordingly. This resulted in a level of image fluorescence that was appropriate for the experiment to be performed; that is, the level of fluorescence was lowered if the effects of McN-A-343 (which elevates fluorescence - see below) were to be examined, and increased if dopamine (which conversely, lowers the level of fluorescence - see below) was to be used. Such alterations optimized the drug-induced responses obtained. Once set up, these parameters were not changed during an experiment and they did not affect the experimental results. The images of the fluo-3-filled

neurones could differ quite markedly in appearance from one preparation to another (see figures in this section); this was largely attributed to subtle variations between preparations during the isolation process, the orientation of each isolated neurone in the experimental chamber and the plane of focus chosen within the neurone.

### 3.3.2. The effect of McN-A-343 on intracellular calcium in isolated BA1 motoneurones

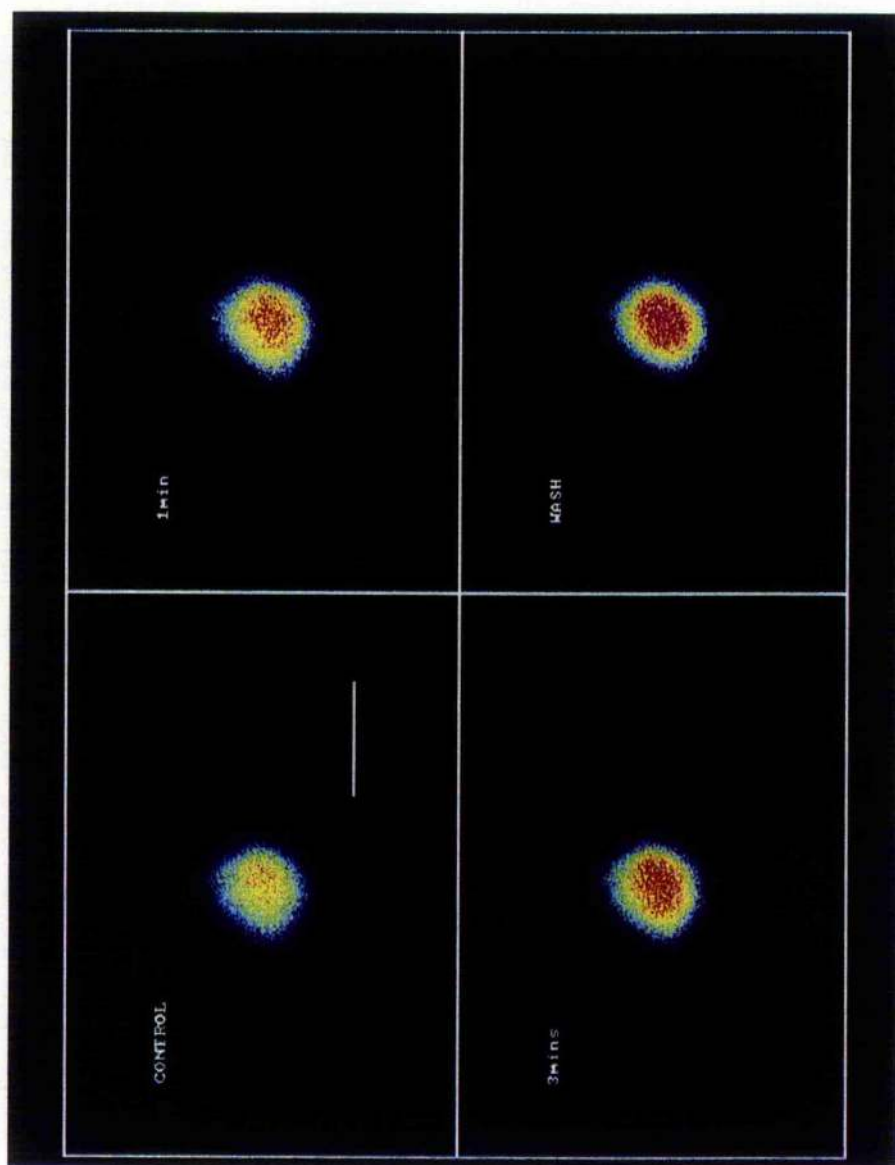
When the vertebrate muscarinic  $M_1$ -subtype agonist, McN, was bath-applied to isolated BA1 motoneurones, it consistently increased  $[Ca^{2+}]_i$  (range tested being  $10^{-4}M$  to  $1.1 \times 10^{-2}M$  McN;  $n = 11$ ). Figure 3.3.1. shows the effect of  $10^{-4}M$  McN on an isolated BA1 motoneurone presented as a series of pseudocolour images. When images are presented in pseudocolour the relative  $[Ca^{2+}]_i$  in descending order are shown as white, red, yellow/green, and blue/purple. In this preparation there was a relatively rapid large response to the bath-application of McN ( $10^{-4}M$ ). After 1 minute in the presence of McN,  $[Ca^{2+}]_i$  increased - this is shown by the increase in area of red colour; after a further 2 minutes (the '3mins' frame),  $[Ca^{2+}]_i$  had increased further, as indicated by the increase in the level of fluorescence. McN ( $10^{-4}M$ ) was seen to increase  $[Ca^{2+}]_i$  in 4 different preparations. On examination of the preparation 90 minutes after washing,  $[Ca^{2+}]_i$  remained elevated. This was not an unusual phenomenon in isolated BA1 motoneurones; following a rapid and/or large increase in  $[Ca^{2+}]_i$  by McN, it was difficult to reverse the agonist-induced response with washing (see Figure 3.3.1.). There are known to be three main ways in which  $[Ca^{2+}]_i$  are lowered. Firstly, by the plasma membrane bound  $Ca^{2+}$ ATPase, which actively pumps  $Ca^{2+}$  out of the neurone, secondly, by active sequestration into the cytoplasmic organelles (from which it was released) such as smooth endoplasmic

Figure 3.3.1. The effect of  $10^{-4}\text{M}$  McN-A-343 (McN) on  $[\text{Ca}^{2+}]_i$  of isolated BA1 motoneurones.

The bath-application of McN ( $10^{-4}\text{M}$ ) increased  $[\text{Ca}^{2+}]_i$  in isolated BA1 motoneurones. In this preparation,  $[\text{Ca}^{2+}]_i$  was seen to be elevated at 1 and 3 minutes after the application of McN. In isolated BA1 motoneurones it was difficult to reverse the McN-induced effect on  $[\text{Ca}^{2+}]_i$  with washing, even with prolonged wash periods. In this preparation,  $[\text{Ca}^{2+}]_i$  remained elevated following 90 minutes washing.

Scale =  $100\mu\text{m}$





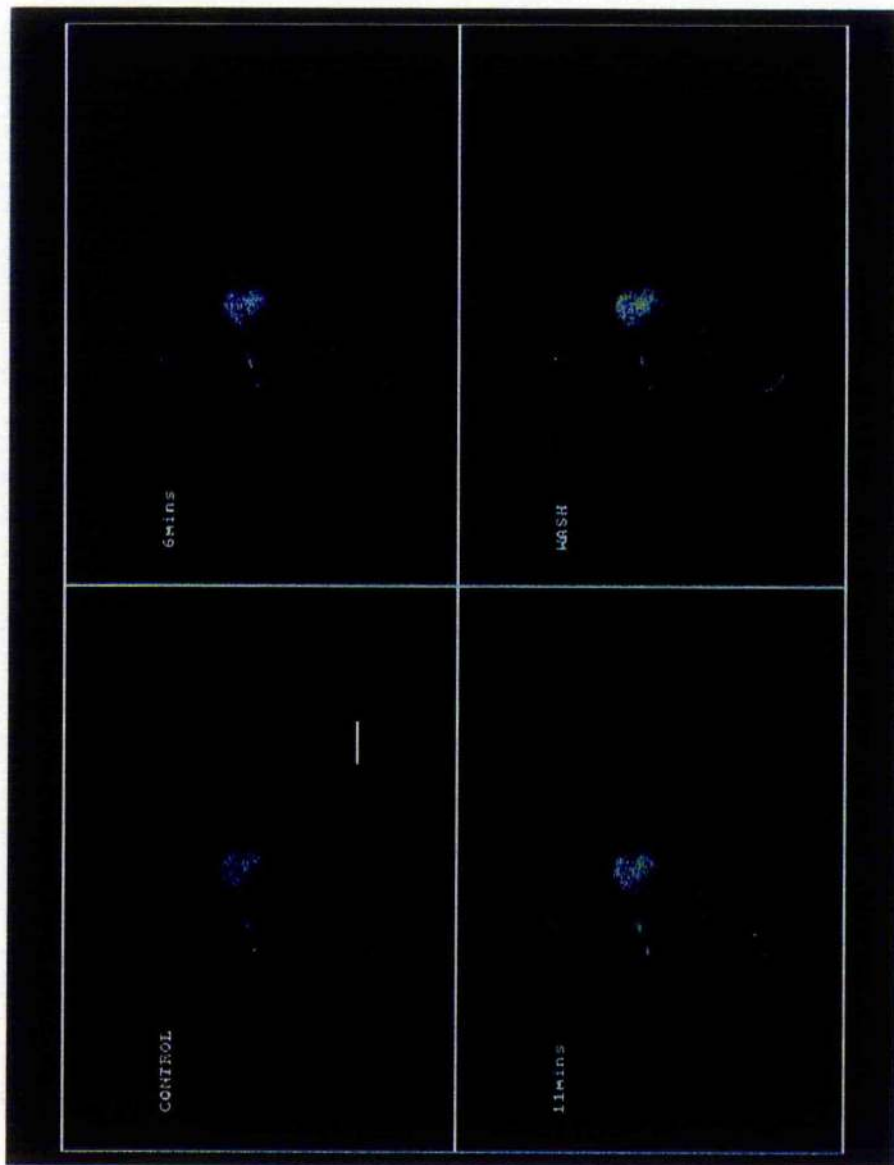
reticulum and mitochondria, and thirdly, by the  $\text{Na}^+$ - $\text{Ca}^{2+}$  exchange mechanism, which operates across the surface plasma membrane (for further details see Discussion). As  $[\text{Ca}^{2+}]_i$  elevation is the result of second messenger activation of a cascade pathway (which are known to act over a long time course), and these mechanisms for the lowering of  $[\text{Ca}^{2+}]_i$  have slower time courses than the direct movement of ions through voltage-dependent ion channels, prolonged wash periods (usually 60 minutes) are used to see reversal of the agonist-induced increase in  $[\text{Ca}^{2+}]_i$ . Since, this was not the case for isolated BA1 motoneurons in the present study, yet such a protocol was suitable for the reversal of McN-induced elevation of  $[\text{Ca}^{2+}]_i$  in an isolated cockroach motoneurone under similar experimental conditions (see Section 3.3.3.), it is suggested that there could be differences between neurone types regarding the relative contributions of the different cellular mechanisms for the lowering of  $[\text{Ca}^{2+}]_i$  in insect neurones.

When the bath concentration of McN applied to isolated BA1 motoneurons was increased to  $10^{-3}\text{M}$ , a similar effect on  $[\text{Ca}^{2+}]_i$  was evoked (see Figure 3.3.2.). In the control image of this preparation, the cell body is seen as the purple/faint green circular area and the axon and dendritic fields (purple areas above and below the axon) can be faintly seen (for a clearer picture of this preparation, see the control image in Figure 3.3.8.). In the presence of  $10^{-3}\text{M}$  McN,  $[\text{Ca}^{2+}]_i$  slowly increased in the soma, axonal and dendritic regions (see frames at 6 and 11 minutes) of the neurone. As observed in Figure 3.3.1, the McN-induced increase in  $[\text{Ca}^{2+}]_i$  was sustained. That is, it did not reverse following washing (the 'WASH' frame, after 32 minutes), and was still elevated after 47 minutes washing had commenced (not shown). This extremely long time course of the McN-induced response of isolated BA1 motoneurons meant that dose-dependent relationship using the same preparation was not possible.

Figure 3.3.2. The effect of  $10^{-3}\text{M}$  McN-A-343 on  $[\text{Ca}^{2+}]_i$  of isolated BA1 motoneurons.

The bath-application of McN ( $10^{-3}\text{M}$ ) increased  $[\text{Ca}^{2+}]_i$  in isolated BA1 motoneurons. In this preparation,  $[\text{Ca}^{2+}]_i$  was seen to be elevated at 6 and 11 minutes after the application of McN. As seen in Figure 3.3.1, in isolated BA1 motoneurons it was difficult to reverse the McN-induced effect on  $[\text{Ca}^{2+}]_i$  with washing. In this preparation, the McN-induced in  $[\text{Ca}^{2+}]_i$  was sustained (seen following 32 minutes washing).

Scale =  $100\mu\text{m}$



Increasing the concentration of bath-applied McN still further, also induced an increase in  $[Ca^{2+}]_i$  in isolated BA1 motoneurones, and the nature of the response indicated that the McN-induced effect was dose-dependent. Figure 3.3.3i and 3.3.3ii show a rapid and dramatic rise in  $[Ca^{2+}]_i$  following the bath-application of  $10^{-2}M$  McN in an isolated BA1 motoneurone. Figure 3.3.3ii shows the corresponding black and white frames for the observed increases in  $[Ca^{2+}]_i$  shown in Figure 3.3.3i. On comparing the two figures, it can be seen that visualizing the images in pseudocolour provides greater detail about the change in degree and distribution in fluo-3 fluorescence, and therefore, the change in  $[Ca^{2+}]_i$ .

To demonstrate that the increases in  $[Ca^{2+}]_i$  following the bath application of McN was the result of muscarinic receptor activation, rather than the activation of another neurotransmitter receptor type, or the consequence of non-specific changes in the neurone, McN ( $10^{-4}M$ ) was bath-applied to isolated BA1 motoneurones in the presence of the cholinergic antagonist, atropine ( $10^{-4}M$ ; Figure 3.3.4.). In the 'control (atropine)' frame an isolated BA1 motoneurone is shown following its incubation for 105 minutes in  $10^{-4}M$  atropine. The cell body of the neurone is clearly distinguishable, and its axonal stump is seen as the structure leaving the cell body on the top left side of the neurone. The isolated neurone was then challenged with  $10^{-4}M$  McN, in the presence of the antagonist; after 5 minutes McN did not increase in  $[Ca^{2+}]_i$  (see '5mins' frame;  $n = 5$ ).

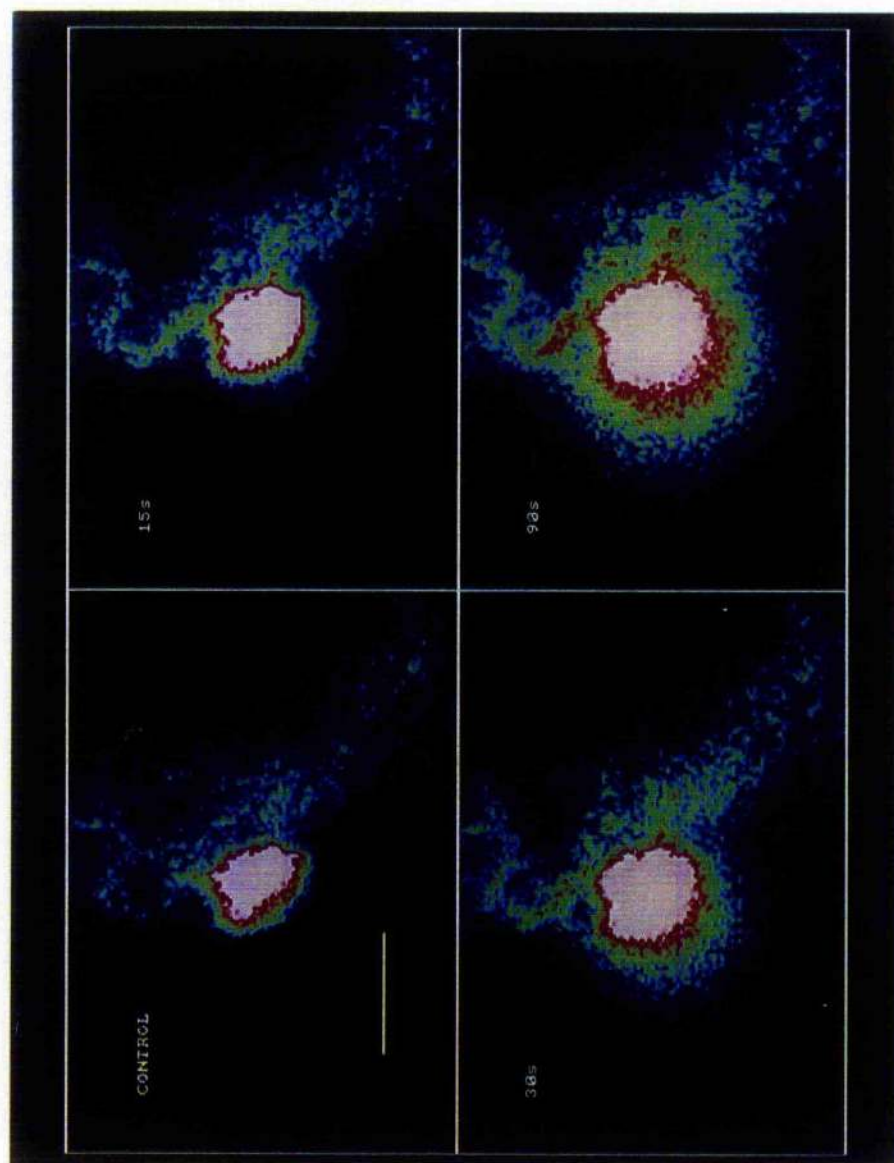
### 3.3.3. The effect of McN-A-343 on intracellular calcium in isolated $D_f$ motoneurones

A series of experiments was undertaken using the fast coxal depressor motoneurone of the cockroach (*Periplaneta americana*) third thoracic ganglion to compare the effects of McN with those observed in the BA1 motoneurone of the

Figure 3.3.3. The effect of  $10^{-2}\text{M}$  McN-A-343 on  $[\text{Ca}^{2+}]_i$  of isolated BA1 motoneurones.

In this preparation, the bath-application of McN ( $10^{-2}\text{M}$ ) was seen to rapidly and dramatically increase  $[\text{Ca}^{2+}]_i$  within 90s following the application of McN (also seen at 15s and 30s). No attempt was made to reverse this McN-induced increase in  $[\text{Ca}^{2+}]_i$  by washing the preparation. In addition to the pseudocolour image of this experiment (Figure 3.3.3i), the corresponding black and white frames are shown overleaf (Figure 3.3.3ii), to illustrate the improved level of detail obtained from the pseudocolour images, regarding changes in  $[\text{Ca}^{2+}]_i$ .

Scale =  $100\mu\text{m}$



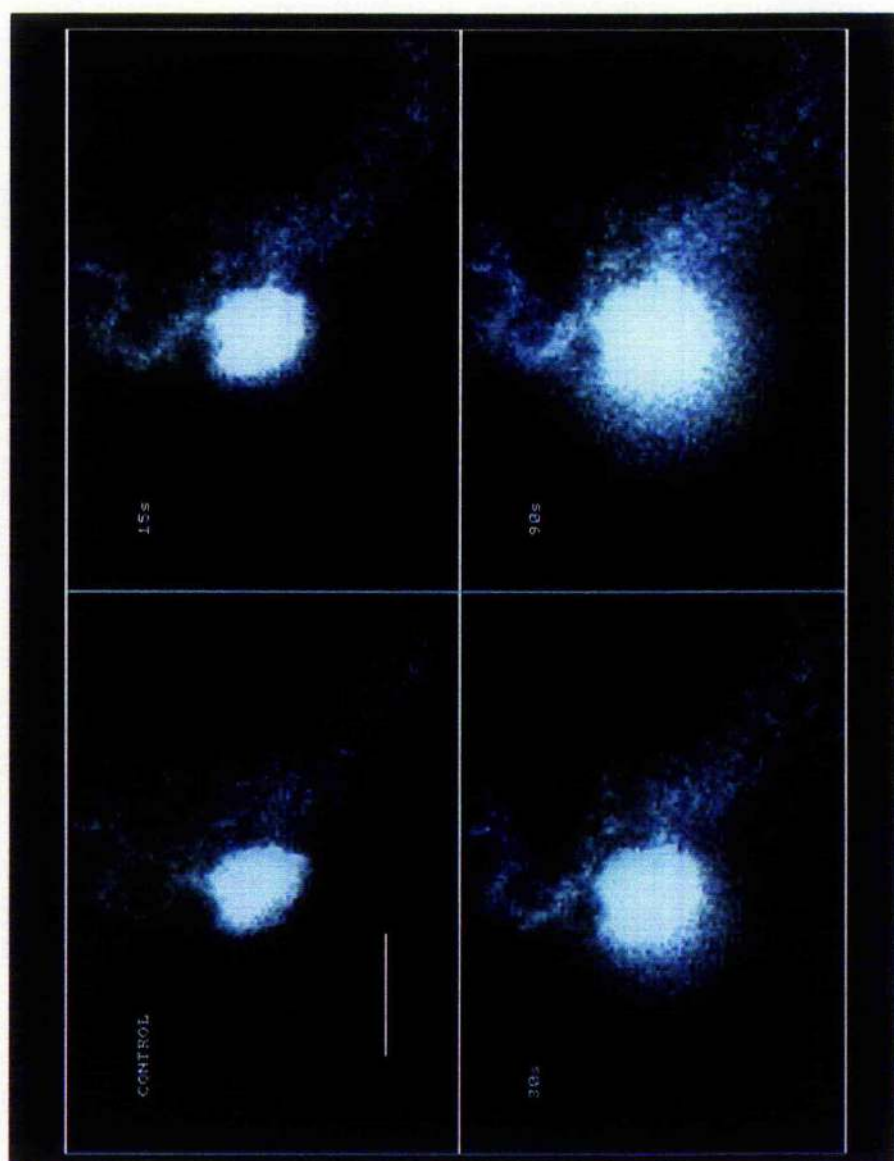
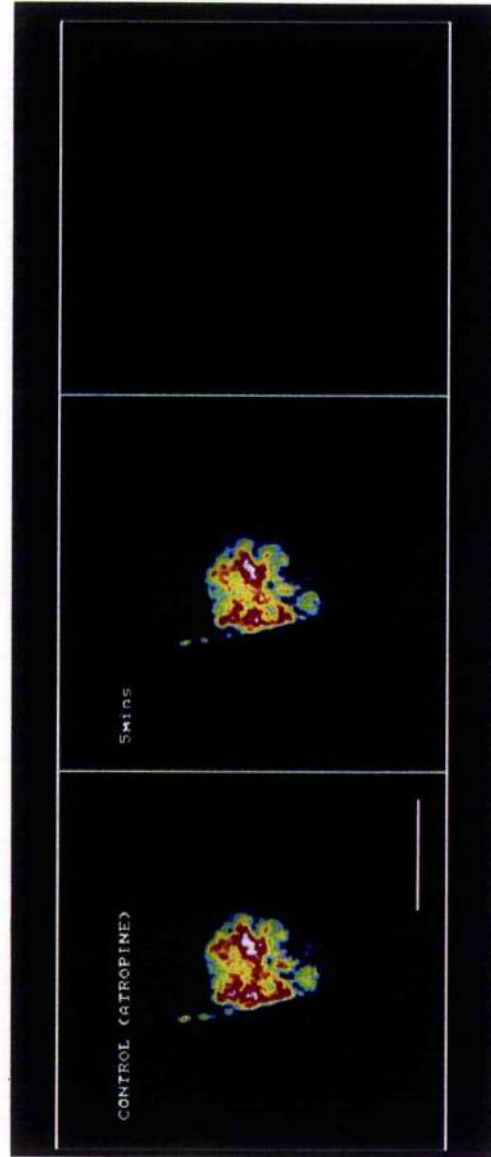




Figure 3.3.4. The effect of  $10^{-4}\text{M}$  McN-A-343 on  $[\text{Ca}^{2+}]_i$  of isolated BA1 motoneurons is blocked by the cholinergic antagonist, atropine ( $10^{-4}\text{M}$ ).

Scale =  $100\mu\text{m}$



locust. This neurone was chosen for comparison since its electrophysiological and pharmacological properties have been studied extensively in this laboratory. The experimental protocol was the same as that used for BA1. The  $D_f$  motoneurone soma has a similar location on the ventral surface of the ganglion to that of BA1 in the mesothoracic ganglion in the locust, *Schistocerca gregaria*. The only significant change in the protocol was the use of cockroach saline, rather than locust saline, for the experiments (composition given in Appendix 2). Prior to isolation, the fluo-3-filled  $D_f$  somata had resting membrane potentials similar to those obtained in the absence of the dye ( $-77.6 \pm 0.9\text{mV}$ ; mean  $\pm$  S.E.M.;  $n = 15$ ; David and Sattelle, 1984).

As observed in the isolated BA1 motoneurone, McN induced an increase in  $[\text{Ca}^{2+}]_i$  in isolated  $D_f$  motoneurons (range tested  $10^{-4}\text{M}$  to  $10^{-2}\text{M}$  McN,  $n = 10$  out 11; 6 in the presence of  $50\mu\text{M}$  verapamil). To demonstrate that cellular responses to McN were the result of the release of  $\text{Ca}^{2+}$  from intracellular stores evoked by the agonist, rather than a  $\text{Ca}^{2+}$  influx through voltage-dependent  $\text{Ca}^{2+}$  channels ( $I_{\text{Ca}}$ ), the  $\text{Ca}^{2+}$  channel blocker, verapamil, was used to block these ion channels. As verapamil at this concentration blocks 85 - 90% of the inward  $\text{Ca}^{2+}$  current in  $D_f$  (J. D. Mills, personal communication), it would suggest that a McN-induced increase in  $[\text{Ca}^{2+}]_i$  in the presence of verapamil was the result of  $\text{Ca}^{2+}$  release from intracellular stores. Furthermore, it would demonstrate that any drug-induced response was due to the direct action of the agonist on the neurone, rather than to an indirect effect mediated synaptically via other neurones.

The responses of an isolated  $D_f$  motoneurone to McN, in the absence and presence of verapamil are shown in Figure 3.3.5. Figure 3.3.5i shows the rise in  $[\text{Ca}^{2+}]_i$  following the bath-application of  $10^{-3}\text{M}$  McN ( $n = 3$ ; 2 in the presence of  $50\mu\text{M}$  verapamil). In this preparation the soma and axon are clearly distinguishable. McN ( $10^{-3}\text{M}$ ) evoked an increase in  $[\text{Ca}^{2+}]_i$  in both regions (seen

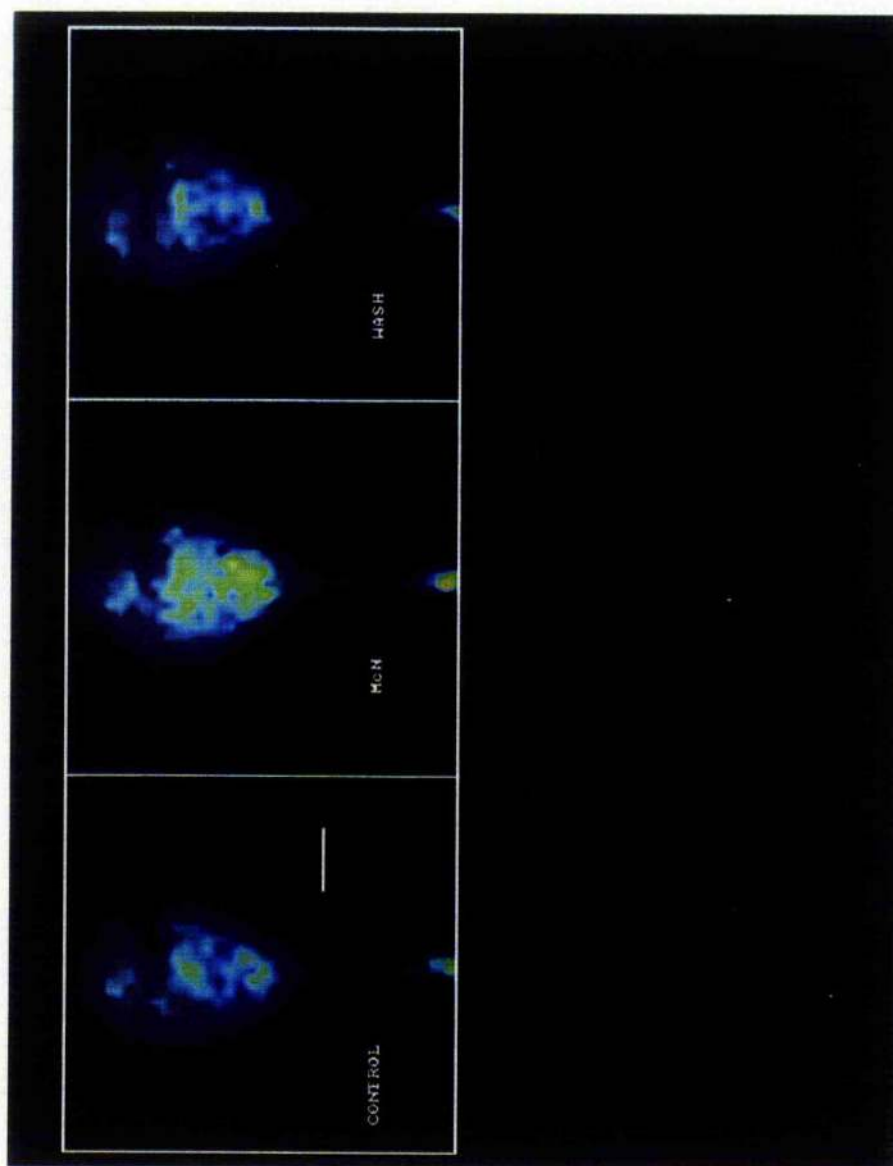
Figure 3.3.5. The effect of  $10^{-3}\text{M}$  McN-A-343 on  $[\text{Ca}^{2+}]_i$  of isolated  $D_f$  motoneurons.

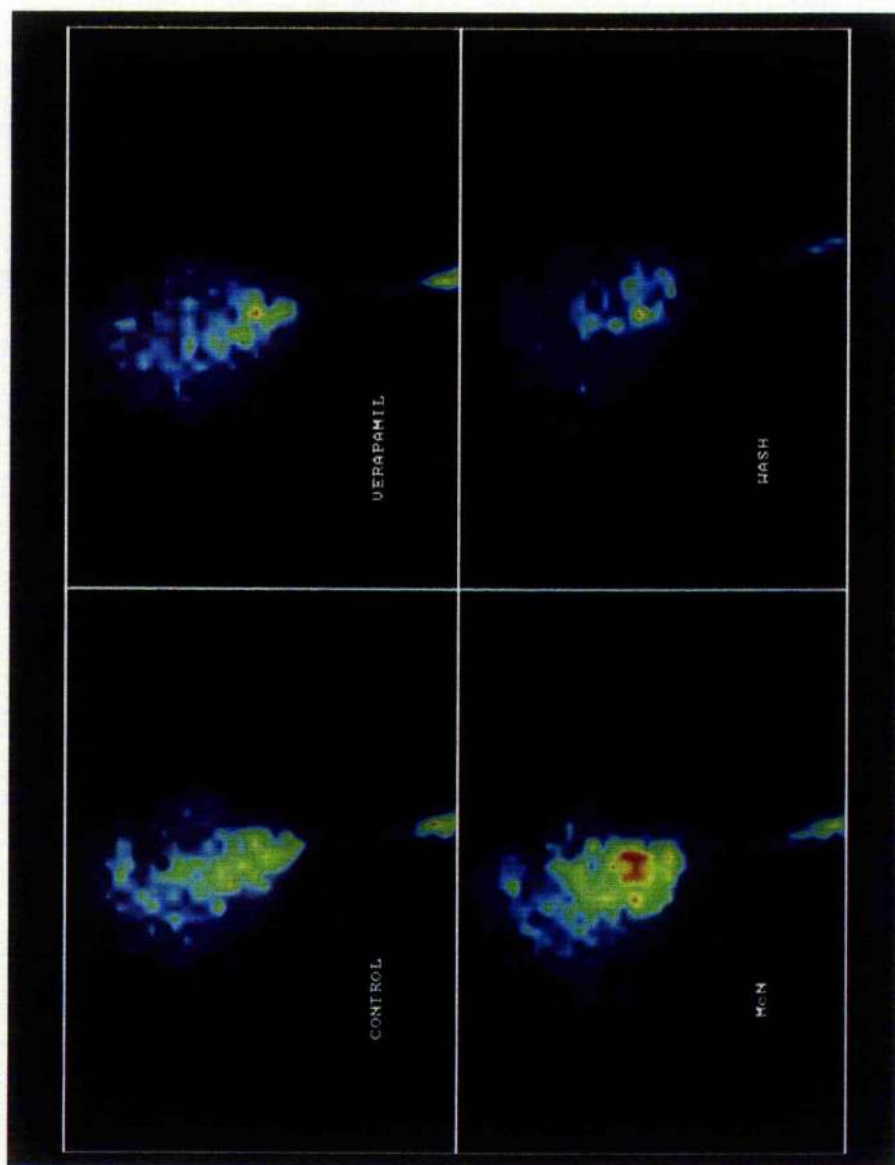
i. The bath-application of McN ( $10^{-3}\text{M}$ ) increased  $[\text{Ca}^{2+}]_i$  in isolated  $D_f$  motoneurons. In this preparation,  $[\text{Ca}^{2+}]_i$  was seen to be elevated 1 minute after the application of McN. Unlike that observed in isolated BA1 motoneurons, the McN-induced increase in  $[\text{Ca}^{2+}]_i$  reversed with relative ease with washing (wash frame seen 14 minutes after washing).

Scale =  $50\mu\text{m}$

ii. To investigate whether the McN-induced increase in  $[\text{Ca}^{2+}]_i$  of isolated  $D_f$  motoneurons (see Figure 3.3.5i) occurred primarily as the result of the stimulation of  $\text{Ca}^{2+}$  release from intracellular stores, or as an increase in  $\text{Ca}^{2+}$  influx through voltage-dependent  $\text{Ca}^{2+}$  channels, the effect of McN ( $10^{-3}\text{M}$ ) was tested in the presence of the blocker of voltage-dependent  $\text{Ca}^{2+}$  channels, verapamil ( $50\mu\text{M}$ ). Using the same preparation as before, in the presence verapamil ( $50\mu\text{M}$ ) alone,  $[\text{Ca}^{2+}]_i$  decreased (seen after 7 minutes). However, McN ( $10^{-3}\text{M}$ ) increased  $[\text{Ca}^{2+}]_i$  in the presence verapamil ( $50\mu\text{M}$ ). This effect reversed on washing; after 60 minutes,  $[\text{Ca}^{2+}]_i$  was observed to be lower than that in the control frame.

Scale same as Figure 3.3.5i





after 1 minute). The change in  $[Ca^{2+}]_i$  reversed on washing; this is seen in the third frame ('wash') which shows the neurone 14 minutes post-washing (compare to Figure 3.3.1.). When the preparations were placed in verapamil saline (cockroach saline with 50  $\mu$ M verapamil added), the level of intracellular  $Ca^{2+}$  concentration decreased ( $n = 5$  out of 6; see Figure 3.3.5ii). The 'verapamil' frame in Figure 3.3.5ii was obtained when the verapamil-induced reduction in  $[Ca^{2+}]_i$  had stabilized (after 7 minutes). This reduction in  $Ca^{2+}$  was interesting as it indicated the presence of resting  $Ca^{2+}$  influx in the neurone (see Discussion). The subsequent bath-application of  $10^{-3}$ M McN evoked an increase in  $[Ca^{2+}]_i$  in the presence of verapamil, suggesting that the rise in  $[Ca^{2+}]_i$  occurred through an  $I_{Ca}$ -independent mechanism. Furthermore, the McN-evoked rise in  $[Ca^{2+}]_i$  (seen after 5 minutes) was reversed on washing; in this preparation, 60 minutes after washing,  $[Ca^{2+}]_i$  was found to be below that of the control image. The reason why McN-evoked changes in  $[Ca^{2+}]_i$  were more readily reversible in  $D_f$  motoneurons compared to BA1 motoneurons is not clear; the results could suggest that the ways by which  $D_f$  motoneurons regulate  $[Ca^{2+}]_i$  are more effective.

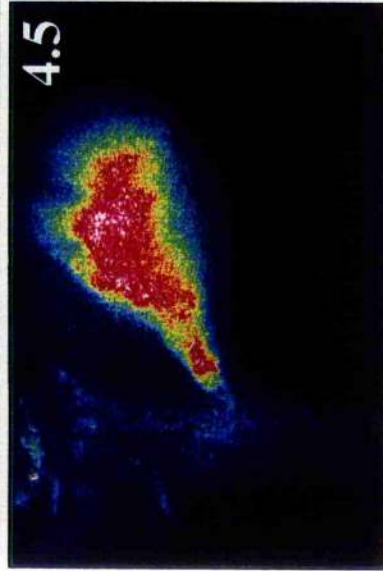
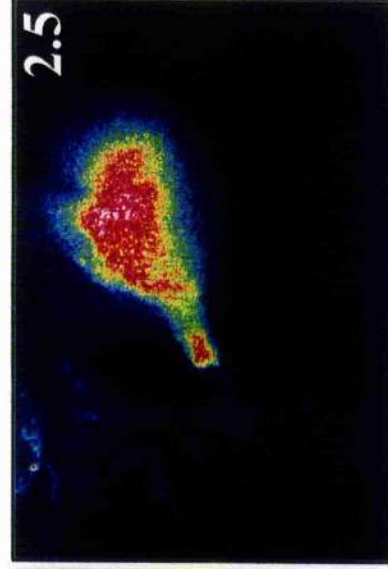
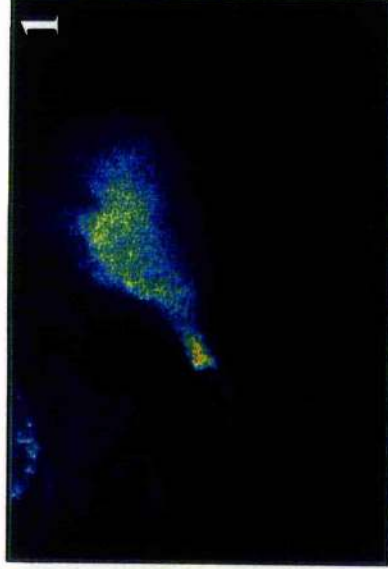
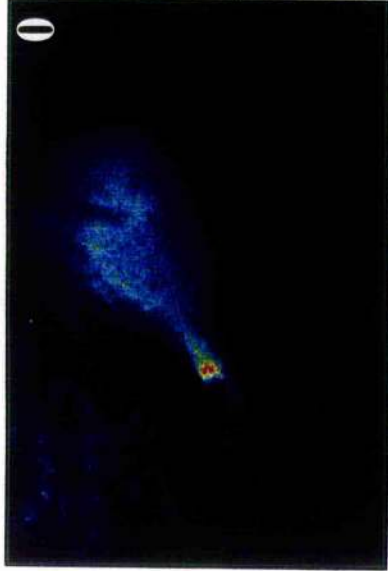
The effect of  $10^{-2}$ M McN on an isolated  $D_f$  motoneurone is shown in Figure 3.3.6. ( $n = 1$ ). In this preparation the morphology of the neurone was very clear; the cell body, axon, and dendritic field (seen at the top left of each frame) can all be clearly identified. The '0' frame is the control image; the subsequent frames 1, 2.5, 4.5 are the images (in minutes) of the preparation, following the bath-application of  $10^{-2}$ M McN.  $[Ca^{2+}]_i$  was seen to dramatically increase in the cell body and axon during the 4.5 minute observation period. An increase in  $[Ca^{2+}]_i$  was also observed in the dendritic field. As shown in the 'wash' frame, the dramatic McN-induced increase in  $[Ca^{2+}]_i$  was reversed on washing (seen after 20 minutes).

Figure 3.3.6. The effect of  $10^{-2}\text{M}$  McN-A-343 on  $[\text{Ca}^{2+}]_i$  of an isolated  $\text{D}_f$  motoneurone.

In this preparation the bath-application of  $10^{-2}\text{M}$  McN evoked a rapid and dramatic increase in  $[\text{Ca}^{2+}]_i$ , to highlight the morphological features of this isolated  $\text{D}_f$  motoneurone. The effect of McN is shown 1, 2.5 and 4.5 minutes following application; furthermore, the increase in  $[\text{Ca}^{2+}]_i$  was seen to be reversed by washing (seen after 20 minutes), and  $[\text{Ca}^{2+}]_i$  was observed to be lower than that in the control frame (0 minutes).

Scale =  $100\mu\text{m}$





### 3.3.4. The effect of dopamine on intracellular calcium in isolated BA1 motoneurones

The bath-application of dopamine (DA) induced a dose-dependent reduction in  $[Ca^{2+}]_i$  of isolated BA1 motoneurones (range tested  $10^{-4}M$  to  $2.2 \times 10^{-2}M$  DA;  $n = 16$  out of 17; see Figures 3.3.7i, 3.3.7ii, and 3.3.8). Figures 3.3.7i and 3.3.7ii show the effects of  $10^{-4}M$  and  $10^{-3}M$  DA, respectively, on the same isolated BA1 motoneurone. In this preparation the soma is seen as the relatively large red-coloured region and the dendritic fields are seen as the green and purple-coloured regions surrounding the soma. The axonal stump is seen as the white region on the lower right-hand side of the cell. The reason for the apparently high  $[Ca^{2+}]_i$  in the axonal stump compared to the soma, is due to the fact that on leaving the soma the stump sharply descended through the neuropile; when the preparation was then viewed from below, the focal plane transected the axonal stump (and not the soma) and consequently, the axon appeared to have a higher  $[Ca^{2+}]_i$  than the rest of the neurone. For both the experiments shown, the laser scanning controls were set to automatically scan and save the acquired images to the optical disk every 5 seconds. This procedure ensured that accurate time intervals between frames were obtained.

The effects of  $10^{-4}M$  DA on the isolated BA1 motoneurone are shown in Figure 3.3.7i. In this preparation, within 5s of the bath-application of DA intracellular  $[Ca^{2+}]_i$  was lowered. In the subsequent frames  $[Ca^{2+}]_i$  progressively increased, to reach an apparently stable level below that of the control. No further changes in the levels of fluorescence were seen 30s after beginning DA application. The effect of DA on intracellular  $[Ca^{2+}]_i$  in this preparation is said to be transient, since, the  $[Ca^{2+}]_i$  returned towards control levels in the continued presence of DA. Washing commenced 120s after the application of DA; after 125

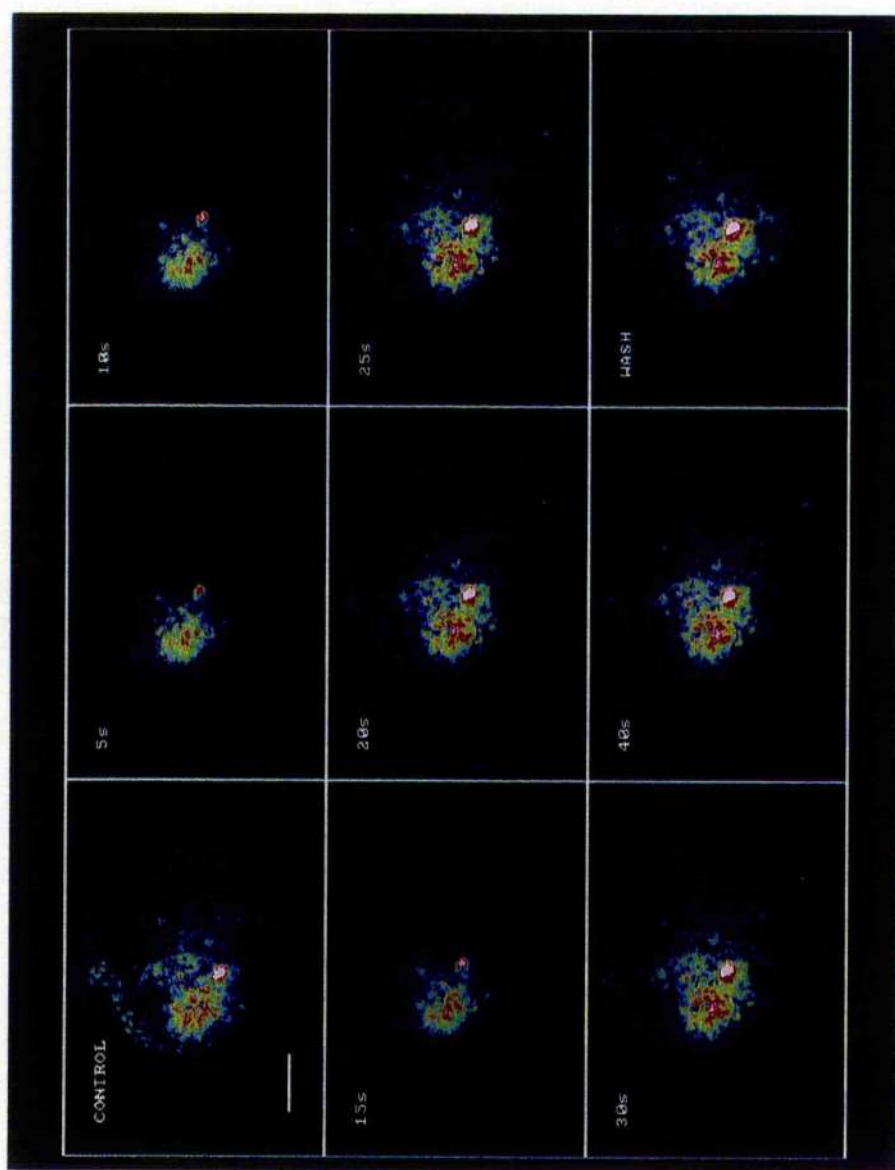
Figure 3.3.7. The dose-dependent effect of dopamine ( $10^{-4}\text{M}$  and  $10^{-3}\text{M}$ ) on  $[\text{Ca}^{2+}]_i$  of isolated BA1 motoneurons.

The bath-application of DA induced a dose-dependent lowering of  $[\text{Ca}^{2+}]_i$  in isolated BA1 motoneurons.

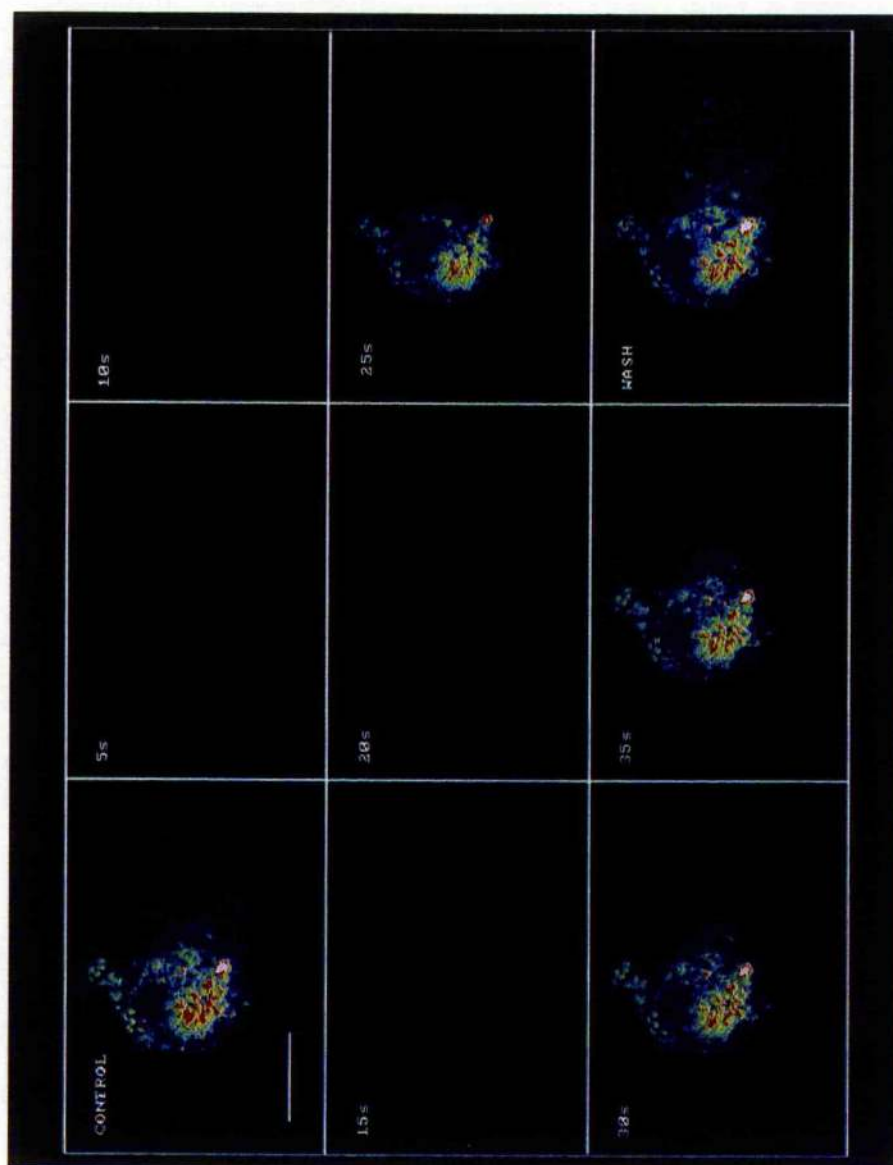
i. In this isolated BA1 motoneurone preparation, DA ( $10^{-4}\text{M}$ ) evoked a transient decrease in  $[\text{Ca}^{2+}]_i$ . Within 5s of application,  $[\text{Ca}^{2+}]_i$  was lowered; in subsequent frames  $[\text{Ca}^{2+}]_i$  is seen to return to a level close to that of the control frame. No further increase is seen after 30s. Washing commenced 120s after the application of DA, and no further changes in  $[\text{Ca}^{2+}]_i$  were apparent (wash frame seen after 125 minutes).

ii. The bath-application of  $10^{-3}\text{M}$  DA induced a dramatic transient lowering of  $[\text{Ca}^{2+}]_i$ , which was greater in magnitude than that observed induced by  $10^{-4}\text{M}$  DA in the same preparation (Figure 3.3.7i).  $[\text{Ca}^{2+}]_i$  was dramatically lowered within 5s of DA application of DA. It remained diminished for a further 15s, before increasing, to return to a level close to that seen observed in the control frame. Washing commenced 120s after the application of DA, and no further changes in  $[\text{Ca}^{2+}]_i$  were apparent (wash frame seen after 120 minutes).

Scale =  $100\mu\text{m}$



11



minutes washing the levels of fluorescence appeared to be slightly higher in the soma and axonal stump and lower in the dendritic regions.

Since this preparation appeared to recover from the decrease in  $[Ca^{2+}]_i$  evoked by  $10^{-4}M$  DA, it was possible to demonstrate the dose-dependent nature of the DA response, using this preparation. Increasing the concentration of DA to  $10^{-3}M$  induced a more marked response, compared to that evoked by  $10^{-4}M$  DA. Figure 3.3.7ii shows the effects of  $10^{-3}M$  DA on the same neurone. Like  $10^{-4}M$  DA, the bath-application of  $10^{-3}M$  DA decreased  $[Ca^{2+}]_i$  in isolated BA1 motoneurons ( $n = 4$ ). Within 5s of the bath-application of DA  $[Ca^{2+}]_i$  was dramatically lowered, and it remained diminished for a further 15s. At 25s following DA administration,  $[Ca^{2+}]_i$  had increased. This increase in  $Ca^{2+}$  continued so that at 30s, the level of fluorescence was similar to that in the control image. No further changes in  $[Ca^{2+}]_i$  were apparent. The neurone was washed at 120s after the application of DA. At 2 hours post-washing, the level of fluorescence was close to that seen in the control frame. Since the application of DA evoked a reduction in fluorescence throughout the neurone, the results suggest that there are DA receptors present on both the somal and dendritic plasma membranes.

Figure 3.3.8. shows the DA responses obtained from a different isolated BA1 motoneurone preparation. This neurone was previously used to demonstrate the effects of  $10^{-3}M$  McN (see Figure 3.3.2.). The reason why the morphology of the neurone is clearer in this figure, than in Figure 3.3.2., is that the focal plane was altered so that both dendritic fields and the cell body could be seen. Initially,  $10^{-3}M$  DA was bath-applied to the neurone. In the presence of  $10^{-3}M$  DA for 4 minutes (at which the response to DA had stabilized), the somal  $[Ca^{2+}]_i$  had slightly decreased. On the subsequent bath-application of the  $10^{-2}M$  DA, a further decrease in somal  $[Ca^{2+}]_i$  and a decrease in dendritic  $[Ca^{2+}]_i$  was observed. The

Figure 3.3.8. The dose-dependent effect of dopamine ( $10^{-3}\text{M}$  and  $10^{-2}\text{M}$ ) on  $[\text{Ca}^{2+}]_i$  of isolated BA1 motoneurones.

Using the preparation shown in Figure 3.3.2.,  $10^{-3}\text{M}$  and  $10^{-2}\text{M}$  DA was observed to induce a dose-dependent reduction in  $[\text{Ca}^{2+}]_i$  in this neurone.  $10^{-3}\text{M}$  DA decreased  $[\text{Ca}^{2+}]_i$  in the motoneurone soma (seen after 4 minutes). However, increasing the bath concentration of DA to  $10^{-2}\text{M}$ , resulted in a further reduction in somal  $[\text{Ca}^{2+}]$  and a reduction in dendritic  $[\text{Ca}^{2+}]$  (seen after 7 minutes). 30 minutes washing resulted in partial recovery from the DA-induced response (see wash frame).

Scale =  $100\mu\text{m}$





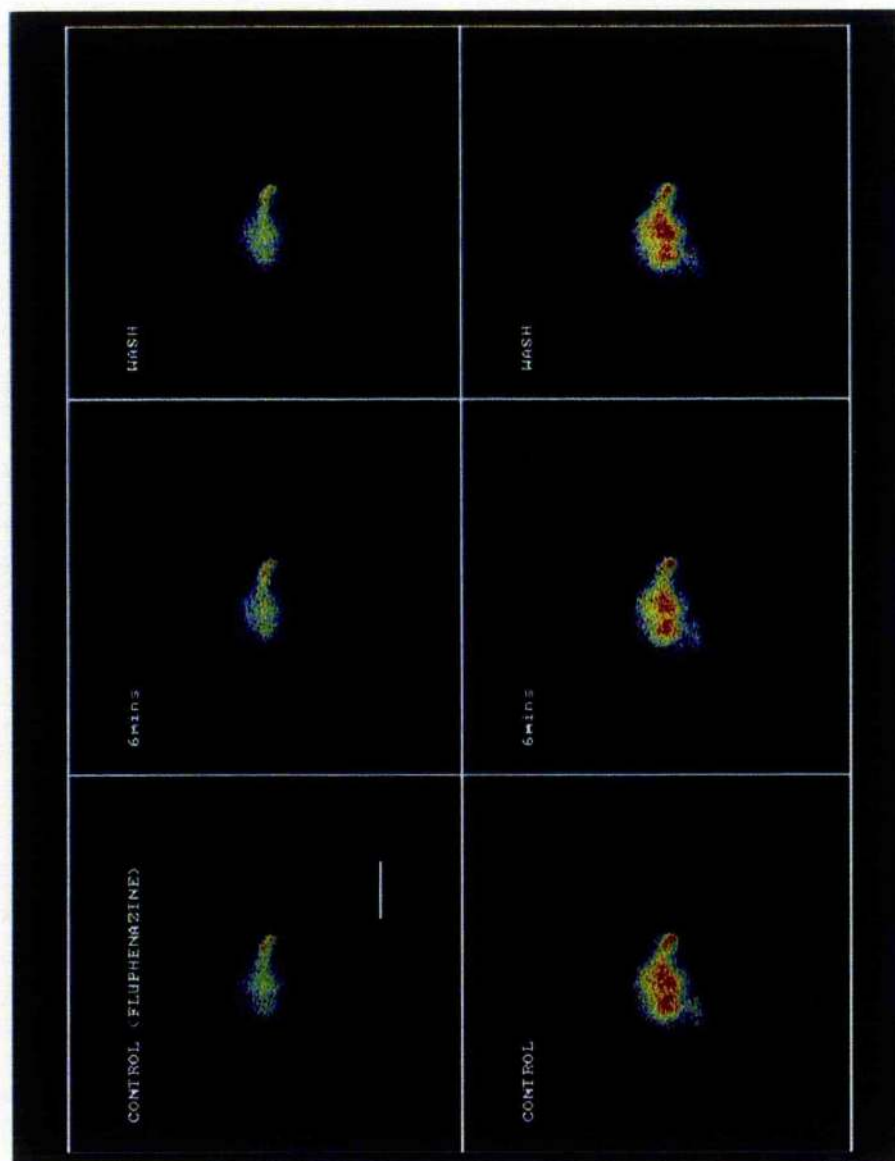
frame showing the effect of  $10^{-2}\text{M}$  DA on BA1 was obtained 7 minutes after the application of DA. However, on washing the preparation, partial recovery from the DA-evoked response was observed after 30 minutes. The preparation was continually monitored during the experiment and a rapid change in  $[\text{Ca}^{2+}]_i$  (as seen in Figure 3.3.7i and Figure 3.3.7ii) was not observed in this preparation.

In order to demonstrate that the DA-induced reduction in  $[\text{Ca}^{2+}]_i$  described above was due to the activation of DA receptors on the BA1 motoneurone, the vertebrate  $\text{D}_1/\text{D}_2$  receptor subtype antagonist, fluphenazine, was used to block the DA receptors on this neurone. A general DA receptor antagonist was used in these experiments because the precise identity of the BA1 motoneurone DA receptors has yet to be determined. Fluphenazine ( $10^{-4}\text{M}$ ) blocked the response to DA ( $10^{-4}\text{M}$ ) in isolated BA1 motoneurons ( $n = 3$ ; see Figure 3.3.9.). The 'control (fluphenazine)' frame shows the isolated neurone prior to the addition of DA, having been left in fluphenazine for 115 minutes. Following the bath-application of  $10^{-4}\text{M}$  DA in the presence of fluphenazine, no change in fluorescence (and therefore  $[\text{Ca}^{2+}]_i$ ) was observed. After the neurone was washed with antagonist-free saline the fluorescence remained unaltered. After a prolonged period of washing to remove the fluphenazine (5 hours 10 minutes), DA ( $10^{-4}\text{M}$ ) evoked a decrease in  $[\text{Ca}^{2+}]_i$  at 6 minutes after DA-application. This effect was seen to be partially reversed 20 minutes after washing. The  $[\text{Ca}^{2+}]_i$  was elevated in the lower set of frames because  $10^{-4}\text{M}$  McN was applied to the neurone between the two DA applications. By raising the  $[\text{Ca}^{2+}]_i$ , the DA-evoked reduction in  $[\text{Ca}^{2+}]_i$  was more marked.

Figure 3.3.9. The effect of  $10^{-4}\text{M}$  dopamine on  $[\text{Ca}^{2+}]_i$  of isolated BA1 motoneurons is blocked by the  $\text{D}_1/\text{D}_2$  dopaminergic antagonist, fluphenazine ( $10^{-4}\text{M}$ ).

The DA-induced ( $10^{-4}\text{M}$ ) reduction in  $[\text{Ca}^{2+}]_i$  has been shown to be mediated by DA receptor activation, since, in the presence of fluphenazine ( $10^{-4}\text{M}$ ; greater than 60 minutes; in this experiment, 115 minutes),  $10^{-4}\text{M}$  DA (6 minutes) fails to decrease  $[\text{Ca}^{2+}]_i$  (see upper horizontal panel, middle frame). However, following removal of the antagonist by washing with fresh locust saline (lower horizontal panel, 'CONTROL' frame), DA was seen to lower  $[\text{Ca}^{2+}]_i$  (seen after 6 minutes; lower horizontal panel, middle frame). Partial recovery of the DA-induced response was observed 20 minutes after washing (lower horizontal panel, 'WASH' frame).

Scale =  $100\mu\text{m}$



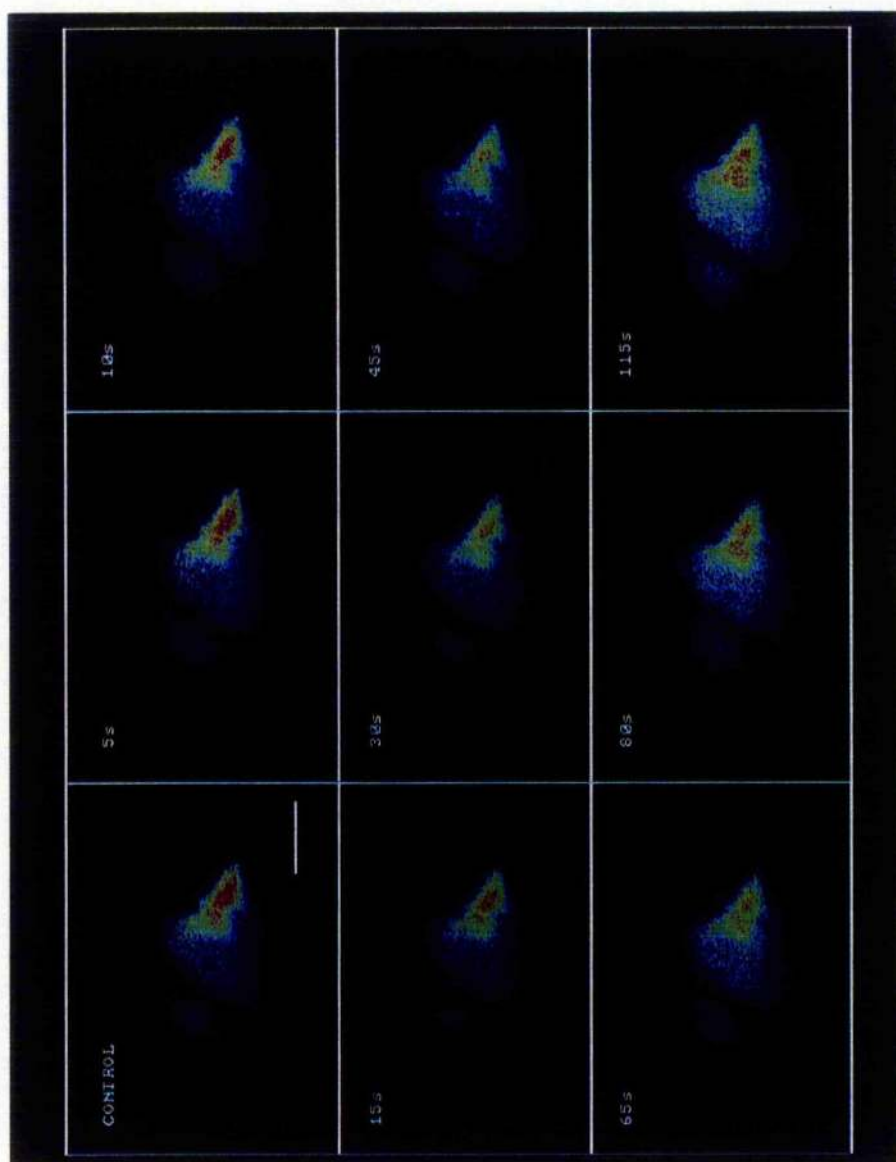
### 3.3.5. The effects of dopamine on intracellular calcium in isolated D<sub>f</sub> motoneurones

Using isolated D<sub>f</sub> motoneurones, DA decreased  $[Ca^{2+}]_i$  in a similar manner to that observed in isolated BA1 motoneurones (see Figure 3.3.7i);  $10^{-3}M$  DA reduced  $[Ca^{2+}]_i$  in 4 out of 5 preparations tested. Figure 3.3.10. shows the transient decrease in  $[Ca^{2+}]_i$  induced using  $10^{-3}M$  DA in one of these preparations. The dark band crossing the left-hand side of this neurone was tracheal tissue passing underneath the cell soma. In this preparation  $10^{-3}M$  DA evoked a reduction in  $[Ca^{2+}]_i$  which was maximal after 45s. Following this, in the continued presence of  $10^{-3}M$  DA,  $[Ca^{2+}]_i$  began to return towards resting level; the effects of washing were not examined in this preparation.

Figure 3.3.10. The effect of dopamine ( $10^{-3}\text{M}$ ) on  $[\text{Ca}^{2+}]_i$  of isolated  $\text{D}_f$  motoneurones.

DA ( $10^{-3}\text{M}$ ) induces lowering of  $[\text{Ca}^{2+}]_i$  in isolated  $\text{D}_f$  motoneurones, which resembles that observed in isolated BA1 motoneurones. In this isolated  $\text{D}_f$  motoneurone, DA evoked a transient reduction in  $[\text{Ca}^{2+}]_i$ , which had a time course slower than observed in the BA1 motoneurone preparation in Figures 3.3.7i and 3.3.7ii. The effects of washing were not examined.

Scale =  $100\mu\text{m}$



## DISCUSSION

Using the  $\text{Ca}^{2+}$ -sensitive fluorescent dye, fluo-3, and confocal microscopy techniques, evidence was obtained to support the electrophysiological data previously described (see Chapter 2), indicating that muscarinic receptors and dopamine receptors are present on the isolated soma of the first basalar (BA1) motoneurone of the locust (*Schistocerca gregaria*). Similar results were obtained in a comparative study using the fast coxal depressor ( $\text{D}_f$ ) motoneurone of the cockroach (*Periplaneta americana*).

The bath-application of the vertebrate  $\text{M}_1$  muscarinic agonist, McN-A-343 (McN) to either preparation causes an increase in  $[\text{Ca}^{2+}]_i$ , whilst dopamine (DA) reduces  $[\text{Ca}^{2+}]_i$ . With the exception of the McN-induced increase in isolated BA1 motoneurons, the effects on  $[\text{Ca}^{2+}]_i$  were reversed on washing. Possible reasons for the poor reversibility of this response include higher stability of intermediary compounds comprising the cascade pathway mediating the agonist-induced response, and slower metabolic pumping for the reversal of the agonist-induced increase in  $[\text{Ca}^{2+}]_i$  (see below for further details). Using the isolated BA1 motoneurone preparation, the response to McN was inhibited by the cholinergic antagonist, atropine ( $10^{-4}\text{M}$ ), suggesting that the response to McN was mediated by cholinergic receptors. When isolated  $\text{D}_f$  motoneurons were bathed in saline containing a blocker of the voltage-dependent  $\text{Ca}^{2+}$  channels, verapamil ( $50\mu\text{M}$  verapamil in cockroach saline), the bath-application of McN ( $10^{-3}\text{M}$ ) was still able to evoke an increase in  $[\text{Ca}^{2+}]_i$ . This observation indicated that McN did not act upon the neurones by increasing  $\text{Ca}^{2+}$  influx. Although not demonstrated directly in this study, this is most likely to result from  $\text{IP}_3$ -induced  $\text{Ca}^{2+}$  release from intracellular stores, since previous work has implicated this pathway in the response of  $\text{D}_f$  to McN (David and Pitman, 1994; see below). Following

incubation in the non-specific dopaminergic antagonist, fluphenazine ( $10^{-4}\text{M}$ ), the isolated BA1 motoneurone failed to respond to the application of DA. This observation supports the conclusion that DA receptors mediate the response of BA1 to DA. These observations support the findings of the pharmacological studies presented in Sections 2.3.2.3. and 2.3.4., to confirm the existence of functional muscarinic and dopamine receptors in this neurone, and the likelihood that receptor activation underlies the agonist-induced depolarization in the BA1 motoneurone soma. Furthermore, these results support data obtained using electrophysiological recording techniques that demonstrate the presence of muscarinic receptors on these motoneurons *in situ* (Anderson, 1995; David and Pitman, 1993a, 1996a). It is understood that the cellular response to dopamine has not previously been demonstrated in any isolated insect neurone. Since, the changes in  $[\text{Ca}^{2+}]_i$  can be dramatic and relatively long in duration, it is likely that these agonists may have important modulatory roles in these neurones.

It was noted that relatively high concentrations of the agonists were required to elicit changes in  $[\text{Ca}^{2+}]_i$  in these insect motoneurons; similar concentrations are required to evoke changes in membrane potential and membrane currents under current- and voltage-clamp (see Sections 2.3.2.3. and 2.3.4.; Anderson, 1995; David and Pitman, 1993a). High concentrations of pharmacological antagonists were also needed to block the agonist-induced responses. Possible explanations for such a requirement for high drug concentrations include (i) differences in the biophysical properties of the receptor proteins compared to those of vertebrate preparations and (ii) highly invaginated neuronal plasma membrane preventing the agonists from reaching receptors; if this is the case, it would imply the 'true' sensitivity of the isolated BA1 motoneurone to agonists is greater than demonstrated in the current study (see Discussion, Chapter 2). Another reason for using high concentrations of



antagonists was that, when using a qualitative probe (such as fluo-3) antagonism of an agonist-induced response can only be demonstrated by full block of the agonist response. This may be because these G-protein coupled neurotransmitters activate an enzyme cascade upon agonist-receptor binding and activation of few receptors may, therefore, produce an observable response.

The results of the current studies using fluo-3, demonstrate that atropine (ATR) and fluphenazine (both  $10^{-4}\text{M}$ ) are effective antagonists of muscarinic and dopaminergic receptor activation, respectively, in the isolated BA1 motoneurone. These findings conflict with those presented in Section 2.3.4.; that is, McN- and DA-induced membrane depolarization was not blocked by these antagonists. In light of the current results, it is proposed that the main reason for the ineffectiveness of the antagonists encountered in the earlier experiments is agonist saturation at the receptor binding sites. The ineffectiveness of ATR to block the arecoline-induced muscarinic response but not that of McN-induced increase in  $\text{Ca}^{2+}$ , is that arecoline (in the presence of  $\alpha\text{-BTX}$ ) has a greater affinity for the muscarinic receptor on the somal membrane than McN, and therefore is able to displace ATR more easily than McN. It had been suggested earlier that, at a concentration of  $10^{-4}\text{M}$ , ATR could be acting as a cholinergic agonist (Benson, 1992), to render it ineffective as an antagonist of the muscarinic response. Evidence to suggest this, was not observed during the present series of experiments. That is, ATR was not observed to increase  $[\text{Ca}^{2+}]_i$ , as would be expected of a muscarinic agonist (unpublished observation).

#### *Cellular events following muscarinic receptor activation by McN-A-343*

Under current-clamp, McN does not have a significant effect on the resting membrane potential in either the cockroach  $\text{D}_f$  or locust BA1 motoneurone. In the present study, the bath-application of  $10^{-4}\text{M}$  McN to isolated BA1 motoneurones

did not appear to alter the membrane potential or membrane input resistance (see Section 2.3.2.3), although it has been reported that when tested on BA1 motoneurons *in situ*, in 2 out of 5 preparations McN ( $10^{-4}\text{M}$ ) induced a membrane depolarization of 2mV after 15 minutes, which was accompanied by an increase in input resistance (Anderson, 1995). Similar observations have been made, under current-clamp, from the  $D_f$  motoneurone *in situ* (J. D. Mills, personal communication). However, a recent report has suggested that this cockroach motoneurone is insensitive to McN (Bai and Sattelle, 1994); it is thought possible that the voltage-dependent nature of the McN response (see Discussion, Chapter 2) was overlooked in that study, given the substantial volume of evidence regarding the cellular response of this agonist, examined under voltage-clamp, by David and Pitman (1992, 1993a, c, 1994, 1995, 1996a, b).

From examining the McN-induced response under voltage-clamp, it has been shown that the agonist induces an apparent inward current in the  $D_f$  motoneurone, by decreasing  $I_{Ca}$  (probably by inducing  $Ca^{2+}$ -dependent inactivation) which, in turn, causes a reduction in  $I_{K(Ca)}$  (David and Pitman, 1996b). Since the  $I_{Ca}$  channel blocker, verapamil, has been shown to block approximately 85 - 90% of the  $I_{Ca}$  current in this neurone (J. D. Mills, personal communication), it appears that the majority of the observed McN-induced increase in  $[Ca^{2+}]_i$  observed in this neurone in the presence of verapamil, arises from release from intracellular stores (i.e. a  $I_{Ca}$ -independent manner).

There are two explanations for the apparent lack of response of the  $D_f$  motoneurone under current-clamp at resting membrane potential (usually between -70mV and -80mV), to the bath-application of McN. Firstly, the neurone has a small  $Ca^{2+}$  conductance at these potentials, and secondly,  $E_K$  of the  $D_f$  motoneurone is close to its resting membrane potential. Although there are thought to be two components of  $I_{Ca}$  in  $D_f$  motoneurons *in situ*, these are only

activated at potentials positive to  $-60\text{mV}$  (J. D. Mills, personal communication). Therefore, as few  $I_{\text{Ca}}$  channels are open at resting membrane potential, muscarinic receptor activation has little effect on membrane potential or input resistance unless the neurone is depolarized. This supports the evidence that McN acts to increase  $[\text{Ca}^{2+}]_i$  in a  $I_{\text{Ca}}$ -independent mechanism in this neurone. It may be expected that this  $\text{Ca}^{2+}$  released from intracellular stores induces an increase in  $\text{K}^+$  conductance by activating  $I_{\text{K}(\text{Ca})}$ . This is actually observed (David and Pitman, 1996b). However, no change in membrane potential is associated with the McN response because it is close to  $E_{\text{K}}$ .

Although the kinetics of  $I_{\text{Ca}}$  current of the BA1 motoneurone have not been studied, the presence of this current has been demonstrated under voltage clamp using verapamil,  $\text{Ba}^{2+}$  and other  $\text{K}^+$  channel blockers (Anderson, 1995). The bath-application of McN to the motoneurone *in situ*, having blocked the  $\text{K}^+$  channels, did not appear to affect  $I_{\text{Ca}}$  (McN induces its effects on the membrane potential and input resistance of the neurone by decreasing both a  $I_{\text{K}(\text{Ca})}$  current and a voltage-dependent  $\text{K}^+$  current: Anderson, 1995). This would imply that the McN-induced increase in  $[\text{Ca}^{2+}]_i$  observed in the isolated BA1 motoneurone seen in the current study was the result of increased  $\text{Ca}^{2+}$  release from intracellular stores rather than by an increase in  $I_{\text{Ca}}$ , as proposed for McN-induced increases in  $D_f$  motoneurone. Furthermore, there is evidence from radioligand binding studies to support this. It has been demonstrated that muscarinic agonists increase phosphatidylinositol turnover in locust CNS tissue (Trimmer and Berridge, 1985, Duggan and Lunt, 1986, Qazi and Lunt, 1991).

#### *Mechanism for McN-induced increase in intracellular calcium*

It is now established that, in a number of different insect preparations, cellular events following muscarinic receptor activation can be mediated by

increased phosphatidylinositol turnover, so that, muscarinic agonists act via the second messenger, inositol triphosphate ( $IP_3$ ), to modulate  $[Ca^{2+}]_i$  (Trimmer and Berridge, 1985; Duggan and Lunt, 1986; David and Pitman, 1994). This is based on data obtained from both radioligand binding studies and electrophysiological experiments. David and Pitman, in particular, have extensively studied this phenomenon using cockroach neural tissue. They have provided three lines of evidence to support the involvement of  $IP_3$  in the increase in  $[Ca^{2+}]_i$ , following muscarinic receptor activation. Firstly, under voltage-clamp, pressure-injection of  $IP_3$  into  $D_f$  motoneurons induces a biphasic current response, which resembles that observed following muscarinic receptor activation (David and Pitman, 1993b). Secondly, when examining the mass content of  $IP_3$  in whole nerve cords with a binding assay, McN increased the  $IP_3$  content of the tissue. This response was blocked using the established vertebrate  $M_1$  antagonist, pirenzepine (David and Pitman, 1994). Finally, the inhibitor of  $IP_3$  breakdown, lithium ( $Li^+$ ), potentiates the muscarinic receptor-mediated increase in  $IP_3$  content of whole nerve cords and prolongs the McN-induced modulation of ligand-gated ion channel function in  $D_f$  motoneurons (David and Pitman, 1996a).

In the present study, examination of agonist-induced changes in  $[Ca^{2+}]_i$  were restricted to global changes within the isolated motoneurone. This was because the fastest rate the laser could scan the preparation and the computer write the image data to the optical disk, whilst maintaining image resolution, was 0.2Hz. Had improved time resolution been available, changes in  $[Ca^{2+}]_i$  with faster kinetics, such as  $Ca^{2+}$  waves and oscillations, may have been observed (see Pozzan *et al*, 1994). Further examination of muscarinic agonist-induced increases in  $[Ca^{2+}]_i$  would be of interest to the present study, particularly using a quantitative fluorescent probe, such as fura-2. This is because membrane potential

oscillations were observed with arecoline-induced membrane depolarizations of the isolated BA1 motoneurone, in the presence of  $\alpha$ -BTX. Such an observation is thought to be linked to  $[Ca^{2+}]_i$  oscillations (see Berridge, 1993). It has been suggested that the key to the generation of such rhythmic  $[Ca^{2+}]_i$  events is the bell-shaped dependency on  $[Ca^{2+}]_i$  of the  $IP_3$  receptor for its function (for detailed reviews see Berridge, 1993; Pozzan, *et al*, 1994). That is, as  $[Ca^{2+}]_i$  increases, so does CICR ( $Ca^{2+}$ -induced  $Ca^{2+}$  release) until a maximum is reached, at which point, further increases in  $[Ca^{2+}]_i$  inhibit the  $IP_3$  receptor resulting in almost complete inhibition of CICR. Since the function of both  $IP_3$  and ryanodine receptors is also sensitive to modulation by protein kinases, receptor phosphorylation may also contribute to these events (see Pozzan *et al*, 1994).

#### *Cellular events following the activation of insect dopamine receptors*

If neurotransmitter receptor activation results in a change in  $[Ca^{2+}]_i$ , as demonstrated in the current series of experiments, the mechanisms by which this occurs are unlikely to be simple. For example, calcium-sensitive proteins, in particular the protein kinases, may be involved and their effects on cell function can be complex (see Swope *et al*, 1992). As described in Discussion 2.4, the identity and the nature of the transduction mechanisms activated following agonist binding to the insect DA receptor protein(s) have yet to be fully determined. Briefly, a DA receptor of *Drosophila* has been shown to be homologous to the  $D_1/D_5$  vertebrate DA receptor (Gotzes *et al*, 1994), and the pharmacological properties of the DA receptor of the  $D_3$  cockroach motoneurone resemble more closely those of the vertebrate  $D_1$ -like receptor than those of the  $D_2$ -like receptor. However, the ionic basis of the DA-induced current of this neurone has yet to be clarified and it is not yet clear whether second messenger pathways are involved (Pitman and Davis, 1988; Davis and Pitman, 1991). The cockroach salivary gland

acinar cell DA receptor, which also resembles the vertebrate D<sub>1</sub>-like receptor rather than the D<sub>2</sub>-like receptor (Evans and Green, 1990, 1991), has been linked to both cAMP production (Gray *et al*, 1984) and the activation of phospholipase C (PLC) (A. M. Evans, unpublished observations). These two transduction mechanisms are believed to have separate physiological roles in this preparation: cAMP is associated with the secretory response of the glands (Gray *et al*, 1984), whilst it has been proposed that IP<sub>3</sub>, one of the products of PLC activation, is linked to the hyperpolarizing response observed in the cells (A.M. Evans, unpublished observations).

*Possible mechanisms by which DA decreases intracellular calcium*

The possible involvement of cytosolic calcium-binding proteins (see Blaustein, 1988; Alberts *et al*, 1983) and the Na<sup>+</sup>-Ca<sup>2+</sup> exchange mechanism (see Lederer *et al*, 1990) cannot be excluded as mechanisms for the lowering of [Ca<sup>2+</sup>]<sub>i</sub>. However, I believed that they would be unable to elicit responses of the amplitude and time course observed following the bath-application of DA; evidence for the neurotransmitter-mediated modulation of these mechanisms has not been published. An experiment to determine whether metabolic pumping processes are responsible for the DA-induced lowering of [Ca<sup>2+</sup>]<sub>i</sub> would be the replication of these experiments at different environmental temperatures and the investigation of any temperature sensitivity of the response.

It is thought most likely that DA stimulates Ca<sup>2+</sup> sequestration into intracellular stores by Ca<sup>2+</sup>ATPase to lower [Ca<sup>2+</sup>]<sub>i</sub>, given the nature and time courses observed of the DA-induced response. However, other mechanisms that result in the reduction of [Ca<sup>2+</sup>]<sub>i</sub> cannot be excluded. Whether the DA receptor is coupled to phosphatidylinositol hydrolysis (resulting in the elevation of cytosolic diacylglycerol and IP<sub>3</sub>) or the stimulation of adenylate cyclase (to elevate



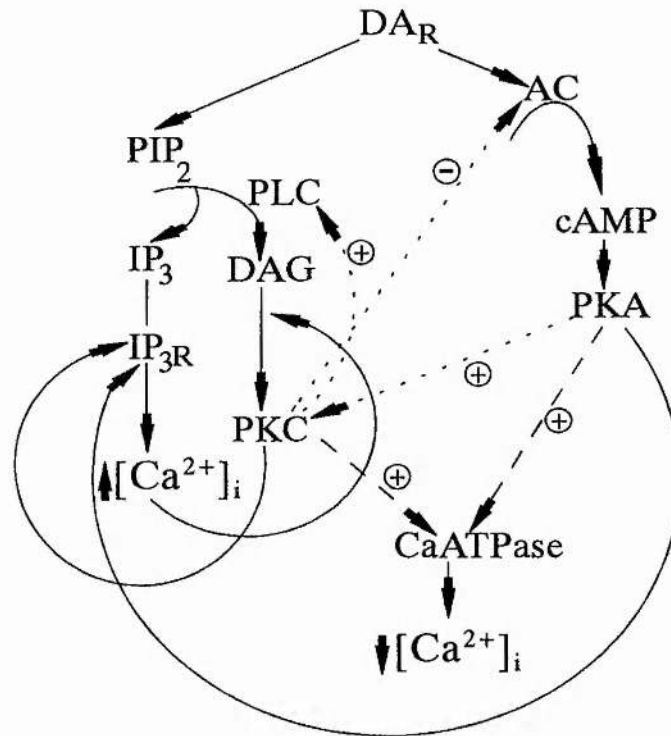


Figure 3.4.1. Schematic diagram summarizing a hypothesis of the cellular events of DA regulation of  $[Ca^{2+}]_i$  in isolated BA1 motoneurons and D<sub>f</sub> motoneurons. Both AC- and PLC-coupled transduction pathways may be involved in DA-induced lowering of  $[Ca^{2+}]_i$ . The changes in  $[Ca^{2+}]_i$  observed in this study may be the balance of the activation of both AC and PLC. As cross-reactivity of these two second messengers has recently been described, DA modulation of  $[Ca^{2+}]_i$  may be complex. See text for further details.

**Key:** AC - adenylate cyclase; Ca<sup>2+</sup> - calcium ions; CaATPase - calcium-activated ATPase; cAMP - cyclic adenosine monophosphate; DAG - diacylglycerol; DAR - dopamine receptor; IP<sub>3</sub> - inositol trisphosphate; IP<sub>3</sub>R - inositol trisphosphate receptor; PIP<sub>2</sub> - phosphatidyl inositol diphosphate; PKA - cAMP-dependent protein kinase; PKC - Ca<sup>2+</sup>/DAG-dependent protein kinase; PLC - phospholipase C; +/- - stimulatory/inhibitory action

**solid lines** represent events that are known to occur in neural tissue.

**dotted lines** represent known modulatory interactions the protein kinases have on the cascade pathways.

**broken lines** represent the mechanisms thought likely to be involved in Ca<sup>2+</sup> sequestration following DAR activation in these neurones.

cytosolic cAMP), it is proposed that DA may stimulate sequestration by the activation of cAMP-dependent protein kinase (PKA) and/or  $\text{Ca}^{2+}$ /diacylglycerol-dependent protein kinase (PKC) (see Figure 3.4.1). Both kinases have been reported to be involved in the enhancement of  $\text{Ca}^{2+}$  uptake into intracellular organelles (Figure 3.4.1, broken lines). It has been demonstrated that PKA stimulates  $\text{Ca}^{2+}$  uptake into isolated platelet vesicles by examining the effects of PKA and an inhibitor of this kinase on sequestration (Hettasch and Le Breton, 1987); PKC has been reported to stimulate  $\text{Ca}^{2+}$  uptake in intact platelet cells by increasing the maximum velocity ( $V_m$ ) of the enzyme responsible for sequestration,  $\text{Ca}^{2+}$ ATPase (Tao *et al*, 1992). However, these mechanisms by which DA could modulate  $[\text{Ca}^{2+}]_i$  may be complicated further, as cross-reactivity of these two second messenger pathways has recently been described (Figure 3.4.1, dotted lines). Using cloned rat DA  $D_{1A}$  receptors, it has been demonstrated that activation of PKA can result in the activation of PKC which in turn, stimulates PLC (Yu *et al*, 1996), and in rat kidney cells, PKC is reported to inhibit cAMP formation by the inhibition of AC (Teitelbaum and Berl, 1994). Other known interactions which may be of importance for PKA/PKC-mediated regulation of  $[\text{Ca}^{2+}]_i$  are also illustrated in Figure 3.4.1. Both protein kinases are known to stimulate  $\text{IP}_3$ -induced  $\text{Ca}^{2+}$  release via  $\text{IP}_3$  receptors, and  $\text{Ca}^{2+}$  itself is involved in the activation of PKC (see Pozzan *et al*, 1994).

Therefore, if the insect neuronal DA receptors examined in this study resemble those in the cockroach salivary gland, i.e. activation of DA could result in the production of AC and PLC, then the different time courses observed of the DA-induced decrease in  $[\text{Ca}^{2+}]_i$  may be explained as the balance between the PKA- and PKC- induced  $\text{Ca}^{2+}$  sequestration and the  $\text{IP}_3$ -induced  $\text{Ca}^{2+}$  release. For example, a rapid decrease in  $[\text{Ca}^{2+}]_i$  may be the result of a rapid production of cAMP activating PKA, to cause rapid  $\text{Ca}^{2+}$  sequestration. The rise in  $[\text{Ca}^{2+}]_i$



following this could be a rebound effect occurring as a consequence of rapid lowering of  $[Ca^{2+}]_i$ , or the effects of  $IP_3$ -induced  $Ca^{2+}$  release which may outlast the effects of cAMP. Slower response times could arise from the simultaneous activation of PLC and AC.  $Ca^{2+}$  sequestration could still occur in this case because  $Ca^{2+}$ , together with DAG (the other breakdown product of  $PIP_2$  hydrolysis along with  $IP_3$ ), activates PKC to stimulate  $Ca^{2+}$  uptake into the smooth endoplasmic reticulum and mitochondria (see Figure 3.4.1.).

To summarize:

It has been demonstrated using the  $Ca^{2+}$ -sensitive dye, fluo-3 in conjunction with the vertebrate  $M_1$  muscarinic agonist, McN-A-343, and dopamine, that functional  $M_1$ -like muscarinic receptors and dopamine receptors are present on the soma of the first basalar (BA1) motoneurone of the locust and the fast coxal depressor ( $D_f$ ) motoneurone of the cockroach.

McN-A-343 induced an increase in  $[Ca^{2+}]_i$  in both insect neurone preparations. It is understood to occur from muscarinic acetylcholine receptor-mediated  $IP_3$  release of  $Ca^{2+}$  from intracellular  $Ca^{2+}$  stores, rather than via an increase in a voltage-dependent  $Ca^{2+}$  current. The McN-induced increase in  $[Ca^{2+}]_i$  in the BA1 motoneurone soma was blocked using the cholinergic antagonist, atropine.

Dopamine induced a decrease in  $[Ca^{2+}]_i$  in both insect neurone preparations. Since, the pharmacological profile of the DA receptors on these neurones has not yet been established, a hypothesis has been proposed for the mechanism of  $Ca^{2+}$  sequestration. It is thought that protein kinases may be involved in the lowering of  $[Ca^{2+}]_i$ . The DA-induced decrease in  $[Ca^{2+}]_i$  in the BA1 motoneurone soma was blocked using the dopaminergic antagonist, fluphenazine.

## **Chapter 4**

### **A study of cultured isolated locust neurones**

## INTRODUCTION

The suitability of isolated invertebrate neurone preparations for the study of elements of synapse formation and neuromodulation has been established (see Section 1.4.2). Species of Mollusca and Annelida lend themselves particularly suitable as experimental models for such investigations. However, techniques required to maintain insect neurones (particularly those from adults) in long-term culture, have remained elusive. Furthermore, there is currently no firm evidence that insect neurones are able to form functional neurone-neurone synaptic connections *in vitro*. A brief synopsis of the progress of isolated insect neurone cultures is given below.

Prior to 1980 there was little literature available that described the use of isolated insect nerve cell cultures for the investigation of specific neuropharmacological problems (for reviews see Beadle and Hicks, 1985; Thomas *et al*, 1987). Most of the work had been based on the use of embryonic and nymphal tissue rather than material obtained from adult animals. Usherwood and his co-workers first reported successful culture of dissociated locust (*Locusta migratoria*) neurones (Giles *et al*, 1978). They reported that, when cultured alone, embryonic and third instar neurones exhibited neuritic outgrowth. The degree of neurite growth of neurones from instars, however, was greatly enhanced when co-cultured with the embryonic neurones and morphological connectivity was observed.

A system for culturing dissociated insect neurones was pioneered by Chen and Levi-Montalcini, who, in developing a successful chemically defined growth medium (colloquially known as '5 + 4'), maintained dissociated embryonic cockroach neurones *in vitro* (Chen and Levi-Montalcini, 1970a, b). The culture medium had previously been shown to support the axonal outgrowth from intact

embryonic cockroach (*Periplaneta americana*) brains and ganglia *in vitro* (Chen and Levi-Montalcini, 1969). It was reported that these dissociated neurones, when cultured alone (in the absence of glial cells), exhibited limited neurite outgrowth and survived for approximately 2 months with little morphological change; however, in the presence of embryonic foregut explants, the neurones survived for 4 to 5 months, developed a dense, organized fibrillar network, that connected the muscle explant which exhibited muscular contractions. Furthermore, electron microscopy techniques showed the presence of synaptic vesicles and the thickening of presynaptic membranes. To date, ultrastructural examinations of cockroach neurone cultures have indicated the presence of synapses. However, unequivocal evidence from electrophysiological studies supporting the formation of synaptic connections, has been limited (Hicks and Beadle, 1980; Beadle *et al*, 1982; see Lees and Beadle, 1988). Since the work of Chen and Levi-Montalcini (1970a, b), it has been found that the presence of foregut is not necessary for extensive growth of these cultures (Schlapfer *et al*, 1972; Hicks and Beadle, 1980).

Most of the work of the 1980's progressed towards a greater understanding of the pharmacology of isolated insect neurones, which was facilitated by improved culture techniques. Short-term cultures of freshly dissociated adult neurones and long-term cultures of embryonic and nymphal neurones were employed as models for investigations of the neuropharmacology of the insect nervous system. Of particular importance to studies of isolated neurones *in vitro* was the development of the 'adapted hanging column' technique, by Beadle and his co-workers, which reduced the level of debris contamination in culture preparations (Beadle and Hicks, 1985; Beadle and Lees, 1986). Techniques used for the pharmacological studies included the various configurations of the patch-clamp technique, the voltage-clamp technique, ligand binding studies and

neurotransmitter uptake studies. These allowed an in-depth study of various receptor populations of insect neurones, in particular, acetylcholine, GABA and glutamate receptors, in addition to the actions of insecticides and pesticides. Whilst neural tissue of the locust (*Schistocerca* and *Locusta*), housefly (*Musca*), fruitfly (*Drosophila*) and moth (*Spodoptera*) have been used, that of the cockroach (*Periplaneta americana*) has been most thoroughly investigated (for reviews see Beadle and Hicks, 1985; Beadle and Lees, 1986; Lees and Beadle, 1988).

#### *Use of adult locust neuronal tissue*

The use of freshly isolated adult locust (*Schistocerca gregaria*) nerve cells to obtain the electrophysiological properties and pharmacological profiles of these neurones was first described by Usherwood and his co-workers (Usherwood *et al*, 1980). However, their attempts to culture the dissociated neurones were unsuccessful. In 1985, Suter and Usherwood described an *in vitro* technique which was used to investigate the effects of various neurotransmitters and putative transmitters on isolated adult neurones (Suter & Usherwood, 1985; Giles & Usherwood, 1985). More recently, Benson and his co-workers used the method of Usherwood *et al* (1980), in conjunction with current- and voltage-clamp recording techniques, to examine the electrophysiological pharmacology of 'nicotinic' and 'muscarinic' cholinergic responses and multiple serotonin-activated currents of freshly dissociated adult thoracic *Locusta* neurones (Benson and Neumann, 1987; Benson, 1992; Bermudez *et al*, 1992).

Whilst embryonic insect tissue has been proven amenable to long-term electrophysiological and pharmacological studies, maintaining isolated adult insect neurones in culture has proven to be difficult. It is worthwhile to pursue this area of research as it has been shown that experimental data obtained from neurones *in vitro* is qualitatively similar to that obtained from neurones *in situ* and

*in vivo* (Suter and Usherwood, 1985; Anderson, 1995; David and Sattelle, 1984). *In vitro* studies have been carried out on adult cockroach and housefly neurones (Pinnock and Sattelle, 1987; Harrison *et al*, 1990). However, these cells exhibited limited neuritic outgrowth and remained in culture for periods of up to 7 days.

The first successful method by which isolated adult thoracic cockroach neurones could be maintained in long-term culture, that is, for up to three weeks in the absence of glial cells, was described by Howes *et al* (1991). In addition to describing the morphology and plasticity of neuritic outgrowth from the neurones, the functional status of the cells was demonstrated using the calcium-sensitive fluorescent dye, fura-2. This culture technique has recently been refined to enable the growth of adult cockroach dorsal unpaired median (DUM) neurones *in vitro* for several weeks (Newland *et al*, 1993). These neurones retained their *in vivo* membrane characteristics and typical morphological growth patterns; using a different experimental protocol, similar findings have been reported (Lapied *et al*, 1993).

Following the work of Howes *et al* (1991) there have been further reports of the use of adult insect neurones in tissue culture studies. Adult hawkmoth thoracic leg motoneurones have been maintained *in vitro*, using the growth medium devised by Hayashi and Hildebrand (1990) for the cultivation of pupal hawkmoth antennal lobe neurones, in order to examine the modulation of ionic currents associated with metamorphosis (Hayashi and Levine, 1992). Kirchhof and Bicker (1992) have recently described a technique which enabled dissociated fifth instar and adult thoracic neurones from two locust species, *Locusta migratoria* and *Schistocerca gregaria*, to be maintained in culture. They reported neuritic outgrowth from *Schistocerca* neurones, but not *Locusta* neurones, to be enhanced when the cells were grown in haemolymph-enriched culture medium. However, under these conditions, the degree of neuritic branching decreased and

there was no report of evidence of synaptogenesis. Finally, Rössler and his co-workers have established both larval and adult locust medial neurosecretory cells in culture. In addition to showing the morphology and electrophysiological properties of the cultured neurones, using whole-cell patch-clamp techniques, they have examined the calcium channel currents of these cells (Rössler and Bickmeyer, 1993; Bickmeyer *et al*, 1994).

#### *Neuromuscular junction formation*

The formation of neuromuscular junctions using insect tissue *in vitro* has been easier to achieve than synaptogenesis between neurones. Using *Drosophila melanogaster*, Seecof showed that it was possible to follow the differentiation of nerve cells and myocytes from neuroblasts and myoblasts and reported the formation of neuromuscular junctions *in vitro* (Seecof & Teplitz, 1971; Seecof *et al*, 1972). Furthermore, following the report of an improved methodology permitting the full neuronal differentiation of embryonic cockroach neurones *in vitro* (Beadle *et al*, 1982), Beadle and his co-workers showed myogenesis and neuromuscular junction formation in cultures of *Periplaneta americana* myoblasts and neurones which resembled those on adult insect muscle (Bermudez *et al*, 1986).

The overall aim of the current work is to be able to study synaptic transmission and its modulation at the wing-hinge stretch receptor neurone (SR)-first basalar motoneurone (BA1) synapse, in the absence of heterosynaptic modulation, using primary neuronal culture techniques. Of particular interest are presynaptic 'muscarinic' receptors which autoregulate the release of acetylcholine at this monosynaptic connection (Leitch *et al*, 1993; Leitch and Pitman, 1995).

Although it had been demonstrated that adult cockroach (Howes *et al*, 1991) and adult tobacco hawkmoth neurones (Hayashi and Levine, 1992) could be supported *in vitro*, at the time of this study there was no evidence of isolated adult locust neurones being maintained in culture and fully differentiated adult dissociated insect neurones forming synaptic connections in culture. Evidence of synaptogenesis is necessary if the characteristics of the SR-BA1 synapse are to be studied.

The aims of the current investigations were (i) to develop a protocol for the maintenance of dissociated, unidentified, adult locust neurones (existing as a homogeneous cell population) in culture, (ii) assess the ability of culture media routinely used in insect neuronal culture studies, to support neuronal growth and development of isolated adult insect neurones (iii) culture the isolated adult BA1 motoneurone using the technique developed for the maintenance of unidentified adult locust neurones and (iv) using a conventional single microelectrode intracellular recording technique, investigate the electrophysiological properties of the cultured neurones.



## MATERIALS AND METHODS

### 4.2.1. Culturing of unidentified dissociated locust neurones

#### 4.2.1.1. Dissection and preparation

The procedure used for preparing primary isolated unidentified neurone cultures was adapted from the technique described by Howes *et al* (1991). This protocol was devised because it was wished to exclude the use of degradative enzymes used in many investigations for the isolation of neurones from nervous tissue. Such enzymes may have a deleterious effect on the health of the cells prior to their placement in culture.

Locusts were anaesthetized using 100% carbon dioxide for approximately 2 to 3 minutes, before they were surface-sterilized by rinsing them in 70% ethanol for approximately 30s. All procedures were carried out under aseptic conditions; work was performed in a laminar flow cabinet or under an ethanol (70%) sterilized plastic cabinet using sterile dissecting techniques.

Animals were pinned out ventral surface uppermost, on a Sylgard-filled Petri dish, having had their head and legs removed. The cuticle of the thorax was removed to expose the pro-, meso- and metathoracic ganglia. The three ganglia were dissected free of the body cavity and placed in fresh sterile culture medium (see below for further details). At this point fat and tracheal tissue surrounding each ganglion were removed. The ganglia were then rinsed in three changes of fresh medium to minimize the level of microbial contamination prior to desheathing. Each ganglion was isolated from the adjacent and the interganglionic connectives and peripheral nerves cropped short. The ganglia were then transferred to a 5ml sterile aliquot tube (Teklab, U.K.) containing 1.0ml of culture medium where they were mechanically dissociated by repeated trituration (3 to 4 times) using a sterilized glass Pasteur pipette (John Poulten Ltd) which had been

flame-polished (see Figure 4.2.1). The pipette had been thoroughly wetted before use by drawing culture medium up and down the pipette. The wetting prevented the neurones from adhering to the glass walls of the pipette.

The suspension of cell bodies was then passed through a sterile nylon mesh (Mesh 190, H. Simon Ltd) wetted with culture medium using a Pasteur pipette (as described above), and transferred into a plastic culture dish. The purpose of the mesh was to remove the larger pieces of debris, such as remnants of the ganglionic sheath and glial cells. The culture medium was either spread out over the bottom of a culture dish (Celcult; diameter 35mm, vented) or 4 - 5 drops of the suspension was placed into the centre of a specially prepared plastic culture dish (see Figure 4.2.1). This dish (Falcon 1006; diameter 50mm, tight-seal) had four small pieces of glass microscope slide which had been flamed and covered in Vaseline, and arranged in it as shown. A glass coverslip was then lowered onto the culture medium supported by the Vaseline-covered glass fragments. The coverslips and glass pieces were stored under ethanol (70%) and flamed before use - coverslips were allowed to cool before being placed over the culture medium. After placing the lid onto the dish the suspension was allowed to settle for 1 hour. The culture medium was then replaced with fresh medium and the preparation was inverted. Inverting preparations is reported to prevent the fine debris not removed by passing the neurone suspension through the nylon mesh from settling on the growth surface. Such debris inhibits neurite growth and obscures neuronal processes that do develop. This protocol is an adaptation of that described by Beadle and Hicks (1985) which was based on a technique described by Shields, Dübendorfer and Sang (1975).

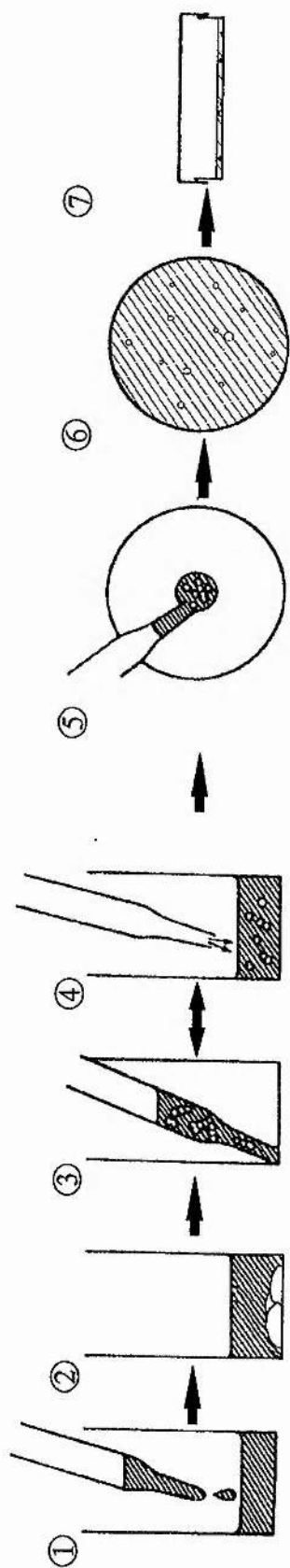
The Petri dishes containing the isolated neurones were then transferred to a sterile plastic box - usually four culture dishes were set up for each experiment. An open culture dish containing sterile distilled water was placed inside the sterile

Figure 4. 2. 1. Schematic diagram of the preparation of isolated locust thoracic neurone cultures.

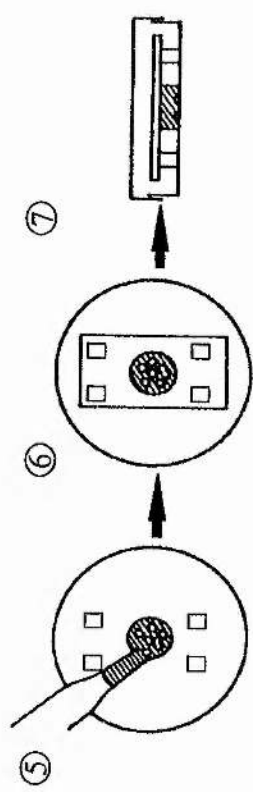
A 5ml sterile aliquot tube contained 1ml of sterile culture medium; this medium was used to wet the internal surfaces of the sterile flame-polished glass Pasteur pipette, prior to use. The medium was drawn up and down the pipette; this prevented dissociated neurones adhering to the glass ①. ② The dissected thoracic locust ganglia, separated from their interganglionic connectives and peripheral nerve trunks were placed into the growth medium. Using the wetted pipette, the thoracic ganglia were triturated; that is, the neural tissue was dissociated by repeatedly (3 to 4 times) passing it up and down the sterile flame-polished Pasteur pipette to isolate the neurone somata ③ and ④.

Then **either** the suspension of dissociated thoracic locust neurones (1ml) was then passed through a wetted (with sterile culture medium) sterile nylon mesh (for clarity this is not shown), and into a plain plastic culture dish, using the flame-polished Pasteur pipette ⑤. By gently tilting the culture dish in various planes, the dissociated neurones and culture medium were spread across the bottom of the dish ⑥. ⑦ shows the dissociated neurone culture preparation in profile, following the placement of the lid onto the dish. This protocol was adapted from the technique described by Howes *et al*, 1991.

**Or** the suspension of dissociated neurones was passed through the wetted sterile nylon mesh (again, for clarity it is not shown), and approximately 4 drops of the suspension were placed in the centre of a specially prepared plastic culture dish. The dish had four small pieces of glass microscope slide firmly placed on the surface of the dish (as illustrated), which were held in position with Vaseline ⑧. A sterile glass coverslip was then placed over the droplet of culture medium, to be supported by the pieces of glass ⑨. ⑩ shows the profile of this preparation, known as the 'hanging column (or drop)' preparation, after Shields *et al* (1975). Once replacing the lid on the culture dish, the preparation was left for 1 hour, allowing the neurones to adhere to the surface of the dish. The culture medium was then replaced with fresh medium, and the preparation was inverted. To exchange the culture medium for fresh medium, using fine forceps, the coverslip is very carefully lifted from the glass supports, thus, enabling replacement of the medium. This preparation is an adaptation of that described by Beadle and Hicks (1985), and was implemented to improve the likelihood that neurone-neurone contacts were observed.



or



box to maintain a humid atmosphere, and so prevent evaporation of water from the culture medium. The box was then placed inside a Perspex container and sealed with plastic insulating tape. Cultures were maintained in air at 29°C using a Grant incubator. Approximately 75% of the culture medium was replaced with fresh medium every 3 to 4 days; although neurones can survive with no apparent detrimental effects when the medium is replaced only once every 7 days (I. Bermudez, personal communication). Cultures were observed daily using an inverted phase contrast microscope (normally Olympus, CK-2, however, also Cooke, Troughton and Simms Ltd, M264 was used). Neuritic outgrowth was recorded photographically using an Olympus OM-2 camera; the films (Agfapan) were developed by the University of St. Andrews Photographic Department. The electrical properties of isolated cells in growth medium were observed using a conventional single intracellular microelectrode recording technique.

Microelectrodes were drawn from thin-walled filamented capillary glass (Clark Electromedical Instruments; external diameter, 1.5mm; internal diameter 1.17mm) using a Narishige PE-2 vertical puller. They were filled with 1M KAc which gave resistance values of 10 to 20 M $\Omega$ . Membrane responses to injected current were observed in some neurones; the current pulses were applied using a Grass SD9 stimulator which was connected to a laboratory-made amplifier/bridge. The electrical activity of the cultured neurones was monitored using a Gould 1421 oscilloscope and hard copies of the data were plotted using a Bryans X-Y 24000 Recorder.

#### 4.2.1.2. Culture Media

Several culture media are known to support the growth of insect neurones in culture; these include Chen and Levi-Montalcini's '5 + 4' medium (Gibco) which supports adult cockroach neurones *in vitro* (Howes *et al*, 1991), and a

supplemented Liebovitz L15 medium which supports hawkmoth olfactory neurones *in vitro* (Hayashi & Hildebrand, 1990). These media were tested for their ability to support adult locust neurones in culture. In the case of the latter medium, it was also used in a parallel study using dissociated fifth instar neurones, to compare the patterns of neuritic growth and development of these neurones, with that of the adult neurones. The medium was tested with and without the fetal calf serum (FCS; Integra Biosciences, UK) supplement. The compositions of these media are given in Appendix 7.

#### 4.2.1.3. Preparation of culture dishes

Since Howes *et al* (1991) reported adult cockroach neuritic growth to be promoted in the presence of cockroach haemolymph, the effect of locust haemolymph on neurite outgrowth was examined. For the preparation of haemolymph-coated culture dishes, the hindleg of an anaesthetized, surface-sterilized locust was removed at its base from the thorax and one drop of haemolymph per dish was squeezed from it, to fall into the culture dish containing 0.5ml of medium. The haemolymph was then allowed to spread out and settle for two hours. Prior to use, each dish was rinsed three times with sterile medium.

#### 4.2.2. Culturing isolated first basalar motoneurones

A protocol was developed which combined the techniques used to isolate BA1 for electrophysiological studies (see Section 2.2.4.2.) with those described for the culturing of unidentified locust neurones so that the BA1 motoneurone could be cultured.

Once the thoracic ganglia were removed from the locust they were secured on a Perspex slide and the mesothoracic ganglion was desheathed, as previously described. The preparation was then transferred to the isolation bath, which was

filled with sterile culture medium instead of locust saline. The BA1 cell body was isolated with a small cluster of other neighbouring neurones, as previously described (see Section 2.2.4.2.) and then rinsed in two changes of sterile medium to minimize microbial contamination. The cluster of cells was then plated out on plastic culture dishes (Celcult; 35mm, vented) containing 1.0ml growth medium and treated in the same manner as the unidentified dissociated locust neurones.



## RESULTS

### 4.3.1. Maintenance of isolated unidentified locust neurones in culture

The protocol described for the isolation and long-term maintenance of dissociated adult cockroach neurones *in vitro* (adapted from Howes *et al*, 1991) was successful for the culturing of isolated adult locust (*Schistocerca gregaria*) neurones. Using an inverted phase-contrast microscope to examine the neurone cultures, viable somata of various sizes (diameters of 50 to 130 $\mu$ m) were observed adhered to the surface of the culture dishes. The following criteria were used as determinants of cell viability (i) the neurones were 'phase-bright' when viewed using the inverted phase microscope, (ii) their cytoplasm appeared to be agranular, (iii) neuritic outgrowth was observed (both photomicrographs and sketches of the neurones annotated with some of their prominent structural features have been included in the results) and (iv) when examined using electrophysiological recording techniques, properties such as resting membrane potential and the response to injected current appeared similar to those reported *in situ*.

When dissociated adult locust neurones were cultured in Chen and Levi-Montalcini's '5 + 4' growth medium, the isolated neurones tended to extend single neurites which were relatively straight in their morphology - branching of neurites was rarely seen (see Figures 4.3.1i and 4.3.1ii). The neurones were usually maintained in culture for time periods of up to five days. Figures 4.3.1i and 4.3.1ii show a neurone, at three days in culture using '5 + 4' culture medium, which had extended a single neurite with varicosities (small nodule-like structures) along its length. The reason why this neurone has a slightly different appearance to other neurones shown later in this section, is because this preparation was viewed using an M264 microscope (Cooke, Troughton and



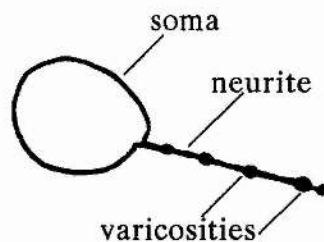
Figure 4.3.1. Neuritic outgrowth from a dissociated unidentified adult thoracic locust neurone cultured in Chen and Montalcini's '5 + 4' (5 parts Schneider's *Drosophila* medium revised to 4 parts Minimum Essential Medium (Eagle) with Hanks' salts) growth medium.

i. A photomicrograph showing the typical neuritic extensions produced from dissociated adult thoracic locust neurones, seen from a neurone on the third day in culture. Single, straight neurites usually emanated from the cell soma; neuritic branching was rarely seen. In this example, varicosities (small nodule-like structures) were observed along the length of the neurite. However, their physiological basis and role was not investigated.

ii. An annotated sketch of the photomicrograph shown in Figure 4.3.1i, illustrating the morphological features described above.

Scale = 100 $\mu$ m

ii



i



—

Simms, Ltd); the other culture preparations were viewed using an Olympus CK-2 microscope.

When haemolymph-coated culture dishes were used in association with '5 + 4' medium, the ability of neurones to adhere to the surface of the dish appeared to be reduced. That is, there was an increase in the proportion of cells floating in suspension to those adhered to the culture dish. However, the neurones that did adhere, exhibited improved neuritic outgrowth (not shown). Neurones that failed to adhere to the culture dish failed both to extend neurites and to survive in culture. The finding of improved neuritic outgrowth of locust (*Schistocerca gregaria*) neurones in the presence of haemolymph is in agreement with Kirchhof and Bicker (1992) who reported enhancement of nymphal *Schistocerca gregaria* neuronal outgrowth when cultured in haemolymph-conditioned medium. The main problem with the cultures in this study was the population of neurones was contaminated with non-neurone-like cells (the growth of which was supported by the '5 + 4' medium) and unidentified debris, which appeared to prevented cell adhesion. The non-neurone-like cells were believed to be muscle cells as their appearance resembled the cells described as muscle cells by Bermudez *et al* (1986). The presence of muscle fibres was not totally unexpected, since the haemolymph was obtained by squeezing the muscular hindlegs of locusts. In future studies, to improve the success rate of neuritic growth using '5 + 4' medium in the presence of haemolymph, it is suggested that haemolymph is obtained from the locust body cavity as described by Kirchhof and Bicker (1992). This technique enables the collection of larger volumes of 'clean' haemolymph per animal for use in locust neurone culture studies.

When the results described above were compared with those of other insect neurones in culture (particularly Howes *et al*, 1991; Hayashi and Hildebrand, 1990; Hayashi and Levine, 1992; R. M. Pitman, personal

communication), it appeared that there could be either (i) unknown factors or conditions hindering cell survival and neuritic outgrowth, or (ii) certain currently unidentified factors necessary for more extensive, branched neurite outgrowth and sustained neuronal viability not present in the '5 + 4' medium. It was believed that these factors could be important criteria if synaptogenesis was to be observed. Although this growth medium supported cell adhesion and initial neuritic outgrowth of isolated adult locust neurones, it was decided to test the ability of the chemically undefined growth medium of Hayashi and Hildebrand (1990), for the long-term development of dissociated adult locust neurones in culture. In addition, dissociated neurones from fifth instar locusts were cultured, in order to compare their neuritic outgrowth and viability in culture with that of adult neurones. The medium devised by Hayashi and Hildebrand for the maintenance of dissociated tobacco hawkmoth neurones *in vitro* contains 10% FCS. The medium was tested for its ability to support dissociated locust neurone viability and neuritic development in the absence, and presence, of FCS.

In the absence of 10% FCS, this medium enhanced the neuritic outgrowth and viability of adult locust neurones, compared to that observed when the '5 + 4' culture medium was used (compare Figure 4.3.1 with Figure 4.3.6). Such cultures could usually be maintained for one week and sometimes up to two weeks. The ability of the medium to support fifth instar neurones *in vitro* was very similar to that observed with adult neurones, in terms of duration and patterns of neuritic outgrowth. Owing to technical photographic difficulties, most of the examples shown in the figures are of fifth instar neurones in culture. However, similar observations were made of cultured adult neurones.

Locust neurones cultured in the medium developed by Hayashi and Hildebrand produced two forms of neuritic processes: neurites and filopodia. Neurites were the broader projections emanating from the cell body (see Figures

4.3.2Ai and 4.3.2Aii), and filopodia were the finer neuritic projections that extended from the tip of the neurites (see Figures 4.3.2Ai and 4.3.2Aii) or directly from the cell body itself (see Figures 4.3.2Bi and 4.3.2Bii). The patterns of neurite outgrowth from the soma also differed. Two dominant forms were noted: (i) multipolar outgrowth (meaning neuritic processes extended from many points around the soma), which was seen in the absence of a prominent axonal stump emanating from the soma (see Figures 4.3.2A and 4.3.2B) and (ii) monopolar growth, (growth from one distinct point) which was induced by the presence of a prominent axonal stump from the soma (see Figure 4.3.3i and 4.3.3ii). In the former type of pattern of outgrowth, it was believed that the soma did lack an axonal stump rather than the stump protruding at an angle which left it unseen, for example, underneath the soma. This opinion came from two lines of evidence. First, when focussing between the neuritic processes (whose in-focus focal plane is very close to that of the surface of the culture dish) and the cell body of a neurone, there were only subtle differences in the in-focus focal planes of both features. Consequently, it would seem unlikely that an axonal stump would be present underneath the cell body. Second, when isolated neurones (isolated from the crayfish (*Pacifastacus leniusculus*) central nervous system so that a segment of axon is also present) are placed in culture medium, the soma settles first on the surface of the culture dish. Consequently, the axonal stump does not interfere with the cell body adhering to the culture dish (S. Falconer, personal communication). It has been suggested that the presence of an axonal stump induces monopolar outgrowth by preferentially targeting an axonal transport system, which is involved in the movement of building materials (such as microtubules and actin filaments), from the somatic region of the neurone into the remaining primary neurite stump, for neuritic regeneration (Kirchhof and Bicker, 1992).

Figure 4.3.2. Varied forms of neuritic outgrowth were observed from dissociated thoracic locust neurones, when cultured in Hayashi and Hildebrand's chemically undefined growth medium (in the absence of fetal calf serum).

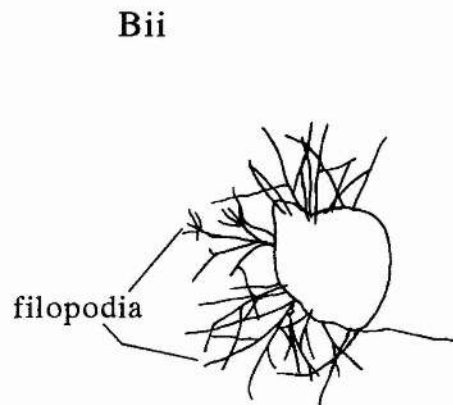
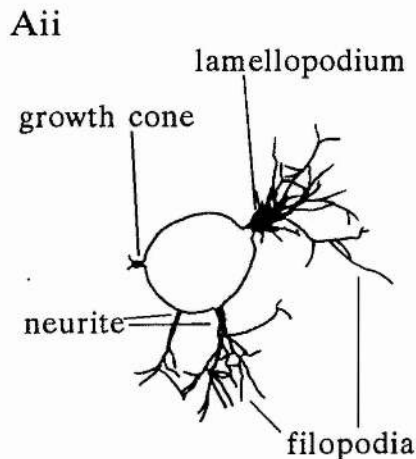
Ai. This photomicrograph shows a dissociated locust fifth instar neurone with 3 prominent neurites emanating from the cell body, in a multipolar fashion. From the tips of the neurites, finer processes known as filopodia extend.

Aii. An annotated sketch of the photomicrograph shown in Figure 4.3.2Ai, illustrating the neuritic extensions and filopodia described. A lamellopodium is a flattened growth projection from which filopodia may extend.

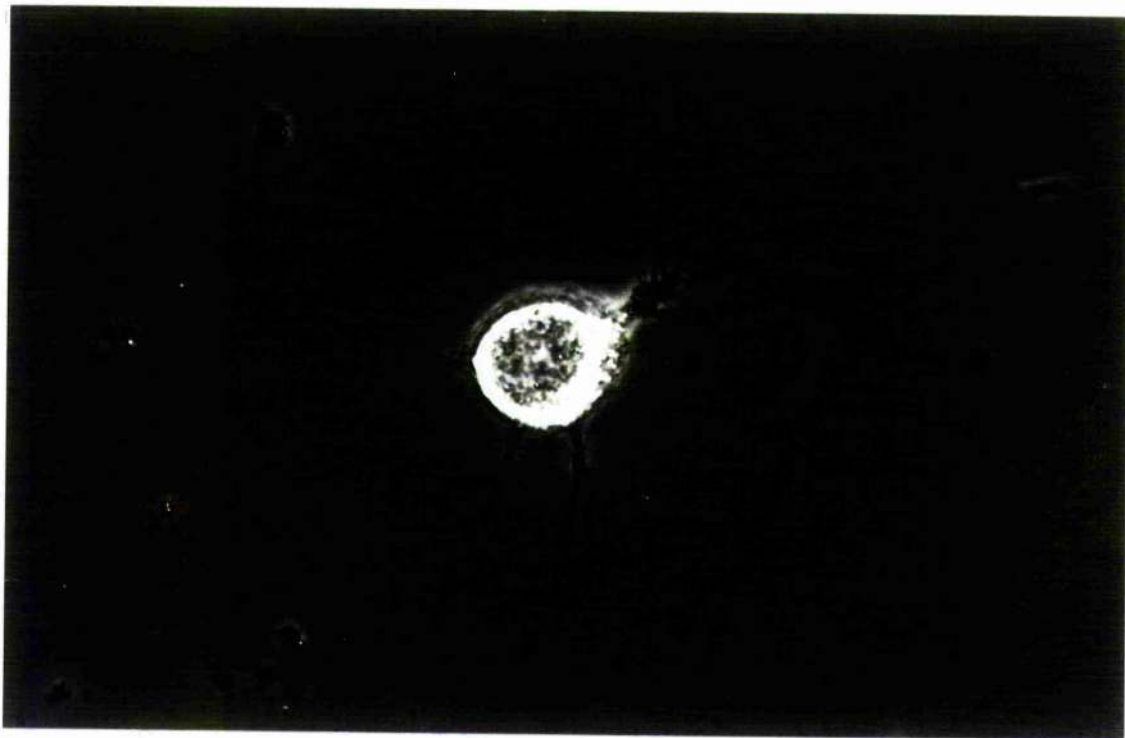
Bi. Rather than extending from the tips of neurites, filopodia could also be projected directly from the cell body.

Bii. An annotated sketch of the photomicrograph shown in Figure 4.3.2Bi, illustrating the multipolar filopodial growth directly emanating from the cell body.

Scale = 100 $\mu$ m



Ai



Bi

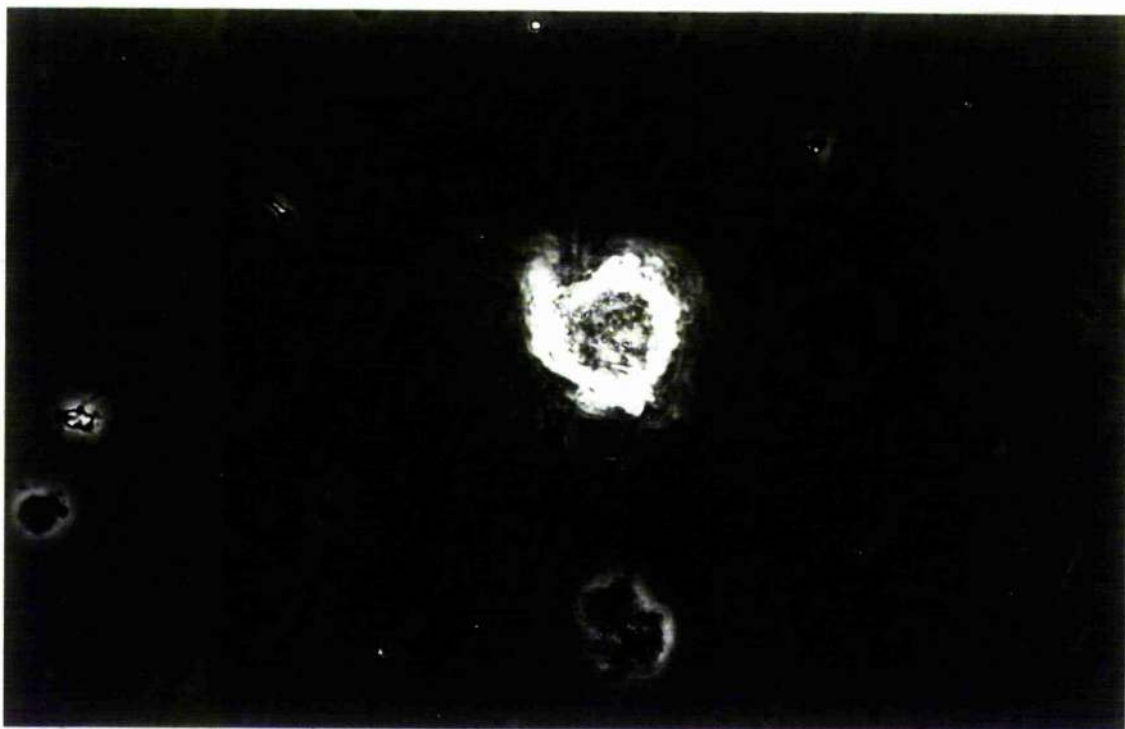
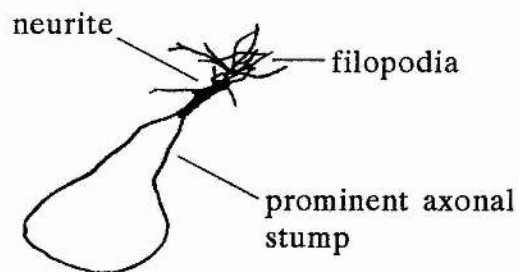


Figure 4.3.3. Directed neuritic outgrowth from dissociated locust thoracic neurones

i. In the presence of a prominent axonal stump, the pattern of neuritic outgrowth was seen to be monopolar, that is growth was directed from the tip of the axonal stump, rather than from many points around the cell soma (see Figure 4.3.2.).

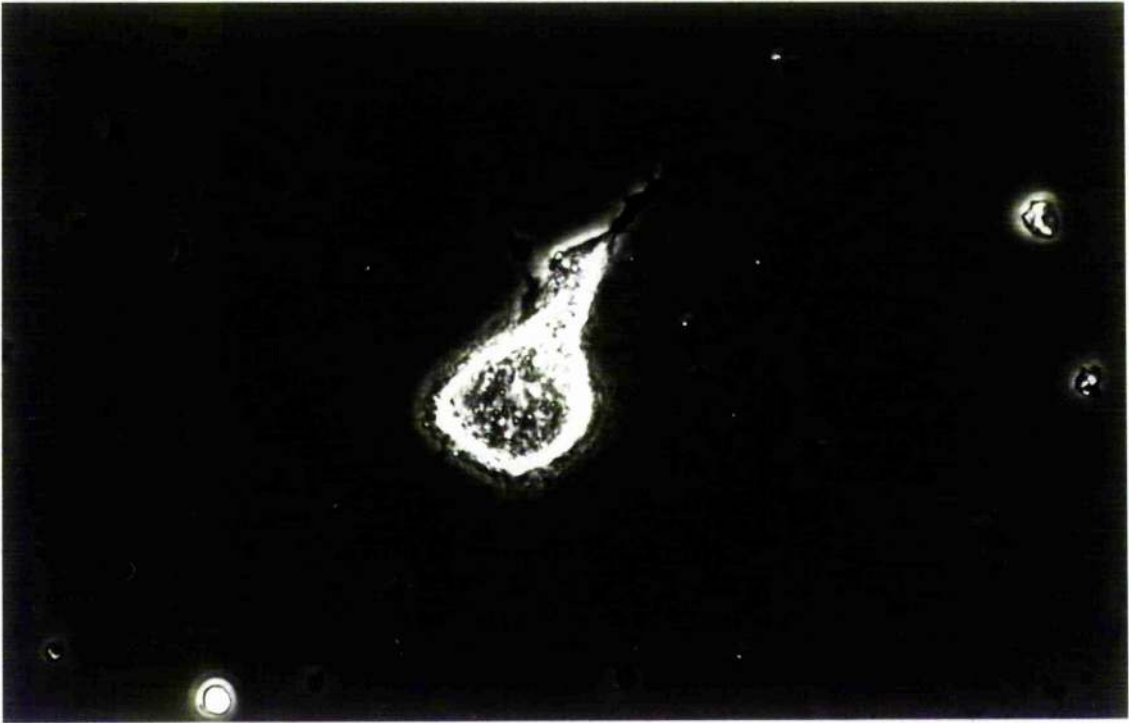
ii. An annotated sketch of the photomicrograph shown in Figure 4.3.2Bi, illustrating the multipolar filopodial growth directly emanating from the cell body.

Scale = 100 $\mu$ m





i



When isolated cells were positioned in close proximity to one another, they tended to exhibit enhanced neuritic growth and branching, so that in some cases there appeared to be cell contact. Neurones positioned close together have been designated the L and R neurones, depending on whether they were located to the left-hand (L) or right-hand (R) side of the photomicrographs. Figure 4.3.4 shows two dissociated fifth instar neurones without prominent axonal stumps, in close proximity, that appeared to have made neuritic contact on the third day in culture. Whilst the L neurone extended a number of filopodia, the R neurone exhibited a greater degree of neuritic outgrowth. There also appeared to be several growth cones and lamellopodia associated with the R neurone (see Figures 4.3.4i and 4.3.4ii). Both neurones exhibited multipolar growth, however, the R neurone showed a tendency to concentrate its outgrowth at opposing poles of the neurone. Unfortunately, as the development of these neurones could not be continually monitored using a video recorder, it could not be determined whether one neurone extended filopodia to contact the other, or whether the filopodia contacted each other at a site between both neurones.

Figures 4.3.5Ai and 4.3.5Bi show another two dissociated fifth instar neurones cultured in close proximity to one another; Figure 4.3.5Ai shows the neurones after 2 days and Figure 4.3.5Bi shows them on the 3 day in culture. Both these neurones had prominent axonal stumps, and exhibited monopolar neuritic growth, with a high degree of branching from the tips of the axon segments. At 2 days in culture the R neurone appeared to have a relatively long axonal stump compared to that of the L neurone - it is possible that some of its length could be attributed to new neurite growth (Figures 4.3.5Ai and 4.3.5Aii). At the tip of this neuritic process, a lamellopodium and growth cones (from which filopodia grew) were seen. The morphology of the R neurone differed slightly. Whilst it was not completely clear whether all of its axonal stump had adhered to the surface of the

i

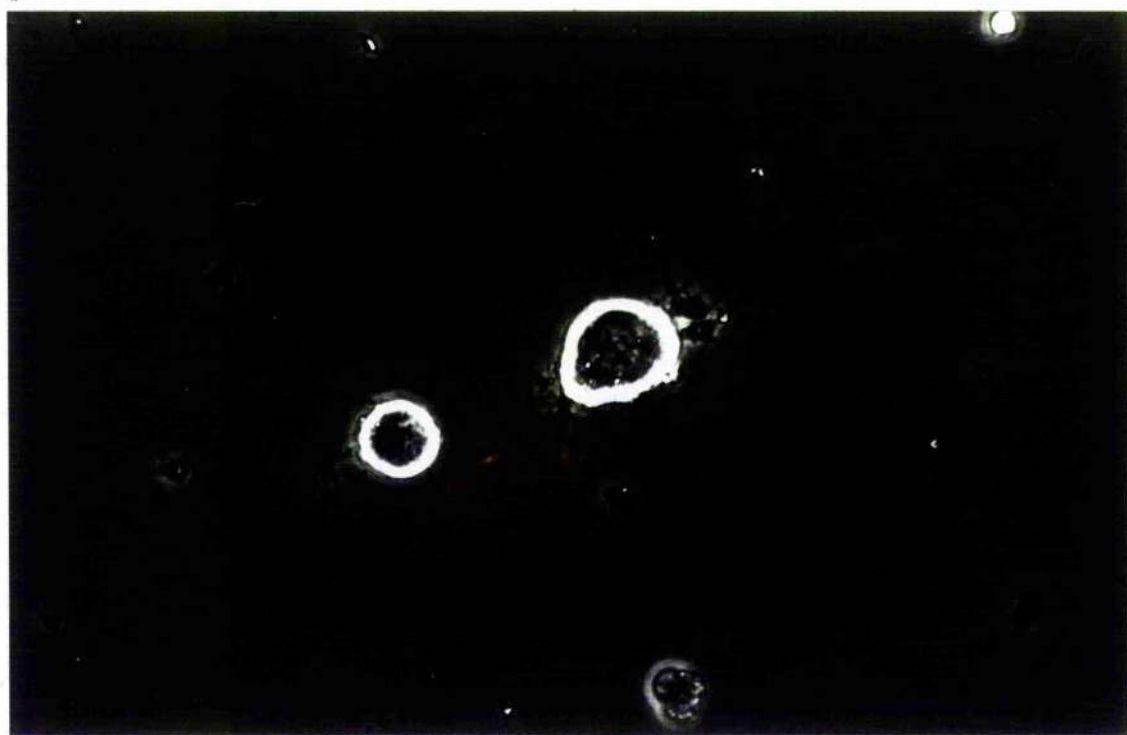


Figure 4.3.4. Neurones without prominent axonal stumps, plated in close proximity to one another, were seen to extend neuritic processes which appeared to contact one another.

i. This photomicrograph shows two dissociated fifth instar neurones (left-hand (L) and right-hand (R), respectively), that have appeared to have made cell contact on the third day in culture. Filopodia were produced by both the L and R neurones, however, additional morphological features associated with the neuritic outgrowth were observed. Structures resembling growth cones and lamellopodia were associated with the R neurone (see Figure 4.3.4ii)

ii. An annotated sketch of the photomicrograph shown in Figure 4.3.4i, illustrating the morphological features emanating from both neurones.

Scale = 100 $\mu$ m

ii

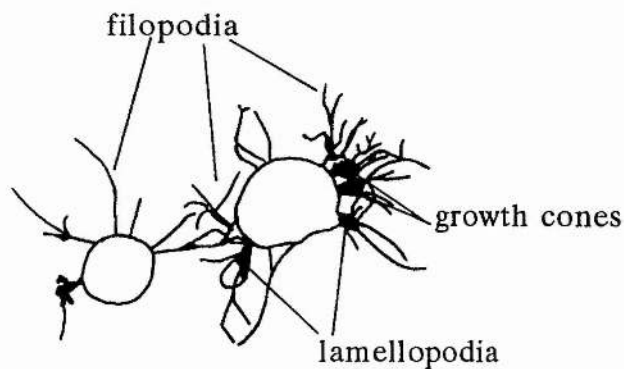


Figure 4.3.5. Neurones with prominent axonal stumps, plated in close proximity to one another, were seen to extend neuritic processes which appeared to contact one another.

Ai. A photomicrograph showing the two neurones both with prominent axonal stumps on the second day in culture. Monopolar neuritic outgrowth with a high degree of branching emanated from both neurones; neuritic processes from one neurone appeared to make contact with processes from the other.

Aii. An annotated sketch of the photomicrograph shown in Figure 4.3.5Ai, illustrating the morphological features of these neurones.

Bi. A photomicrograph showing the same preparation on the third day in culture. It appeared that the neurones underwent a degree of morphological reorganization, since the axonal stumps appear shorter, compared to the previous day *in vitro*.

Bii. An annotated sketch of the photomicrograph shown in Figure 4.3.5Bi, illustrating the morphology of these two neurones on the third day in culture.

Ci. After 6 days in culture, this neuronal culture began to show signs of ageing and deterioration, in particular, increased cytoplasmic granularity and degeneration of neuritic processes.

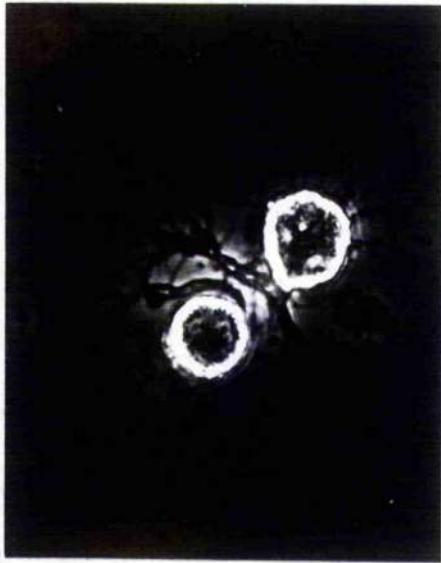
Cii. An annotated sketch of the photomicrograph shown in Figure 4.3.5Ci, illustrating the signs of neuronal ageing.

Scale = 100 $\mu$ m

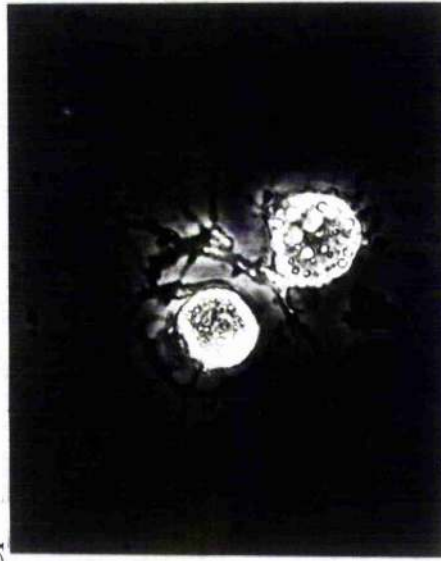
Ai



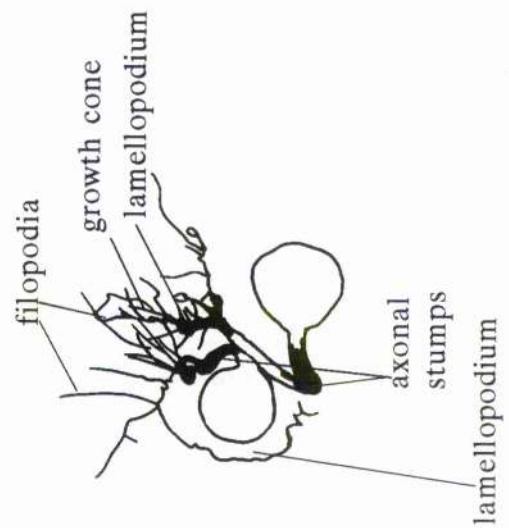
Bi



Ci



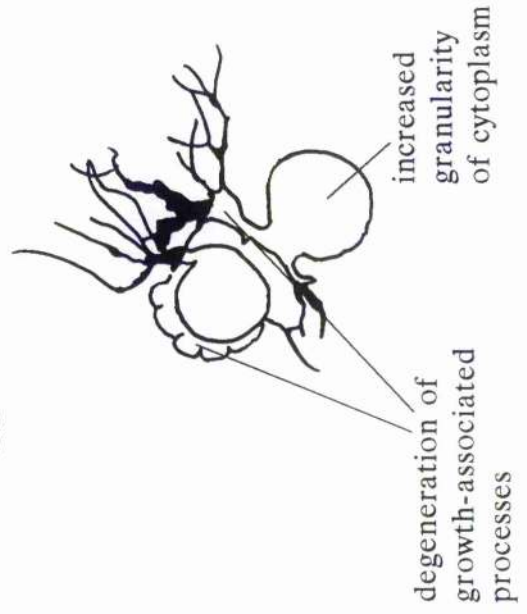
Aii



Bii



Cii



culture dish, filopodia were seen in the vicinity of its tip. One feature of the L neurone, which was not often seen associated with cultured locust neurones, was a lamellopodium surrounding the soma. Filopodia had also extended from this morphological feature (see Figures 4.3.5Ai and 4.3.5Aii). After 3 days in culture, both neurones appeared to have undergone neuritic reorganization, since, both axonal stumps had been shortened and their positioning had been adjusted (Figures 4.3.5Bi and 4.3.5Bii). The process of the R neurone appeared to have been adjusted so that the filopodia extending from the tips of both R and L neurone axonal stumps exhibited a degree of overlap. When comparing the filopodia present after 2 days in culture, those observed after 3 days in culture appeared to be broader. In addition, the lamellopodia around the L neurone still appeared to be present (the shadow around the cell), despite a slight change in focal plane. Whether the patterns of outgrowth observed from these somata and those shown in Figure 4.3.4i have enabled the formation of synaptic connections, is not yet known. There is evidence to show that extensive neuritic growth is not a requirement for synaptogenesis between isolated molluscan neurones (Haydon, 1988; S. Harris; personal communication), so whether such insect neurones that are in close anatomical proximity, can actually become synaptically connected remains to be determined. Figure 4.3.5Ci and Figure 4.3.5Cii show the neurones described above after 6 days in culture. Prominent features of neuronal ageing were observed at this time. Characteristics of ageing included degeneration of filopodia, lamellopodia and axonal stumps and an increase in cytoplasmic granularity. The increase in microbial contamination frequently associated with the ageing of the cultures was not obvious in this photomicrograph.

When using the culturing technique adapted from Howes *et al* (1991) two problems were encountered: (i) the isolated somata tended to be widely distributed across the whole dish and (ii) that presence of debris in the growth medium and on



the surface of the culture dish persisted. The debris consists of remnants of disrupted glial cells and fine pieces of ganglionic sheath and connective tissue not removed by the nylon mesh filter. In addition to being a potential source of microbial contamination, it is known to inhibit neuritic outgrowth (Lees and Beadle, 1988). Consequently, experiments were performed using the adapted version of the 'hanging column' technique described by Beadle and Hicks (1985) (see Section 4.2.). This technique brought the isolated neurones closer to one another, so increasing the probability of the development of synaptic connections and reduced the level of debris suspended in the culture medium.

Figures 4.3.6i and 4.3.6ii show adult locust neurones in close proximity to one another displaying apparent directional formation and extension of neuritic processes, after 3 days in culture. Whilst the L neurone and the R neurone were clearly distinguishable, a second smaller neurone (S) was observed attached to the R neurone. The S neurone had a 'in-focus' focal plane that was different to that of the R neurone, so could not be clearly seen. The L neurone exhibited multipolar neuritic and filopodial outgrowth which appeared to directed towards the R neurones. Numerous growth cones and varicosities were associated with these processes (Figure 4.3.6ii). Both the R and S neurones extended neuritic outgrowth, however, the growth of the R neurone was much more extensive than that of the S neurone. Neurites and growth cones, a prominent lamellopodia-like structure, and numerous filopodia emanated from the R neurone, whilst just a number of filopodia appeared to been extended from the S neurone (Figure 4.3.6ii). As the growth processes of the L neurone were directed towards the R neurone, those of the R neurone extended towards the L neurone. Since one of the aims of this work was to determine conditions required for synaptogenesis between dissociated locust neurones, the pattern of neuritic growth in this preparation was of interest. It suggested that neurones in close proximity to each

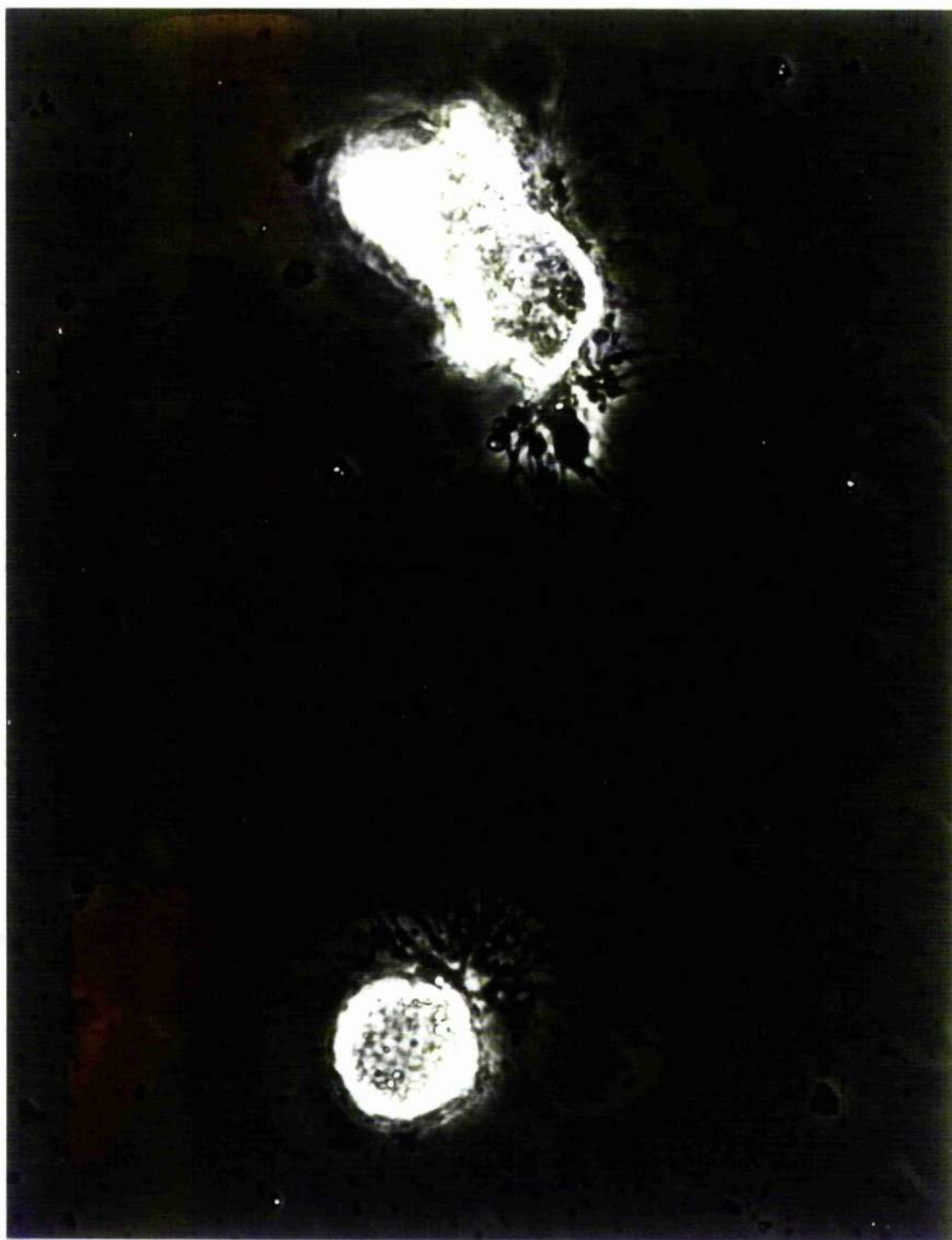


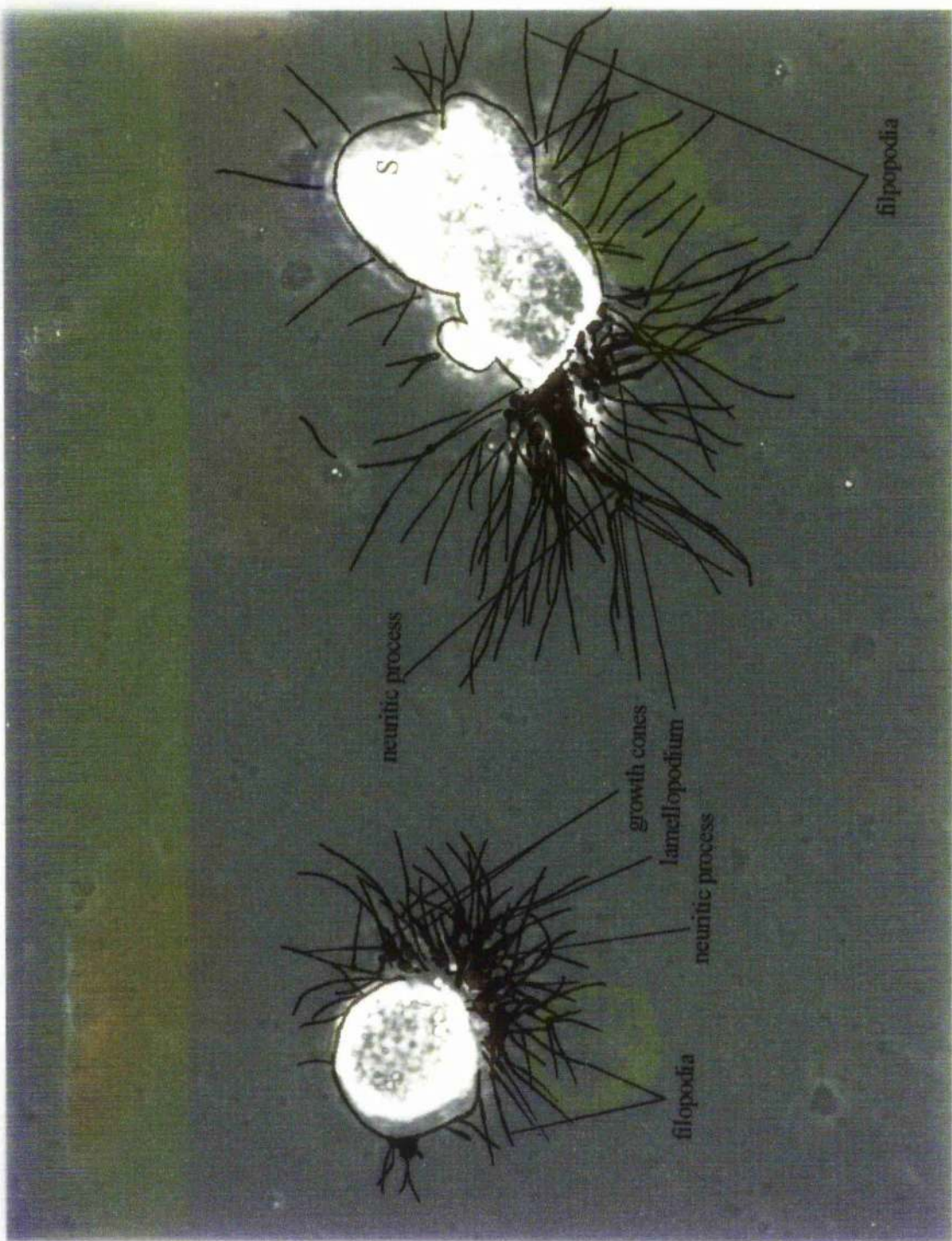
Figure 4.3.6. The adapted version of the 'hanging column' technique described by Beadle and Hicks (1985) was successful for culturing dissociated adult locust neurones when using Hayashi and Hildebrand's growth medium (in the absence of fetal calf serum).

i. A photomicrograph showing two dissociated adult locust neurones in close proximity to each other after 3 days in culture. The neurones exhibited a relatively high degree of neuritic outgrowth, both with apparent directional patterns of growth. A third smaller neurone (shown as S) was also observed attached to the neurone located to the right-hand side of the photomicrograph.

ii. An overlaying annotated sketch of the photomicrograph shown in Figure 4.3.6i, illustrating the morphological features associated with the growth processes.

Scale = 50 $\mu$ m





other could show a good degree of directional outgrowth, when cultured in the medium of Hayashi and Hildebrand. Whether such observations are physiologically significant for cell contact has yet to be determined; this preparation had to be discarded before neuritic contact was observed between the two neurones.

A degree of debris contamination is still evident in Figure 4.3.6. It is believed that it originated from the 1 hour period allowed for the adhesion of the neurones to the plastic culture dish. Unlike the somata, it was difficult to dislodge by washing with fresh culture medium. Therefore, removal of the debris from the medium prior to neuronal plating was attempted (protocol adapted from Amar, 1991). Once the medium holding the neurones had been filtered using the nylon mesh, instead of being placed directly into the culture dish, it was collected in a siliconized, sterilized 1.0ml Eppendorf tube. These plastic tubes were siliconized and sterilized by rinsing the inside surfaces with dimethyldichlorosilane solution in trichloroethane (BDH), allowing them to dry and then rinsing with them with ethanol (70%). This treatment prevented isolated neurones from adhering to the internal surfaces of the tubes. Having collected the suspension of neurones (1.0ml) in an Eppendorf tube, they were centrifuged at 500 to 1000rpm for approximately 3 minutes. The supernatant containing the neurone somata was then carefully removed and replaced with fresh growth medium. The neurones were then spun again using the same procedure, however, instead of using 1.0ml of fresh medium to resuspend the neurones, 0.1ml of medium was used. The suspension of cells was then plated out as a one droplet in the centre of the culture dish and the preparations were treated as those for the 'hanging column' technique. This procedure both reduced the level of debris in the medium and the distances between dissociated neurones. Unfortunately, due to problems of microbial contamination, photographic evidence of this is not available.



When the culture medium was supplemented with 10% FCS, as described by Hayashi and Hildebrand (1990), the ability of neurones to adhere to the surface of the culture dishes appeared to be compromised. That is, in the presence of FCS, the proportion of cells adhered to the culture dish compared to those suspended in the culture medium was reduced. Dagan and Levitan (1981) have reported similar findings, such that FCS was used to prevent the adhesion of isolated neurones to glassware. For future studies which examine the ability of this supplemented medium to support locust (*Schistocerca gregaria*) neurones in culture, it is suggested that the neurones should be initially plated out in FCS-free Hayashi and Hildebrand's medium, which is then replaced with the FCS-supplemented growth medium after 1 to 2 hours; this time period would allow for the adhesion of the isolated neurones to the surface of the culture dish to occur.

#### 4.3.2. Maintenance of first basalar motoneurones in culture

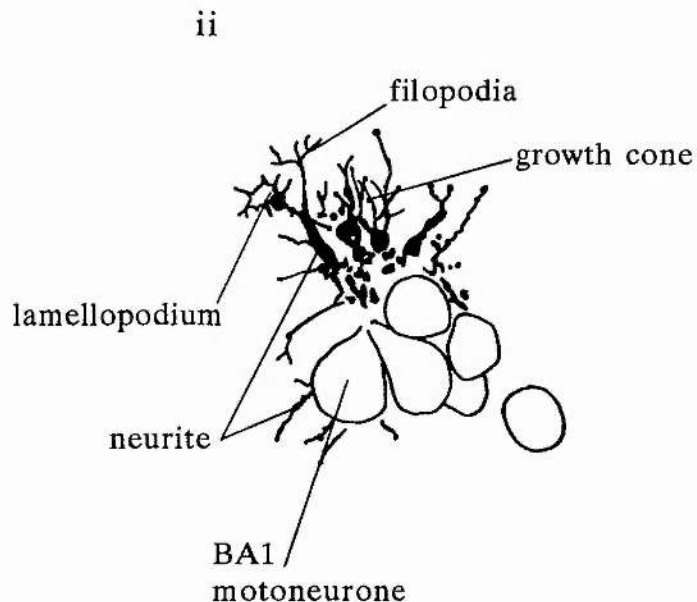
Once appropriate culture conditions had been established to support dissociated locust neurones *in vitro*, attempts were made to determine whether BA1 motoneurones could be maintained in culture using the same conditions. Following isolation of a BA1 motoneurone as one of a small cluster of neurones (usually no more than 7 somata), it was plated onto the surface of a culture dish, containing Hayashi and Hildebrand's growth medium in the absence of FCS. Figure 7i shows a neuronal cluster after 4 days in culture and the neurone believed to be BA1 is indicated in Figure 4.3.7ii. Isolated somata cultured as small clusters of neurones tended to exhibit enhanced neuritic outgrowth, when compared to that seen with dissociated neurones. Prominent neurites were extended from the neurones, and lamellopodia, growth cones and filopodia similar to those seen previously with cultured isolated neurones, were also observed (Figure 4.3.7ii). These latter features are not clearly seen because the focal plane was closer to that

Figure 4.3.7. The isolated adult locust first basalar motoneurone maintained in culture.

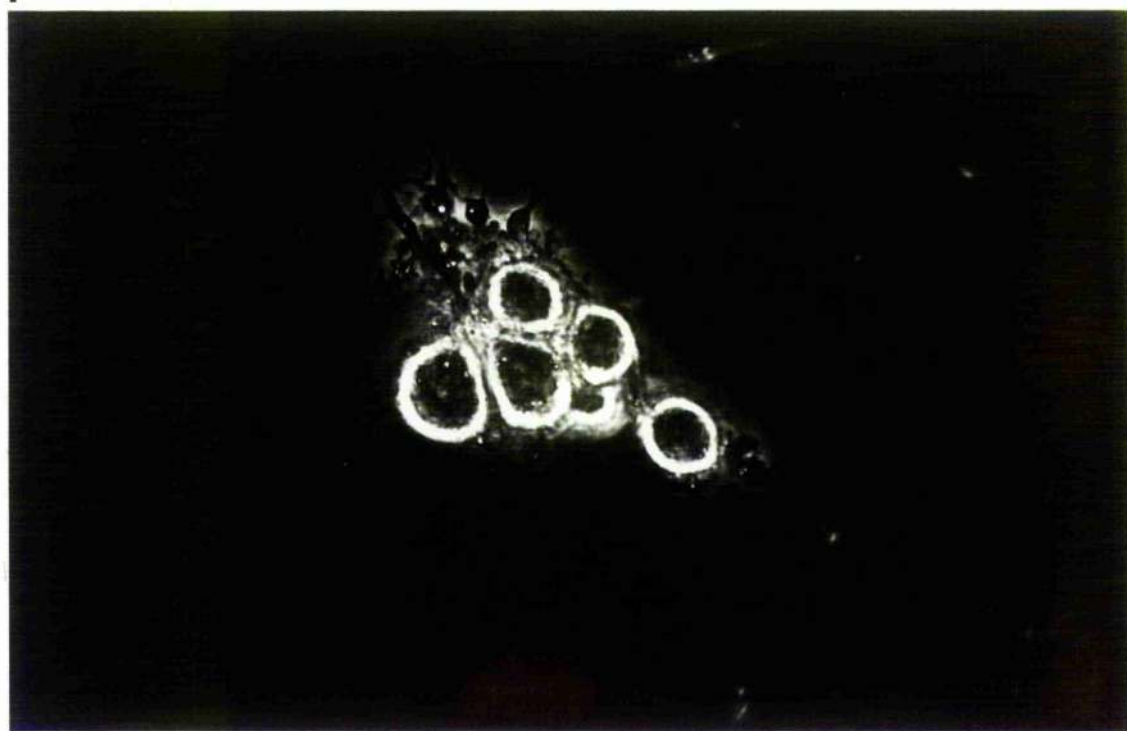
i. A photomicrograph showing the first basalar motoneurone isolated as one of a small cluster of neurones from the mesothoracic ganglion of an adult locust, after 4 days *in vitro*. It was observed that isolated neurones cultured as a small cluster of neurones, tended to exhibit enhanced neuritic outgrowth, as shown here.

ii. An annotated sketch of the photomicrograph shown in Figure 4.3.7i, identifying the BA1 motoneurone soma, and illustrating the different morphological features associated with neuritic outgrowth.

Scale = 100 $\mu$ m



i



of the 'in-focus' plane required to clearly see the somata in this photomicrograph. A possible explanation for the improved neuritic outgrowth from these somata in culture may be the neurones themselves and glial cells associated with them, provide physical support so that these neurones experience less trauma during isolation than do dissociated neurones.

#### 4.3.3. Electrophysiological properties of isolated locust neurones.

Once a protocol for the culturing of dissociated locust neurones was established, the electrophysiological properties of freshly isolated and cultured somata were examined. Table 4.3.1. summarizes the resting membrane potentials recorded from the isolated locust neurones. The properties of dissociated neurones were compared to those which were isolated in clusters. The values obtained for the resting membrane potentials of the isolated neurones were similar to those previously reported for isolated locust neurones *in vitro*, and thus provided a good indication of neuronal viability (Usherwood *et al*, 1980; Kirchhof and Bicker, 1992). When the differences in the resting membrane potential values of dissociated neurones maintained in locust saline and culture medium were examined, they were found not to be statistically different ( $P > 0.05$ ; unpaired two-tailed t-test). These observations provided further evidence that the culture medium devised for the maintenance of isolated *Manduca sexta* neurones, in the absence of FCS, was suitable for supporting adult thoracic locust neurones *in vitro*.

In addition to the resting membrane potential values obtained, another indication that the neurones had survived the process of isolation and remained viable, was indicated by the membrane activity characteristics of the isolated neurones once *in vitro*. These could vary quite dramatically and this was not dependent on whether the neurone was maintained in locust saline or growth



Table 4.3.1. Comparison of the membrane potentials of freshly isolated and cultured locust neurones.

Using the single microelectrode recording technique described in Section 2.2.4.3., the resting membrane potential values were estimated. Freshly isolated neurones were placed in locust saline, whilst cultured neurones were maintained in the medium devised by Hayashi and Hildebrand (for the culturing of sphinx moth neurones) in the absence of fetal calf serum (FCS). The ratio of  $\text{Na}^+ : \text{K}^+$  in locust saline and in culture medium were similar (150:5 and 139:5.4, respectively; see Appendices 2 and 7).

In addition to the mean values ( $\pm$ S.E.M.) of the resting membrane potentials observed and the number of neurones recorded in each category, the respective ranges are also shown. Where two 'n' values are given, that is, when a neurone in a cluster of neurones was recorded from, the first value is the number of clusters used, and the second is the number of neurones recorded from these clusters.

Freshly isolated neurones maintained in locust saline		Cultured neurones maintained in growth medium devised by Hayashi and Hildebrand (1990) in the absence of fetal calf serum	
<u>Dissociated</u>	<u>Member of a cluster</u>	<u>Dissociated</u>	<u>Member of a cluster</u>
-42.6 $\pm$ 2.9mV (n = 10)	-46.0 $\pm$ 2.9mV (n = 4/n = 7)	-48.5 $\pm$ 2.7mV (n = 4)	-42.7 $\pm$ 1.1mV (n = 2/n = 3)
range: -28 to -57mV	range: -35 to -60mV	range: -40 to -53mV	range: -40 to -44mV

medium. The membrane potential of the neurones following impalement could be either spontaneously active (that is, large and regular action potentials ('spikes') were produced), or quiescent and stable. Neurones with stable membrane potentials could be induced to either 'spike' on rebound, following the injection of hyperpolarizing current, or elicit multiple membrane oscillations or a single transient membrane oscillation with the injection of depolarizing current (see below).

Figure 4.3.8A shows an excerpt of the intracellular recording from a freshly isolated neurone, maintained in locust saline, following microelectrode impalement. This neurone evoked regular 'spikes' with an amplitude of  $83.6 \pm 0.7\text{mV}$  (mean  $\pm$  S.E.M.; number of 'spikes' = 8) at a frequency of 0.8Hz. The repolarizing phase of each 'spike' was associated with a prominent membrane afterhyperpolarization. Usherwood *et al* (1980) reported a frequency range of 0.5 to 5Hz for action potential generation in isolated adult locust neurones. When such activity was observed from relatively large somata, i.e. the diameter was approximately 80 to 100 $\mu\text{m}$ , it was suggested that the neurone could be a dorsal unpaired medial (DUM) neurone (Kerkut *et al*, 1969a; Pitman and Kerkut, 1970; Lapied *et al*, 1993).

If an isolated neurone did not exhibit spontaneous membrane activity on impalement, its membrane potential was said to be stable and 'resting', for example, see Figure 4.3.8Bi. However, upon the injection of depolarizing current, some of these neurones exhibited membrane oscillations (see Figures 4.3.8Bi, 4.3.9A and B), whilst in others, a single graded depolarizing transient was evoked (see Figure 4.3.10). Figure 4.3.8Bi shows an isolated neurone (resting membrane potential, -40mV) after 48 hours in culture. Upon depolarizing current injection (70ms; 0.24V), this neurone produced small membrane oscillations. On termination of the current pulse, the membrane potential did not return to the

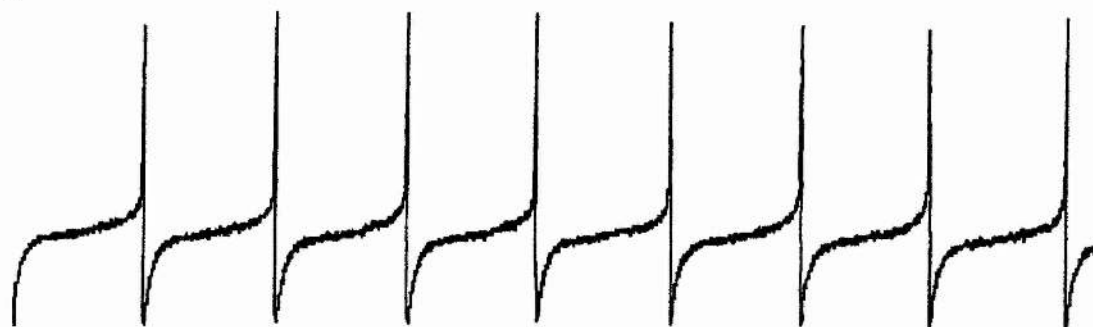
Figure 4.3.8. Both freshly isolated and dissociated adult locust neurones in culture elicit spontaneous membrane activity.

A. Upon microelectrode impalement, this freshly isolated neurone preparation (maintained in locust saline) was seen to evoke regular action potentials ('spikes'). Each 'spike' was associated with prominent membrane afterhyperpolarizations.

B. Some neurones that did not exhibit spontaneous membrane activity on microelectrode impalement, that is, had a resting membrane potential, could be induced to show such activity, following the injection of hyperpolarizing current into the cell.

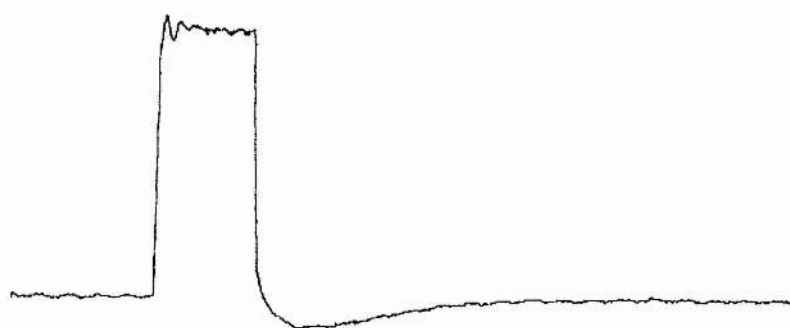
In this dissociated locust preparation (48 hours in culture; maintained in Hayashi and Hildebrand's (1990) growth medium in the absence of fetal calf serum, resting membrane potential,  $-40\text{mV}$ ), small membrane oscillations were produced on depolarizing current injection ( $70\text{ms}$ ;  $0.24\text{V}$ ; Bi). However, following the injection of hyperpolarizing current (membrane potential was held at approximately  $-65\text{mV}$  for 3 minutes), spontaneous membrane spiking was observed on rebound (Bii).

A



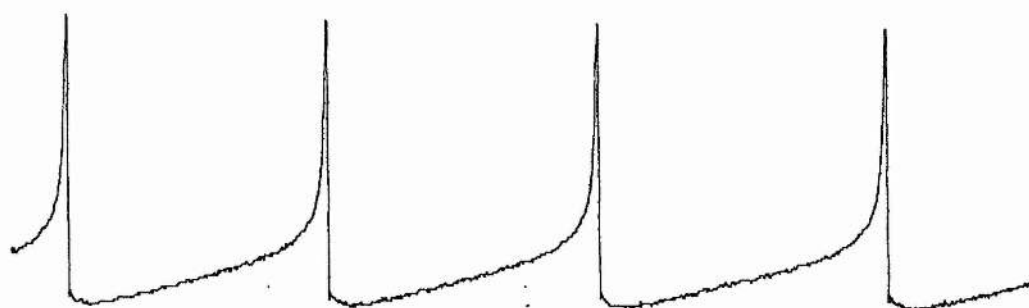
20mV  
1s

Bi



10mV  
70ms

Bii



10mV  
120ms

resting membrane potential, but a membrane afterhyperpolarization was observed. Following the injection of hyperpolarizing current through the bridge/amplifier, so that the membrane potential was held at approximately -65mV for 3 minutes, this neurone was seen to elicit spontaneous spiking activity (Figure 4.3.8Bii). These 'spikes' with an amplitude of  $39.3 \pm 0.2\text{mV}$  (mean  $\pm$  S.E.M.; number of 'spikes' = 4) were generated at a frequency of 4Hz (Figure 4.3.8Bii).

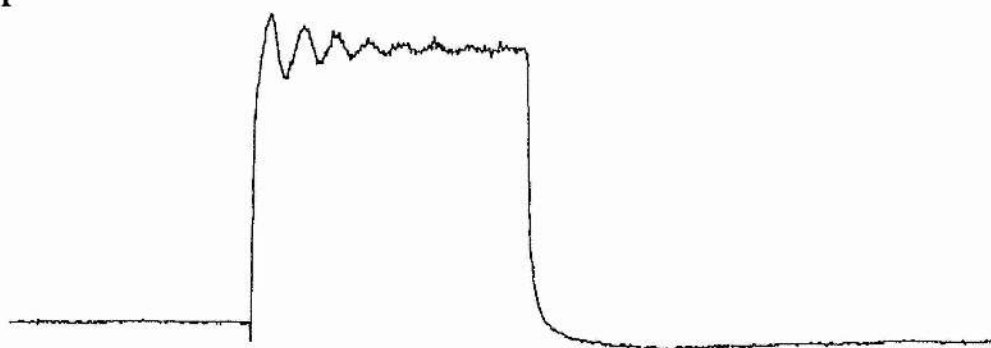
Figures 4.3.9Ai and 4.3.9Aii show the membrane oscillations, evoked on membrane depolarization, from a freshly isolated soma (resting membrane potential, -31mV), maintained in locust saline. Upon injection of a depolarizing current pulse (50ms; 0.23V), multiple membrane oscillations were seen, and it was noted that the amplitude of the membrane oscillations declined with time (Figure 4.3.9Ai). No membrane afterhyperpolarization was observed on termination on the stimulus pulse. Similar observations were recorded when the membrane potential of this neurone was hyperpolarized through the bridge/amplifier to -60mV. When the membrane was depolarized by the injection of a depolarizing current pulse (the duration and amplitude of which was the same as used previously: 50ms; 0.23V), although the amplitude of the membrane oscillations increased, 'spikes' were not produced. Figure 4.3.9B illustrates that similar membrane activity was observed when isolated neurones were maintained in the culture medium devised by Hayashi and Hildebrand (1990). It is shown that upon depolarizing current injection (50ms; 0.21V), an isolated neurone with a resting membrane potential of -44mV, produced membrane oscillations with similar characteristics shown in Figure 4.3.9A, after 3 hours in the culture medium. Such cells, whether maintained in locust saline or culture medium were not seen to generate action potentials when the stimulus size and duration was increased. This is a typical characteristic of isolated and *in situ* insect

Figure 4.3.9. Locust neurones *in vitro* could produce membrane oscillations upon membrane depolarization which were not associated with the production of spontaneous 'spiking' activity.

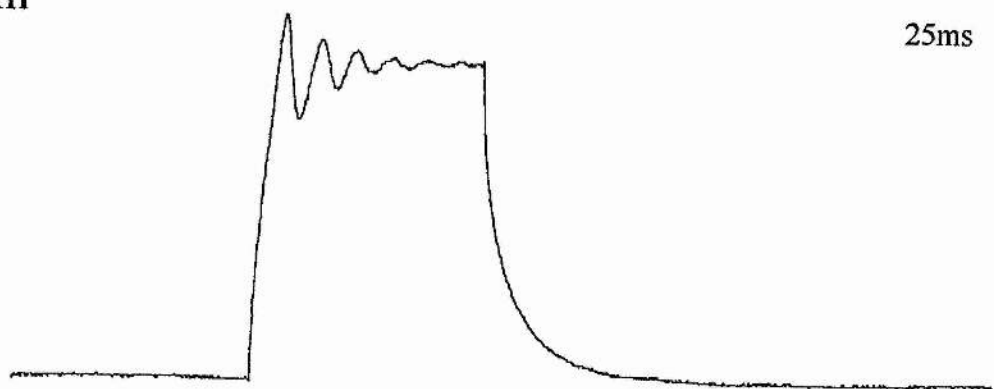
A. The injection of depolarizing current (50ms; 0.23V) into a freshly isolated soma maintained in locust saline (resting membrane potential -31mV), evoked multiple oscillations, which declined in amplitude with time (Ai). When hyperpolarizing current was injected into the neurone (membrane potential approximately -60mV), and the depolarizing current pulse was tested again, the amplitude of the oscillations increased, 'spikes' were not produced. (Aii).

B. Similar observations were made from an isolated neurone, maintained for 3 hours in culture medium (Hayashi and Hildebrand, 1990), upon depolarizing current injection (50ms; 0.21V; resting membrane potential, -44mV).

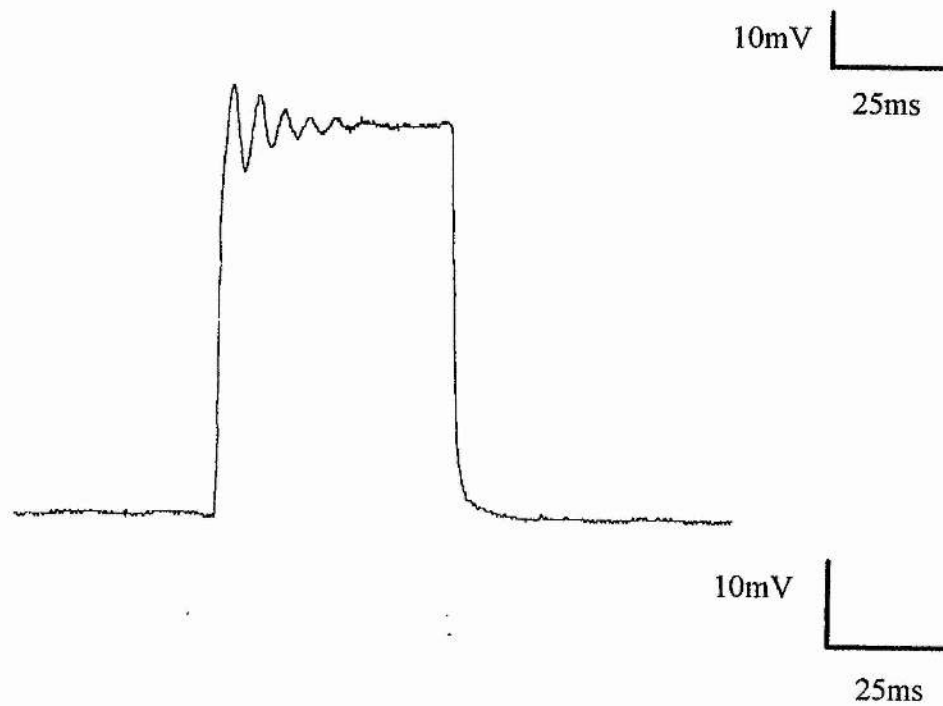
Ai



Aii



B





motoneurons (see Figure 2.3.1B; Usherwood *et al*, 1980; Pitman, 1988; L. J. Anderson, personal communication).

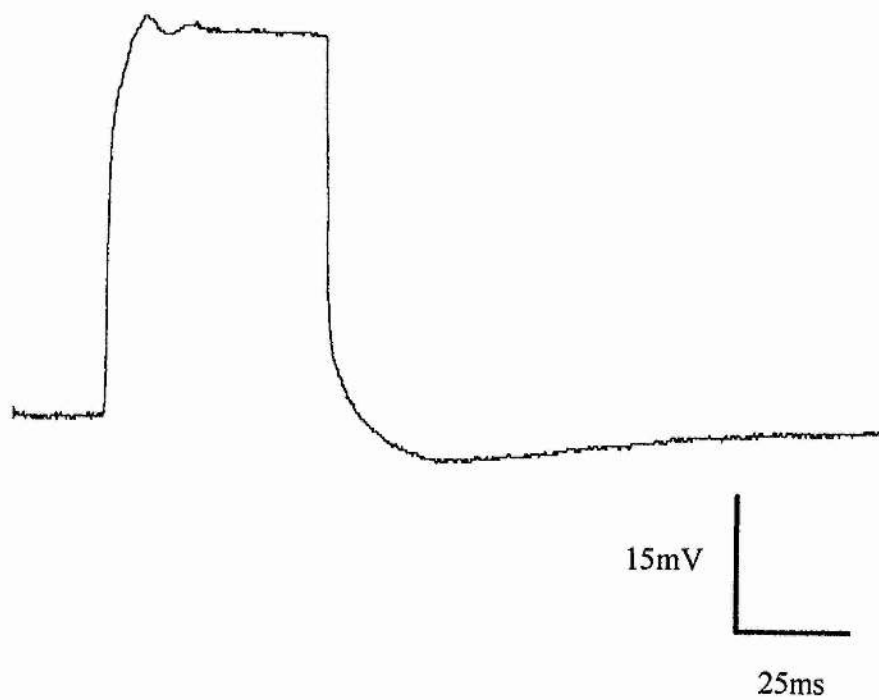
Finally, some isolated locust neurones failed to show 'spiking' activity or membrane oscillations in response to depolarizing current injection (see Figure 4.3.10). Figures 4.3.10Ai and Aii show intracellular recordings from a cell body (resting membrane potential, -40mV) within a cluster of neurones after 5 days in culture. Upon depolarizing current injection (50ms; 0.15V) a small transient membrane depolarization was evoked, and on termination of the current pulse a membrane afterhyperpolarization was observed (Figure 4.3.10Ai). As shown in Figure 4.3.10Aii, neurones exhibiting such membrane activity, could not be induced to evoke multiple membrane oscillations or 'spiking' activity by hyperpolarizing the membrane potential (-60 to -70mV for 20 minutes) or increasing the stimulus duration (and also the stimulus amplitude, not shown). Although one cannot exclude the possibility of time-dependent changes on neuronal membrane activity of somata in culture in these preliminary studies, similar recordings have been obtained from freshly isolated neurones and cultured (Usherwood *et al*, 1980).

The main growth-limiting factor in this study appeared to be microbial contamination. Despite implementing aseptic culturing techniques with the given laboratory conditions, the preparations were often found to be contaminated in their second week in culture, and this meant they had to be discarded. Thus, in addition to a greater understanding of factors influencing neuritic growth and development of adult insect neural tissue, improved sterile conditions would benefit the maintenance and study of synaptogenesis between isolated unidentified and identified locust neurones *in vitro*, in this laboratory.

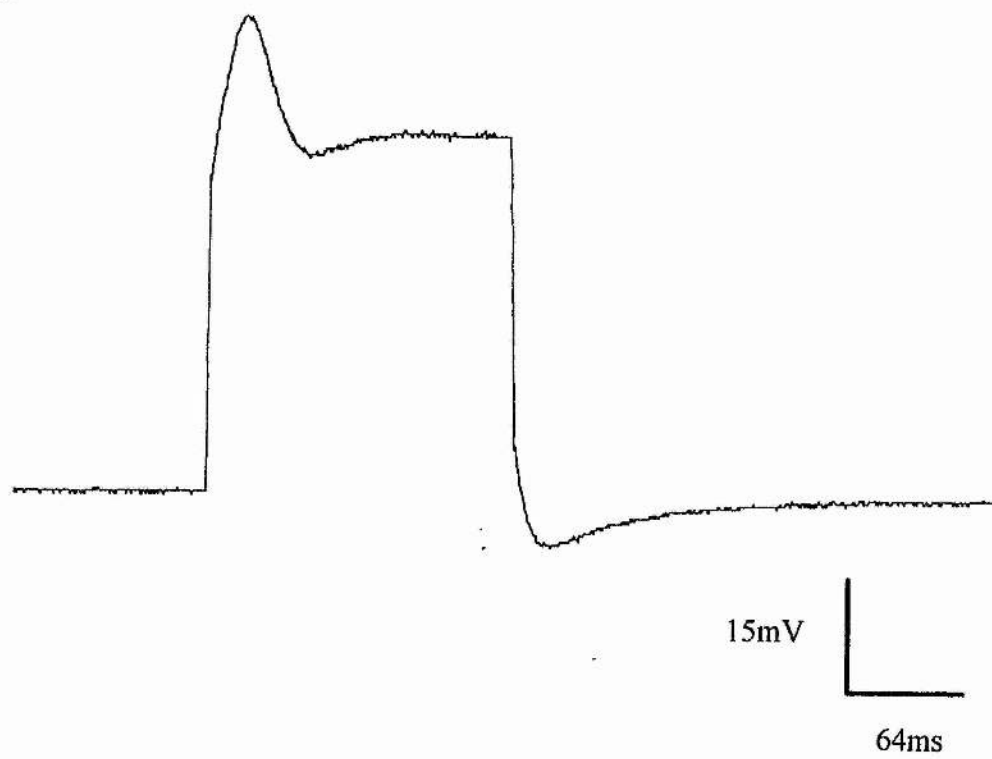
Figure 4.3.10. Locust neurones *in vitro* could fail to show spontaneous 'spiking' activity or multiple membrane oscillations in response to depolarizing current injection.

Intracellular recordings from a neurone within a cluster of neurones (resting membrane potential  $-40\text{mV}$ ) showed that upon depolarizing current injection (50ms;  $0.15\text{V}$ ), the neurone produced a single transient membrane depolarization (Ai). Membrane hyperpolarization, increasing the current pulse duration and increasing the stimulus amplitude (not shown) failed to induce 'spiking' or multiple membrane oscillations on depolarizing current injection in such neurones (Aii), although the amplitude of the transient depolarizing response was increased.

Ai



Aii



## DISCUSSION

From the results presented in this Chapter, it has been demonstrated that it is possible to maintain isolated unidentified adult thoracic neurones and the BA1 motoneurone from the locust (*Schistocerca gregaria*) *in vitro*. When intracellular recordings were made from the freshly isolated, dissociated or cultured cells, the electrophysiological properties of the cells were similar to those previously reported for locust neurones *in vitro* (Holden *et al*, 1978; Usherwood *et al*, 1980) and *in situ* (Goodman and Heitler, 1979; Anderson, 1995). Dissociated somata, whether cultured using the adapted technique of Howes *et al* (1991) or an adaptation of the 'hanging column' technique (Beadle and Hicks, 1985) and neurones, including the BA1 motoneurone isolated as small clusters, extended growth processes when cultured. These neurones could be maintained *in vitro* for up to two weeks. Therefore, the approaches used to isolate neurones from the thoracic ganglia of the adult locust, and the protocol employed to maintain these neurones in culture were considered successful.

One of the criteria set for the present investigation was that neurones were to be cultured as a homogeneous population of cells, since, it was thought desirable to reduce the possibility of tissue matter of unknown identity that could have an adverse effect upon cell adhesion and consequently neuronal viability. To achieve this, thoracic ganglia were triturated using flame-polished glass Pasteur pipettes, to aid disintegration of non-neuronal tissue such as connective tissue, tracheolar tissue and glial cells. In addition, prior to plating, the suspension of neurones was passed through a sterile nylon mesh; the mesh acted as a filter, for the removal of debris. Debris has been reported to prevent neuritic growth from isolated neurones (Lees and Beadle, 1988). It was thought that if glial cells were present, they too could affect neuritic outgrowth from the isolated neurones, since,

they are able to exhibit prolific growth when cultured using similar conditions for the maintenance of isolated neurones *in vitro* (Howes *et al*, 1993; Keen *et al*, 1994). Both the cell body and the cellular processes of cultured glial cells have a characteristic flat morphology (Hicks *et al*, 1981), however, using the experimental protocol described, cells with such a morphological profile were not evident in the current experiments. Glial cells represent a population of cells, the major physiological role of which is thought to be involved in repair of the central nervous system following injury (Howes *et al*, 1993). They are found within the ganglionic environment in close proximity to neurones, to the extent that they penetrate neuronal structures (Carlson and Saint Marie, 1990; Keen *et al*, 1994). In addition, glial cells possess a range of neurotransmitter receptors (which include acetylcholine, GABA, serotonin and glutamate receptors) and ion channels (including  $\text{Ca}^{2+}$ ,  $\text{Na}^{+}$  and  $\text{K}^{+}$  channels), and thus, can be involved in glial-neuronal interactions (for recent reviews see Coles and Abbott, 1996; Verkhratsky and Kettenmann, 1996).

Degradative enzymes can be used to facilitate the softening of the ganglionic sheath and digestion of connective tissue surrounding the neuronal cell bodies, thus, easing the process of trituration and neurone isolation. Collagenase or a collagenase/dipase mixture are often used (for example, Howes *et al*, 1991; Kirchhof and Bicker, 1992), however, the use of degradative enzymes can be associated with decreased neuronal viability and was therefore avoided in the present study. It is known that the duration that the neural tissue is exposed to these enzymes, as well as the temperature at which the preparations are incubated to facilitate the action of the enzyme, are critical to neuronal viability and the success of the cultures (Harrison *et al*, 1990).

The recovery of viable cell bodies using the technique of trituration established in this study was relatively high, although it was not calculated

numerically. Isolated somata with diameters ranging from 50 to 130 $\mu$ m were recovered and cultured. The degree of recovery was assessed from the high number of 'phase bright' cell bodies that adhered to the surface of each culture dish displaying neuritic outgrowth. The high degree of recovery aided the study of the electrophysiological properties of the isolated neurones, verifying the viable nature of these cells.

Neuritic outgrowth from the cultured dissociated neurones and those neurones isolated as small clusters took several forms, (i) neurites, (ii) growth cones, (iii) lamellopodia and (iv) filopodia (also known as 'microspikes'); the different structures were identified according to Smith (1988). A neurite was considered to be the broader processes extending either from the cell body itself or the end of an axonal stump; at the tip of a neurite a growth cone was found. In some preparations nodule-like structures were observed. The nature of the features was not known; ultrastructure examination using electron microscopy techniques is required to clarify this. However, it had been suggested that these could be the remains of retracted growth cones (B. Powell, personal communication). Actively growing growth cones are the portion of the axon responsible for navigation and elongation; when observed using time-lapse video microscopy, they show continual locomotory activity (Smith, 1988). Lamellopodia are known as the membranous sheets extended (and retracted) by growth cones, from which fine spike-like protusions, the filopodia, emanate; filopodia were often found to protrude directly from the cell body itself. The major cytoskeletal elements responsible for neuritic outgrowth and pathfinding are microtubule elements found within the neuritic processes and actin filaments which are differentially organized within neurites, lamellopodia and filopodia (Smith, 1988). Prominent lamellopodia, as observed from isolated crustacean neurones *in vitro* (Grau and Cooke, 1992; Panchin *et al*, 1993), were not observed during the current series of

experiments. Furthermore, they do not appear to be a common feature of the neuritic outgrowth of insect neurones in culture, whether of embryonic, nymphal or adult origin (see Lees and Beadle, 1988; Giles and Usherwood, 1985; Howes *et al*, 1990; Kirchhof and Bicker, 1992).

It was noted that neurones cultured in the medium devised by Hayashi and Hildebrand (in the absence of FCS) adhered rapidly to the plastic culture dishes and tended to produce neuritic processes at a relatively rapid initial rate over the first few days in culture, which was then followed by a second, slower growth phase. It was found that cells that were to exhibit neuritic outgrowth, displayed growth within the first 24 to 36hrs, following plating. If initial growth processes were not extended from a neurone during this period, they were not usually observed at all (unpublished observation). This may suggest that the growth medium was suitable for maintaining adult locust neurones in short-term culture. However, for sustained periods *in vitro*, currently unidentified growth factors necessary for long-term survival are absent in the medium of Hayashi and Hildebrand (1990) in the absence of FCS. Adult cockroach neurones, when cultured in '5 + 4' medium, exhibit a sigmoid-shaped growth profile (Howes *et al*, 1991). That is, following a short lag phase, most neurones exhibited initial neuritic outgrowth at day 5 in culture; those that had not; did not tend to exhibit initial neuritic outgrowth following day 10. It has previously been noted that the presence of an axonal stump reduces the time required for the initiation of neuritic growth from *Aplysia* cell bodies (Schacher and Proshansky, 1983), although this relationship was not investigated in the present study. It is suggested that this could occur as a consequence of preferential axonal transport of building materials into the neuritic stump. This suggestion has previously been proposed to explain the restriction of multipolar outgrowth that occurs in the presence of an axonal stump (Kirchhof and Bicker, 1992). It is not known whether the rate of growth or



the age of the cultured insect neurone will be critical for synaptogenesis to occur *in vitro*. It has been reported that synaptic contact between *Helisoma* neurones requires mutually actively growing neurites (Hadley *et al*, 1985), although, it has been suggested that extensive neuritic outgrowth is not necessary for synaptogenesis (S. Harris, personal communication). In support of this, it has been demonstrated that soma-soma chemical synapses form between isolated identified *Helisoma* neurones (Haydon, 1988).

The requirements for neuritic growth and the formation of synaptic connections for insect neurones are not currently known. Whilst such factors are understood for other invertebrate species (see Section 1.4.2), those required by insect neurones have yet to be established. In order to maintain the viability and growth of neurones in culture, it is well known that the choice of culture medium and surface substrate is critical. Chen and Levi-Montalcini's growth medium, '5 + 4', was found to support neuritic growth from locust somata, however, outgrowth was greater in the present study when the neurones were cultured in the medium devised by Hayashi and Hildebrand (1990) in the absence of FCS. This medium contained a number of additional components not found in '5 + 4', which are thought likely be associated with the increased neuritic outgrowth and improved neuronal viability observed. One notable addition was the ecdysteroid, 20-hydroxyecdysone (20-HE); steroid hormones such as 20-HE are understood to have an important regulatory role during neural postembryonic development (Prugh *et al*, 1992). 20-HE has been shown to promote neuronal outgrowth and survival of hawkmoth neurones (Bennett and Truman, 1985; Prugh *et al*, 1992; Oland and Hayashi, 1993) and locust neural tissue (Vanhems *et al*, 1990). It is thought that 20-HE acts indirectly to enhance neuritic growth; evidence from embryonic locust tissue explants suggests that the steroid interacts with growth factors (for example, insulin and the locust neurohormone neuroparsin) to improve



neuritic outgrowth (Vanhems *et al*, 1990). However, as insulin and neuroparsin have been reported not to affect neuritic growth of isolated embryonic pars intercerebralis neurosecretory cells *in vitro*, it has been suggested that there are additional substrate-associated growth-promoting factors *in vitro* (Vanhems *et al*, 1993). As blood and neural tissue have growth promoting properties (Howes *et al*, 1991; Kirchhof and Bicker, 1992; Vanhems *et al*, 1990) it has been proposed that a growth promoting factor is common to both (Vanhems *et al*, 1993).

When the surfaces of the plastic culture dishes were coated with locust haemolymph, obtained in a manner similar to that described by Howes *et al* (1991), it appeared to have a two-fold effect on the dissociated locust neurones in this study. Although the haemolymph seemed to enhance neuritic outgrowth of neurones that had adhered to the surface of the dishes, the haemolymph appeared to reduce the ability of the neurones to stick to the dish surface. Schacher and Proshansky (1983) reported a similar observation, that is, haemolymph did not appear to be linked with increased cell substrate adhesion in *Aplysia* neuronal cultures. A similar observations was also made when the medium of Hayashi and Hildebrand was supplemented with FCS, as originally described for the culturing of dissociated *Manduca sexta* neurones (Hayashi and Hildebrand, 1990). Therefore, it was suggested that although haemolymph had conditioning properties which could enhance neuritic outgrowth, another factor(s) was present, which may also be present in FCS, that interferes with cell-substrate interactions. This suggestion is supported by a recent study which reported an increase in the probability of detachment of dissociated locust (*Locusta* but not *Schistocerca gregaria*) neurones in culture, when haemolymph-conditioned medium was used (Kirchhoff and Bicker, 1992).

The membrane properties of the freshly isolated and cultured neurones were similar to those previously described for isolated locust neurones *in vitro* and

*in situ* (Usherwood *et al*, 1980; Anderson, 1995; present study), whether maintained in locust saline or in culture medium. Following microelectrode penetration, neurones were found to elicit spontaneous action potentials or have a stable, 'resting' membrane potential. Upon injection of depolarizing current, these neurones produced multiple membrane oscillations or a single transient depolarization associated with membrane depolarization.

It was noted in this study, and that of Usherwood and his colleagues (1980), that the membrane potential values of dissociated neurones are slightly less negative than those recorded from neurones *in situ*. It has been suggested that the values obtained *in situ* could be the true values, and the less negative levels observed *in vitro* are the result of environmental differences experienced by the neurones. For example, whilst the composition of the locust saline is based on the ionic composition of locust haemolymph, it is possible that it does not exactly mimic it. Alterations of the ionic ratios would affect the electrophysiological properties and the viability of the isolated neurones. When intracellular recordings were made from neurones maintained in the culture medium, there was concern that the ionic composition of the medium differed sufficiently from locust saline to affect their electrophysiological properties. However, as given in Appendix 7, the concentrations of the major ions of the medium ( $K^+$ ,  $Na^+$  and  $Ca^{2+}$ ) resemble those of the locust saline used. Furthermore, as the resting membrane potentials recorded from dissociated neurones maintained in locust saline and from those in culture medium were found to be not statistically significant ( $P > 0.05$ ), it is unlikely, that differences seen were the consequence of differences in ionic composition. On the other hand, it could be that these are the true membrane potential values for the neurones *in situ*. However, if the centre of the ganglion becomes relatively hypoxic and as a consequence,  $K^+$  conductance increases, this

could lead to a more negative membrane potential value being recorded *in situ* (see Martin *et al*, 1994).

As these studies have been only been preliminary, conclusive explanations for the different types of membrane activity would be premature, particularly as the identity of dissociated neurones is not known. It is known, however, that spontaneous spiking activity is associated with dorsal unpaired median (DUM) neurones both *in vitro* and *in situ* (Kerkut *et al*, 1969a; Pitman and Kerkut, 1970; Lapied *et al*, 1993; Newland *et al*, 1993) and the production of membrane oscillations on membrane depolarization are characteristic of insect motoneurones (Usherwood *et al*, 1980; Pitman, 1988; Anderson, 1995; present study). It is believed the differences observed in neuronal membrane activity can be mainly attributed to inter-neurone differences of the balance of inward and outward currents and to the kinetic properties of the respective ion channels which determine membrane activity. Pharmacological and voltage-clamp studies will be necessary for the further understanding of the currents underlying the different forms of membrane excitability. However, there are several factors which could influence the resting membrane potential and properties of isolated neurones. These may include the isolation process itself and the absence of glial cells i.e. the neurones are in an environment that differs from that *in situ* and *in vivo*. Evidence that the process of dissection and isolation can alter membrane activity comes from two sources. Firstly, it has been demonstrated that the cockroach fast coxal depressor motoneurone ( $D_f$ ) develops the ability to produce action potentials in the absence of pharmacological treatment, 1 to 4 hours following dissection. Whilst the mechanisms for this developmental change remains to be determined, it has been shown to be a  $Ca^{2+}$ -dependent event (Hancox and Pitman, 1992). Secondly, it has been noted that the proportion of spontaneously 'spiking' neurones is greater *in vitro* than expected (Holden *et al*, 1978); it is suggested that

the process of isolation contributes to this observation. The physiological effects of neuronal isolation at cellular level are therefore worthy of investigation.

Although there is sufficient evidence to demonstrate the morphological, electrophysiological and pharmacological similarities between isolated cultured insect neurones and their counterparts *in situ*, the degree to which these neurones fully resemble those *in situ* and *in vivo* has been questioned. When examined ultrastructurally, the characteristics of cultured dissociated embryonic cockroach neurones do generally agree with that of neurones in explant cultures (Hicks and Beadle, 1980). However, several anomalies have been noted and it is suggested that these could contribute to the difficulties encountered when culturing insect neurones long-term (particularly those from adult neural tissue) and forming functional synaptic connections. Firstly, is the absence of the Golgi system and its vesicular structures in these isolated neurones (Hicks *et al*, 1981). The Golgi apparatus has an important role in cellular function - its primary function is modification and trafficking of macromolecules such as proteins, glycoproteins, glycolipids and carbohydrates (Alberts *et al*, 1983). Secondly, despite demonstrating the contacting of adjacent neuritic processes, to date, conclusive evidence (both ultrastructural and electrophysiological) for synaptic connectivity between isolated neurones is lacking (Beadle *et al*, 1979; Hicks and Beadle, 1980). Therefore, it is suggested in future experiments, when it appears that neuritic processes have made contact, that the ultrastructure of the neurones is examined using electron microscopy techniques - this was not possible in the current study.

Whilst these observations may reflect the degree of suitability of the growth media chosen for the culture studies (that is, it may lack certain components, whether organic or inorganic in origin that are critical for the complete support of the cells *in vitro*), it may indicate that the use of glial-free

cultures for the maintenance of insect neurones *in vitro*, does not provide an entirely suitable environment for the neurones. In this study, when small clusters of neurones were cultured, improved neuritic outgrowth was observed; it was suggested that this may result from the support of glial cells and other components of the connective tissue present in the cluster. There is evidence indicating that neurones have a protective role for glial cells in culture. Glial cells will survive the process of trituration and grow in culture when associated with neurones in small clumps (Hicks *et al*, 1981). Therefore, both of these points warrant consideration when examining the conditions required for the study of synaptogenesis between isolated locust neurones in future investigations.

To summarize:

From the results obtained it has been shown possible to maintain isolated adult locust (*Schistocerca gregaria*) neurones *in vitro*. Two approaches used to isolate neurones from the thoracic ganglia have been successful. Dissociated somata, whether cultured using the adapted technique of Howes *et al* (1991) or the adapted 'hanging column' technique (Beadle and Hicks, 1985), and neurones isolated as small clusters of neurones which included the BA1 motoneurone, extend growth processes when cultured.

When intracellular recordings were made from freshly isolated and cultured cells, the electrophysiological properties of the cells were similar to those reported from other locust neurones *in vitro* and *in situ*.

In order to maintain the viability and growth of neurones in culture, the choice of culture medium is critical. Chen and Levi-Montalcini's '5 + 4' supported neuritic growth from dissociated locust somata. However, outgrowth was enhanced when the neurones were cultured in the medium devised by Hayashi and Hildebrand (1990) in the absence of fetal calf serum.

Consequently, it appears that isolated adult locust neurone cultures could be suitable for further *in vitro* studies investigating neurophysiological problems, such as neuromodulation and the formation of synaptic connections.

## **Chapter 5**

### **General Discussion**

## GENERAL DISCUSSION

In the current study it was demonstrated that the freshly isolated first basalar motoneurone soma of the locust, *Schistocerca gregaria*, was a suitable model for the study of the electrophysiological and pharmacological profile of this locust flight motoneurone *in vitro*. A technique was developed to isolate the motoneurone soma from its ganglionic environment and maintain it in a viable state for current- and voltage-clamp studies, which were employed to study the electrophysiological and pharmacological properties of the neurone. Since there was no evidence of synaptic activity on the isolated BA1 motoneurone preparation during the study, it confirmed that the neurone was completely isolated from other neuronal contacts, and that drug-induced responses were directly mediated by neurotransmitter receptors present on the BA1 motoneurone soma membrane, rather than as a secondary effect, that is, the consequence of indirect synaptic modulation.

From the pharmacological investigations it was demonstrated that nicotinic ( $\alpha$ -BTX-sensitive) and muscarinic ( $\alpha$ -BTX-insensitive;  $M_1$ -like) acetylcholine receptors, picrotoxin-sensitive GABA receptors and DA receptors coexist on the soma membrane of the first basalar motoneurone. The bath-application of cholinergic agonists and DA evoked an excitatory membrane response, whilst GABA and the vertebrate GABA<sub>A</sub> and GABA<sub>C</sub> receptor subtype agonist, muscimol, evoked inhibitory responses. It was found that the cholinergic pharmacological profile of the isolated BA1 motoneurone was consistent with that of the motoneurone *in situ* (Anderson, 1995; Leitch and Pitman, 1995). The presence of GABA and DA receptors on this motoneurone has not been described before.



Cholinergic receptor-mediated events underlie all insect sensory systems, and established examples of this include the cercal sensory neurone and giant interneurone synapse of the cockroach (Sattelle *et al*, 1983), and the winghinge stretch receptor and the first basalar motoneurone of the locust (Leitch *et al*, 1993; Leitch and Pitman, 1995). Although not apparent from data presented in this study, it has been established that nicotinic receptors mediate large, fast physiological responses, whilst muscarinic receptors mediate slow membrane responses (Trimmer and Weeks, 1989; Benson, 1992; Le Corrone and Hue, 1993). Unlike nicotinic receptors which are associated with postsynaptic neuronal membranes, muscarinic receptors are found on both pre- and postsynaptic neuronal membranes and have significantly different physiological effects (for detailed review see Trimmer, 1995). The pharmacological profiles and effects mediated by the respective receptor populations are distinctive. Activation of those located at presynaptic sites on sensory terminals results in inhibition of acetylcholine release (i.e. they act as negative feedback autoreceptors) to reduce the effectiveness of the sensory afferent input. These muscarinic receptors are seen to show some pharmacological similarity to the vertebrate M<sub>2</sub> muscarinic receptor subtype (Hue *et al*, 1989; Le Corrone *et al*, 1991; Leitch and Pitman, 1995). In contrast, activation of the muscarinic receptors on postsynaptic neurones results in membrane depolarization, lowering of spike threshold and consequently an increase in membrane excitability of the postsynaptic neurone. These observations result from an agonist-induced generation of an inward membrane current (Le Corrone and Hue, 1993; Trimmer, 1994; Anderson, 1995). These receptors, however, do not conform to the vertebrate classification system. Although they are blocked by the vertebrate M<sub>1</sub> receptor antagonist, pirenzepine, Anderson (1995) reported that the receptors of the BA1 motoneurone are sensitive to a range of muscarinic receptor subtype-selective ligands and, therefore, have a broad

muscarinic pharmacology. Similar findings have been recorded from the cockroach  $D_f$  motoneurone (David and Pitman, 1993a). Using dissociated unidentified locust neurones, a thorough investigation has demonstrated that the muscarinic receptor population of these neurones most closely resembles that of the vertebrate  $M_1$  and  $M_3$  receptor subtypes (Benson, 1992).

The muscarinic receptors present on the BA1 soma membrane were termed  $M_1$ -like because it was found using the  $Ca^{2+}$ -sensitive fluorescent dye, fluo-3, with confocal microscopy techniques, that bath-applying the vertebrate  $M_1$  receptor subtype agonist, McN-A-343, consistently increased  $[Ca^{2+}]_i$  in the BA1 motoneurone. Similar observations were made from the isolated  $D_f$  motoneurone in this study, and an increase in  $[Ca^{2+}]_i$  has already been associated with muscarinic receptor activation in this motoneurone (David and Pitman, 1996a). However, this does not exclude the possibility that the receptors also show sensitivity to some vertebrate  $M_2$  and  $M_3$  receptor subtype selective ligands. Further studies are required to investigate the pharmacological profile and physiological role of these receptors, as well as the ionic dependency of the muscarinic response of the BA1 motoneurone. Recent preliminary data have shown that muscarinic receptor activation may be involved in lowering spike threshold of this motoneurone (Anderson, 1995).

The modulatory effects of muscarinic agonists upon behavioural patterns regulated by CPGs has been demonstrated in several insect preparations, where they have an overall excitatory effect. For example, carbachol, muscarine and pilocarpine have been shown to drive bursts of activity in the pharyngeal muscles of *Drosophila*; these bursts resemble a motor pattern thought to be involved in feeding (Gorczyca *et al.*, 1991). When pilocarpine is applied to isolated locust thoracic ganglia, it induces dose-dependent oscillations in leg motoneurones

which resemble those seen during normal walking (Ryckebusch and Laurent, 1993).

It was found that the GABA response of the isolated BA1 motoneurone was similar to that mediated by the vertebrate GABA<sub>A</sub> and GABA<sub>C</sub> receptors. That is, the response to GABA had an estimated reversal potential close to that expected for E<sub>Cl</sub>, the GABA-induced current did not show voltage-dependent rectification and the induced membrane response was blocked by the GABA<sub>A</sub> antagonist, picrotoxin. Furthermore, the GABA response was mimicked by the vertebrate GABA<sub>A</sub> and GABA<sub>C</sub> agonist, muscimol. The effect of a chloride-mediated inhibitory GABA response on unidentified dissociated (Usherwood *et al*, 1980, Lees *et al*, 1987; Neumann *et al*, 1987) and insect neurones *in situ* is well documented (Kerkut *et al*, 1969a; Pitman and Kerkut, 1970; Pinnock *et al*, 1988, Sattelle *et al*, 1988; Dubas, 1991). The presence of GABA receptors with a pharmacological profile resembling the vertebrate GABA<sub>B</sub> receptor subtype has yet to be investigated in this preparation.

Regarding the physiological role of GABAergic neurotransmission in locust flight pattern generation, there is physiological and immunocytological evidence to suggest that some of the inhibitory interneurons of the flight CPG are GABAergic and that they trigger picrotoxin-sensitive postsynaptic potentials in postsynaptic neurones (Robertson and Pearson, 1985; Robertson and Wisniowski, 1988). It is anticipated that GABA-mediated afferent input would act to reduce membrane excitability in the postsynaptic neurones. Consequently, in the BA1 motoneurone, which is responsible for wing lowering in the flight pattern cycle, this would result in shortening of the wing downstroke, and therefore, could increase wingbeat frequency.

This study presents the first evidence of an effect by DA on an isolated insect neurone, although the amine has been shown to have excitatory effects on

dorsal unpaired midline neurones of the sixth abdominal ganglion (Kerkut *et al*, 1969a) and the prothoracic common inhibitory ( $D_3$ ) neurone of the cockroach *in situ* (Pitman and Davis, 1988; Pitman and Baker, 1989). Since another biogenic amine, octopamine, has been shown to evoke plateau potentials in locust neurones (Rameriz and Pearson, 1991a, b), it has been suggested that DA may have a similar effect on insect neurone membrane excitability. However, preliminary studies investigating this possibility upon the  $D_f$  motoneurone *in situ* have been inconclusive; DA evokes membrane depolarization in the  $D_f$  motoneurone *in situ*, however, clear evidence for additional effects on membrane excitability has yet to be obtained (J. D. Mills, personal communication). DA and octopamine are found within the central nervous system of many insects, including those of the locust (*Schistocerca gregaria*) and the cockroach (*Periplaneta americana*) (for reviews see Evans, 1980; Pitman, 1985; Nässel, 1996). However, although the trigger for octopamine release is known (that is, stress), that for DA release is not known. Furthermore, apart from acting as a neurotransmitter for salivary gland secretion, the physiological roles of DA have not been established.

When DA alone was applied to isolated BA1 motoneurones, it evoked membrane depolarization. Consequently, it was of great interest to discover that DA in the presence of GABA, this agonist could induce either membrane depolarization or hyperpolarization and induce long-term enhancement of the inhibitory response evoked by GABA, irrespective of whether membrane depolarization or hyperpolarization was induced. These phenomena clearly warrant further investigation using voltage-clamp recording techniques, in order to establish the underlying ionic dependency of the events observed. Since it was demonstrated that DA lowered  $[Ca^{2+}]_i$  in the isolated BA1 motoneurone, using the  $Ca^{2+}$ -sensitive fluorescent dye fluo-3, it is suggested that a change in  $[Ca^{2+}]_i$  plays a significant part of DA-induced effects on neuronal membrane properties,

whether in the absence or presence of GABA. Any involvement of extracellular  $\text{Ca}^{2+}$  in this response could be tested by performing the experiments in low  $\text{Ca}^{2+}$  locust saline. It may also be of interest to examine any potential dependency upon the  $\text{Na}^+/\text{Ca}^{2+}$  exchange mechanism for the DA-induced lowering of  $[\text{Ca}^{2+}]_i$  by using low  $\text{Na}^+$  locust saline. Given the long time course of the DA-induced effects on the GABA response, it may be anticipated that protein kinases are involved in this DA-mediated effect, since, receptor protein phosphorylation by protein kinases is an established mechanism for modulating vertebrate ligand-gated ion channel function (see Swope *et al*, 1992; Raymond *et al*, 1993). In fact protein kinases are understood to play a central role in synaptic plasticity which underlies the development of memory (see Raymond *et al*, 1993). A similar proposal regarding the involvement of protein kinases in neuromodulation has recently been made regarding the modulatory effect of muscarinic receptor mediated changes in  $[\text{Ca}^{2+}]_i$  on nicotinic acetylcholine- and GABA- gated ion channels of the cockroach  $\text{D}_f$  motoneurone (David and Pitman, 1996a). It would be of interest to examine the potential modulatory effect(s) of DA on the nicotinic response of this neurone, in addition to the effects of muscarinic agonists on both ligand-gated ion channel mediated response of the BA1 motoneurone. In order to examine the involvement of protein kinases in DA-mediated modulation of ion channel function, it is suggested that the effect(s) of injecting the catalytic subunits of PKA and PKC upon these responses is investigated. It is also suggested that the effects of the catalytic subunit of  $\text{Ca}^{2+}$ /calmodulin-dependent protein kinase II are investigated, since this kinase has recently been shown to potentiate the GABA receptor-mediated current of rat neurones *in vitro* (Wang *et al*, 1995).

Evidence from other insect preparations indicates that DA may have a physiological role as a modulator of locust flight. It has been demonstrated that when injected into the thoracic ganglia at nanomolar concentrations, the three

biogenic amines, DA, octopamine, and serotonin are involved in initiating, maintaining and terminating flight behaviour in *Manduca sexta*, respectively (Classen and Kammer, 1986). Similarly, these biogenic amines have differential effects on the escape circuit of the cockroach (Goldstein and Camhi, 1991; Casagrand and Ritzmann, 1992). In this instance, the application of DA enhances the response of leg motoneurons to activation of interneurons in the abdominal nerve cord, by electrical or wind stimulation. Serotonin, on the other hand, decreases the response of the motoneurons. Although the precise actions of the amines have yet to be established in these examples, it is understood that they could exert their effects by modulating membrane excitability and/or synaptic efficacy of neurones comprising the CPGs that generate the behavioural activities observed. Subsequently, it would not seem unreasonable to suggest that DA may act to have a similar modulatory role upon the flight CPG of the locust.

Evidence to support this comes from another invertebrate preparation in which the concept of neuromodulation is established and has been investigated in detail. DA is a neuromodulator in the lobster stomatogastric nervous system, which controls the activity of the crustacean stomach during feeding (see Harris-Warrick and Flamm, 1986). The CPG controlling the pyloric rhythm which regulates the pumping and filtering movement in the posterior region of the stomach, contains 14 identified neurones in six major classes, the synaptic connectivity and transmitter used by the component neurones, have been elucidated (Eisen and Marder, 1982; Miller and Selverston, 1982a, b). DA is found to modulate the pyloric rhythm by both direct effects on the baseline firing properties of the component neurones, and modulation of the strength of synaptic connections in the network (Flamm and Harris-Warrick, 1986a, b; Harris-Warrick *et al*, 1993; Johnson and Harris-Warrick, 1990). In both the pyloric and lateral pyloric neurones of this CPG, DA induces an increase in membrane excitability



and causes the activity to be phase-advanced in the pyloric motor pattern. Recent investigations examining the ionic mechanisms underlying these effects have shown that the amine decreases the transient potassium current ( $I_{K(A)}$ ) in both cell types, however, in the lateral pyloric neurones it also enhances a hyperpolarization-evoked inward current ( $I_h$ ) (Harris-Warrick *et al*, 1995a, b).

In addition to the electrophysiological and pharmacological studies performed on freshly isolated BA1 motoneurone somata discussed above, in the current study a neuronal culture technique was established for the maintenance of isolated adult locust neurones *in vitro*. Using the growth medium devised by Hayashi and Hildebrand (1990), however, without fetal calf serum, these neurones extended neuritic processes, and were maintained in a viable state for one to two weeks - neuronal viability was determined using a single intracellular microelectrode recording technique. By being able to maintain isolated adult locust neurones in culture, it is intended that these preparations will be used in future investigations to examine the regulation of the excitable properties of the BA1 motoneurone. It is believed that neurotransmitter interactions play an important role in the intact animal for flight pattern generation under varying environmental conditions. It is also intended that such a preparation will be used to study elements of synaptic transmission mediated by the presynaptic neurone of the BA1 motoneurone, the forewing hinge stretch receptor neurone, in particular, the modulation of acetylcholine release by presynaptic muscarinic receptors. Although not described here, a protocol has been established in the current study for the location and isolation of the forewing hinge stretch receptor from the thoracic cavity. Consequently, it will be possible to study the modulation of cellular mechanisms underlying synaptic transmission at an identified synapse central to locust flight.

## **Bibliography**



- Abdallah, A. E. M., Eldefrawi, M. E. and Eldefrawi, A. T. (1991)** Pharmacological characterization of muscarinic receptors of insect brains. *Arch. Insect Biochem. Physiol.*, **17**, 107-118
- Aguilar, J. S. and Lunt, L. G. (1984)** Cholinergic binding sites with muscarinic properties on membranes from the supraoesophageal ganglion of the locust (*Schistocerca gregaria*). *Neurochem. Int.*, **6** (4), 510-507
- Aidley, D. J. (1991)** *'The physiology of excitable cells'*. Third Edition, Cambridge University Press, UK
- Albert, P. R., Neve, K. A., Bunzow, J. R. and Civelli, O. (1990)** Coupling of a cloned rat dopamine-D<sub>2</sub> receptor to inhibition of adenylyl cyclase and prolactin secretion. *J. Biol. Chem.*, **265** (4), 2098-2104
- Alberts, B., Bray, D., Lewis, J., Raff, M., Roberts, K., and Watson, J. D. (1983)** *'Molecular Biology of the Cell'*. Garland Publishing, New York, USA
- Altman, J. S. (1980)** Toluidine blue as a rapid stain for nerve cell bodies in intact ganglia. In *'Neuroanatomical Techniques. Insect Nervous System.'* Eds. Strausfeld N. J. and Miller, T. A., New York, USA, Springer-Verlag, 21-24
- Altman, J. S. and Tyrer, N. M. (1977)** The locust wing-hinge stretch receptors. 1. Primary sensory neurones with enormous central arborizations. *J. Comp. Neurol.*, **172**, 409-430
- Amar, M. (1991)** Etude biophysique et pharmacologique des canaux ioniques de la membrane de neurones en cultures d'un insecte: La Blatte *Periplaneta americana*. PhD Thesis, Universite Paris VII, Jussieu, Paris
- Amar, M., Thomas, P., Wonnacott, S. and Lunt, G. G. (1995)** A nicotinic acetylcholine-receptor subunit from insect brain forms a non-desensitizing homo-oligomeric nicotinic acetylcholine-receptor when expressed in *Xenopus* oocytes. *Neurosci. Letts.*, **199** (2), 107-110
- Anderson, L. J. (1995)** Alpha-bungarotoxin-resistant cholinergic receptors on an identified locust flight motoneurone. PhD Thesis, University of St. Andrews
- Anthony, N. M., Harrison, J. B. and Sattelle, D. B. (1993)** GABA receptor molecules of insects. In *'Comparative Molecular Neurobiology'*. Ed. Pichon, Y., Birkhäuser Verlag, Basel, Switzerland, 172-209
- Arechiga, H., Chiquet, M., Kuffler, D. P. and Nicholls, J. G. (1986)** Formation of specific connections in culture by identified leech neurones containing serotonin, acetylcholine and peptide transmitters. *J. exp. Biol.*, **126**, 15-31

- Aydar, E., Taylor, A. R., Beadle, D. J. and Bermudez, I. (1995)** A novel electropharmacological profile of insect GABA receptors. *J. Physiol. (Lond.)*, **483**, 196P
- Aziz, S. A. and Eldefrawi, M. E. (1973)** Cholinergic receptors of the central nervous system of insects. *Pest. Biochem. Physiol.* **3**, 168-174
- Bai, D. and Sattelle, D. B. (1994)** Muscarinic acetylcholine receptors on an identified insect motor neurone in the cockroach, *Periplaneta americana*. *Neurosci. Letts.*, **175**, 161-165
- Bai, D. and Sattelle, D. B. (1995)** A GABA<sub>B</sub> receptor on an identified insect motor neurone. *J. exp. Biol.*, **198**, 889-894
- Baines, R. A. and Bacon, J. P. (1994)** Pharmacological analysis of the cholinergic input to the locust VPLI neuron from an extracellular photoreceptor system. *J. Neurophysiol.*, **72** (6), 2864-2874
- Barker, J. L. and Mathers, D. A. (1981)** GABA analogues activate channels of different duration on cultured mouse spinal neurons. *Science*, **212**, 358-361
- Barnard, E. A., Wieckowski, J. and Chiu, T. H. (1971)** Cholinergic receptor molecules and cholinesterase molecules at mouse skeletal junctions. *Nature*, **234**, 207-209
- Barnes, S., Syed, N. I., Bullock, A. G. M. and Lukowiak, K. (1994)** Modulation of ionic currents by dopamine in an interneurone of the respiratory central pattern generator of *Lymnaea stagnalis*. *J. exp. Biol.*, **189**, 37-54
- Baxter, D. A. and Byrne, J. H. (1989)** Serotonergic modulation of two potassium currents in pleural sensory neurons of *Aplysia*. *J. Neurophysiol.*, **62**, 665-667
- Beadle, D. J. and Hicks, D. (1985)** Insect nerve culture. In 'Comprehensive insect physiology, biochemistry and pharmacology.' Volume 5. Eds. Kerkut, L. and Gilbert, G., Pergamon Press, Oxford, 181-211
- Beadle, D. J., Hicks, D. and Middleton, C. (1982)** Fine structure of *Periplaneta americana* neurons in long-term culture. *J. Neurocytol.*, **11**, 611-626
- Beadle, D. J. and Lees, G. (1986)** Insect neuronal cultures: a new tool in insect neuropharmacology. In 'Neuropharmacology and pesticide action.' Eds. Ford, M. G., Lunt, G. G., Reay, R. C. and Usherwood, P. N. R., Ellis Horwood, London, 423-444
- Beadle, D. J., Livingstone, C. D. and Read, S. (1979)** Ultrastructural localisation of acid phosphatase, non-specific esterase and  $\beta$ -glucuronidase in the mid-gut-

epithelium of *Tenebrio molitor*, *Schistocerca gregaria* and *Carausius morosus*. *Histochemie*, **28**, 243-249

**Ben-Barak, J. B. and Dudai, Y. (1979)** Cholinergic binding sites in rat hippocampal formation: properties and ontogenesis. *Brain Res.*, **166**, 245-257

**Bennett, K. L. and Truman, J. W. (1985)** Steroid-dependent survival of identifiable neurons in cultured ganglia of the moth *Manduca sexta*. *Science*, **229**, 58-60

**Benson, J. A. (1989)**  $M_1$ -like muscarinic receptors mediate cholinergic activation of an inward current in isolated neuronal somata from locust thoracic ganglia. *Soc. Neurosci. Abstr.*, **15**, 365

**Benson, J. A. (1992)** Electrophysiological pharmacology of the nicotinic and muscarinic cholinergic responses of isolated neuronal somata from locust thoracic ganglia. *J. exp. Biol.*, **170**, 203-233

**Benson, J. A. (1993)** The electrophysiological pharmacology of neurotransmitter receptors on locust neuronal somata. In '*Comparative Molecular Neurobiology*'. Ed. Pichon, Y. Birkhäuser Verlag, Basel, Switzerland, 390-413

**Benson, J. A. and Neumann, R. (1987)** Nicotine and muscarine evoke different responses in isolated neuronal somata from locust thoracic ganglia. *Soc. Neurosci. Abstr.*, **13**, 938

**Bermudez, I., Beadle, D. J. and Benson, J. A. (1992)** Multiple serotonin-activated currents in isolated neuronal somata from locust thoracic ganglia. *J. exp. Biol.*, **165**, 43-60

**Bermudez, I., Lees, G., Botham, R. P. and Beadle, D. J. (1986)** Myogenesis and neuromuscular junction formation in cultures of *Periplaneta americana* myoblasts and neurones. *Dev. Biol.*, **116**, 467-476

**Berridge, M. J. (1993)** Inositol trisphosphate and calcium signalling. *Nature*, **361**, 315-325

**Bertrand, D., Ballivet, M., Gomez, M., Bertrand, S., Phannavong, B. and Gundelfinger, E. D. (1994)** Physiological properties of neuronal nicotinic receptors reconstituted from the vertebrate  $\beta 2$  subunit and *Drosophila*  $\alpha$  subunits. *Eur. J. Neurosci.*, **6** (5), 869-875

**Bezprozvanny, M. L., Watras, J. and Ehrlich, B. E. (1991)** Bell-shaped calcium-response curves of  $\text{Ins}(1,4,5)\text{P}_3$ -gated and calcium-gated channels from endoplasmic reticulum of cerebellum. *Nature*, **351**, 751-754

**Bickmeyer, U., Rössler, W. and Wiegand, H. (1994)** Calcium channel currents in cultured pars intercerebralis neurosecretory cells of adult *Locusta migratoria*. *J. exp. Biol.*, **197**, 393-398

**Blake, A. D., Anthony, N. M., Chen, H. H., Harrison, J. B., Nathanson, N. M. and Sattelle, D. B. (1993)** *Drosophila* nervous system muscarinic acetylcholine receptor: transient functional expression and localization by immunocytochemistry. *Mol. Pharmacol.*, **44**, 716-724

**Blatz, A. L. and Magleby, K. L. (1986)** Single apamin-blocked Ca-activated K<sup>+</sup> channels of small conductance in cultured rat skeletal muscle. *Nature*, **323**, 718-720

**Blaustein, M. P. (1988)** Calcium transport and buffering in neurons. *TINS*, **11** (10), 438-443

**Bodmer, R., Dagan, D. and Levitan, I. B. (1984)** Chemical and electrotonic connections between *Aplysia* neurons in primary culture. *J. Neurosci.*, **4** (1), 228-233

**Bormann, J., Hamill, O. P. and Sakmann, B. (1987)** Mechanism of anion permeation through channels gated by glycine and  $\gamma$ -aminobutyric acid in mouse cultured spinal neurons. *J. Physiol. (Lond.)*, **385**, 243-286

**Bormann, J. and Feigenspan, A. (1995)** GABA<sub>C</sub> receptors. *TINS*, **18** (12), 515-519

**Borst, A. and Egelhaaf, M. (1992)** *In vitro* imaging of calcium accumulation in fly interneurons as elicited by visual motion stimulation. *Proc. Natl. Acad. Sci.*, **89**, 4139-4143

**Bossy, B., Ballivet, M. and Spierer, P. (1988)** Conservation of neural nicotinic acetylcholine receptors from *Drosophila* to vertebrate central nervous system. *EMBO J.*, **7** (3), 611-618

**Bowery, N. G. (1993)** GABA<sub>B</sub> receptor pharmacology. *Ann. Rev. Pharmacol. Toxicol.*, **33**, 109-147

**Bowman, W. C. and Rand, M. J. (1980)** 'Textbook of pharmacology', Blackwell Scientific Publications

**Boyle, M. B., Klein, M. Smith, S. J. and Kandel, E. R. (1984)** Serotonin increases intracellular Ca<sup>2+</sup> transients in voltage clamped sensory neurons of *Aplysia californica*. *Proc. Natl. Acad. Sci., USA*, **75**, 3512-3516

- Braha, O., Edmonds, B., Sacktor, T., Kandel, E. R. and Klein, M. (1993)** The contributions of protein kinase A and protein kinase C to the actions of 5HT on L-type  $\text{Ca}^{2+}$  current of the sensory neurons in *Aplysia*. *J. Neurophysiol.*, **13**, 1839-1851
- Brakenhoff, G. J., Van Spronsen, E. A., Van der Voort, H. T. M. and Nanninga, N. (1989)** Three-Dimensional Confocal Fluorescence Microscopy. In 'Methods in Cell Biology. Volume 30. Fluorescence microscopy of living cells in culture. Part B.' Eds. Taylor, D. L. and Wang, Y.-L., Academic Press, Inc., San Diego, California, USA, 379-398
- Breer, H (1981)** Comparative studies on cholinergic activities in the central nervous system of *Locusta migratoria*. *J. Comp. Physiol.*, **141**, 271-275
- Breer, H., Kleene, R. and Hinz, G. (1985)** Molecular forms and subunit structure of the acetylcholine receptor in the central nervous system of insects. *J. Neurosci.*, **5**, 3386-3392
- Breer, H. and Knipper, M. (1984)** Characterization of acetylcholine release from insect synaptosomes. *Insect Biochem.*, **14**, 337-344
- Brisson, A. and Unwin, P. N. T. (1985)** Quaternary structure of the acetylcholine receptor. *Nature*, **315**, 474-477
- Brookes, J. P. and Hall, Z. W. (1975)** Acetylcholine receptors in normal and denervated muscle. 1. Purification and interaction with [ $^{125}\text{I}$ ]- $\alpha$ -bungarotoxin. *Biochem.* **14** (10), 2092-2099
- Brown, D. A. and Adams, P. R. (1980)** Muscarinic suppression of a novel voltage-sensitive  $\text{K}^+$  current in a vertebrate neurone. *Nature*, **283**, 673-676
- Brown, D. A. and Fumagalli, L. (1977)** Dissociation of the  $\alpha$ -bungarotoxin binding and receptor block in the rat superior cervical ganglion. *Brain Res.* **129**, 165-168
- Bulloch, A. G. M. and Hauser, G. C. (1990)** Sprouting by isolated *Helisoma* neurons - enhancement by glutamate. *Int. J. Dev. Neurosci.*, **8** (4), 391
- Burrows, M. (1975)** Monosynaptic connexions between wing stretch receptors and flight motoneurons of the locust. *J. exp. Biol.*, **62**, 189-219
- Byrne, J. H. and Kandel, E. R. (1996)** Presynaptic facilitation revisited: state and time dependence. *J. Neurosci.*, **16** (2), 425-435

- Campbell, J. I. (1961)** The anatomy of the nervous system of the mesothorax of *Locusta migratoria migratorioides* R and F. *Proc. Zool. Soc., Lond.*, **137**, 403-432
- Carew, T. J., Walters, E. T. and Kandel, E. R. (1981)** Classical conditioning in a simple defensive withdrawal reflex in *Aplysia*. *J. Neurosci.* **1**, 1426-1437
- Carlson, S. D. and Saint Marie, R. L. (1990)** Structure and function of insect glia. *Ann. Rev. Entomol.*, **35**, 597-621
- Casagrand, J. L. and Ritzmann, R. E. (1992)** Biogenic amines modulate synaptic transmission between identified giant interneurons and thoracic interneurons in the escape system of the cockroach. *J. Neurobiol.*, **23**, 644-655
- Castellucci, V. L. and Kandel, E. R. (1976)** Presynaptic facilitation as a mechanism for behavioural sensitization in *Aplysia*. *Science*, **194**, 1176-1178
- Catarsi, S., Ching, S., Merz, D. C. and Drapeau, P. (1995)** Tyrosine phosphorylation during synapse formation between identified leech neurons. *J. Physiol. (Lond.)*, **485** (3), 775-786
- Catarsi, S. and Drapeau, P. (1993)** Tyrosine kinase-dependent selection of transmitter responses induced by neuronal contact. *Nature*, **363** (6427), 353-355
- Chen, J. S. and Levi-Montalcini, R. (1969)** Axonal outgrowth and cell migration *in vitro* from nervous system of cockroach embryos. *Science*, **166**, 631-632
- Chen, J. S. and Levi-Montalcini, R. (1970a)** Axonal growth from insect neurons in glia-free cultures. *Proc. Natl. Acad. Sci.*, **66**, 32-39
- Chen, J. S. and Levi-Montalcini, R. (1970b)** Long-term cultures of dissociated nerve cells from the embryonic nervous system of the cockroach *Periplaneta americana*. *Arch. Ital. Biol.*, **108**, 503-537
- Choi, D. W. (1988)** Calcium-mediated neurotoxicity: relationship to specific channel types and role in ischemic damage. *TINS*, **11** (10), 465-469
- Claassen, D. E. and Kammer, A. E. (1986)** Effects of octopamine, dopamine and serotonin on production of flight motor output by thoracic ganglia of *Manduca sexta*. *J. Neurobiol.*, **17** (1), 1-14
- Cohan, C. S. and Kater, S. B. (1986)** Suppression of neurite elongation and growth cone motility by electrical activity. *Science*, **232**, 1638-1640
- Coles, J. A. and Abbott, N. J. (1996)** Signalling from neurones to glial cells in invertebrates. *TINS*, **19** (8), 358-362



**Collier, M. L. and Hume, J. R. (1995)** Unitary chloride channels activated by protein kinase C in guinea pig ventricular myocytes. *Circulation Res.*, **76** (2), 317-324

**Conti-Troconi, S. M., McLane, K. E., Raferty, M. A., Grando, S. A. and Protti, M. P. (1994)** The nicotinic acetylcholine receptor - structure and autoimmune pathology. *Crit. Rev. Biochem. Mol. Biol.*, **29** (2), 69-123

**Cox, T. (1993)** Low-affinity mixed acetylcholine-responsive receptors at the apical membrane of frog tadpole skin. *Am. J. Physiol.*, **264** (Cell Physiol. **33**), C552-C558

**Crepel, F. and Krupa, M. (1988)** Activation of protein kinase-C induces a long term depression of glutamate sensitivity of cerebellar Purkinje cells. An *in vitro* study. *Brain Res.* **458**, 397-401

**Cutting, G. R., Lu, L., O'Hara, B. F., Kasch, L. M., Montrose-Rafizadeh, C., Donovan, D. M., Shimada, S., Antonarakis, S. E., Guggino, W. B., Uhl, G. R. and Kazazian Jr., H. H. (1991)** Cloning of the  $\gamma$ -aminobutyric acid (GABA)  $\rho 1$  cDNA: a GABA receptor subunit highly expresses in the retina. *Proc. Natl. Acad. Sci., USA*, **88**, 2673-2677

**Dagan, D. and Levitan, I. B. (1981)** Isolated identified *Aplysia* neurons in cell culture. *J. Neurosci.*, **1** (7), 736-740

**Dale, N. and Kandel, E. R. (1993)** L-Glutamate may be the fast excitatory transmitter of *Aplysia* sensory neurons. *Proc. Natl. Acad. Sci. USA*, (**90**), 7163-7167

**Dale, N. Schacher, S. and Kandel, E. R. (1988)** Long-term facilitation in *Aplysia* involves increase in transmitter release. *Science*, **239**, 282-285

**David, J. A. and Pitman, R. M. (1990)** Functional muscarinic receptors on an identified neurone in the isolated metathoracic ganglion of the cockroach *Periplaneta americana*. *J. Physiol. (Lond.)*, **429**, 66P

**David, J. A. and Pitman, R. M. (1992)** The pharmacology of muscarinic receptor on the soma membrane of an identified cockroach motoneurone. *J. Physiol. (Lond.)*, **446**, 326P

**David, J. A. and Pitman, R. M. (1993a)** The pharmacology of alpha-bungarotoxin-resistant acetylcholine receptors on an identified cockroach motoneurone. *J. Comp. Physiol. A*, **172**, 359-368

- David, J. A. and Pitman, R. M. (1993b)** Evidence for functional inositol 1,4,5-trisphosphate receptors in the CNS of the cockroach *Periplaneta americana*. *J. Physiol. (Lond.)*, **473**, 248P
- David, J. A. and Pitman, R. M. (1993c)** Activation of receptors with mixed muscarinic/nicotinic pharmacology modulates a calcium current in an insect motoneurone. *J. Physiol. (Lond.)*, **459**, 98P
- David, J. A. and Pitman, R. M. (1994)** Inositol 1,4,5-trisphosphate production is linked to muscarinic acetylcholine receptors in the CNS of the cockroach, *Periplaneta americana*. *J. Physiol. (Lond.)*, **480P**, 97P
- David, J. A. and Pitman, R. M. (1995)** Muscarinic agonists modulate calcium-dependent outward currents in an identified motoneurone. *Brain Res.*, **669**, 153-156
- David, J. A. and Pitman, R. M. (1996a)** Muscarinic receptor activation modulates ligand-gated ion channels in an insect motoneuron via changes in intracellular calcium. *Proc. Roy. Soc. Lond. B*, **263**, 469-474
- David, J. A. and Pitman, R. M. (1996b)** Modulation of  $\text{Ca}^{2+}$  and  $\text{K}^{+}$  conductances in an identified insect neurone by the activation of an  $\alpha$ -bungarotoxin-resistant cholinergic receptor. *J. exp. Biol.*, **199**, 1921-1930
- David, J. A. and Sattelle, D. B. (1984)** Actions of cholinergic pharmacological agents on the cell body membrane of the fast coxal depressor motoneurone of the cockroach (*Periplaneta americana*). *J. exp. Biol.*, **108**, 119-136
- David, J. A. and Sattelle, D. B. (1990)** Ionic basis of membrane potential and of acetylcholine-induced currents in the cell body of the cockroach fast coxal depressor motoneurone. *J. exp. Biol.*, **151**, 21-39
- Davis, J. L. P. and Pitman, R. M. (1991)** Characterization of receptors mediating the actions of dopamine on an identified inhibitory motoneurone of the cockroach. *J. exp. Biol.*, **155**, 203-217
- de Jong, H. R. and Rosen, O. M. (1977)** Self-phosphorylation of cyclic guanosine 3':5'-monophosphate-dependent protein kinase from bovine lung. *J. Biol. Chem.*, **252**, 2780-2783
- Djamgoz, M. B. A. (1995)** Diversity of GABA receptors in the vertebrate retina. *TINS*, **18** (3), 118-130
- Dohlman, H. G., Thorner, J., Caron, M. C. and Lefkowitz, R. J. (1991)** Model systems for the study of seven-transmembrane segment receptors. *Ann. Rev. Biochem.*, **60**, 653-688



**Dolly, J. O. and Barnard, E. A. (1975)** Complete purification of the acetylcholine receptor protein from mammalian muscle. *FEBS Letts.*, **57** (3), 267-271

**Downing, J. E. G. and Role, L. W. (1987)** Activators of protein kinase C enhance acetylcholine receptor desensitisation in sympathetic ganglion neurons. *Proc. Natl. Acad. Sci. USA*, **84**, 7739-7743

**Drew, C. A., Johnston, A. R. and Weatherby, R. P. (1984)** Bicuculline-insensitive GABA receptors: studies on the binding of (-)-baclofen to rat cerebellar membranes. *Neurosci. Letts.*, **52**, 317-321

**Dubas, F. (1991)** Actions of putative amino acid neurotransmitters on the neuropile arborizations of locust flight motoneurons. *J. exp. Biol.*, **155**, 337-365

**Dudai, Y. (1977)** Demonstration of an  $\alpha$ -bungarotoxin-binding nicotinic receptor in flies. *FEBS Letts.*, **76** (2), 211-213

**Dudai, Y. and Amsterdam, A. (1977)** Nicotinic receptors in the brain of *Drosophila melanogaster* demonstrated by autoradiography with [ $^{125}$ I] $\alpha$ -bungarotoxin. *Brain Res.*, **130**, 551-555

**Dudai, Y. and Ben-Barak, J. (1977)** Muscarinic receptor in *Drosophila melanogaster* demonstrated by binding of [ $^3$ H] quinuclidinyl benzilate. *FEBS Letts.*, **81** (1), 134-136

**Duggan, M. J. and Lunt, G. G. (1986)** Second messengers linked to the muscarinic acetylcholine receptor in locust (*Schistocera gregaria*) ganglia. In 'International conference on insect neurochemistry and neurophysiology.'; Second edition. Eds. Borkovic, A. B. and Gelman, D. B., New Jersey, Humana, 251-254

**Dyer, D., Tigyi, G. and Miledi, R. (1992)** The effect of active serum albumin on PC12 cells: II. Intracellular  $\text{Ca}^{2+}$  transients and their role in neurite retraction. *Mol. Brain Res.*, **14**, 302-309

**Eisen, J. S. and Marder, E. (1982)** Mechanisms underlying pattern generation in lobster stomatogastric ganglion as determined by selective inactivation of identified neurons. III. Synaptic connections of electrically coupled pyloric neurons. *J. Neurophysiol.*, **48**, 1392-1415

**Eldefrawi, M. E., Eldefrawi, A. T. and O'Brien, R. D. (1971)** Binding sites for cholinergic ligands in a particulate fraction of *Electrophorus* electroplax. *Proc. Natl. Acad. Sci. USA*, **68**, 1047-1050

- Enz, R., Brandstätter, J. H., Hartveit, E., Wässle, H. and Bormann, J. (1995)** Expression of GABA receptor  $\rho 1$  and  $\rho 2$  subunits in the retina of brain of the rat. *Eur. J. Neurosci.*, **7**, 1495-1501
- Evans, A. M. and Green, K. L. (1990)** Characterization of the dopamine receptor mediating the hyperpolarisation in the cockroach salivary gland acinar cells *in vitro*. *Br. J. Pharmacol.*, **101**, 103-108
- Evans, A. M. and Green, K. L. (1991)** Effects of selective  $D_1$  and  $D_2$  dopamine agonists on cockroach salivary gland acinar cells *in vitro*. *Br. J. Pharmacol.*, **104**, 787-792
- Evans, P. D. (1980)** Biogenic amines in the insect nervous system. *Adv. Insect Physiol.*, **15**, 317-473
- Feigenspan, A. and Bormann, J. (1994)** Modulation of GABA<sub>C</sub> receptors in rat retinal bipolar cells by protein kinase C. *J. Physiol. (Lond.)*, **481** (2), 325-330
- Feigenspan, A., Wässle, H. and Bormann, J. (1993)** Pharmacology of GABA receptor  $Cl^-$  channels in rat retinal bipolar cells. *Nature*, **361**, 159-162
- Felder, C. C., Williams, H. L. and Axelrod, J. (1991)** A transduction pathway associated with receptors coupled to the inhibitory guanine nucleotide binding protein  $G_i$  that amplifies ATP-mediated arachidonic acid release. *Proc. Natl. Acad. Sci. USA*, **88**, 6477-6480
- Fernández-de-Miguel, F. and Drapeau, P. (1995)** Synapse formation and function: insights from identified leech neurons in culture. *J. Neurobiol.*, **27** (3), 367-379
- French-Constant, R. H. and Rocheleau, T. (1992)** *Drosophila* cyclodiene resistance gene shows conserved genomic organisation with vertebrate  $\gamma$ -aminobutyric acid<sub>A</sub> receptor. *J. Neurochem.*, **59** (4), 1562-1565
- Flamm, R. E. and Harris-Warrick, R. M. (1986a)** Aminergic modulation in lobster stomatogastric ganglion. I. Effects on motor pattern and activity of neurons within the pyloric circuit. *J. Neurophysiol.*, **55** (5), 847-865
- Flamm, R. E. and Harris-Warrick, R. M. (1986b)** Aminergic modulation in lobster stomatogastric ganglion. II. Target neurons of dopamine, octopamine, and serotonin within the pyloric circuit. *J. Neurophysiol.*, **55** (5), 866-881
- Fleming, J. R. and Pitman, R. M. (1983)** Histochemical localization of biogenic amines in cockroach neurones. *J. Physiol. (Lond.)*, **334**, 98-99P

- Fuchs, P. A., Henderson, L. P. and Nicholls, J. G. (1982)** Chemical transmission between individual retzius and sensory neurones of the leech in culture. *J. Physiol. (Lond.)*, **323**, 195-210
- Fukuda, K., Higashida, H., Kubo, T., Maeda, A., Akiba, I., Bujo, H., Mishina, M. and Numa, S. (1988)** Selective coupling with K<sup>+</sup> currents of muscarinic acetylcholine receptor subtypes in NG108-15 cells. *Nature*, **335**, 355-358
- Fumagalli, L., De Renzi, G. and Miani, N. (1976)** Acetylcholine receptors: number and distribution in intact and deafferented superior cervical ganglion of the rat. *J. Neurochem.*, **27**, 47-52
- Funte, L. R. and Haydon, P. G. (1993)** Synaptic target contact enhances presynaptic calcium influx by activating cAMP-dependent protein kinase during synaptogenesis. *Neuron*, **10**, 1069-1078
- Gage, P. W. (1992)** Activation and modulation of neuronal K<sup>+</sup> channels by GABA. *TINS*, **5** (2), 46-51
- Gerschenfeld, H. M. (1973)** Chemical transmission in invertebrate central nervous system and neuromuscular junction. *Physiol. Rev.*, **53**, 1-119
- Gettrup, E. (1962)** Thoracic proprioceptors in the flight system of locusts. *Nature*, **193**, 498-499
- Giles, D. P., Joy, R. T. and Usherwood, P. N. R. (1978)** Growth of isolated locust neurones in culture. *J. Physiol. (Lond.)*, **276**, 74P
- Giles, D. P. and Usherwood, P. N. R. (1985)** Locust nymphal neurones in culture: a new technique for studying the physiology and pharmacology of insect central neurones. *Comp. Biochem. Physiol.*, **80C**, 53-59
- Ginsborg, B. L., House, C. R. and Mitchell, M. R. (1980)** On the role of calcium in the electrical responses of cockroach salivary gland cells to dopamine. *J. Physiol. (Lond.)*, **303**, 325-335
- Glanzman, D. L., Kandel, E. R. and Schacher, S., (1990)** Target-dependent structural changes accompanying long-term synaptic facilitation in *Aplysia* neurons. *Science*, **249**, 799-802
- Goldsmith, B. A. and Abrams, T. W. (1992)** cAMP modulates multiple K<sup>+</sup> currents, increasing spike duration and excitability in *Aplysia* sensory neurons. *Proc. Natl. Acad. Sci., USA*, **89**, 11481-11485

- Goldstein, R. S. and Camhi, J. M. (1991)** Different effects of the biogenic amines dopamine, serotonin and octopamine on the thoracic and abdominal portions of the escape circuit in the cockroach. *J. Comp. Physiol. A.*, **168**, 103-112
- Goodman, C. S. and Heitler, W. J. (1979)** Electrical properties of insect neurones with spiking and non-spiking somata: normal, axotomized, and colchicine-treated neurones. *J. exp. Biol.*, **83**, 95-121
- Goodman, C. S. and Spitzer, N. C. (1980)** Embryonic development of neurotransmitter receptors in grasshoppers. In '*Receptors for Neurotransmitters, Hormones and Pheromones in Insects*'. Eds. Sattelle, D. B., Hall, L. M. and Hildebrand, J. G., Elsevier/North Holland, Amsterdam, 195-207
- Gorczyca, M. G., Budnik, V., White, K. and Wu, C. F. (1991)** Dual muscarinic and nicotinic action on a motor program in *Drosophila*. *J. Neurobiol.*, **22**, 391-404
- Gotzes, F., Balfanz, S. and Baumann, A. (1994)** Primary structure and functional characterisation of a *Drosophila* dopamine receptor with high homology to human D<sub>1/5</sub> receptors. *Receptor and Channels*, **2**, 131-141
- Grau, S. M. and Cooke, I. M. (1992)** Peptidergic neurons of the crab, *Cardisoma carnifex*, in defined culture maintain characteristic morphologies under a variety of conditions. *Cell Tissue Res.*, **270**, 303-317
- Gray, D. C., Ginsborg, B. L. and House, C. R. (1984)** Cyclic AMP as a possible mediator of dopamine stimulation of cockroach gland cells. *Q. J. exp. Physiol.*, **69**, 171-186
- Green, W. N., Ross, A. F. and Claudio, T. (1991a)** cAMP stimulation of acetylcholine receptor expression is mediated through posttranslational mechanisms. *Proc. Natl. Acad. Sci. USA*, **88** (3), 854-858
- Green, W. N., Ross, A. F. and Claudio, T. (1991b)** Acetylcholine receptor assembly is stimulated by phosphorylation of its gamma subunit. *Neuron*, **7** (4), 659-666
- Greengard, P., Jen, J., Narin, A. C. and Stevens, C. F. (1991)** Enhancement of the glutamate response by cAMP-dependent protein kinase in hippocampal neurons. *Science*, **253**, 1135-1138
- Grewe, C. W. and Kebedian, J. W. (1982)** Dopamine stimulates production of cyclic AMP by the salivary gland of the cockroach *Nauphoeta cinerea*. *Cell. Mol. Neurobiol.*, **2** (1), 65-69
- Grolleau, F., Lapied, B., Buckingham, S. D., Mason, W. D. and Sattelle, D. B. (1996)** Nicotine-induced increase in [Ca<sup>2+</sup>]<sub>i</sub> in isolated adult neurosecretory cells

of the cockroach *Periplaneta americana* detected using fura-2. *J. Physiol. (Lond.)*, **491P**, 107P

**Grundy, H. F. (1990)** Fundamental pharmacodynamics; receptors and responses. In '*Lecture notes on pharmacology*'. Blackwell Scientific Publications, UK, 90-123

**Gundelfinger, E. D. (1992)** How complex is the nicotinic receptor system of insects? *TINS*, **15** (6) 206-211

**Hadley, R. D., Bodnar, D. A. and Kater, S. B. (1985)** Formation of electrical synapses between isolated, cultured *Helisoma* neurons requires mutual neurite elongation. *J. Neurosci.*, **5** (12), 3145-3153

**Hadley, R. D., Kater, S. B. and Cohan, C. S. (1983)** Electrical synapse formation depends on interaction of mutually growing neurites. *Science*, **221**, 466-468

**Hancox, J. C. (1991)** Non-linear membrane properties of insect motoneurons. PhD Thesis, University of St. Andrews

**Hancox, J. C. and Pitman, R. M. (1992)** A time dependent excitability change in the soma of an identified insect motoneurone. *J. exp. Biol.*, **162**, 251-263

**Hanke, W. and Breer, H. (1986)** Channel properties of an insect neuronal acetylcholine receptor protein reconstituted in planar lipid bilayers. *Nature*, **321**, 171-174

**Harris, R., Cattell, K. J. and Donnellan, J. F. (1981)** The purification and molecular characterisation of a putative nicotinic-muscarinic acetylcholine receptor from housefly heads. *Insect. Biochem.*, **11** (4), 371-385

**Harris-Warrick, R. M., Coniglio, L. M., Barazangi, N., Guckenheimer, J. and Gueron, S. (1995a)** Dopamine modulation of transient potassium current evokes phase shifts in a central pattern generator network. *J. Neurosci.*, **15**, 342-358

**Harris-Warrick, R. M., Coniglio, L. M., Levini, R. M., Gueron, S. and Guckenheimer, J. (1995b)** Dopamine modulation of two subthreshold currents produces phase shifts in activity of an identified motoneuron. *J. Neurophysiol.*, **74** (4), 1404-1420

**Harris-Warrick, R. M. and Flamm, R. E. (1986)** Chemical modulation of a small central pattern generator circuit. *TINS*, **9**(9), 432-437

**Harris-Warrick, R. M., Flamm, R. E., Johnson, B. R., Katz, P. S., Keihn, O. and Zhang, B. (1993)** Amine modulation in the crustacean stomatogastric



ganglion. In 'Proceedings of Neurotox '91.' Ed. Duce, I. R., Elsevier, Cambridge, UK, 305-321

**Harrison, J. B., Leech, C. A., Katz, J. and Sattelle, D. B. (1990)** Embryonic and adult neurones of the housefly (*Musca domestica*) in culture. *Tissue and Cell*, **22** (3), 337-347

**Haugland, R. P. (1992)** Calcium indicators, chelators and ionophores. In 'Handbook of fluorescent probes and research chemicals.', Fifth edition. Ed. Larison, K. D. Molecular Probes Inc., Eugene, Oregon, USA, 113-128

**Hayashi, J. H. and Hildebrand, J. G. (1990)** Insect olfactory neurones *in vitro*: Morphological and physiological characterisation of cells from the developing antennal lobes of *Manduca sexta*. *J. Neurosci.*, **10** (3), 848-859

**Hayashi, J. H. and Levine, R. B. (1992)** Calcium and potassium currents in leg motoneurones during postembryonic development in the hawkmoth *Manduca sexta*. *J. exp. Biol.*, **171**, 15-42

**Haydon, P. G. (1988)** The formation of chemical synapses between cell-cultured neuronal somata. *J. Neurosci.*, **8** (3), 1032-1038

**Haydon, P. G. and Drapeau, P. (1995)** From contact to connection: early events during synaptogenesis. *TINS*, **18** (4), 196-201

**Haydon, P. G. and Kater, S. B. (1988)** The differential regulation of formation of chemical and electrical connections in *Helisoma*. *J. Neurobiol.*, **19**, 636-655

**Haydon, P. G., McCobb, D. P. and Kater, S. B. (1984)** Serotonin selectively inhibits growth cone motility and synaptogenesis of specific neurons. *Science*, **226**, 561-564

**Henderson, L. P., Kuffler, D. P., Nicholls, J. G. and Zhang, R.-J. (1983)** Structural and functional analysis of synaptic transmission between identified leech neurones in culture. *J. Physiol. (Lond.)*, **340**, 347-358

**Hepler, J. R. and Gilman, A. G. (1992)** G proteins. *TIBS*, **17**, 383-387

**Hermans-Borgmeyer, I., Zopf, D., Ryseck, R.-P., Hovemann, B., Betz, H. and Gundelfinger, E. D. (1986)** Primary structure of a developmentally regulated nicotinic acetylcholine receptor protein from *Drosophila*. *EMBO J.*, **5** (7), 1503-1598

**Hettasch, J. M. and Le Breton, G. C. (1987)** Modulation of  $Ca^{2+}$  fluxes in isolated platelet vesicles: effects of cAMP-dependent protein kinase and protein

kinase inhibitor on  $\text{Ca}^{2+}$  sequestration and release. *Biochimica et Biophysica Acta*, **931**, 49-58

**Hicks, D. B. and Beadle, D. J. (1980)** An investigation of the ultrastructure of neuronal cultures of *Periplaneta americana*. In '*Insect Neurobiology and Pesticide Action*'. Society of the Chemical Industry, London, UK, 193-200

**Hicks, D., Beadle, D. J., Giles, D. P. and Usherwood, P. N. R. (1981)** Ultrastructure of dissociated nerve cells of *Periplaneta americana* (L) (Dictyoptera: Blattidae) growing in culture. *Int. J. Insect Morphol. Embryol.*, **10**, 225-233

**Hill, D. R. and Bowery, N. G. (1981)**  $^3\text{H}$ -baclofen and  $^3\text{H}$ -GABA bind to bicuculline-insensitive  $\text{GABA}_\text{B}$  sites in rat brain. *Nature*, **290**, 149-152

**Hille, B. (1994)** Modulation of ion-channel function by G-protein coupled receptors. *TINS*, **17** (12), 531-536

**Hochner, B. and Kandel, E. R. (1992)** Modulation of a transient  $\text{K}^+$  current in the pleural sensory neurons of *Aplysia* by serotonin and cAMP: implications for spike broadening. *Proc. Natl. Acad. Sci.*, **89**, 11476-11480

**Hodgkin, A. L. and Keynes, R. D. (1955)** The potassium permeability of a giant nerve fibre. *J. Physiol. (Lond.)*, **128**, 253-281

**Hoffmann, P. W., Ravindran, A. and Haganir, R. L. (1994)** Role of phosphorylation in desensitization of acetylcholine receptors expressed in *Xenopus* oocytes. *J. Neurosci.*, **14** (7), 4185-4195

**Holden, J. S., Suter, C. and Usherwood, P. N. R. (1978)** Isolation of neurone somata exhibiting pharmacological responses from the locust nervous system. *J. Physiol. (Lond.)*, **276**, 4-5P

**House, C. R. (1973)** An electrophysiological study of neuroglandular transmission in the isolated salivary glands of the cockroach. *J. exp. Biol.*, **58**, 29-43

**Howes, E. A., Armett-Kibel, C. and Smith, P. J. S. (1993)** A blood-derived attachment factor enhances *in vitro* growth of two glial cell types from adult cockroach. *Glia*, **8**, 33-41

**Howes, E. A., Cheek, T. R. and Smith, P. J. S. (1991)** Long-term growth *in vitro* of isolated, fully differentiated neurones from the central nervous system of an adult insect. *J. exp. Biol.*, **156**, 591-605

**Huang, Z.-Y. and Knowles, C. O. (1990)** Nicotinic and muscarinic cholinergic receptors in honey bee (*Apis mellifera*) brain. *Comp. Biochem. Physiol.*, **97C**, 275-281

**Hue, B., Lapied, B. and Malécot, C. O. (1989)** Do presynaptic muscarinic receptors regulate acetylcholine release in the central nervous system of the cockroach *Periplaneta americana*? *J. exp. Biol.*, **142**, 447-451

**Huganir, R. L. (1987)** Biochemical mechanisms that regulate the properties of ion channels. In '*Neuromodulation: the biochemical control of neuronal excitability*'. Eds. Kaczmarek, L. K. and Levitan, I. B., Oxford University Press Inc, New York, 64-85

**Huganir, R. L. and Greengard, P. (1990)** Regulation of neurotransmitter receptor desensitization by protein phosphorylation. *Neuron*, **5**, 555-567

**Huganir, R. L., Miles, K. and Greengard, P. (1984)** Phosphorylation of the nicotinic acetylcholine receptor by an endogenous tyrosine-specific protein kinase. *Proc. Natl. Acad. Sci. USA*, **81**, 6968-6972

**Hulme, E. C., Birdsall, N. M. J. and Buckley, N. J. (1990)** Muscarinic receptor subtypes. *Ann. Rev. Toxicol.*, **30**, 633-673

**Hwang, T. C., Horie, M., Nairn, A. C. and Gadsby, D. C. (1992)** Role of GTP-binding proteins in the regulation of mammalian cardiac chloride conductance. *J. Gen. Physiol.*, **99** (4), 465-489

**Ivanina, T., Perets, T., Thornhill, W. B., Levin, G., Dascal, N. and Lotan, I. (1994)** Phosphorylation by protein kinase A of RCK1 K<sup>+</sup> channels expressed in *Xenopus* oocytes. *Biochem.*, **33** (29), 8786-8792

**Johnson, B. R. and Harris-Warrick, R. M. (1990)** Aminergic modulation of graded synaptic transmission in the lobster stomatogastric ganglion. *J. Neurosci.*, **10** (7), 2066-2076

**Jonas, P., Baumann, A., Merz, B. and Gundelfinger, E. D. (1990)** Structure and developmental expression of the D $\alpha$ 2 gene encoding a novel nicotinic acetylcholine receptor protein of *Drosophila melanogaster*. *FEBS Letts.*, **269** (1), 264-268

**Jones, M. V. and Westbrook, G. L. (1996)** The impact of receptor desensitization on fast synaptic transmission. *TINS*, **19** (3) 96-101

**Jouaville, L. S., Ichas, F., Holmuhamedov, E. L., Camacho, P. and Lechleiter, J. D. (1995)** Synchronization of calcium waves by mitochondrial substrates in *Xenopus laevis* oocytes. *Nature*, **377**, 483-441



**Kaczmarek, L. K., Finbow, M., Revel, J. P. and Strumwasser, F. (1979)** The morphology and coupling of *Aplysia* bag cells within the abdominal ganglion and in cell culture. *J. Neurobiol.*, 10, 535-550

**Kaczmarek, L. K. and Levitan, I. B. (1987)** What is Neuromodulation? In 'Neuromodulation: the biochemical control of neuronal excitability'. Eds. Kaczmarek, L. K. and Levitan, I. B., Oxford University Press Inc, New York, 3-16

**Kao, J. P. Y., Harootunian, A. T. and Tsien, R. Y. (1989)** Photochemically generated cytosolic calcium pulses and their detection by fluo-3. *J. Biol. Chem.*, 264 (14), 8179-8184

**Karlin, A. (1993)** Structure of nicotinic acetylcholine receptors. *Curr. Op. Neurobiol.*, 3, 299-309

**Karlin, A. and Cowburn, D. (1973)** The affinity-labelling of partially purified acetylcholine receptor from electric tissue of *Electrophorus*. *Proc. Natl. Acad. Sci., USA*, 70, 3636-3640

**Katz, P. S. and Frost, W. N. (1996)** Intrinsic neuromodulation: altering neuronal circuits from within. *TINS*, 19 (2), 54-61

**Kebabian, J. W. and Calne, D. B. (1979)** Multiple receptors for dopamine. *Nature*, 277, 93-96

**Kebabian, J. W. and Neumeyer, J. L. (1994)** 'The RBI handbook of receptor classification'. Research Biochemicals International, Natick, Massachusetts, USA

**Keen, L., Amar, M., Beadle, D. J. and Bermudez, I. (1994)** Cockroach glial cell cultures: morphological development and voltage-gated potassium channels. *Tissue and Cell*, 26 (2), 209-221

**Kerkut, G. A., Pitman, R. M. and Walker, R. J. (1969a)** Iontophoretic applications of acetylcholine and GABA onto insect central neurones. *Comp. Biochem. Physiol.*, 31, 611-633

**Kerkut, G. A., Pitman, R. M. and Walker, R. J. (1969b)** Sensitivity of neurones of the insect central nervous system to iontophoretically applied acetylcholine or GABA. *Nature*, 222, 1075-1076

**Kirchhof, B. and Bicker, G. (1992)** Growth properties of larval and adult locust neurones in primary cell culture. *J. Comp. Neurol.*, 323, 411-422

- Klein, M., Camardo J., and Kandel, E. R. (1982)** Serotonin modulates a specific potassium current in the sensory neurons that show presynaptic facilitation in *Aplysia*. *Proc. Natl. Acad. Sci. USA*, **79**, 5713-5717
- Klein, M. and Kandel, E. R. (1980)** Mechanism of calcium current modulation underlying presynaptic facilitation and behavioural sensitization in *Aplysia*. *Proc. Natl. Acad. Sci. USA*, **77**, 6912-6916
- Klein, M., Shapiro, E. and Kandel, E. R. (1980)** Synaptic plasticity and the modulation of the  $Ca^{2+}$  current. *J. exp. Biol.*, **89**, 117-157
- Knipper, M. and Breer, H. (1988)** Subtypes of muscarinic receptors in the nervous system of insects. *Comp. Biochem. Physiol.*, **90C**, 275-280
- Knipper, M. and Breer, H. (1989)** Muscarinic receptors modulating acetylcholine release from insect synaptosomes. *Comp. Biochem. Physiol.*, **93C**, 287-292
- Kokay, I. C. and Mercer, A. R. (1996)** Characterisation of dopamine receptors in insect (*Apis mellifera*) brain. *Brain Res.*, **706**, 47-56
- Krebs, E. G. and Beavo, J. A. (1979)** Phosphorylation-dephosphorylation of enzymes. *Ann. Rev. Biochem.*, **48**, 923-959
- Krnjevic, K. (1974)** Chemical nature of synaptic transmission in vertebrates. *Physiol. Rev.*, **54**, 418-540
- Kuba, K., Nohimi, M. and Hua, S.-Y. (1992)** Intracellular dynamics in response to  $Ca^{2+}$  release in autonomic neurones. *Can. J. Physiol. Pharmacol.*, **70**, S64-S72
- Kubo, T., Bujo, H., Akiba, I., Nakai, J., Mishina, M. and Numa, S. (1988)** Location of a region of the muscarinic acetylcholine receptor involved in selective effector coupling. *FEBS Letts.*, **241** (1-2), 119-125
- Kubo, T., Fukuda, K., Mikami, A., Maeda, A., Takahashi, H., Mishina, M., Haga, T., Haga, K., Ichiyama, A., Kangawa K., Kojima, M., Matsuo, H., Hirose, T. and Numa, S. (1986a)** Cloning, sequencing and expression of complementary DNA encoding the muscarinic acetylcholine receptor. *Nature*, **323**, 411-416
- Kubo, T., Maeda, A., Sugimoto, K., Akiba, I., Mikami, A., Takahashi, H., Haga, T., Haga, K., Ichiyama, A., Kangawa K., Matsuo, H., Hirose, T. and Numa, S. (1986b)** Primary structure of porcine cardiac muscarinic acetylcholine receptor deduced from the cDNA sequence. *FEBS Letts.* **209** (2), 367-372

**Kusama, T., Spivak, C. E., Whiting, P., Dawson, V. L., Schaeffer, J. C. and Uhl, G. R. (1993)** Pharmacology of GABA  $\rho 1$  and  $\alpha/\beta$  receptor expressed in *Xenopus* oocytes and COS cells. *Br. J. Pharmacol.*, **109**, 200-206

**Lapied, B. and Hue, B. (1991)** Sensitive nicotinic, mixed and muscarinic receptors in isolated identified adult insect neurones. *Pestic. Sci.*, **32**, 377-279

**Lapied, B., Tribut, F. and Hue, B. (1992)** Effects of McN-A-343 on insect neurosecretory cells: evidence for muscarinic-like receptor subtypes. *Neurosci. Letts.*, **139**, 165-168

**Lapied, B., Tribut, F., Sinakevitch, I., Hue, B. and Beadle, D. J. (1993)** Neurite regeneration of long-term cultured adult insect neurosecretory cells identified as DUM neurons. *Tissue and Cell*, **25** (6), 893-906

**Larkman, A. U. and Jack, J. J. B. (1995)** Synaptic plasticity: hippocampal LTP. *Curr. Op. Neurobiol.*, **5**, 324-334

**Le Corrionc, H. and Hue, B. (1993)** Pharmacological and electrophysiological characterisation of a postsynaptic muscarinic receptor in the central nervous system of the cockroach. *J. exp. Biol.*, **181**, 257-278

**Le Corrionc, H., Lapied, B. and Hue, B. (1991)**  $M_2$ -like presynaptic receptors modulate acetylcholine release in the cockroach (*Periplaneta americana*) central nervous system. *J. Insect Physiol.*, **37**, 647-652

**Lederer, W. J., Niggli, E. and Hadley, R. W. (1990)** Sodium-calcium exchange in excitable cells: fuzzy space. *Science*, **248** (4953), 283

**Lees, G. and Beadle, D. J. (1988)** Cockroach neuronal cultures as models for investigating the neuropharmacology of the insect nervous system. In 'Cell culture approaches to invertebrate neuroscience'. Eds. Beadle, D. J., Lees, G. and Kater, S. B., Academic Press, London, UK, 109-147

**Lees, G., Beadle, D. J. and Botham, R. P. (1983)** Cholinergic receptors on cultured neurones from the CNS of embryonic cockroaches. *Brain Res.*, **288**, 49-59

**Lees, G., Beadle, D. J., Neumann, R. and Benson, J. A. (1987)** Responses to GABA by isolated insect neuronal somata: pharmacology and modulation by a benzodiazepine and a barbiturate. *Brain Res.*, **401**, 267-278

**Leitch, B. and Pitman, R. M. (1995)** Modulation of transmitter release from the terminals of the locust wing stretch receptor neuron by muscarinic antagonists. *J. Neurobiol.*, **28** (4), 455-464

- Leitch, B., Pitman, R. M. and Crockford, K. J. (1993)** Muscarinic receptors at the synapse between locust wing stretch receptors and an identified motoneurone. *Brain Res. Assoc. Abstr.*, **10**, 31
- Levitan, I. B. (1988)** Modulation of ion channels in neurons and other cells. *Ann. Rev. Neurosci.*, **11**, 119-136
- Levitan, I. B. and Kaczmarek, L. K. (1987)** Ion currents and ion channels: substrates for neuromodulation. In '*Neuromodulation: the biochemical control of neuronal excitability*'. Eds Kaczmarek, L. K. and Levitan, I. B., Oxford University Press Inc., New York, 18-35
- Liao, C.-F., Themmen, A. P. N., Joho, R., Barberis, C., Birnbaumer, M. and Birnbaumer, L. (1989)** Molecular cloning and expression of a fifth muscarinic acetylcholine receptor. *J. Biol. Chem.* **264** (12), 7328-7337
- Lin, S. S. and Levitan, I. B. (1987)** Concanavalin A alters the synaptic specificity between cultured *Aplysia* neurons. *Science*, **237**, 648-650
- Lincoln, T. M. and Cornwell, T. L. (1993)** Intracellular cyclic GMP receptor proteins. *FASEB. J.*, **7**, 329-338
- Lindstrom, J., Merlie, J. and Yogeewaran, G. (1979)** Biochemical properties of acetylcholine receptor subunits from *Torpedo californica*. *Biochem.*, **18** (21), 4465-4470
- Liu, Y. and Lasater, E. M. (1994)** Calcium currents in turtle retinal ganglion cells. II Dopamine modulation via a cyclic AMP-dependent mechanism. *J. Neurophysiol.*, **71** (2), 743-752
- López, J. R., Ghanbari, R. A. and Terzic, A. (1996)** A  $K_{ATP}$  channel opener protects cardiomyocytes from  $Ca^{2+}$  waves: a laser confocal microscopy study. *Am. Physiol. Soc.*, **270**, H1384-H1389
- Lummis, S. C. R. and Sattelle, D. B. (1985)** Binding of N-[propionyl- $^3H$ ]propionylated  $\alpha$ -bungarotoxin and L-[benzyl-4- $^3H$ ] quinuclidinyl benzilate to CNS extracts of the cockroach *Periplaneta americana*. *Comp. Biochem. Physiol.*, **80C**, 75-83
- Lummis, S. C. R., Pinnoch, R. D. and Sattelle, D. B. (1987)** GABA receptors of the insect central nervous system. In '*Sites of action for neurotoxic pesticides*'. Eds. Hollingworth R. M. and Green, M. B., Americ. Chem. Soc., Washington DC, USA, 14-24
- MacDonald, R. L. and Olsen, R. W. (1994)** GABA<sub>A</sub> receptor channels. *Ann. Rev. Neurosci.*, **17**, 569-602

**MacDonald, R. L., Rodgers, C. J. and Twyman, R. E. (1989a)** Kinetic properties of the GABA<sub>A</sub> receptor main conductance state of mouse spinal cord neurones in culture. *J. Physiol. (Lond.)*, **419**, 479-499

**MacDonald, R. L., Rodgers, C. J. and Twyman, R. E. (1989b)** Barbiturate regulation of kinetic properties of the GABA<sub>A</sub> receptor channel of mouse spinal neurones in culture. *J. Physiol. (Lond.)*, **417**, 483-500

**Majewski, H. and Barrington, M. (1995)** Modulation of neurotransmitter release. In *'Neurotransmitter release and its modulation: biochemical mechanisms, physiological function and clinical relevance.'* Eds. Powis, D. A. and Bunn, S. J., Cambridge University Press, Cambridge, UK, 163-181

**Margiotta, J. F., Berg, D. K. and Dionne, V. E. (1987)** Cyclic AMP regulates the proportion of functional acetylcholine receptors on chick ciliary ganglion neurons. *Proc. Natl. Acad. Sci. USA*, **84**, 8155-8159

**Marshall, J., Buckingham, S. D., Shingai, R., Lunt, G. G., Goosey, M. W., Darlison, M. G., Sattelle, D. B. and Barnard, E. A. (1990)** Sequence and functional expression of a single  $\alpha$  subunit of an insect nicotinic acetylcholine receptor. *EMBO J.*, **9** (13), 4391-4398

**Martin, R. L., Lloyd, H. G. E. and Cowan, A. I. (1994)** The early events of oxygen and glucose deprivation: setting the scene for neuronal death? *TINS*, **17** (6), 251-257

**Masuda-Nakagawa, L. M. and Nicholls, J. G. (1991)** Extracellular-matrix molecules in development and regeneration of the leech CNS. *Phil. Trans. Roy. Soc. Lond. B*, **331** (1261), 323-335

**Mattson, M. P. and Kater, S. B. (1987)** Calcium regulation of neurite elongation and growth cone mobility. *J. Neurosci.*, **7** (12), 4034-4043

**McCobb, D. P., Haydon, P. G. and Kater, S. B. (1985)** Dopamine: an additional regulator of neurite outgrowth in *Helisoma*. *Soc. Neurosci. Abstr.*, **11**, 761

**McCobb, D. P. and Kater, S. B. (1986)** Serotonin inhibition of growth cone motility is blocked by acetylcholine. *Soc. Neurosci. Abstr.*, **12**, 1117

**McDonald, B. J. and Moss, S. J. (1994)** Differential phosphorylation of intracellular domains of  $\gamma$ -aminobutyric acid type A receptor subunits by calcium/calmodulin type 2-dependent protein kinase and cGMP-dependent protein kinase. *J. Biol. Chem.*, **269** (27), 18111-18117



- McKernan, R. M. and Whiting, P. J. (1996)** Which GABA<sub>A</sub>-receptor subtypes really occur in the brain? *TINS*, **19**(4), 139-143
- Merz, D. C. and Drapeau, P. (1994)** Cell-surface contact mediates neuronal recognition and synapse formation between 2 identified leech neurons. *J. Neurobiol.*, **25** (8), 1029-1037
- Millar, N. S., Baylis, H. A., Reaper, C., Bunting, R., Mason, W. T. and Sattelle, D. B. (1995)** Functional expression of a cloned *Drosophila* muscarinic acetylcholine receptor in a stable *Drosophila* cell line. *J. exp. Biol.*, **198**, 1842-1850
- Millar, N. S., Buckingham, S. D. and Sattelle, D. B. (1994)** Stable expression of a functional homo-oligomeric *Drosophila* GABA receptor in a *Drosophila* cell line. *Proc. Roy. Soc. Lond. B*, **258**, 307-314
- Miller, J. P. and Selverston, A. I. (1982a)** Mechanisms underlying pattern generation in lobster stomatogastric ganglion as determined by selective inactivation of identified neurons. II. Oscillatory properties of pyloric neurons. *J. Neurophysiol.*, **48** (6), 1378-1391
- Miller, J. P. and Selverston, A. I. (1982b)** Mechanisms underlying pattern generation in lobster stomatogastric ganglion as determined by selective inactivation of identified neurons. IV. Network properties of pyloric system. *J. Neurophysiol.*, **48** (6), 1416-1432
- Miller, R. J. (1988)** Calcium signalling in neurons. *TINS*, **11** (10), 415-419
- Minta, A., Kao, J. Y. P. and Tsien, R. Y. (1989)** Fluorescent indicators for cytosolic calcium based on rhodamine and fluorescein chromophores. *J. Biol. Chem.*, **264** (14), 8171-8178
- Mishina, M., Tobimatsu, T., Imoto, K., Fujita, Y., Fukuda, K., Kurasaki, M., Takahashi, H., Morimoto, Y., Hirose, T., Inayama, S., Takahashi, T., Kuno, M. and Numa, S. (1985)** Location of functional regions of acetylcholine-receptor  $\alpha$ -subunit by site-directed mutagenesis. *Nature*, **313** (6001), 364-369
- Mody, I., De Koninck, Y., Otis, T. S. and Soltesz, I. (1994)** Bridging the cleft at GABA synapses in the brain. *TINS*, **17** (12), 517-525
- Montarolo, P. G., Goelet, P., Castellucci, V. F., Morgan, J. and Kandel, E. R. (1986)** A critical period of macromolecular synthesis in long-term heterosynaptic facilitation in *Aplysia*. *Science*, **234**, 1249-1254

- Moran, O. and Dascal, N. (1989)** Protein kinase C modulates transmitter responses in *Xenopus* oocytes injected with rat brain RNA. *Mol. Brain Res.*, **5**, 193-202
- Moss, S. J., Gorrie, G. H., Amato, A. and Smart, T. G. (1995)** Modulation of GABA<sub>A</sub> receptors by tyrosine phosphorylation. *Nature*, **377**, 344-348
- Moss, S. J., Smart, T. G., Blackstone, C. D. and Huganir, R. L. (1992)** Functional modulation of GABA<sub>A</sub> receptors by cAMP-dependent protein phosphorylation. *Science*, **257** (5070), 661-665
- Müller, W., Petrozzino, J. J., Griffith, L. C., Danho, W. and Connor, J. A. (1992)** Specific involvement of Ca<sup>2+</sup>-calmodulin kinase II in cholinergic modulation of neuronal responsiveness. *J. Neurophysiol.*, **68** (6), 2264-2269
- Nairn, A. C., Hemmings, H. C., Jr., and Greengard, P. (1985)** Protein kinases in the brain. *Ann. Rev. Biochem.*, **54**, 931-976
- Nakayama, H., Okuda, H. and Nakashima, T. (1993)** Phosphorylation of rat brain nicotinic acetylcholine receptor by cAMP-dependent protein kinase *in vitro*. *Mol. Brain Res.*, **20** (1-2), 171-177
- Nässel, D. R. (1996)** Neuropeptides, amines and amino acids in an elementary insect ganglion - functional and chemical anatomy of the unfused abdominal ganglion. *Prog. Neurobiol.* **48**(4-5), 325-420
- Nathanson, N. M. (1987)** Molecular properties of the muscarinic acetylcholine receptor. *Ann. Rev. Neurosci.*, **10**, 195-236
- Neumann, R., Lees, G., Beadle, D. J. and Benson, J. A. (1987)** Responses to GABA and other neurotransmitters in insect central neuronal somata *in vitro*. In 'Sites of action for neurotoxic pesticides'. Eds. Hollingworth, R. M. and Green, M. B., Americ. Chem. Soc., Washington DC, USA, 25-43
- Newland, P. L., Smith, P. J. S. and Howes, E. A. (1993)** Regenerating adult cockroach dorsal unpaired median neurones *in vitro* retain their *in vivo* membrane characteristics. *J. exp. Biol.*, **179**, 323-329
- Nicholls, J. G., Liu Y., Payton, B. W. and Kuffler, D. P. (1990)** The specificity of synapse formation by identified leech neurones in culture. *J. exp. Biol.*, **153**, 141-154
- Nishizuka, Y. (1984)** The role of protein kinase C in cell surface signal transduction and tumor promotion. *Nature*, **308** (5961), 693-698



- Noda, M., Takahashi, H., Tanabe, T., Toyosata, M., Furutani, Y., Hirose, T., Asai, M., Inayama, S., Miyata, T. and Numa, S. (1982) Primary structure of  $\alpha$ -subunit precursor of *Torpedo californica* acetylcholine receptor deduced from cDNA sequence. *Nature*, **299**, 793-797
- Oland, L. A. and Hayashi, J. H. (1993) Effects of the steroid hormone 20-hydroxyecdysone and prior sensory input on the survival and growth of moth central olfactory neurons *in vitro*. *J. Neurobiol.*, **24**, 1170-1186
- Olsen, R. W., Meunier, J.-C. and Changeux, J.-P. (1972) Progress in the purification of the cholinergic receptor protein from *Electrophorus electricus* by affinity chromatography. *FEBS Letts.*, **28** (1), 96-100
- Olsen, R. W. and Tobin, A. J. (1990) Molecular biology of GABA<sub>A</sub> receptors. *FASEB J.*, **4**, 1469-1480
- Onai, T., FitzGerald, M. G., Arakawa, S., Gocayne, J. D., Urquhart, D. A., Hall, L. M., Fraser, C. M., McCrombie, W. R. and Venter, J. C. (1989) Cloning, sequence analysis and chromosome localization of a *Drosophila* muscarinic acetylcholine receptor. *FEBS Letts.*, **255** (2), 219-225
- Panchin, Y. V., Arshavsky, Y. I., Selverston, A. and Cleland, T. A. (1993) Lobster stomatogastric neurons in primary culture. 1. Basic characteristics. *J. Neurophysiol.*, **69** (6), 1976-1992
- Pearson, K. G. and Ramirez, J. M. (1990) Influence of input from the forewing stretch receptors on motoneurons in flying locusts. *J. exp. Biol.*, **151**, 317-340
- Pearson, K. G., Reye, D. N. and Robertson, R. M. (1983) Phase-dependent influences of wing stretch receptors on flight rhythm in the locust. *J. Neurophysiol.*, **49** (5), 1168-1181
- Peralta, E. G., Ashkenazi, A., Winslow, J. W., Ramachandran, J. and Capon, D. J. (1988) Differential regulation of PI hydrolysis and adenylyl cyclase by muscarinic receptor subtypes. *Nature*, **334**, 434-437.
- Peralta, E. G., Ashkenazi, A., Winslow, J. W., Smith, D. H., Ramachandran, J. and Capon, D. J. (1987) Distinct primary structures, ligand-binding properties and tissue-specific expression of four human muscarinic acetylcholine receptors. *EMBO J.* **6** (13), 3923-3929
- Pinkas-Kramarski, R., Stein, R., Zimmer, Y. and Sokolovsky, M. (1988) Cloned rat M3 muscarinic receptors mediate phosphoinositide hydrolysis but not adenylate cyclase inhibition. *FEBS Letts.* **239** (2), 174-178.

**Pinnock, R. D., David, J. A. and Sattelle, D. B. (1988)** Ionic events following GABA receptor activation in an identified motor neuron. *Proc. Roy. Soc. Lond. B*, **232**, 457-470

**Pinnock, R. D. and Sattelle, D. B. (1987)** Dissociation and maintenance of neurones from adult cockroach (*Periplaneta americana*) and housefly (*Musca domestica*). *J. Neurosci. Methods*, **20**, 195-202.

**Pitman, R. M. (1971)** Transmitter substances in insects: a review. *Comp. Gen. Pharmacol.*, **2**, 347-371.

**Pitman, R. M. (1975)** The ionic dependence of action potentials induced by colchicine in an insect motoneurone cell body. *J. Physiol. (Lond.)*, **247**, 511-520

**Pitman, R. M. (1985)** Pharmacology of the insect central nervous system. In 'Comprehensive Insect Physiology, Biochemistry and Pharmacology.' Eds. Kerkut, G. A. and Gilbert, L. I. Pergamon, Oxford, 5-54

**Pitman, R. M. (1988)** Delayed effects of anoxia upon the electrical properties of an identified cockroach motoneurone. *J. exp. Biol.*, **135**, 95-108

**Pitman, R. M. and Baker, J. R. (1989)** Dopamine responses recorded from a common inhibitory motoneurone of the cockroach (*Periplaneta americana*). *Comp. Biochem. Physiol.*, **92C**, 245-251

**Pitman, R. M., David, J. A. and Hancox, J. C. (1993)** Modulation of insect neurone properties. In 'Comparative Molecular Neurobiology'. Ed. Pichon Y., Birkhäuser Verlag, Basel, Switzerland, 414-424

**Pitman, R. M. and Davis, J. P. L. (1988)** Pharmacological differentiation of responses to dopamine, octopamine, and noradrenaline recorded from a cockroach motoneurone. *Pestic. Sci.*, **24**, 311-323

**Pitman, R. M. and Kerkut, G. A. (1970)** Comparison of the actions of iontophoretically applied acetylcholine and gamma aminobutyric acid with the EPSP and IPSP in cockroach central neurons. *Comp. Gen. Physiol.*, **1 (2)**, 221-230

**Pitman, R. M., Tweedle, C. D. and Cohen, M. J. (1972)** Branching of central neurones: intracellular cobalt injection for light and electron microscopy. *Science*, **176**, 412-414

**Pozzan, T., Rizzuto, R., Volpe, P. and Meldolesi, J. (1994)** Molecular and cellular physiology of intracellular calcium stores. *Physiol. Rev.*, **74 (3)**, 595-636

- Prugh, J., Della Croce, K. and Levine, R. B. (1992)** Effects of the steroid hormone, 20-hydroxyecdysone, on the growth of neurites by identified insect motoneurons *in vitro*. *Dev. Biol.*, **154**, 331-347
- Qazi, S. and Lunt, G. G. (1991)** Muscarinic receptors in locust ganglia are coupled to phosphatidyl inositol turnover and to adenylate cyclase. *Soc. Neurosci. Abstr.*, **17**, 584
- Qian, H. and Dowling, J. E. (1993)** Novel GABA responses from rod-driven retinal horizontal cells. *Nature*, **361**, 162-164
- Qian, H. and Dowling, J. E. (1994)** Pharmacology of novel GABA receptors found on rod horizontal cells of the white perch retina. *J. Neurosci.*, **14** (7), 4299-4307
- Raferty, M. A. (1973)** Isolation of acetylcholine receptor- $\alpha$ -bungarotoxin complexes from *Torpedo californica* electroplax. *Arch. Biochem. Biophys.*, **154**, 270-276
- Raferty, M. A., Vandlen, R. L., Reed, K. L. and Lee, T. (1975)** Characterization of *Torpedo californica* acetylcholine receptor: its subunit composition and ligand-binding properties. *Symp. Quant. Biol.*, **40**, 193-292
- Ramirez, J.-M. and Orchard, I. (1990)** Octopaminergic modulation of the forewing stretch receptor in the locust, *Locusta migratoria*. *J. exp. Biol.*, **149**, 255-279
- Ramirez, J.-M. and Pearson, K. G. (1991a)** Octopamine induced bursting plateau potentials in insect neurones. *Brain Res.*, **549**, 332-337
- Ramirez, J.-M. and Pearson, K. G. (1991b)** Octopaminergic modulation of interneurons in the flight system of the locust. *J. Neurophysiol.*, **66** (3), 1522-1537
- Rang, H. P. and Dale, M. M. (1987)** 'Pharmacology'. Churchill Livingstone, UK
- Rauh, J. J., Lummis, S. C. R. and Sattelle, D. B. (1990)** Pharmacological and biochemical properties of insect GABA receptors. *TIPS*, **11**, 325-329
- Raymond, L. A., Blackstone, C. D. and Haganir, R. L. (1993)** Phosphorylation of amino acid neurotransmitter receptors in synaptic plasticity. *TINS*, **16**, 147-153
- Ready, D. F. and Nicholls, J. G. (1979)** Identified neurones isolated from leech CNS make selective connections in culture. *Nature*, **281**, 67-69

- Reiter, M. J., Cowburn, D. A., Prives, J. M. and Karlin, A. (1972)** Affinity labelling of the acetylcholine receptor in the electroplax: electrophoretic separation in sodium dodecyl sulfate. *Proc. Natl. Acad. Sci., USA*, **69**, 1168-1172
- Reye, D. N. and Pearson, K. G. (1987)** Projections of the wing stretch receptors to central flight neurons in the locust. *J. Neurosci.*, **7**, 2476-2487
- Reynolds, J. A. and Karlin, A. (1978)** Molecular weight in detergent solution of acetylcholine receptor from *Torpedo californica*. *Biochem.*, **17** (11), 2035-2038
- Robertson, R. M. and Pearson, K. G. (1985)** Neural circuits in the flight system of the locust. *J. Neurophysiol.*, **53** (1), 110-128
- Robertson, R. M. and Wisniewski, L. (1988)** GABA-like immunoreactivity of identified interneurons in the flight system of the locust, *Locusta migratoria*. *Cell Tiss. Res.*, **254**, 331-340
- Roskoski, R., Vulliet, P. R. and Glass, D. B. (1987)** Phosphorylation of tyrosine hydroxylase by cyclic GMP-dependent protein kinase. *J. Neurochem.*, **48** (3), 840-845
- Ross, A., Rapauno M., and Prives, J. (1988)** Induction of phosphorylation and cell surface redistribution of acetylcholine receptors by phorbol esters and carbamylcholine in cultured chick muscle cells. *J. Cell Biol.*, **107**, 1139-1145
- Ross, A. F., Green, W. N., Hartman, D. S. and Claudio, T. (1991)** Efficiency of acetylcholine receptor subunit assembly and its regulation by cAMP. *J. Cell Biol.*, **113**, 623-626
- Rössler, W. and Bickmeyer, U. (1993)** Locust medial neurosecretory cells *in vitro*: morphology, electrophysiological properties and effects of temperature. *J. exp. Biol.*, **183**, 323-339
- Rykebusch, S. and Laurent, G. (1993)** Rhythmic patterns evoked in locust leg motor neurons by the muscarinic agonist pilocarpine. *J. Neurophysiol.*, **69** (5), 1583-1595
- Safran, A., Sagi-Eisenberg, R., Neumann, D. and Fuchs, S. (1987)** Phosphorylation of the acetylcholine receptor by protein kinase C and identification of the phosphorylation site within the receptor  $\delta$  subunit. *J. Biol. Chem.*, **262**, 10506-10510
- Sattelle, D. B., David, J. A., Harrow, I. D. and Hue, B. (1980)** Actions of  $\alpha$ -bungarotoxin on identified insect neurones. In '*Receptors for neurotransmitters, hormones and pheromones in insects.*' Eds. Sattelle, D. B., Hall, L. M. and Hildebrand, J. G., Elsevier/North-Holland Biomedical Press, Amsterdam, 125-139

**Sattelle, D. B., Harrow, I. D., Hue, B., Pelhate, M., Gepner, J. I. and Hall, L. M. (1983)**  $\alpha$ -Bungarotoxin blocks excitatory synaptic transmission between cercal sensory neurones and giant interneurone 2 of the cockroach, *Periplaneta americana*. *J. exp. Biol.*, **107**, 473-489

**Sattelle, D. B., Pinnock, R. D., Walford, K. A. and David, J. A. (1988)** GABA receptors on the cell-body of an identified motor neuron. *Proc. Roy. Soc. Lond. B*, **232**, 443-456

**Sawruk, E., Udri, C., Betz, H. and Schmitt, B. (1990)** SBD, a novel structural subunit of the *Drosophila* nicotinic acetylcholine receptor, shares its genomic localization with two  $\alpha$ -subunits. *FEBS Letts.*, **273** (1-2), 177-181

**Schacher, S. (1988)** Identified *Aplysia* neurons maintained in dissociated cell culture: regeneration, synapse formation and synaptic plasticity. In '*Cell culture approaches to invertebrate neuroscience*'. Eds. Beadle, D. J., Lees, G. and Kater, S. B., Academic Press, London, UK, 53-84

**Schacher, S. and Proshansky, E. (1983)** Neurite regeneration by *Aplysia* neurons in dissociated cell culture: modulation by *Aplysia* hemolymph and the presence of the initial axonal segment. *J. Neurosci.*, **3** (12), 2403-2413

**Schacher, S., Rayport, S. G. and Ambron, R. T. (1985)** Giant *Aplysia* neuron R2 reliably forms strong chemical connections *in vitro*. *J. Neurosci.*, **5** (11), 2851-2856

**Schlapfer, W. T., Haywood, P. and Barondes, S. H. (1972)** Cholinesterase and choline acetyltransferase activities develop in whole explant but not in dissociated cell cultures of cockroach brain. *Brain Res.*, **39**, 540-544

**Schloss, P., Betz, H., Schroeder, C. and Gundelfinger, E. D. (1991)** Neuronal nicotinic acetylcholine receptors in *Drosophila* antibodies raised against an  $\alpha$ -like and a non- $\alpha$ -subunit recognise the same high affinity  $\alpha$ -bungarotoxin binding complex. *J. Neurochem.*, **57** (5), 1556-1562

**Schmidt, J. and Raferty, M. A. (1972)** Use of affinity chromatography for acetylcholine receptor purification. *Biochem. Biophys. Res. Comm.*, **49** (2), 572-578

**Schofield, P. R., Darlinson, M. G., Fujita, N., Burt, D. R., Stephenson, F. A., Rodriguez, H., Rhee, L. M., Ramachandran, J., Reale, V., Glencourse, T. A., Seeburg, P. H. and Barnard, E. A. (1987)** Sequence and functional expression of the GABA<sub>A</sub> receptor shows a ligand-gated receptor super-family. *Nature*, **328**, 221-227



- Scholz, K. P. and Byrne, J. H. (1987)** Long-term sensitization in *Aplysia*: biophysical correlates in tail sensory neurons. *Science*, **235**, 685-687
- Schulman, H. (1995)** Protein phosphorylation in neuronal plasticity and gene expression. *Curr. Op. Neurobiol.*, **5**, 375-381
- Seecof, R. L. and Teplitz, R. L. (1971)** *Drosophila* neurone differentiation *in vitro*. *Curr. Topic Mic. Immunol.*, **55**, 77-85
- Seecof, R. L., Teplitz, R. L., Gerson, I., Ikeda, K. and Donady, J. J. (1972)** Differentiation of neuromuscular junctions in cultures of embryonic *Drosophila* cells. *Proc. Nat. Acad. Sci.*, **69** (3), 566-570
- Seeman, P. S. and Van Tol, H. M. (1994)** Dopamine receptor pharmacology. *TIPS*, **15**, 264-270
- Sessler, F. M., Liu, W., Kirifides, M. L., Mouradin, R. D., Lin, R. C. S. and Waterhouse, B. D. (1995)** Noradrenergic enhancement of GABA-induced input resistance changes in layer V regular spiking pyramidal neurons of rat somatosensory cortex. *Brain Res.*, **675**, 171-182
- Shapiro, R. A., Wakimoto, B. T., Subers, E. M. and Nathanson, N. M. (1989)** Characterization and functional expression in mammalian cells of genomic and cDNA clones encoding a *Drosophila* muscarinic acetylcholine receptor. *Proc. Natl. Acad. Sci. USA*, **86**, 9039-9043
- Shields, G., Dübendorfer, A. and Sang, J. H. (1975)** Differentiation *in vitro* of larval cell types from early embryonic cells of *Drosophila melanogaster*. *J. Embryol. exp. Morphol.*, **33**, 159-175
- Shimada, S., Cutting, G. and Uhl, G. R. (1992)**  $\gamma$ -aminobutyric acid A or C receptor?  $\gamma$ -aminobutyric acid  $\rho_1$  receptor RNA induced bicuculline-, barbiturate- and benzodiazepine-insensitive  $\gamma$ -aminobutyric acid responses in *Xenopus* oocytes. *Mol. Pharmacol.*, **41**, 683-687
- Shirvan, M. H., Pollard, H. B. and Heldman, E. (1991)** Mixed nicotinic and muscarinic features of cholinergic receptor coupled to secretion in bovine chromaffin cells. *Proc. Natl. Acad. Sci. USA*, **88**, 4860-4864
- Sibley, D. R. and Monsma Jr., F. J. (1992)** Molecular biology of dopamine receptors. *TIPS*, **13**, 61-68
- Siegelbaum, S. A. and Tsien, R. W. (1983)** Modulation of gated ion channels as a mode of transmitter action. *TINS*, **6**, 307-313

**Sigel, E. and Baur, R. (1988)** Activation of protein kinase C differentially modulates neuronal  $\text{Na}^+$ ,  $\text{Ca}^{2+}$ ,  $\gamma$ -aminobutyric acid type A channels. *Proc. Natl. Acad. Sci. USA*, **85**, 6192-6196

**Simpson, P. B., Challiss, R. A. J. and Nahorski, S. R. (1995)** Neuronal  $\text{Ca}^{2+}$  stores: activation and function. *TINS*, **18** (7), 299-306

**Smith, S. J. (1988)** Neuronal cytom mechanics: the actin-based motility of growth cones. *Science*, **242**, 708-715

**Smith, R. K. and House, C. R. (1977)** Fluid secretion by isolated cockroach salivary glands. *Experientia*, **33**, 1182-1184

**Steiner, F. A. and Pieri, L. (1969)** Comparative microelectrophoretic studies of invertebrate and vertebrate neurones. In '*Mechanisms of synaptic transmission*'. Eds. Akert, K. and Waser, P. G., Elsevier, Amsterdam, 191-199

**Stephenson, F. A. (1995)** The  $\text{GABA}_A$  receptors. *Biochem. J.*, **310**, 1-9

**Streb, H., Irvine, R. F., Berridge, M. J. and Schulz, I. (1983)** Release of  $\text{Ca}^{2+}$  from a nonmitochondrial intracellular store in pancreatic acinar cells by inositol 1,4,5-trisphosphate. *Nature*, **306**, 67-69

**Stryer, L. (1988)** '*Biochemistry*'. W. H. Freeman and Co., New York

**Strumwasser, F., Kaczmarek, L. K. and Viele, D. (1978)** The peptidergic bag cell neurones of *Aplysia*: morphological and electrophysiological studies of dissociated cells in tissue culture. *Soc. Neurosci. Abstr.*, **4**, 207

**Study, R. E. and Barker, J. L. (1981)** Diazepam and (-)-pentobarbital: fluctuation analysis reveals different mechanisms for potentiation of  $\gamma$ -aminobutyric acid responses in cultured central neurons. *Proc. Natl. Acad. Sci., USA*, **78** (11), 7180-7184

**Sugita, S., Goldsmith, J. R., Baxter, D. A. and Byrne, J. H. (1992)** Involvement of protein kinase C in serotonin-induced spike broadening and synaptic facilitation of sensorimotor connections in *Aplysia*. *J. Neurophysiol.*, **68**, 643-651

**Suter, C. (1986)** The action of octopamine and other biogenic amines on locust central neurons. *Comp. Biochem. Physiol.*, **84C**, 181-187

**Suter, C. and Usherwood, P. N. R. (1985)** Action of acetylcholine and antagonists on somata isolated from locust central neurones. *Comp. Biochem. Physiol.*, **80C**, 221-229



**Sutherland, E. W. and Rall, T. W. (1958)** Fractionation and characterisation of a cyclic adenine ribonucleotide formed by tissue particles. *J. Biol. Chem.*, **232**, 1077-1091

**Swope, S. L., Moss, S. J., Blackstone, C. D. and Huganir, R. L. (1992)** Phosphorylation of ligand-gated ion channels: a possible mode of synaptic plasticity. *FASEB J.*, **6**, 2514-2523

**Takai, T., Noda, M., Mishina, M., Shimizu, S., Furutani, Y., Kayano, T., Ikeda, T., Kubo, T., Takahashi, H., Takahashi, T., Kuno, M. and Numa, S. (1985)** Cloning, sequencing and expression of cDNA for a novel subunit of acetylcholine receptor from calf muscle. *Nature*, **315**, 761-764

**Tao, J., Johansson, J. S. and Haynes, D. H. (1992)** Protein kinase C stimulates dense tubular  $\text{Ca}^{2+}$  uptake in the intact human platelet by increasing the  $V_m$  of the  $\text{Ca}^{2+}$ -ATPase pump: stimulation by phorbol ester, inhibition by calphostin C. *Biochimica et Biophysica Acta*, **1107**, 213-222

**Teitelbaum, I. and Berl, T. (1994)** Increased cytosolic  $\text{Ca}^{2+}$  inhibits AVP-stimulated adenylyl cyclase activity in rat IMCT cells by activation of PKC. *Am. J. Physiol.*, **266**, F486-F490

**Thomas, M. V. (1984)** Voltage-clamp analysis of a calcium-mediated potassium conductance in cockroach (*Periplaneta americana*) central neurones. *J. Physiol. (Lond.)*, **350**, 159-178

**Thomas, A. P. and Delaville, F. (1991)** The use of fluorescent indicators for measurements of cytosolic-free calcium concentration in cell populations and single cells. In 'Cellular Calcium. A Practical Approach.' Eds. McCormack, J. G. and Cobbold, P. H., Oxford University Press, Oxford, UK, 1-54

**Thomas, W. E., Jordan, F. L. and Townsel, J. G. (1987)** The status of the study of invertebrate neurones in tissue culture - phylum Arthropoda. *Comp. Biochem. Physiol.*, **87A**, 215-222

**Tribut, F., Duval, A. and Lapied, B. (1994)** Two distinct receptors are activated by arecoline on cockroach sixth abdominal ganglion DUM neurones. *J. exp. Biol.*, **186**, 325-331

**Trimmer, B. A. (1992)** The regulation of a muscarinic current in an identified insect motoneuron. *Soc. Neurosci. Abstr.*, **18**, 472

**Trimmer, B. A. (1994)** Characterization of a muscarinic current that regulates excitability of an identified insect motoneuron. *J. Neurophysiol.*, **72** (4), 1862-1873

**Trimmer, B. A. (1995)** Current excitement from insect muscarinic receptors. *TINS*, **18** (2), 104-111

**Trimmer, B. A. and Berridge, M. J. (1985)** Inositol phosphates in the insect nervous system. *Insect Biochem.*, **16** (6), 811-815

**Trimmer, B. A. and Weeks, J. C. (1989)** Effects of nicotinic and muscarinic agents on an identified motoneurone and its direct afferent inputs in larval *Manduca sexta*. *J. exp. Biol.*, **144**, 303-337

**Trimmer, B. A. and Weeks, J. C. (1993)** Muscarinic acetylcholine receptors modulate the excitability of an identified insect motoneuron. *J. Neurophysiol.*, **69**, 1821-1836

**Tsien, R. Y. (1980)** New calcium indicators buffer with high selectivity against magnesium and protons: design, synthesis, and properties of prototype structures. *Biochem.*, **19**, 2396-2404

**Tsien, R. Y. (1989)** Fluorescent indicators of ion concentrations. In '*Methods in Cell Biology. Volume 30. Fluorescence microscopy of living cells in culture. Part B.*' Eds. Taylor, D. L. and Wang, Y.-L., Academic Press, Inc., San Diego, California, USA, 127-156

**Tsien, R. W., Lipscombe, D., Madison, D., Bley, D. and Fox, A. (1988)** Multiple types of neuronal calcium channels and their selective modulation. *TINS*, **11**, 431-438

**Twyman, R. E. and MacDonald, R. L. (1992)** Neurosteroid regulation of GABA<sub>A</sub> receptor single-channel kinetic properties of mouse spinal cord neurons in culture. *J. Physiol. (Lond.)*, **456**, 215-245

**Twyman, R. E., Rogers, C. J. and MacDonald, R. L. (1989)** Pentobarbital and picrotoxin have reciprocal action on single GABA<sub>A</sub> receptor channels. *Neurosci. Letts.*, **96**, 89-95

**Usherwood, P. N. R., Giles, D. P. and Suter, C. (1980)** Studies of the pharmacology of insect neurones *in vitro*. In '*Insect Neurobiology and Pesticide Action.*' Soc. Chem. Ind., London, 115-128

**Uzzan, A. and Dudai, Y. (1982)** Aminergic receptors in *Drosophila melanogaster*: responsiveness of adenylate cyclase to putative neurotransmitters. *J. Neurochem.*, **38** (6), 1542-1550

**Valenzuela, C. F., Machu, T. K., McKernan, R. M., Whiting, P., Vanreenterghem, B. B., McManaman, J. L., Brozowski, S. J., Smith, G. B.,**

- Olsen, R. W. and Harris, R. A. (1995) Tyrosine kinase phosphorylation of GABA<sub>A</sub> receptors. *Mol. Brain Res.*, 1-2, 165-172
- Vallar, L., Muca, C., Magni, M., Albert, P., Bunzow, J., Meldolesi, J. and Civelli, O. (1990) Differential coupling of dopaminergic D<sub>2</sub> receptors expressed in different cell types. *J. Biol. Chem.*, 265 (18), 10320-10326
- Vanhems, E., Delbos, M. and Girardie, J. (1990) Insulin and neuroparsin promote neurite outgrowth in cultured locust CNS. *Eur. J. Neurosci.*, 2, 776 - 782
- Vanhems, E., Delbos, M. and Girardie, J. (1993) *In vitro* growth of locust embryonic pars intercerebralis neurosecretory cells. *Neuroscience*, 52 (2), 361-368
- Van Tol, H. H. M., Bunzow, J. R., Guan, H.-C., Sunahara, R. K., Seeman, P., Niznik, H. B. and Civelli, O. (1991) Cloning of the gene for an human dopamine D<sub>4</sub> receptor with high affinity for the antipsychotic clozapine. *Nature*, 30, 610-614
- Verkhratsky, A. and Kettenmann, H. (1996) Calcium signalling in glial cells. *TINS*, 19 (8), 346-352
- Vijayaraghavan, S., Schmid, H. A., Halvorsen, S. W. and Berg, D. K. (1990) Cyclic AMP-dependent phosphorylation of a neuronal acetylcholine receptor  $\alpha$ -type subunit. *J. Neurosci.*, 10, 3255-3262
- Waelbroeck, M., Tastenoy, M., Camus, J. and Christophe, J. (1991) Binding kinetics of quinuclidinyl benzilate and methyl-quinuclidinyl benzilate enantiomers at neuronal (M1), cardiac (M2), and pancreatic (M3) muscarinic receptors. *Mol. Pharmacol.*, 40, 413-420
- Wall, M. J. and Dale, N. (1993) GABA<sub>B</sub> receptors modulate glycinergic inhibition and spike threshold in *Xenopus* embryo spinal neurones. *J. Physiol. (Lond.)*, 469, 275-290
- Wang, R. A., Cheng, G., Kolaj, M. and Randic, M. (1995) Alpha-subunit of calcium/calmodulin-dependent protein-kinase-II enhances gamma-aminobutyric acid and inhibitory synaptic responses of rat neurons *in vitro*. *J. Neurophysiol.*, 73 (5), 2099-2106
- Weill, D. M., McNamee, M. G. and Karlin, A. (1974) Affinity-labelling of purified acetylcholine receptor from *Torpedo californica*. *Biochem. Biophys. Res. Comm.*, 61 (3), 997-1003
- Wellis, D. P. and Werblin, F. S. (1995) Dopamine modulates GABA<sub>C</sub> receptors mediating inhibition of calcium entry into and transmitter release from bipolar cell terminals in Tiger Salamander retina. *J. Neurosci.*, 15 (7), 4748-4761

- Wess, J. (1993)** Molecular basis of muscarinic acetylcholine receptor function. *TIPS*, **14**, 308-313
- Wilson, D. M. (1961)** The central nervous control of flight in a locust. *J. exp. Biol.*, **38**, 471-490
- Wong, R. G., Hadley, R. D., Kater, S. B. and Hauser, G. C. (1981)** Neurite outgrowth in molluscan organ and cell cultures: the role of conditioning factor(s). *J. Neurosci.*, **1**, 1008-1023
- Wonnacott, S. (1997)** Presynaptic nicotinic ACh receptors. *TINS*, **20** (2), 92-98
- Xu, Y. L., Cleary, L. J. and Byrne, J. H. (1994)** Identification and characterization of pleural neurons that inhibit sensory neurons and motor-neurons in *Aplysia*. *J. Neurosci.*, **14** (6), 3565-3577
- Yang, C. R. and Seamans, J. K. (1996)** Dopamine D1 receptors action in layers v-vi rat prefrontal cortex neurons *in vitro*: modulation of dendritic-somatic signal integration. *J. Neurosci.*, **16** (5), 1922-1935
- Yee, G. H. and Huganir, R. L. (1987)** Determination of the sites of cAMP-dependent phosphorylation on the nicotinic acetylcholine receptor. *J. Biol. Chem.*, **262**, 16748-16753
- Yu, P.-Y., Eisner, G. M., Yamaguchi, I., Mouradian, M. M., Felder, R. A. and Jose, P. A. (1996)** Dopamine D<sub>1A</sub> receptor regulation of phospholipase C isoform. *J. Biol. Chem.*, **271** (32), 19503-19508
- Zoran, M. J., Doyle, R. T. and Haydon, P. G. (1990)** Target-dependent induction of secretory capabilities in an identified motoneuron during synaptogenesis. *Dev. Biol.*, **138**, 202-213
- Zoran, M. J., Doyle, R. T. and Haydon, P. G. (1991)** Target contact regulates the calcium responsiveness of the secretory machinery during synaptogenesis. *Neuron*, **6**, 145-151

## **Appendices**

## APPENDIX 1: COMPOSITION OF TOLUIDINE BLUE STAIN AND BODIAN'S FIXATIVE

### TOLUIDINE BLUE

1g Toluidine Blue

6g borax ( $\text{Na}_2\text{B}_4\text{O}_7$ )

1g boric acid

100ml double distilled water

pH 7.6 - 9.0

### BODIAN'S FIXATIVE

5ml formalin

5ml glacial acetic acid

90ml 80% ethanol

(from Altman, 1980)

## APPENDIX 2: COMPOSITION OF LOCUST AND COCKROACH SALINE

### Composition of locust saline (adapted from Hancox, 1991)

		FINAL CONCENTRATION
4M NaCl	37.5ml	150mM
1M KCl	5ml	5mM
1M CaCl <sub>2</sub>	4ml	4mM
TES	2.292gl <sup>-1</sup>	10mM

(for 1000ml)

The salt solutions and pH buffer TES (N-tris[Hydroxymethyl]methyl-2-aminoethanesulfonic acid) were made up to approximately 950ml with double deionized (MilliQ) water. The pH of the saline was corrected to pH 7.4 with 1.0M NaOH using a Pye Model 292 pH meter (Pye Unicam). The final volume was then made up to 1000ml.

100ml aliquots of locust saline were supplemented with glucose (0.09g; 5mM) and sucrose (3.423g; 100mM) shortly before use, in order to minimize microorganism contamination.

### Composition of cockroach saline (Pitman, 1975)

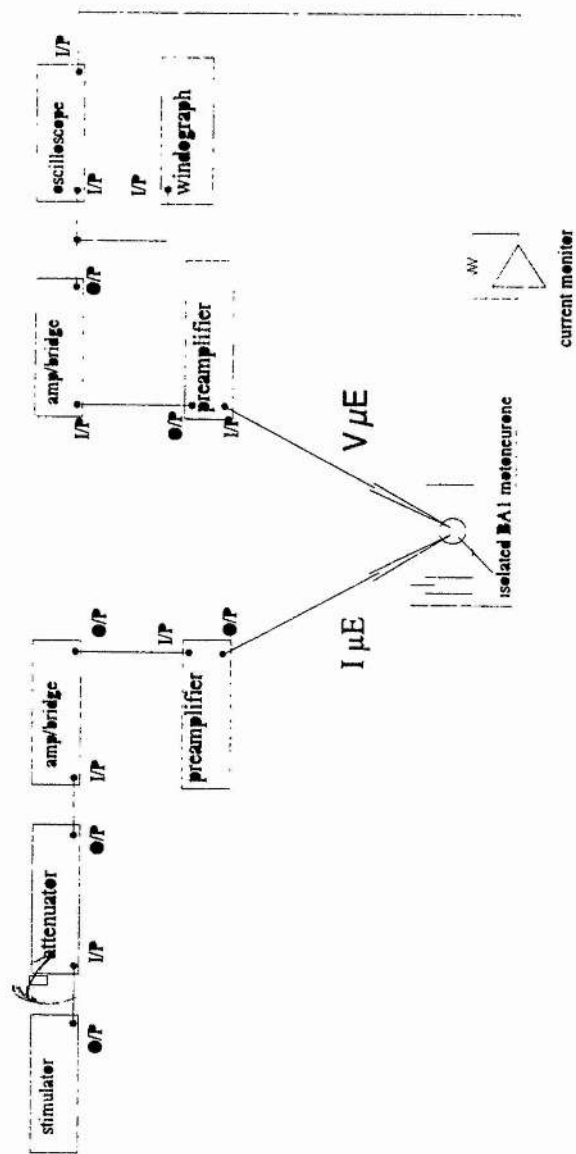
		FINAL CONCENTRATION
4M NaCl	53.5ml	214mM
1M KCl	3.1ml	3.1mM
1M CaCl <sub>2</sub>	9ml	9mM
TES	2.292gl <sup>-1</sup>	10mM

(for 1000ml)

The same procedure described above was used to prepare the cockroach saline, however, the pH of this saline was adjusted to pH 7.2.

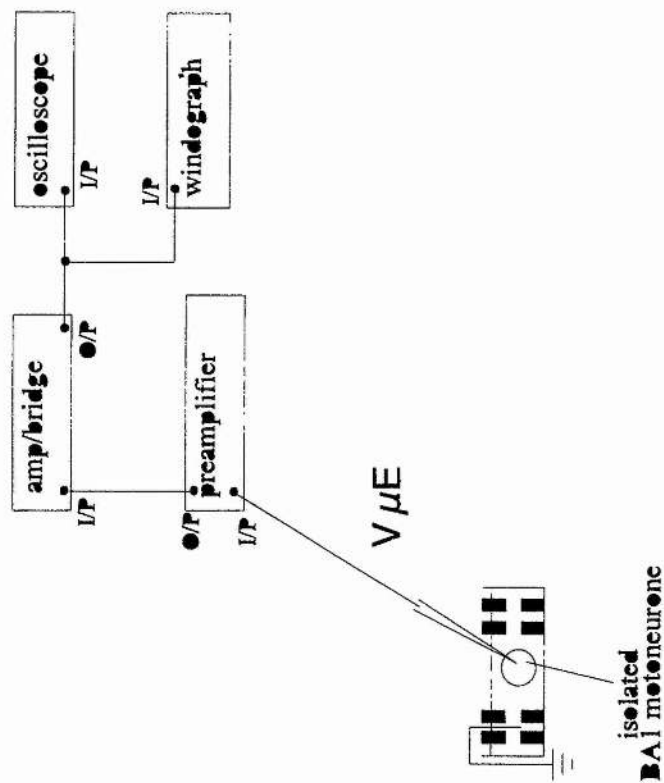


# APPENDIX 3: DIAGRAMATIC REPRESENTATION OF TWO MICROELECTRODE CURRENT CLAMP



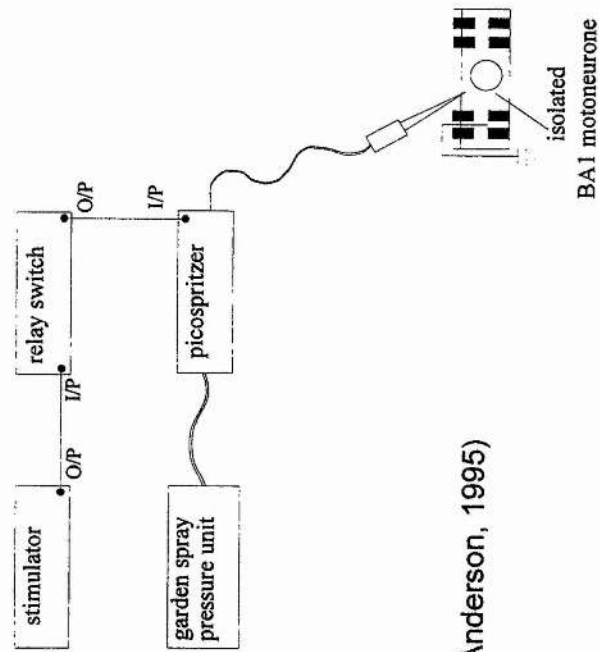
(Adapted from Anderson, 1995)

APPENDIX 4:  
DIAGRAMMATIC REPRESENTATION OF SINGLE MICROELECTRODE CURRENT CLAMP



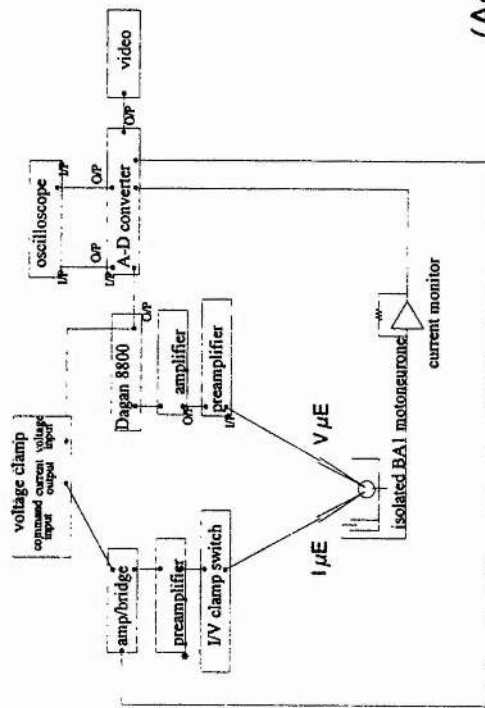
(Adapted from Anderson, 1995)

APPENDIX 5:  
DIAGRAMMATIC REPRESENTATION OF THE  
PRESSURE APPLICATION OF PHARMACOLOGICAL AGENTS



(Adapted from Anderson, 1995)

# APPENDIX 6: DIAGRAMMATIC REPRESENTATION OF TWO MICROELECTRODE VOLTAGE CLAMP



(Adapted from Anderson, 1995)

## APPENDIX 7: COMPOSITION OF THE CULTURE MEDIA<sup>1</sup>

Constituent (mg/l)	Minimum Essential Medium (Eagles with Hank's salts)	Schneider's revised <i>Drosophila</i> medium	Supplemented L-15 medium (H&H) <sup>2</sup> .
<b>Sugars</b>			
fructose			400
galactose			900
glucose	1000	2000	700
trehalose		2000	
<b>Organic acids</b>			
fumaric acid		100	25
$\alpha$ -ketoglutaric acid		200	370
lipoic acid			0.05
malic acid		100	670
succinic acid		100	60
<b>Amino acids</b>			
$\beta$ -alanine		500	5
D,L-alanine			450
L-arginine	126	400	500
L-asparagine			250
L-aspartic acid		400	30
L-cysteine		60	120
L-cystine	24	100	135
L-glutamic acid		800	15
L-glutamine		1800	300
glycine		250	200
L-histidine	42	400	250
L-isoleucine	52	150	250
L-leucine	52	150	125
L-lysine	73	1650	75
L-methionine	15	800	150
L-phenylalanine	32	150	250
L-proline		1700	
D,L-serine		250	200
L-threonine	48	350	600
L-tryptophan	10	100	20
L-tyrosine	36	500	300
L-valine	46	300	200

Vitamins			
biotin		0.44	0.02
Ca-pantothenate	1	0.44	1
choline choride	1	0.44	11
cyancobalamin (B <sub>12</sub> )			2
folic acid	1	0.44	1
inositol	2	0.80	12
niacin			2
nicotinamide	1	0.44	1
p-aminobenzoic acid			5
pyridoxal HCl	1	0.44	1
pyridoxin HCl			1
riboflavin	1	0.444	0.1
thiamine HCl	1	0.44	1
Inorganic salts			
CaCl <sub>2</sub>	185	794	185
KCl	400	1600	400
KH <sub>2</sub> PO <sub>4</sub>	60	450	60
MgCl <sub>2</sub>	100		200
MgSO <sub>4</sub>	100	3700	200
NaCl	8000	2100	8000
NaHCO <sub>3</sub>	350	400	
NaHPO <sub>4</sub>	48	1321	190
Other components			
coenzyme A			0.4
imidazole			60
lactalbumin hydrosylate			2.8
20-hydroxyecdysone			1
phenol red	10	4.40	10.5
sodium pyruvate			550
yeast hydrosylate		2000	2.8

<sup>1</sup>: Values supplied by Gibco (Life Technologies)

<sup>2</sup>: Hayashi and Hildebrand (1990); supplemented Liebovitz L-15 medium

Prior to its use, each medium was supplemented with 0.003% glutamine and had 100iu.ml<sup>-1</sup> penicillin and streptomycin (Gibco) and 0.25µg.ml<sup>-1</sup> Fungizone (Gibco) added to it in order to prevent bacterial and fungal contamination.

The concentrations of Na<sup>+</sup> and K<sup>+</sup> in the prepared Hayashi and Hildebrand medium (in the absence of fetal calf serum) were 139mM and 5.4mM, respectively.

Fetal calf serum (Integra Biosciences) and the 10ml sterile plastic tubes (Teklab) were kindly provided by Dr. A. Riches, St. Andrews University.



## APPENDIX 8: SOURCES OF COMPOUNDS

$\beta$ -alanine	BDH
p-aminobenzoic acid	Sigma
$\gamma$ -aminobutyric acid	Sigma
$\alpha$ -bungarotoxin	Sigma
$\alpha$ -ketoglutaric acid	Sigma
(-)-nicotine	Sigma
(-)-scopolamine hydrochloride	Sigma
( $\pm$ )-verapamil hydrochloride	Sigma
20-hydroxyecdysone	Sigma
3-hydroxytyramine	Sigma
acetylcholine chloride	Sigma
arecoline hydrobromide	Sigma
aspartic acid.	Sigma
atropine sulphate	Sigma
borax	Sigma
boric acid	Griffin and Tatlock Ltd
calcium chloride	BDH
carbamylcholine chloride	Sigma
choline chloride	Sigma
Coenzyme A	Sigma
cyancobalamin (B12)	Sigma
D(-)-fructose	Sigma
D-(+)-glucose	BDH
d-biotin	Sigma
dimethyldichlorosilane in trichloroethane	BDH
DL- $\alpha$ -lipoic acid	Sigma
ethanol	BDH
flupenthixol dihydrochloride	RBI
fluphenazine dihydrochloride	Squibb
formaldehyde	BDH
fumaric acid	BDH
glacial acetic acid	BDH
glutamic acid	Sigma
imidazole	Sigma
L-ascorbic acid	BDH
L-cystine	Sigma
lactalbumin enzymatic hydrolysate	Sigma
lithium acetate	Sigma
Lucifer Yellow CH	Sigma
malic acid	Sigma
McN-A-343	Sigma/RBI
methyl benzoate	BDH
methyl salicylate	BDH
muscimol hydrobromide	RBI

<i>myo</i> -inositol	Sigma
niacin	Sigma
oxotremorine sesquifumarate	Sigma
phenol red (phenolsulfonphthalein)	Sigma
pilocarpine hydrochloride	Sigma
potassium acetate	BDH
potassium chloride	BDH
silicone grease	Radio Spares
sodium chloride	BDH
succinic acid	Sigma
sucrose	Fisons/Tate and Lyle
Sylgard	Dow Corning
TES	Sigma
Toluidine Blue	Gurr
yeast extract	Sigma

## APPENDIX 9: LIST OF ABBREVIATIONS

$\alpha$ -BTX:  $\alpha$ -bungarotoxin  
[Ca<sup>2+</sup>]<sub>i</sub>: intracellular calcium concentration  
20-HE: 20-hydroxyecdysone  
3-APA: 3-aminopropylphosphonic acid  
3-APPA: 3-aminopropylphosphonous acid  
3-APS: 3-aminopropylsulphonic acid  
5HT: serotonin; 5-hydroxytryptamine  
AC: adenylate cyclase  
ACh: acetylcholine; ACh(1) and ACh(2), nicotinic and muscarinic response, respectively  
ADP: adenosine diphosphate  
ADTN: hydrobromide[( $\pm$ )-2-amino-6,7-dihydroxy-1,2,3,4-tetrahydronaphthalene hydrobromide  
AM: acetoxymethyl ester  
AMPA:  $\alpha$ -amino-3-hydroxy-5-methyl-4-isoxalone propionic acid  
ARE: arecoline; arecaidine methyl ester  
ATP: adenosine triphosphate  
ATR: atropine  
Ba<sup>2+</sup>: barium ion  
BA1: first basalar motoneurone  
BAPTA: 1,2-*bis*-(2-aminophenoxy)ethane-N,N,N',N'-tetraacetic acid  
C: carboxy terminus  
Ca<sup>2+</sup>: calcium ion  
Ca<sup>2+</sup>ATPase: calcium-dependent ATPase  
CACA: *cis*-4-aminocrotonic acid  
CaMK: Ca<sup>2+</sup> and calmodulin-dependent protein kinase  
CAMP: *cis*-2-aminomethylcyclopropane carboxylic acid  
cAMP: cyclic adenosine monophosphate  
CCh: carbamylcholine  
Cd<sup>2+</sup>: cadmium ion  
cGMP: cyclic guanosine monophosphate  
CICR: calcium-induced calcium release  
Cl<sup>-</sup>: chloride ion  
CLSM: confocal laser scanning microscopy  
Co<sup>2+</sup>: cobalt ion  
CoA: Coenzyme A  
CPG: central pattern generator  
CTX:  $\omega$ -conotoxin GVIA  
D<sub>3</sub>: prothoracic common inhibitory motoneurone  
DA: dopamine; 3-hydroxytyramine; DA<sub>1</sub>- and DA<sub>2</sub>-, refer to the receptor subtype  
DAG: diacylglycerol  
DAR: dopamine receptor  
D<sub>f</sub>: fast coxal depressor motoneurone  
DHPs: dihydropyridines

DNA: deoxyribonucleic acid  
 DUM: dorsal unpaired median  
 $E_{Ca}$ : calcium equilibrium potential  
 $E_{Cl}$ : chloride equilibrium potential  
 EGTA: ethylene glycol-*bis*-( $\beta$ -aminoethyl)N,N,N',N'-tetraacetic acid  
 $E_K$ : potassium equilibrium potential  
 EM: electron microscopy  
 $E_{Na}$ : sodium equilibrium potential  
 EPSP: excitatory postsynaptic potential  
 FCS: fetal calf serum  
 FTX: funnel web spider toxin  
 GABA:  $\gamma$ -aminobutyric acid; three receptor subtypes GABA<sub>A</sub>, GABA<sub>B</sub>, and GABA<sub>C</sub>  
 GDP: guanosine diphosphate  
 GTP: guanosine triphosphate  
 HHSiD: hexahydro-sila-difenidol  
 HVA: high threshold activation  
 I: current  
 $I_{cation/Ca}$ : calcium-dependent cation current  
 $I_{K(A)}$ : transient (A) potassium current  
 $I_{K(Ca)}$ : calcium-dependent potassium current  
 $I_{K(M)}$ : muscarine-sensitive potassium current (M current)  
 $I_{K(r)}$ : inward rectifying potassium current  
 $I_{K(S)}$ : serotonin-sensitive potassium current (S current)  
 $I_{K(V)}$ : delayed rectifying potassium current  
 $I_K$ : potassium current  
 $I_{Na}$ : sodium current  
 IP<sub>3</sub>: inositol 1,4,5-triphosphate  
 IP<sub>3</sub>R: inositol triphosphate receptor  
 IPSP: inhibitory postsynaptic potential  
 K<sup>+</sup>: potassium ion  
 KAc: potassium acetate  
 Li<sup>+</sup>: lithium ion  
 LiAc: lithium acetate  
 LVA: low threshold activation  
 M1-M7: receptor protein transmembrane spanning domains  
 M<sub>1</sub>/M<sub>2</sub>/M<sub>3</sub>: muscarinic receptor subtype; m1-m5 refers to cloned muscarinic receptors  
 McN: McN-A-343; 4-(N-[3-chlorophenyl]carbamoyloxy)-2-butyryltrimethylammonium chloride  
 N: amino terminus  
 Na<sup>+</sup>: sodium ion  
 Ni<sup>2+</sup>: nickel ion  
 NIC: nicotine  
 NMDA: N-methyl-D-aspartate  
 OXO: oxotremorine; 1-[4-(1-Pyrrolidinyl)-2-butyryl]2-pyrrolidinone

PI: phosphatidylinositol  
PILO: pilocarpine  
PIP<sub>2</sub>: phosphatidylinositol 4,5-bisphosphate  
PKA: cAMP-dependent protein kinase  
PKC: Ca<sup>2+</sup>/phospholipid-dependent protein kinase  
PKG: cGMP-dependent protein kinase  
PLC: phospholipase C  
PPR: principal plantar retractor  
QNB: quinuclidinyl benzilate  
R<sub>i</sub>: input resistance  
RNA: ribonucleic acid  
RyR: ryanodine receptor  
S.E.M.: standard error of the mean  
SLT: supralateral radular tensor  
SR: forewing hinge stretch receptor neurone  
TACA: *trans*-4-aminocrotonic acid  
TAMP: *trans*-2-aminomethylcyclopropane carboxylic acid  
TBPS: *t*-butylbicyclopentachlorophosphate  
TEA: tetraethylammonium ion  
TES: N-tris[Hydroxymethyl]methyl-2-aminoethane-sulphonic acid  
THIP: 4,5,6,7-tetrahydroisoxazole[5,4-c]pyridin-3-ol  
TTX: tetrodotoxin  
UV: ultraviolet light  
V: voltage  
V<sub>m</sub>: maximum velocity